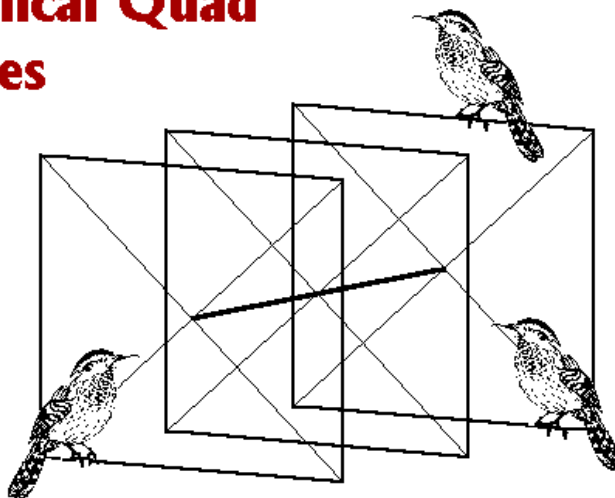


---

# **Cubical Quad Notes**



**Volume 3  
Multi-Band Quad Questions**

**L. B. Cebik, W4RNL**

---

---

***Published by***  
***antenneX Online Magazine***  
**<http://www.antennex.com/>**  
**POB 72022**  
**Corpus Christi, Texas 78472 USA**

---

---

Copyright 2007 by **L. B. Cebik** jointly with ***antenneX Online Magazine***. All rights reserved. No part of this book may be reproduced or transmitted in any form, by any means (electronic, photocopying, recording, or otherwise) without the prior written permission of the author and publisher jointly.

ISBN: 1-877992-80-1

---

## Table of Contents

### Chapter

	Preface to Volume 3 .....	5
	<i>Sneaking Up on 2-Element Common-Feed Quads:</i>	
1	Part 1: Monoband Quad Beams as a Starting Point.....	7
2	Part 2: Dual Band Quad Beams With Separate Feedpoints .....	29
3	Part 3: Dual Band Quad Beams With Common Feedpoints.....	57
4	Part 4: Adjacent-Band Quad Behavior.....	85
	<i>Multi-Element, Multi-Band Quads</i>	
5	A 3-Band, 2-Element Spider-Supported Quad Beam .....	113
6	Why Not Use a 3-Band, 3-Element Quad? .....	139
7	The Quest for the Elusive TBWB4EQ .....	157
8	Notes on Designing Large 5-Band Quads.....	203
9	What Have We Learned?.....	239

## Dedication

This volume of studies of quad antennas is dedicated to the memory of Jean, who was my wife, my friend, my supporter, and my colleague. Her patience, understanding, and assistance gave me the confidence to retire early from academic life to undertake full-time the continuing development of my personal web site (<http://www.cebik.com>). The site is devoted to providing, as best I can, information of use to radio amateurs and others—both beginning and experienced—on various antenna and related topics. This volume grew out of that work—and hence, shows Jean's help at every step.

## Preface to Volume 3 Multi-Band Quad Questions

In Volume 1 of these notes, I reviewed extensively the design of cubical quad beams up to the time of writing (2000). Designs consisted of roughly 3 types. Of course, we began with full size monoband 2-element quads as then designed. We also looked at shrunken quads in order to determine their performance relative to full size versions and their practicality for numerous purposes. Finally, we looked at examples of monoband and multi-band quads with more than 2 elements.

Volume 2 endeavored to re-think the quad beam, with special emphasis on monoband designs. The quad beam suffers from two deficits relative to comparable Yagis. First, the SWR passband tends to be narrower. Second, the front-to-back ratio tends to drop to quite low levels at the edges of any of the wider HF amateur bands. These problems infect quad beams regardless of the number of elements. To rectify these deficiencies, I focused on optimizing the performance of monoband beams and committing the optimization to a series of computer design programs. The result was a series of programs for 1-, 2-, 3-, and 4-element monoband quad designs that required that the user input only the design frequency and the element diameter.

The *unfinished-business box* contained notes on multi-band quad designs. At first sight, one might think that the task at hand consists of optimizing 2-, 3-, and 4-element quads for multi-band service. Unfortunately, the matter is not quite so straightforward. Most quad design work in the 20<sup>th</sup> century used rather standard and close-spaced designs. Early multi-band quads employed planar elements with a constant physical spacing between elements. The designs aimed for physical simplicity and for a feedpoint impedance that permitted a direct match to common coaxial cable impedances. These designs simply hoped for adequate performance and a usefully wide operating passband, and most overlooked their deficiencies. More importantly, they overlooked the detailed work of trying to discover some of the main factors that control the performance of multi-band quads. Element spacing alone does not come close to exhausting the interactions involved in a multi-band quad.

This third volume of notes on the cubical quad begins with 3 chapters that try to sneak up on the question of developing a 2-element multi-band quad with a common feedpoint. We begin with a review of wide-band monoband quads and then combine them into dual-band versions with separate feedpoints. In the process, we shall learn much about how the presence of elements for another band affects the performance of a target band. This information will then let us evaluate the potential for using a common feedpoint for both bands. Including in the common-feedpoint discussion will be some cautions and recommendations relative to modeling these quads.

The conclusions that we can draw from looking at dual-band quads include a recommendation that the bands be separated by a frequency ratio of at least 1.3:1. Since this recommendation seems to exclude combinations such as 10-12 meters or 20-17 meters, we shall spend some time seeing what happens when we close the frequency gap. We shall also examine a 2-element, 3-band quad using spider construction—that is, constant electrical spacing from band to band—to see what we may gain or lose relative to a monoband beam for each of the included bands.

Finally, we shall turn to larger quads, beginning with an account of the good physical and electrical reasons for not building a multi-band 3-element quad. Then we shall examine the search for the elusive ideal 4-element multiband quad and investigate the potential offered by using a pair of phased drivers. Finally, we shall look at very large multi-band quads using variable numbers of elements on one boom. The last two chapters are based on articles that originally appeared in *QEX*: "Notes on Designing Large 5-Band Quads," Nov/Dec, 2003, pp. 12-23, and "The Quest for the Elusive TBWB4EQ," Jul/Aug, 2005, pp. 12-27. I am grateful to ARRL and *QEX* for permission to use the material in these pages.

My ultimate goal is to make some small contributions to the better understanding of quad beam performance and the design factors that mold the performance. As always, the notes are a work in progress, not a finished product. Much remains to be learned, so examine these notes as simply one brick along a very long road.

# Chapter 1

## *Sneaking Up on 2-Element Common-Feed Quads*

### Part 1: Monoband Quad Beams as a Starting Point

Among 2-element quad beam users a question lingers. Which feed system is superior: separate switched drivers or drivers brought to a common feedpoint? The common-feed system is easier for the user, since it eliminates an extra, usually remote, switch box. However, the separate-feed system is usually easier to design and test for proper operation. Many answers to the question abound, ranging from antenna maker claims that users cannot always confirm to simple feelings about the matter.

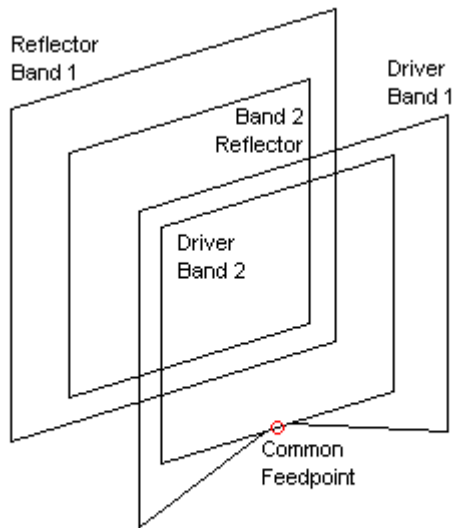


Fig. 1-1

Question: What Happens When We Use a Common Feedpoint for a Multiband Quad Beam?

The common-feed 2-element quad is not a simple system, as **Fig. 1-1** tells us. We

have the elements for at least 2 bands of operation. The elements interact simply by virtue of proximity. Moreover, we have additional interactions occasioned by the use of a common feedpoint. Finally, we can add to the equation the fact that we usually do not know to what we may be comparing either the common-feed or the separate-feed quad. Little wonder that the question tends to raise more heat than light.

Let's revise the basic question so that we can sort out the proper steps on the way to an answer. What happens when we create a multi-band quad and provide it with a common driver feedpoint for all bands?

First, we need a set of starting points, namely, monoband quads from which to build the multi-band quad. Every multi-band quad rests on a set of monoband quads, which the multi-band design alters to compensate for element interaction. In many cases, the designer may not actually examine the monoband quads that underlie the more complex array, but those quads exist anyway. These notes will designate the monoband quads as the place to start so that we can compare multi-band designs and performance to them.

Second, we need to move in logical steps and "sneak up" on the common feed design. After reviewing the performance of the foundational monoband quads, we shall develop from them a series of multi-band designs that use separate feedpoints. These designs will use perfectly square loops for all elements so that the interactions exist at only one level: between reflector wires and driver wires that are equally spaced from each other for the entire perimeter. Only when we know the consequences of this step can we move on to the necessary distortions of the driver wires that occur when we use a common feedpoint.

Third, we must set some limits to the study—or we shall never reach a stopping point. One limitation is setting a frequency ratio between adjacent bands in any multi-band design. The closer 2 bands are in frequency, the greater that the element interaction will be. If the operating frequencies are too close, then seemingly inactive elements become very active, sometimes in unwanted ways. When operating on the lower of two frequencies, the seemingly inactive reflector element may form a director in the wrong direction relative to desired beaming. To

hold interactions to an accountable level, I shall set a minimum frequency ratio of 1.3:1 between adjacent bands. This ratio allows combinations such as 17 and 12 meters, 20 and 15 meters, and 15 and 10 meters. However, it rules out adjacent bands in the upper HF region of the amateur spectrum. There are successful quad beams using these combinations, but they do not reveal their interactions as readily as more widely spaced bands. Remember that our goal is to understand what happens as we move toward a multi-band common-feed quad beam. It is not necessarily to design a quad that we might build.

I shall also limit the study (with one exception) to 2-band quad beams, simply to limit the number of different kinds of sample beams. Instead of examining all possible combinations of multi-band quads, we shall look at multiple examples of two-band quads with different frequency combinations in order to find the reliable trends in the physical shape and performance of these beams. These trends will be the keys to understanding what happens along the road to a common feedpoint. As well, the dual-band quads will give us an opportunity to explore an interesting feeding strategy.

One situation that I shall avoid is a combination of quads involving a 2:1 frequency ratio, such as a 20-meter and 10-meter dual-band quad. On 10 meters, both of the drivers will be at or near resonance and at or near a low impedance value. Hence, we would encounter a greater-than-normal current split between the drivers. However, when used on 10 meters, the 20-meter driver has a circumference of about  $2\lambda$ , and radiation is predominantly off the loop edge. The quad works best when radiation is broadside to the loop, a condition that occurs when closed loops are close to  $1\lambda$  in circumference. By avoiding the 2:1 frequency ratio, we bypass the need for special compensations to overcome the conflict in pattern formation.

The final limitation will involve element spacing. Throughout the multi-banding exercises, I shall maintain the element spacing used in the monoband quads that form our starting points. This specification will result in spider rather than planar quad beams. Planar quad beams have advantages and disadvantages of their own. One primary example is the KC6T quad that I analyzed in volume 1 of *Cubical Quad Notes*. In terms of wavelengths, the spacing between elements

changes as we change bands. Hence, we do not have a ready ability to relate the performance of the multi-band antenna to its root monoband quad components. By preserving element spacing and using what will amount to spider construction with sloping support arms, we can achieve the desired comparisons between original monoband quads and the modifications needed to make them work in various multi-band settings.

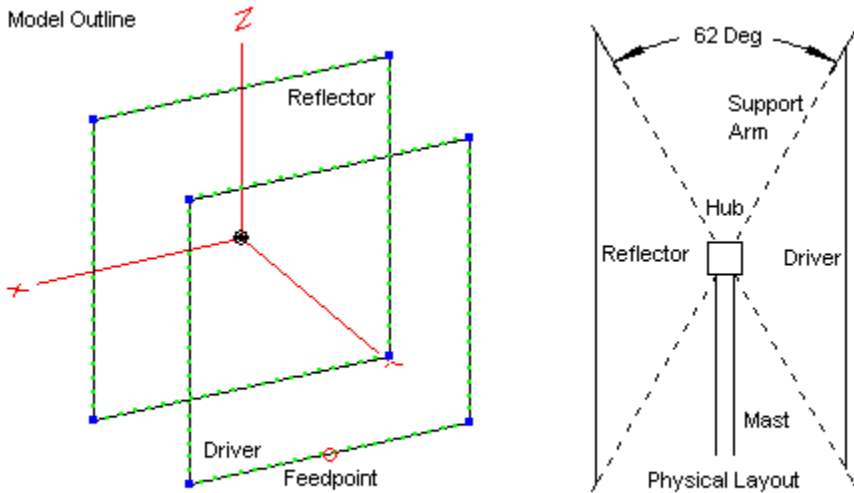
### **Getting Started: Monoband 2-Element Quads**

The multi-element quad beam is essentially a parasitic array with relatively narrow-band performance characteristics. A 2-element driver-reflector design will show a characteristic reduction in forward gain with increasing frequency across the operating passband. This feature the quad shares with the Yagi. (Any well-designed parasitic array with at least one director will show a rising gain with frequency.) However, the key limitations involve the SWR and front-to-back ratio passbands. In Yagi design, 2-element driver-reflector arrays show a low but almost uniform front-to-back ratio across any of the upper HF bands. The SWR passband is often the chief design concern. To widen that passband, we need increased element spacing. The result is a very small reduction in gain at the design frequency, but a wider spread of usable frequencies in which to observe the gain curve.

Designing a monoband 2-element quad involves a number of compromises. In volume 2 of *Cubical Quad Notes*, I described a program and a programmed NEC-Win Plus model that provides optimized 2-element quad beams for any user-selected design frequency and element diameter. The designs rest on extensive hand optimization of models, along with extensive regression analysis to allow use of the designs on wire diameters ranging from  $10E-2$  through  $10E-5 \lambda$  and on frequencies from 3 to at least 300 MHz. A number of interested amateurs have added to the array of formats in which one may perform the calculations. I have also recently set the algorithms into a spreadsheet. For a list of available downloads, see <http://www.cebik.com/quad/q2l2.html>.

**Fig. 1-2** shows the general model outline (using an EZNEC graphic), along with a side view of the quad's physical structure. The angle between the support arms is

62°, that is, about 31° each side of a vertical line drawn through the mast and hub. The precise angle will vary a bit from band to band.



Basic Outlines of Monoband Quads Used in This Study

Fig. 1-2

The angle for the (non-conductive) support arms varies according to the calculated spacing between the elements. The spacing, like all other quad dimensions, is a partial function of the element diameter as measured in wavelengths. In these exercises, I have standardized all quads to the very familiar AWG #14 (0.0641" diameter) copper wire. As measured in wavelengths, the element diameter changes from one band to the next. Since the wire is quite thin, the effects are small. However, the spacing may vary enough to change the overall angle between the reflector and the driver by as much as a full degree or so in the move from 20 down to 10 meters.

Based on the equations, I produced a series of models for the upper HF bands. The dimensions appear in **Table 1-1**. The spacing entry represents the full

dimension. However, for modeling convenience, the loop dimensions appear as 1/2-side lengths. A full side length is twice the value shown, and the loop circumference is 8 times the value in the table. The dimensions are in inches. Multiply these dimensions by 0.0254 to obtain a result in meters.

Table 1-1. 2-Element Monoband Quad Beams

All dimensions derived from NEC-Win Plus programmed model Q2LE.NWP. All dimensions in inches. Driver and reflector lengths are for ½ of each side. Multiply by 2 for full side length and by 8 for circumference.

Design Frequency	14.14	18.118	21.19	24.94	28.40
Driver	105.30	82.27	70.39	59.84	52.58
Reflector	110.83	86.74	74.29	63.24	55.62
Separation	128.33	101.39	87.24	74.53	65.71

These quad designs model very adequately on either NEC-2 or NEC-4. In fact, I remodeled each quad using EZNEC Pro/4 to check on the results of NEC-Win Plus, which uses the NEC-2 core. The reported performance figures are insignificantly different. Although carrying out measurements in inches to 2 decimal places may seem to be beyond normal construction needs, the original model rests on spreadsheet calculations that carry them out to a dozen decimal places. Rounding to the nearest tenth of an inch is perfectly acceptable. Tenths may be easier to convert to the English system of eighths and sixteenths for use with a tape measure.

I selected this particular set of models as the monoband 2-element quads for our study since they provide the widest operating passband of any monoband 2-element quads in my experience. For example, the SWR bandwidth (using the design frequency resonant impedance as a standard) is well below 2:1, even on 10 meters (using the 28-29-MHz span as the antenna passband). However, the 180° front-to-back ratio shows a very high peak at the design frequency, but falls off rapidly.

On the narrow ham bands (17 and 12 meters), I used the band center as the design frequency. However, on the wider upper HF bands (20, 15, and 10 meters), I selected a frequency below the band center. The design frequency selection

criterion was a relatively equal 180° front-to-back ratio at both band edges. The 20-meter design frequency is 14.14 MHz. On 15, the frequency is 21.19 MHz. On 10 meters, 28.4 MHz serves as the design frequency.

Table 1-2. 2-Element Monoband Quad Beams: Modeled Performance (NEC-4)

20 Meters (Design Frequency 14.14 MHz)		Bandwidth: 2.47%		
Frequency MHz	14.0	14.14	14.175	14.35
Free-Space Gain dBi	7.41	7.04	6.94	6.49
180° Front-Back Ratio dB	16.08	38.68	33.40	16.29
Impedance (R +/- jX) Ω	99.9 - j26.1	130.4 - j0.8	137.3 + j3.8	163.7 + j20.9
17 Meters (Design Frequency 18.118 MHz)		Bandwidth: 0.55%		
Frequency MHz	18.068	18.118	18.168	
Free-Space Gain dBi	7.14	7.04	6.93	
180° Front-Back Ratio dB	27.74	44.00	31.11	
Impedance (R +/- jX) Ω	125.3 - j5.6	133.0 - j0.3	140.2 + j4.4	
15 Meters (Design Frequency 21.19 MHz)		Bandwidth: 2.12%		
Frequency MHz	21.0	21.19	21.225	21.45
Free-Space Gain dBi	7.37	7.04	6.98	6.60
180° Front-Back Ratio dB	18.12	46.50	36.21	18.04
Impedance (R +/- jX) Ω	108.3 - j19.5	134.1 + j0.1	138.3 + j2.9	160.7 + j17.0
12 Meters (Design Frequency 24.94 MHz)		Bandwidth: 0.40%		
Frequency MHz	24.89	24.94	24.99	
Free-Space Gain dBi	7.11	7.04	6.96	
180° Front-Back Ratio dB	31.86	53.22	33.39	
Impedance (R +/- jX) Ω	130.0 - j3.4	135.2 + j0.1	140.2 + j3.3	
10 Meters (Design Frequency 28.40 MHz)		Bandwidth: 3.51%		
Frequency MHz	28.0	28.40	28.50	29.0
Free-Space Gain dBi	7.52	7.04	6.91	6.36
180° Front-Back Ratio dB	14.53	59.19	28.26	14.23
Impedance (R +/- jX) Ω	96.7 - j31.6	136.1 + j0.4	144.4 + j5.7	173.3 + j25.8

Although we shall look more closely at the performance curves for each monoband quad, **Table 1-2** summarizes the performance characteristics across the band. It lists the band-edge and band-center values. Where the design frequency is not also the center of the band, the table includes those values as well.

The design-frequency free-space gain is uniformly 7.04 dBi. The 180° front-to-back value at the design frequency tends to climb with frequency, as does the resonant feedpoint impedance. (The reported values result from using calculated figures and do not result from any further modifications to make them "fit" the desired outcome.) The front-to-back ratio at the band edges is about the same for each of the wider bands. (The narrow bands are too narrow and the front-to-back values are too high to be concerned about differences less than 5-6 dB.)

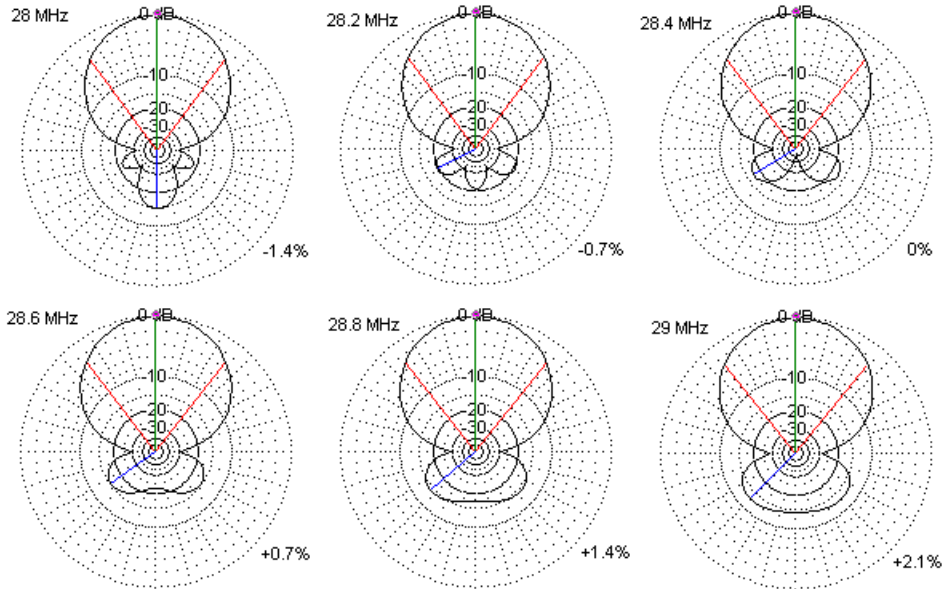
Each upper HF amateur band has a different bandwidth when measured as a percentage of the band-center frequency. The table lists those values as well. It is clear from these sample numbers that as the bandwidth increases, the band-edge front-to-back ratio becomes lower. Three-element Yagis on short booms (under  $0.25\lambda$ ) are capable of about 20 dB front-to-back ratios across the wider ham bands. A 2-element quad may match the 3-element Yagi in gain (with a reverse gain curve relative to frequency), but it simply cannot sustain the front-to-back ratio.

What the numbers in the table cannot show is how the rearward pattern changes with frequency. (The forward lobe remains well behaved throughout.) For that purpose, we need a useful gallery of E-plane patterns. **Fig. 1-3** supplies the need. More importantly, it shows the evolution of the rearward lobes as we move away from the design frequency.

I selected 10 meters for the gallery since that band gives us the widest operating passband of all the upper HF bands. The patterns show both the frequency and how much that frequency departs from the design frequency. Both 17 and 12 meters are so much smaller than the smallest increment of difference in the figure that we can expect their band-edge patterns to resemble the design frequency pattern with only a small loss on the directly rearward null. 20 meters is only about 70% as wide as 10, and 15 meters is only about 60% as wide as 10 meters. Hence, their band-edge patterns will be intermediate between the pair of patterns marking the farthest extremes on 10 meters.

Note: Percentages are the bandwidth departure from the design frequency (= 0%).

Fig. 1-3



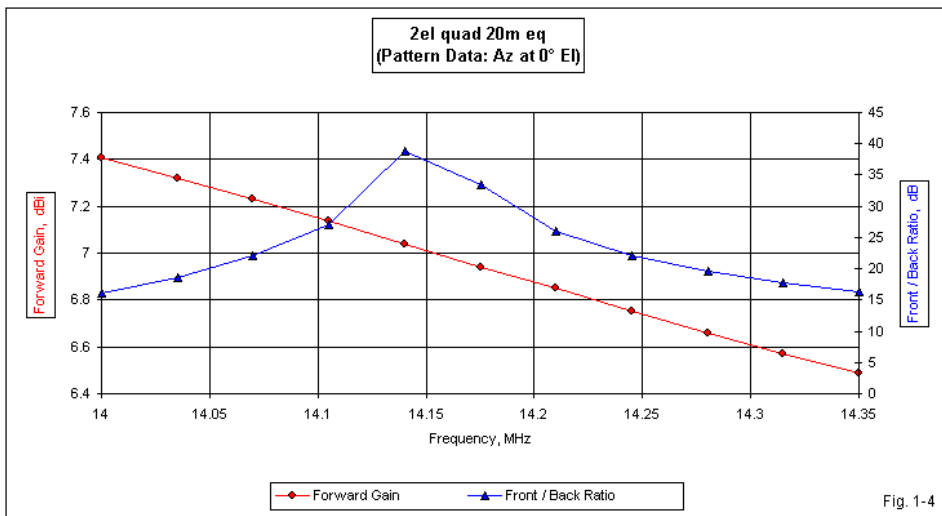
A Gallery of Free-Space E-Plane Patterns for a Monoband 2-Element Quad Beam

One may debate my use of the 180° front-to-back ratio as the desideratum for choosing a design frequency. Admittedly, it is partially a function of modeling convenience, since that figure automatically appears in the basic NEC plot data collection produced by most implementations of the core. However, we should note a significant difference in the overall energy radiated to the rear quadrants both below and above the design frequency. Below the design frequency, we find only a small total area of rearward energy (remembering that we are dealing with only 2 dimensions and ignoring the third). In comparison, above the design frequency, we find a much larger and growing area of total rearward radiation. This condition correlates well with the decreasing forward gain (but continues to ignore the fact that a free-space pattern is actually a 3-dimensional affair). Nevertheless, the band-

edge 180° front-to-back ratio values—and their equality at the band edges—will serve us well as markers of both similarity and of change when we develop dual-band quad beams.

We may collect further detail on the performance changes across each of the upper HF amateur bands by performing frequency sweeps. The graphs to follow emerged from AC6LA's EZPlots Excel function based on EZNEC sweep files. In each case, I subdivided the band into reasonable segments to provide the smoothest curves feasible.

### 20 Meters



The gain and front-to-back curves in **Fig. 1-4** show the performance on 20 meters. The gain curve is nearly, but not quite, linear in the gain reduction per unit of the passband. The rate of decline is about the same as the rate of climb for a short-boom 3-element Yagi using elements of the same diameter. (Since most Yagis would use fatter elements, practical Yagis of such design will show a

somewhat shallower gain-rise curve, ranging from about 6.9 to 7.4 dBi.) The front-to-back ratio peaks at the design frequency and drops to about 16 dB at the band edges.

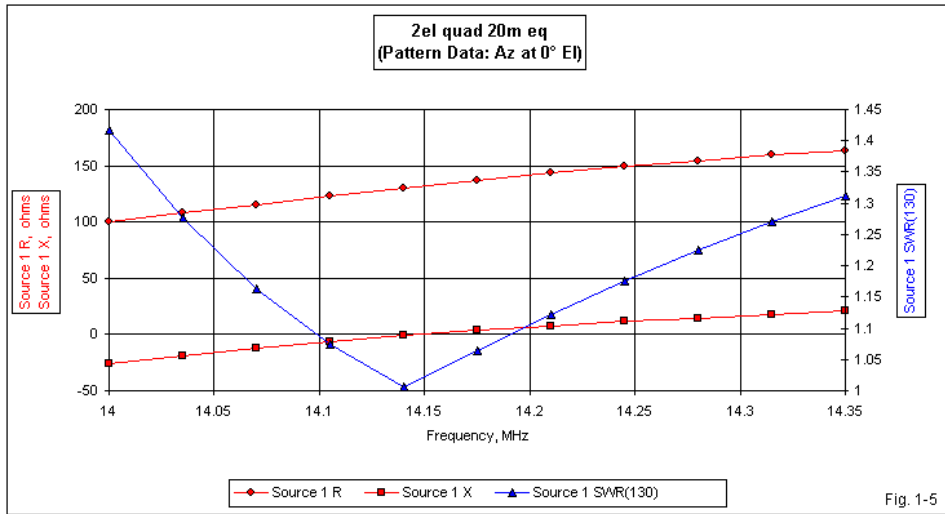


Fig. 1-5

The impedance curves in **Fig. 1-5** have a number of interesting features. The resistance and reactance curves almost parallel each other. Resistance rises about 64 Ω across the band, while the reactance changes by about 47 Ω. With AWG #14 wire on 20 meters, the resonant impedance is about 130 Ω. Using this reference value, we can note that the SWR climbs more rapidly below the design frequency than above it. These features will repeat themselves in subsequent charts, especially for the wider bands.

### 17 Meters

The 17-meter band is only a bit over 1/2% wide. Therefore, we expect flatter gain and front-to-back curves than on the wider 20-meter band. **Fig. 1-6** does not disappoint us. The gain drop is only about 0.2 dB across the band. Because the

graph spreads the smaller passband into 10 parts, the front-to-back curve appears flatter. However, it is every bit as steep as the 20-meter curve. The front-to-back value remains very high over the whole band, suggesting that the use of a 2-element quad may be well suited to the band.

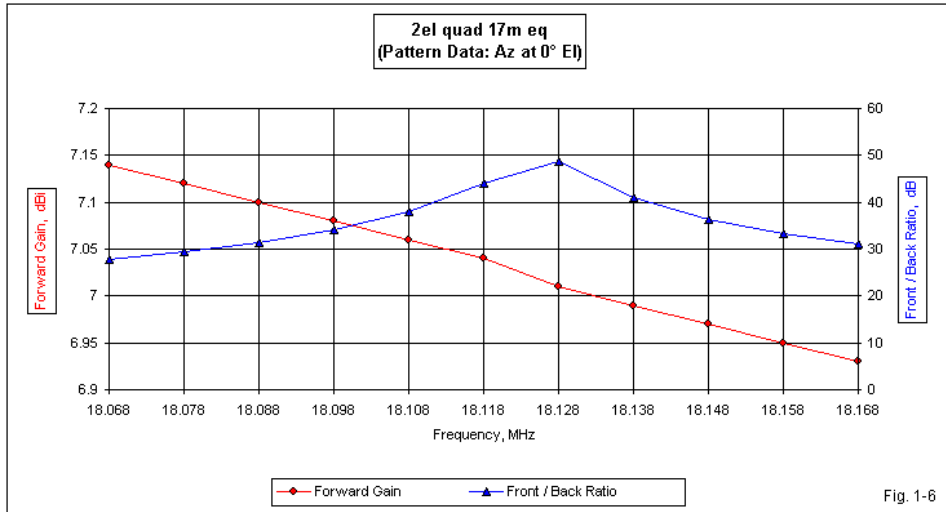


Fig. 1-6

**Fig. 1-7** confirms the impression left by **Table 1-2** that the resistance, reactance, and 133- $\Omega$  SWR are for all practical purposes flat across the band. Only automated graphing spreads the SWR values along the Y-axis. The spread is useful in showing that even over a narrow bandwidth, the SWR rises more rapidly below the design frequency than above it. In most cases, construction variables will result in greater SWR deviations than the changes shown in the graph.

In all cases, the gain figures shown in the graphs are free-space values. The pattern shapes correspond to azimuth patterns at the antenna's take-off or elevation angle of strongest radiation. Over ground, gain may increase by 5 to 5.5 dB, depending upon antenna height, due to ground reflections. In general, the effective height of a quad beam is a height about 2/3 of the way between the lower and

upper wires of any loop.

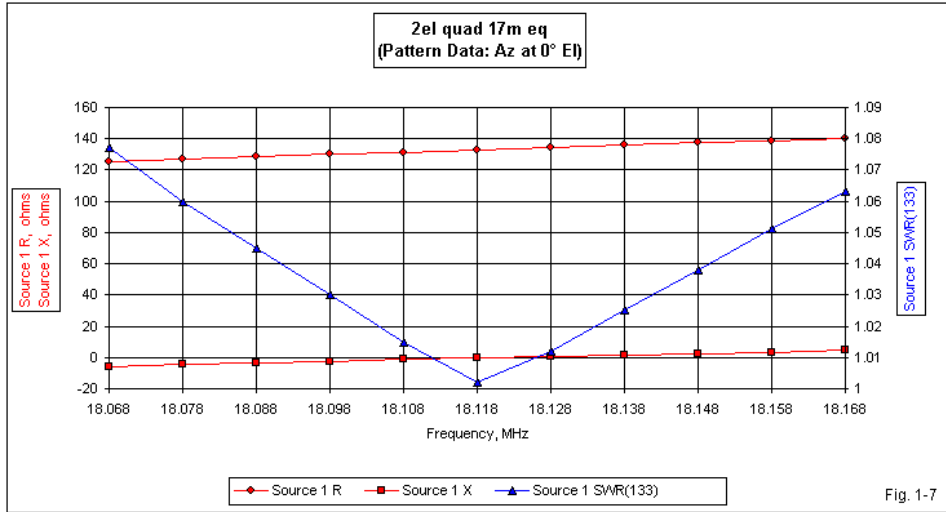
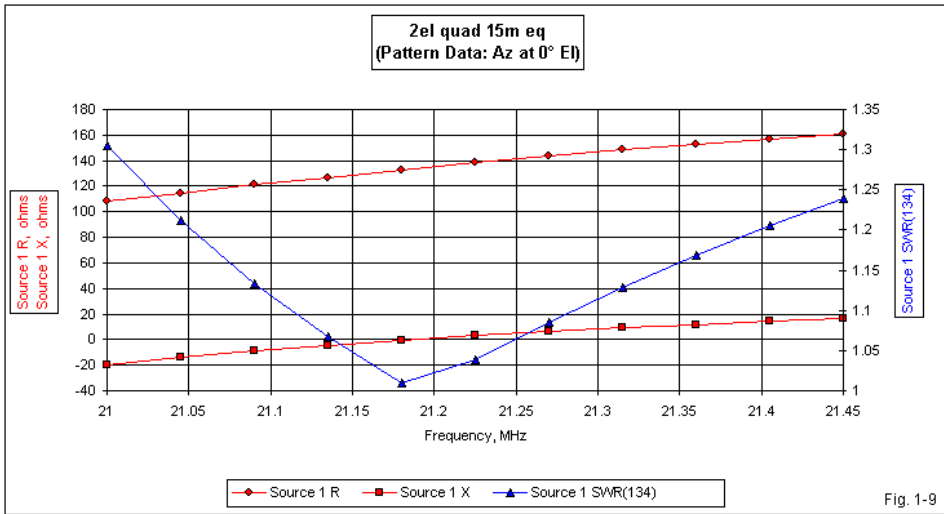
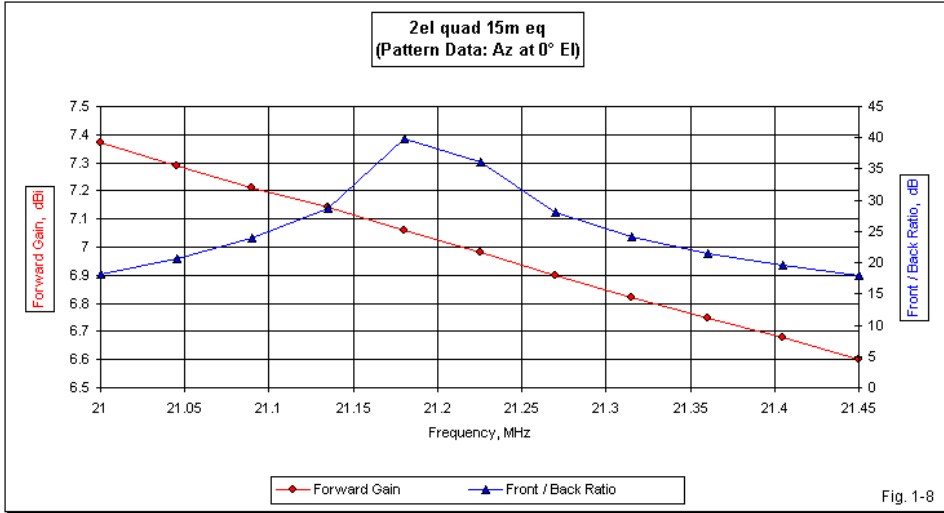


Fig. 1-7

### 15 Meters

15 meters returns us to a wider band, but not as wide as 20 meters when measured as a percentage of the band-center frequency. As shown in **Fig. 1-8**, the band is wide enough to replicate the 20-meter front-to-back pattern. Both bands show a more rapid decrease in the front-to-back value directly below the design frequency than directly above it. However, by the band edges, the ratio has dropped to about 18 dB on 15 (in contrast to about 16 dB on the slightly wider 20 meter band where the wire is also slightly thinner as a fraction of a wavelength).



As we might anticipate from the fact that 15 meters is slightly narrower than 20 meters, the range of resistance and reactance variation in **Fig. 1-9** is somewhat less than in **Fig. 1-5**. The resonant impedance is 134 Ω. The "spooning" of the SWR curve results from the graph's use of 21.18 MHz as a sampling point, when the actual design frequency is 21.19 MHz.

12 Meters

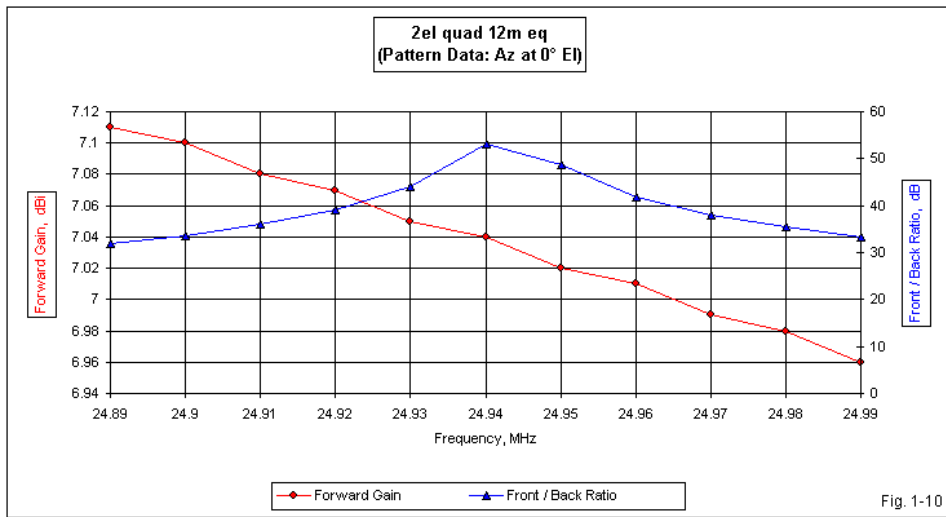


Fig. 1-10

12 meters is the narrowest of the upper-HF amateur bands, when we measure the passband as a percentage of the center frequency (24.94 MHz). Since the band is only 0.4% wide, graphs tend to have a stair-step quality due to the data, which is limited to 2 decimal places. Hence, the gain decrease across the band in **Fig. 1-10** appears somewhat uneven, since the total amount of change is only 0.15 dB. As well, the front-to-back ratio has room only to move slightly off of its peak value. However, if we had used a broader frequency scale, the front-to-back curve would closely resemble the corresponding curves for the wider bands.

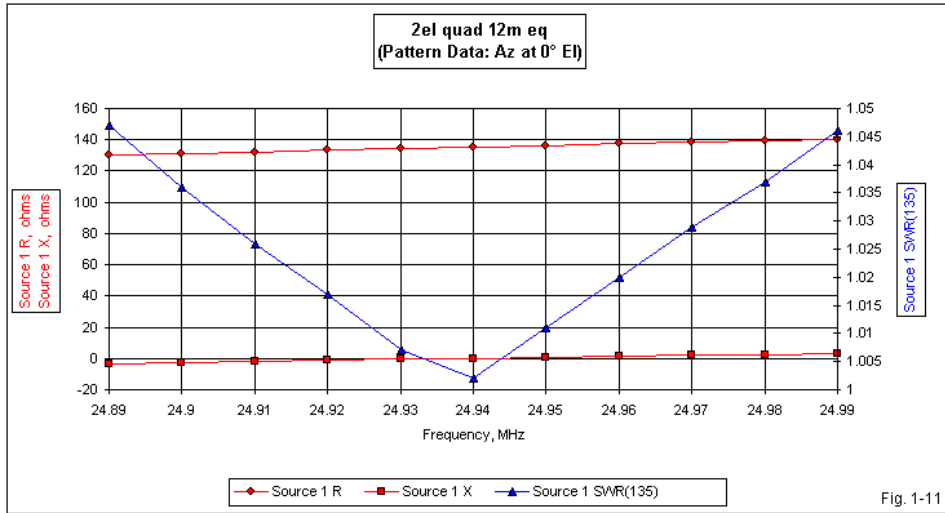
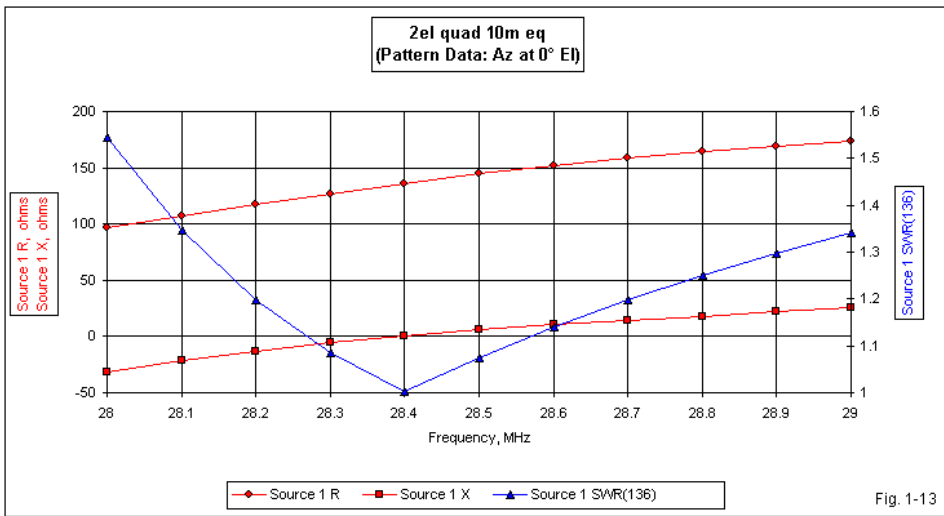
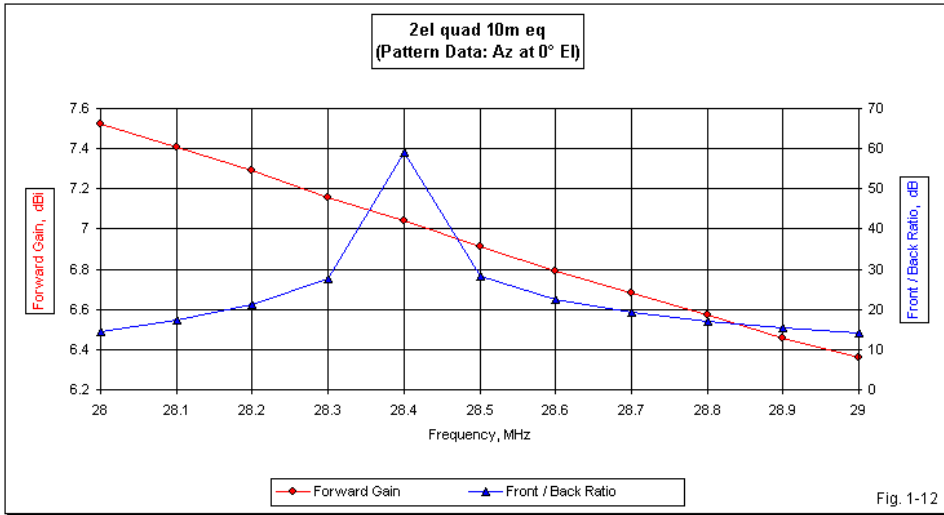


Fig. 1-11

The impedance curves in **Fig. 1-11** show barely any change in the resistance and reactance across the band. The resonant design-frequency resistance (135  $\Omega$ ) continues to rise as we move upward in frequency and the wire diameter grows when measured as a fraction of a wavelength. The SWR does not reach 1.05:1 within the band. Of course, construction variables suggest that a physical copy of this design might not show the perfection that we can obtain in the model.

### 10 Meters

With a bandwidth of about 3.5%, the first MHz of the amateur 10-meter band is the widest within our survey. Therefore, the gain shows the greatest range in **Fig. 1-12**. The 180° front-to-back ratio drops to a little over 14 dB at the band edges, even though its peak value is higher than on any other band. One usual marker of a high-performance array in amateur circles is a front-to-back ratio in excess of 20 dB. The 10-meter 2-element quad achieves this value for only about half the band (from 28.2 to 28.7 MHz). However, at the band edges, the front-to-back ratio is higher than we generally achieve with a 2-element driver-reflector Yagi.



I selected the design frequency to achieve approximately equal 180° front-to-back ratios at the band edges. As a consequence of this decision, the 136-Ω SWR curve—while perfectly acceptable—does not result in equal values at the band edges, as shown in **Fig. 1-13**. A 2-element quad is a bit less sensitive to driver length changes than a 2-element Yagi. Therefore, we might change the driver length to equalize the band edge SWR value while leaving the reflector length to control the front-to-back peak frequency. However, significant changes in the driver length will require corresponding changes in the reflector.

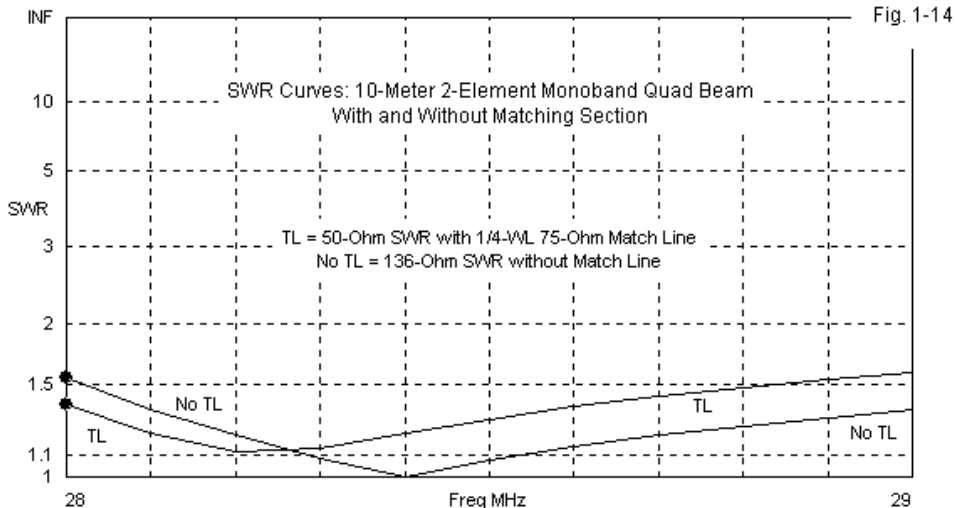
The survey has included a collection of equation-designed monoband quad beams for each of the upper HF amateur bands. I have provided extensive information of the modeled performance curves in order to form a detailed baseline against which we can measure multi-band quads to come. Nevertheless, before we leave the monobanders, we should address at least one or two practicalities. The first matter concerns construction. The models in this sequence presume that all support structures are non-conductive at the operating frequencies. The models also make square corners, although a very small curve at a physical corner to avoid wire crimping would create no operational problems. However, each corner attaches to a support arm. The method of fastening should involve only non-conductive hardware and other components. Metallic clamps, screws, and other fasteners—even if insulated from the element wire—can create 1-turn inductors that may detune the elements, especially since each such conductive fastener is multiplied by 4 for each element. The alternative to a wholly non-conductive fastening system is extensive field adjustment to restore the modeled conditions.

A second practicality involves feeding quads with feedpoint impedance levels that are considerably higher than standard coax feedline values. The most usual matching system is a simple  $1/4\text{-}\lambda$  line using an intermediate characteristic impedance between the feedpoint impedance and the main feedline value. **Table 1-3** provides a sample table of the electrical length of  $1/4\text{-}\lambda$  lines at each of the design frequencies. The physical length of the required line requires that we multiply the electrical length by the listed or (better) measured velocity factor of the actual line used. Coaxial cable velocity factors tend to range from about 0.66 to about 0.80, depending on the dielectric material separating the center conductor from the braid.

Table 1-3. Frequency-Wavelength Reference

Frequency is in MHz. Wavelength and 1/4-Wavelength are in inches. In models, 1/4-wavelength match lines use a length to the nearest inch, with exceptions on 10 meters. Values are electrical lengths. Multiply by the velocity factor of the line used to obtain physical lengths.

Frequency	Wavelength	1/4-Wavelength
14.14	834.71	208.68
18.118	651.44	162.86
21.19	557.00	139.25
24.94	473.25	118.31
28.40	415.59	103.90



Ideally, the matching section characteristic impedance should be the geometric mean between the two terminal impedance values. We arrive at that value by taking the square root of the product of the terminal impedances. For the range of feedpoint impedances in our models and a presumed 50-Ω main feedline, the ideal match line would have a characteristic impedance of about 80 to 82 Ω. 75-Ω line produces perfectly acceptable 50-Ω SWR curves. **Fig. 1-14** shows the basic 10-

meter SWR curve referenced to a 136- $\Omega$  standard and a 50- $\Omega$  SWR curve that results from using a  $1/4\text{-}\lambda$  75- $\Omega$  match line. The values at any frequency differ, but the overall curve falls well within the range of acceptable SWR values. Remember that the matching system does not alter the antenna performance. Given the linear nature of the  $1/4\text{-}\lambda$  match line, it also does not add to the total feedline length and hence does not add any significant amount to line losses. There are a few quad builders who use gamma matching for their drivers. The complexity of the physical structure and of its adjustment has led most quad builders to use the  $1/4\text{-}\lambda$  match-line system.

The 10-meter 2-element wide-band quad completes our survey of designs derived from the calculating program. We are restricting ourselves to HF quads in this inquiry, if only to have a manageable collection of designs. However, the program itself is calibrated from 3 to 300 MHz, and the models derived from both below and above those calibration limits provide very good results in NEC-4. I have derived models for the AM BC band and models for the 70-cm band with consistently good output reports.

Remember that any given wire size becomes thinner in electrical terms as we lower the frequency and electrically fatter as we raise the frequency. The program calibration has wire-size limits that are a function of the element diameter as a fraction of a wavelength. These limits may be more important to arriving at usable quad dimensions than the selected design frequency.

### **Conclusion to Part 1**

We have changed the fundamental question that we pose to common-feedpoint multi-band quads. Instead of asking, "Which kind of feed system is better?" we asked instead, "What happens when we use a common feedpoint for a multi-band quad?" That simple change in question creates a large change in our approach to answers. Instead of directly modeling a common-feedpoint multi-band quad—and drawing all manner of conclusions that might raise more questions than they answer—we have spent the entirety of this chapter laying a foundation for further steps in the exploration.

The monoband quads that we have examined—and to which we shall return continually—represent precisely designed 2-element quad beams having the widest operating bandwidth in all operating categories consistent with having a free-space design-frequency gain of at least 7 dBi. Each quad places the peak 180° front-to-back value and feedpoint resonance on the design frequency. For ease of future references, the design frequencies result in relatively equal front-to-back values at the upper and lower edges of the wider amateur bands.

As a practical matter, we may use any of the programs or models that encapsulate the equations derived from hand optimizing an entire system of quads in order to select a different design frequency. One reason for doing so might be to ensure having at least 20 dB of front-to-back ratio across a favored segment of one or another amateur band. The 2-element quad lends itself well to such operational choices. Indeed, if one only wishes to operate on a subsection of a wide amateur band, then one might even prefer other designs that sacrifice operating bandwidth for slightly more gain.

However, my goal is not to make such selections. Instead, I wish to establish a baseline that we can reliably use in assessing what happens when we attempt to construct multi-band quads. One criticism often leveled against multi-band quads—often based on experience with multi-band Yagis—is that the interaction between elements tends to narrow the operating bandwidth of the antenna on at least one of the bands involved. By starting with a wideband design, we may actually be able to evaluate that claim. As well, we may be able to determine whether the reduction—if actual—results from the basic multi-band process or from trying to use a common feedpoint. We may also note that the criticism that we have recorded is very non-specific in terms of naming which performance parameters might be subject to a narrowing bandwidth in a multi-band quad.

In one sense, then, we have not yet gotten anywhere in our quest to understand the effects of multi-banding quads and feeding the resulting beam. From a different perspective, we have laid a reasonable foundation for actually going some distance to answer our question. If our extended survey of monoband quad performance is the foundation, then the first floor of the multi-band quad edifice involves creating some quads using separate feedlines for each band. In that way, we may proceed

with no shape distortion to any element. That will be our task in the next chapter.

*Note*

The spreadsheet mentioned earlier in this chapter for the design of the monoband quads shown is part of a suite of antenna design calculation programs. The designs cover 1-, 2-, 3-, and 4-element quads (with alternative wide-band and higher-gain versions of 3-element arrays), along with three types of 3-element Yagis (designated high-gain, high-front-to-back, and wide-band versions) and the Moxon-rectangle program. All of the spreadsheet pages presume the use of a uniform element diameter, which limits the use of the Yagi and Moxon programs at HF to wire versions. Stepped-diameter elements require re-design and result in longer elements than uniform-diameter versions. All of the calculations rest on extensive antenna modeling to optimize performance with many wire diameters to yield reliable results from algorithms taken from regression techniques. To obtain the spreadsheet in either Excel or Quattro-Pro format, see <http://www.cebik.com/trans/ant-design.html>

## Chapter 2

### ***Sneaking Up on 2-Element Common-Feed Quads***

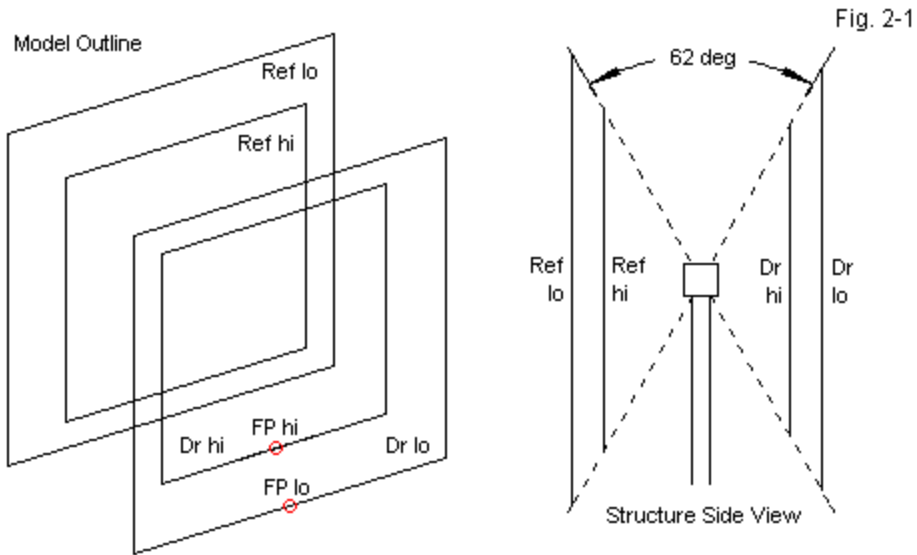
#### **Part 2: Dual Band Quad Beams With Separate Feedpoints**

In Part 1 of this series, we defined our basic question about common-feedpoint multi-band quads this way:

*What happens when we create a multi-band quad and provide it with a common driver feedpoint for all bands?*

We also set some limits to the exploration so that we might reduce the task to manageable proportions. We set a 2-band limit for the multi-band quads, although we shall examine one violation of the limit in this part. We also set a minimum frequency ratio of 1.3:1 between the bands included in the dual-band quads. (However, looking at adjacent upper HF ham-band combination might itself make a good study for the future.) We also noted the need to proceed in stages, looking at dual-band quads of 2 elements each using separate feedpoints for each band before we move on to joining the feedpoints. Our goal is to isolate insofar as possible whatever phenomena (physical or electrical) may be functions of using a common feedpoint and which may result simply from placing 2-element quad beams concentrically on a single support system.

A multi-band quad beam is a combination of monoband quad beams taken through successive modifications until arriving at the final form. To simplify the progression, I adopted spider construction for the beams, as shown in **Fig. 2-1**. In this part of our study, we shall use models like the one on the left to determine what modifications result from the proximity of the two antennas. The sketch of a side view of the resulting dual-band beam shows the spider arms and the nearly constant angle created by the driver and reflector elements for each band. Of course, for modeling runs and for operation, only one of the feedpoints would be active at any one time. The use of separate feedpoints and separate driver loops also helps assure that the models will automatically meet Average Gain Test (AGT) standards, so long as we segment each side so that the segment junctions for loops on different bands align reasonably well. A low-band to high-band segment/side ratio of 1.3 to 1.5 to 1 will generally satisfy this requirement by yielding AGT values from 0.998 to 1.002.



General Outlines of 2-Element, 2-Band Quad Beams with Separate Feeds

Table 2-1. 2-Element Monoband Quad Beams

All dimensions derived from NEC-Win Plus programmed model Q2LE.NWP. All dimensions in inches. Driver and reflector lengths are for  $\frac{1}{2}$  of each side. Multiply by 2 for full side length and by 8 for circumference.

Design Frequency	14.14	18.118	21.19	24.94	28.40
Driver	105.30	82.27	70.39	59.84	52.58
Reflector	110.83	86.74	74.29	63.24	55.62
Separation	128.33	101.39	87.24	74.53	65.71

To ease the design process, I selected monoband 2-element quads that have the broadest operating characteristics that I could devise. **Table 2-1** summarizes the dimensions of each beam in the upper HF series at the listed design frequencies. The side dimensions actually list half-sides for modeling convenience. A loop circumference is 8 times the listed length. Keep in mind that any revision to a loop dimension that may appear in subsequent tables will result

in a revised circumference that differs by 8 times the listed factor from the monoband loop. The element separation is a full measure.

Part 1 was devoted to examining these antennas, band by band, in sufficient detail to form a sort of data base that we might use as a reference in tracking the changes that occur (if any) when we form dual-band quads. For ready reference, **Table 2-2** summarizes the performance data for the monoband beams.

Table 2-2. 2-Element Monoband Quad Beams: Modeled Performance (NEC-4)

20 Meters (Design Frequency 14.14 MHz)		Bandwidth: 2.47%		
Frequency MHz	14.0	14.14	14.175	14.35
Free-Space Gain dBi	7.41	7.04	6.94	6.49
180° Front-Back Ratio dB	16.08	38.68	33.40	16.29
Impedance (R +/- jX) Ω	99.9 - j26.1	130.4 - j0.8	137.3 + j3.8	163.7 + j20.9
17 Meters (Design Frequency 18.118 MHz)		Bandwidth: 0.55%		
Frequency MHz	18.068	18.118	18.168	
Free-Space Gain dBi	7.14	7.04	6.93	
180° Front-Back Ratio dB	27.74	44.00	31.11	
Impedance (R +/- jX) Ω	125.3 - j5.6	133.0 - j0.3	140.2 + j4.4	
15 Meters (Design Frequency 21.19 MHz)		Bandwidth: 2.12%		
Frequency MHz	21.0	21.19	21.225	21.45
Free-Space Gain dBi	7.37	7.04	6.98	6.60
180° Front-Back Ratio dB	18.12	46.50	36.21	18.04
Impedance (R +/- jX) Ω	108.3 - j19.5	134.1 + j0.1	138.3 + j2.9	160.7 + j17.0
12 Meters (Design Frequency 24.94 MHz)		Bandwidth: 0.40%		
Frequency MHz	24.89	24.94	24.99	
Free-Space Gain dBi	7.11	7.04	6.96	
180° Front-Back Ratio dB	31.86	53.22	33.39	
Impedance (R +/- jX) Ω	130.0 - j3.4	135.2 + j0.1	140.2 + j3.3	
10 Meters (Design Frequency 28.40 MHz)		Bandwidth: 3.51%		
Frequency MHz	28.0	28.40	28.50	29.0
Free-Space Gain dBi	7.52	7.04	6.91	6.36
180° Front-Back Ratio dB	14.53	59.19	28.26	14.23
Impedance (R +/- jX) Ω	96.7 - j31.6	136.1 + j0.4	144.4 + j5.7	173.3 + j25.8

When we combine 2 (or more) quad beams concentrically to form a multi-band

array, the elements will interact. Even with a frequency separation of at least 1.3:1 and totally separate loops for each band, we find that the active band elements will induce low-level but significant currents in some of the other loops. **Fig. 2-2** shows the current levels for one of the dual-band beams when operated at each of the 2 design frequencies and after undergoing the required modifications. We should attend mostly to the horizontal wires and their current magnitude curves.

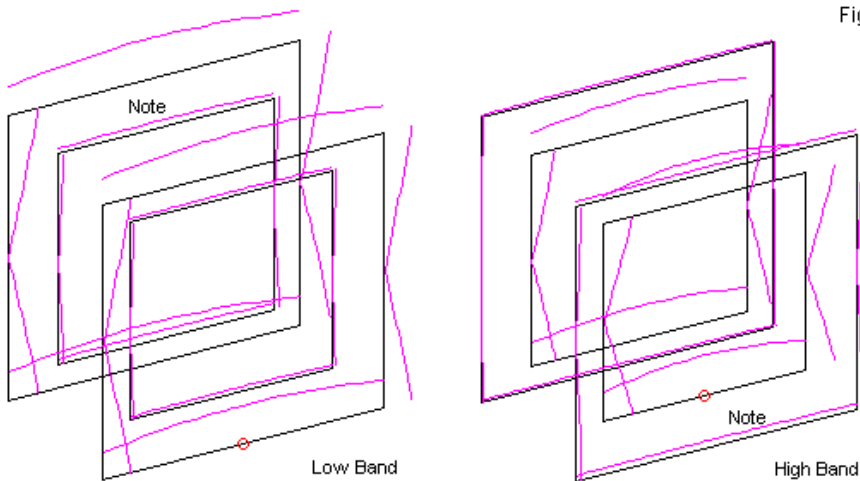


Fig. 2-2

Element Interaction as Indicated by Relative Current Magnitude on Quad Loops

When operated on the lower band, in the left graphic, the larger loops show high current magnitude at the centers of the horizontal wires. However, note that the smaller loops are not inert. The smaller driver shows a relatively low peak current magnitude, but the peak value on the smaller reflector is appreciable. The element is active enough to become part of the overall radiating structure. The other elements require modification to compensate—if possible—for this activity if we are to restore to the degree possible the performance we obtained from the larger 2-element quad in its monoband form.

On the right, the smaller loops for the higher band are active, as indicated by the high current magnitude peaks at the centers of the horizontal wires. In this case, the larger driver loop shows a noticeable level of activity, enough to again require modification of the smaller loops to restore so far as possible monoband performance.

Two consequences follow from the interaction of the elements, even when we use separate feedpoints. One result gives us the design strategy for creating multi-band quads. Each modification to any loop will result in slight changes in the current level on other elements, even for the inert bands. Hence, a small change to a higher-band loop may require a change in previously set lower-band loops—and vice versa. The second result involves intra-band adjustments. Very tiny changes or tweaks to either the driver or the reflector of a monoband quad beam may not require an additional adjustment to the other element. However, larger changes in loop size for either the driver or the reflector will normally require changes in the other element to realign the operating properties across a given band. In most (but not quite all) cases of adjustments that we make in the dual-band quads, we shall have to adjust both the driver and the reflector, since a change in one will itself displace the performance curve.

The final design strategy usually becomes a random set of moves that we might characterize as "a little of this and a little of that," in each case seeing whether the change moves us in the correct direction. In the present situation, we are using a complex set of operating parameters to define the correct direction. We wish to place the peak 180° front-to-back ratio on the design frequency and see roughly equal front-to-back values at the band edges. The monoband quad gain curves give us a good idea of what gain values we should see across the band. As well, we wish to set the design-frequency feedpoint impedance close to resonance.

A portion of our work will be to see what patterns emerge in the required modifications occasioned by creating a dual-band quad with separate feedpoints. If the patterns are consistent in all of the models, then we might ease the design work of future quad builders. Knowing in what directions to modify the quad loops can save a great deal of time and prevent us from messing up the performance

values to a degree that forces us to restart the design from scratch.

### **A 17-12-Meter 2-Element Quad Array Using Separate Feedpoints**

Our first example of a dual-band quad beam with separate driver loops is for the narrow 17- and 12-meter band. On this band, we may use the band center frequencies for design (18.118 and 24.94 MHz). The frequency ratio is 1.38:1. Moreover, properties do not shift within the band limits by an amount that will give us any challenges for band-edge performance. If we can peak the performance on each band somewhere within the band, the result will generally be satisfactory across the band.

**Table 2-3** shows the dimensions of the final version of the 17-12-meter combination. If you compare the numbers with the monoband values in **Table 2-1**, the changes seem slight. However, multiply the changes by 8 to see the effects on the circumference of each loop in the beam. In all of our beams, we are holding the spacing constant to reduce the number of variables that we must manipulate.

Table 2-3. 2-Element 2-Band Quad Beams with Separate Driver Elements

All dimensions in inches. Driver and reflector lengths are for ½ of each side. Multiply by 2 for full side length and by 8 for circumference. Band combinations based on a minimum frequency ratio of 1.3:1.

17-12 Meters		
Design Frequency	18.118	24.94
Driver	82.60	59.40
Reflector	85.90	63.24
Separation	101.40	74.54

The 17-meter driver increases its circumference by nearly 1.5", while the reflector for that band decreases by close to 3-3/8". In contrast, the 12-meter driver requires a circumference reduction of about 1-3/4", but the 12-meter reflector requires no change at all. In the presence of high-band elements, the low-band reflector swells, while the low-band driver shrinks. High-band elements either shrink (driver) or remain unchanged (reflector) in the presence of low-band elements. Let's remember these patterns when we look at other frequency

combinations for subsequent dual-band quads.

**Table 2-4** presents the performance data for our new dual-band 17-12 quad beam. Since both bands are narrow, we may dispense with graphed frequency sweeps, since the curves will be nearly straight lines throughout. Compare the performance values with those for the monoband versions in **Table 2-2**.

Table 2-4. 2-Element 2-Band Quad Beams with Separate Driver Elements  
Each driver uses a  $\frac{1}{4}\lambda$  matchline of 75- $\Omega$  cable. See notes for exceptions.

#### 17-12 Meters

17 Meters (Design Frequency 18.118 MHz)		Bandwidth: 0.55%	
Frequency MHz	18.068	18.118	18.168
Free-Space Gain dBi	7.18	7.04	6.89
180° Front-Back Ratio dB	27.07	36.00	25.21
Impedance (R +/- jX) $\Omega$			
Pre-Match Line	115.4 - j3.9	123.7 - j1.1	130.9 + j0.8
Post-Match Line	48.5 + j1.4	45.3 + j0.4	42.8 - j0.1
50-Ohm SWR	1.04	1.10	1.17
12 Meters (Design Frequency 24.94 MHz)		Bandwidth: 0.40%	
Frequency MHz	24.89	24.94	24.99
Free-Space Gain dBi	7.22	7.16	7.10
180° Front-Back Ratio dB	28.33	34.32	38.55
Impedance (R +/- jX) $\Omega$			
Pre-Match Line	98.8 - j3.7	103.0 + j2.2	107.1 + j7.8
Post-Match Line	56.0 + j2.1	53.9 - j1.0	51.6 - j3.4
50-Ohm SWR	1.13	1.08	1.08

Perhaps the first notable performance feature is the seeming rise in the average gain on 12 meters. However, also note the 12-meter front-to-back values. The peak front-to-back value has moved upward in the band and is no longer exactly centered. The shift in the front-to-back curve also indicates a shift in the 12-meter gain curve. Since the gain rises as we decrease frequency, the higher

gain levels indicate that the gain and front-to-back curves have moved together in the presence of the 17-meter elements. Comparing the 17-meter gain values in the dual-band quad with those of the monoband version, we find much less slippage. However, the front-to-back back value at the high end of the narrow band is quite a bit lower than in the monoband quad.

Perhaps the most noticeable difference between the monoband and dual-band versions of the quads involves the feedpoint impedance. The band-center impedance of the 17-meter quad drops about  $10\ \Omega$  relative to the monoband value, but the range of resistance across the band remains at  $15\ \Omega$ . On 12 meters, we find the greatest impedance decrease: about  $30\ \Omega$  resistive or a drop of about 24%. The range of variation in resistance across the band drops by a like amount.

The chief consequence of the changes in feedpoint impedance lies in the ability of  $1/4\text{-}\lambda$   $75\text{-}\Omega$  match-lines to effect a close match to a  $50\text{-}\Omega$  main feedline. On 17 and even on 12 meters, the mismatch is not significant. However, if the patterns set by this combination of beams hold for the other combinations that cover wider bands, we may see high  $50\text{-}\Omega$  SWR values at the band edges on 20, 15, or 10 meters.

The 17-12-meter dual-band quad forms a good beginning exercise in combining quads. The narrow bandwidth of the two bands allows us to see patterns of physical and performance alteration without introducing the variables that a wider bandwidth might force upon us. Clearly, we cannot simply slap together monoband beams for 17 and 12 and expect peak performance. However, the physical changes to re-center performance are relatively small. As well, although the performance passband shifts slightly on at least one band, we may easily obtain a full-performance dual-band quad. Matching the lower feedpoint impedances appears to present no significant obstacles.

### **A 15-10-Meter 2-Element Quad Array Using Separate Feedpoints**

Our second sample dual-band quad involves wider bands: 15 and 10 meters. As well, the monoband beams for these two bands did not use the band centers as

the design frequencies, but slightly lower frequencies: 21.19 and 28.4 MHz. As the dimensions in **Table 2-5** show (when compared to the monoband dimensions in **Table 2-1**), we obtain the same patterns of element length adjustment in the 15-10 quad as in the 17-12 quad. The circumference of the 15-meter driver increases by a little over 1", while the 15-meter reflector shrinks by nearly 4 inches. The 10-meter driver decreases its circumference by nearly 2", but the reflector remains unchanged. I shall resist any temptation to create a set of equations for these changes, since we have two moderating changes from the 17-12 quad. First, the wire diameter as a fraction of a wavelength changes from one band to the next, since all models use AWG #14 copper wire. Second, the frequency ratio changes from one dual-band quad to the next. The 15-10-meter combination uses a design-frequency ratio of about 1.34:1.

Table 2-5. 2-Element 2-Band Quad Beams with Separate Driver Elements

All dimensions in inches. Driver and reflector lengths are for ½ of each side. Multiply by 2 for full side length and by 8 for circumference. Band combinations based on a minimum frequency ratio of 1.3:1.

15-10 Meters		
Design Frequency	21.19	28.40
Driver	70.65	52.10
Reflector	73.30	55.62
Separation	87.24	65.70

Relative to the monoband performance values in **Table 2-2**, the dual-band performance numbers in **Table 2-6** reveal some patterns that would only be possible to see with the wider-band quads for bands like 15 and 10 meters. Since 15 and 10 meters have different bandwidths, we must be careful of cross-band transfer of changes. However, relative to the band-edge numbers in the monoband tables, the 15-meter performance in the dual-band design shows a much steeper gain decrease and generally lower band-edge front-to-back values. In contrast, again relative to monoband values, the 10-meter section of the dual-band quad shows a shallower gain curve and higher band-edge front-to-back values. The near-resonant (pre-match) impedance values for the two bands are comparable to those obtained with the 17-12 dual quad.

Table 2-6. 2-Element 2-Band Quad Beams with Separate Driver Elements  
Each driver uses a  $\frac{1}{4}\lambda$  matchline of 75- $\Omega$  cable. See notes for exceptions.

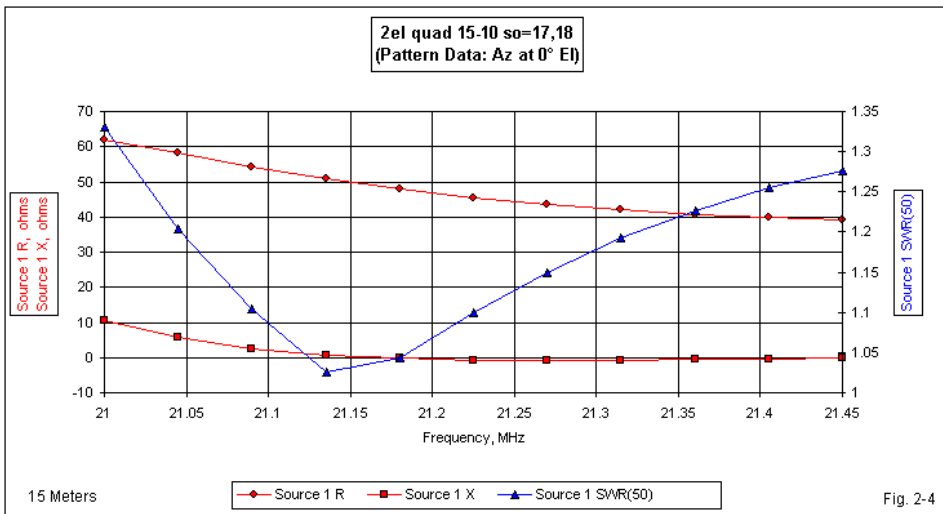
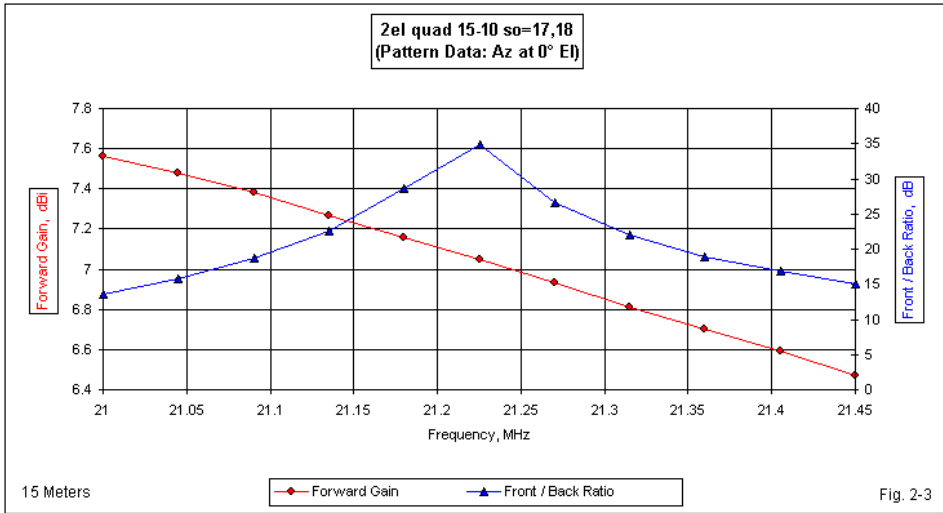
#### 15-10 Meters

15 Meters (Design Frequency 21.19 MHz)		Bandwidth: 2.12%		
Frequency MHz	21.0	21.19	21.225	21.45
Free-Space Gain dBi	7.56	7.14	7.05	6.47
180° Front-Back Ratio dB	13.64	30.69	34.87	15.13
Impedance (R +/- jX) $\Omega$				
Pre-Match Line	87.4 - j15.7	118.3 + j0.3	123.1 + j1.5	142.6 + j3.8
Post-Match Line	61.9 + j10.6	47.4 - j0.3	45.5 - j0.7	39.2 - j0.2
50-Ohm SWR	1.33	1.06	1.10	1.28
10 Meters (Design Frequency 28.40 MHz)		Bandwidth: 3.51%		
Frequency MHz	28.0	28.40	28.50	29.0
Free-Space Gain dBi	7.55	7.17	7.07	6.62
180° Front-Back Ratio dB	14.74	33.98	34.43	16.48
Impedance (R +/- jX) $\Omega$				
Pre-Match Line	73.4 - j46.2	100.7 - j0.8	107.5 + j8.9	138.3 + j50.4
Post-Match Line	53.5 + j33.0	55.1 + j0.8	51.3 - j3.6	35.4 - j10.5
50-Ohm SWR	1.88*	1.10	1.08	1.53

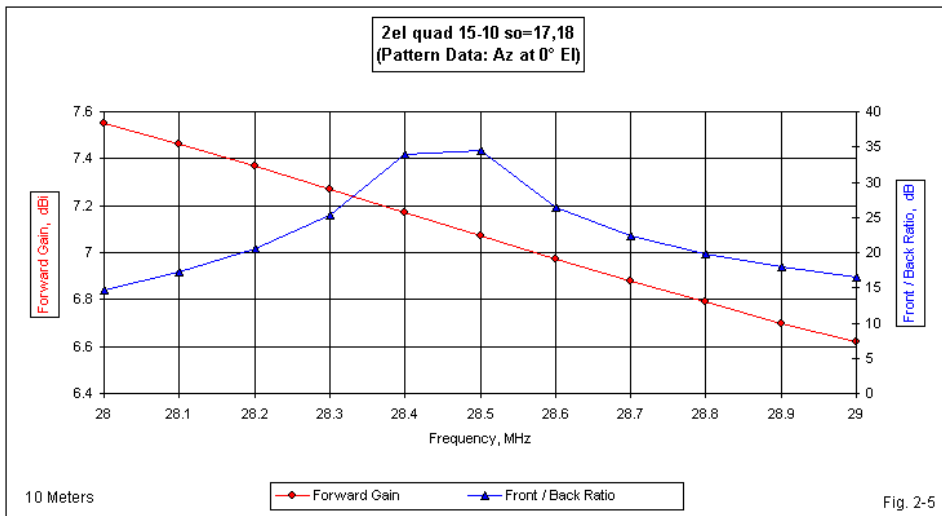
\*Shortening the matchline from 104" to about 100" will equalize band-edge 50- $\Omega$  SWR values.

As a crosscheck on the reality of some of these values, **Fig. 2-3** provides sweep data on the 15-meter gain and 180° front-to-back values. Note that the peak front-to-back ratio is close to the band center, higher in frequency than the design frequency. The higher gain value at the low end of 15 meters confirms that the overall performance pattern has slipped upwards in frequency, just as we saw in a much smaller way with the 17-meter quad.

**Fig. 2-4** graphs the resistance, reactance, and 50- $\Omega$  SWR values for the 15-meter section of the dual-band quad. These values presume a  $\frac{1}{4}\lambda$  75- $\Omega$  matchline between the feedpoint and the 50- $\Omega$  main feedline. If we examine the pre-match impedance values for 15 meters with the monoband values, we find that the total change in resistance across the band is slightly higher in the dual-band quad, but the total change in dual-band 15-meter reactance is considerably smaller. As a result, the  $\frac{1}{4}\lambda$  matching section has little difficulty in effecting a wholly acceptable impedance situation relative to the 50- $\Omega$  main feedline.

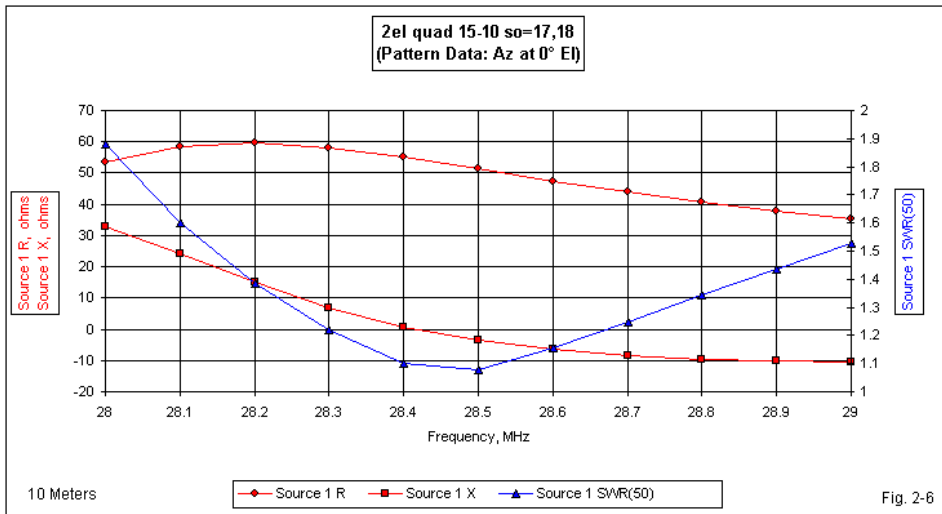


The 10-meter loops form the inner elements of this dual-band quad, and 10 is the widest of the bands in the upper HF amateur region. The inner position of these loops appears to show some advantage in both gain and front-to-back ratio, as suggested by both the tabular values and the sweep graph in **Fig. 2-5**. The performance curves have slipped upward in the band relative to monoband values, similarly to the 12-meter values. However, relative to 10-meter monoband values, the gain curve decreases at a slower rate when the loops are part of the 15-10 quad. As well, the average of the band-edge front-to-back ratios is slightly higher than in the monoband version. (When we turn to a 20-15-meter dual-band quad, we shall be very interested in whether the values for 15 meters show any significant difference from the values that we reviewed earlier, once we give the loops for that band an inner position.)



The match-line values of resistance and reactance on 10 meters do not show the nearly straight lines that we obtained on 15 meters. One factor in the curves shown in **Fig. 2-6** is the width of the band—over 1.5 times wider than 15 meters. A second and possibly more significant factor is the fact that the inner position of the

10-meter elements results in a significant departure in pre-matched values relative to the monoband version of the antenna. The total range of pre-match resistance is slightly lower than in the monoband quad, but the dual-band pre-match reactance shows a spread that is more than 1.6 times the range that we found in the monoband 10-meter quad. As a consequence, a simple  $1/4\text{-}\lambda$   $75\text{-}\Omega$  line achieves an acceptable  $50\text{-}\Omega$  SWR at  $28.0\text{ MHz}$  with very little to spare.



Amateur antenna builders appear to have great difficulty in thinking about match-lines in increments other than  $1/4\lambda$ . Transmission lines effect a continuous impedance transformation along their length (except when perfectly matched to the antenna feedpoint load). Although the transformation calculations are more complex than for resistive loads, there are numerous aids to permit us to find the impedance transformation for virtually any line length. In many cases, we may obtain a flatter SWR curve across a given bandwidth by selecting a line length other than  $1/4\lambda$ . As noted in **Table 2-6**, a  $75\text{-}\Omega$  line with an electrical length of about  $100\text{''}$  will achieve a 10-meter SWR curve with more equal band-edge values than a  $104\text{''}$  ( $1/4\text{-wavelength}$ ) line. (Remember that all line lengths listed in inches

are electrical lengths. Multiply these values by the velocity factor of the line used to obtain the required physical lengths of the match line.)

### **A 20-15-Meter 2-Element Quad Array Using Separate Feedpoints**

The 20-15-meter dual quad is similar to the 15-10 quad in that both cover wider amateur bands. However, the frequency ratio is higher (1.5:1), while both bands are narrower than the 10-meter band. Nevertheless, most of the patterns developed as potentials in connection with the first two dual-band quads receive confirmation in the new model. As shown by a comparison of the dimensions in **Table 2-7** with those in **Table 2-1**, the outer 20-meter reflector increases its circumference by about 1-1/4", while the outer 20-meter driver circumference shrinks by nearly 3-3/4". The inner 15-meter reflector remains unchanged, but the inner 15-meter driver circumference decreases by about 2-1/8". Although wire size as measured in terms of a wavelength and the frequency ratio may play a role in the precise amount of modification required for any element in the dual quad, the positions of the elements determine the general patterns of increasing and decreasing loop size.

Table 2-7. 2-Element 2-Band Quad Beams with Separate Driver Elements

All dimensions in inches. Driver and reflector lengths are for 1/2 of each side. Multiply by 2 for full side length and by 8 for circumference. Band combinations based on a minimum frequency ratio of 1.3:1.

20-15 Meters		
Design Frequency	14.14	21.19
Driver	105.60	69.85
Reflector	109.90	74.29
Separation	128.34	87.24

The performance values in **Table 2-8**, when compared to the monoband values in **Table 2-2**, again show the same patterns as in the 15-10-meter quad. On 20 meters, the dual-band gain curve shows a steeper decline than does the monoband curve. The 20-meter band-edge 180° front-to-back values are lower relative to monoband values. However, the inner 15-meter quad shows the opposite trends. Its gain curve is shallower than is the monoband curve, while the dual-band band-edge front-to-back ratios are equal to or higher than the

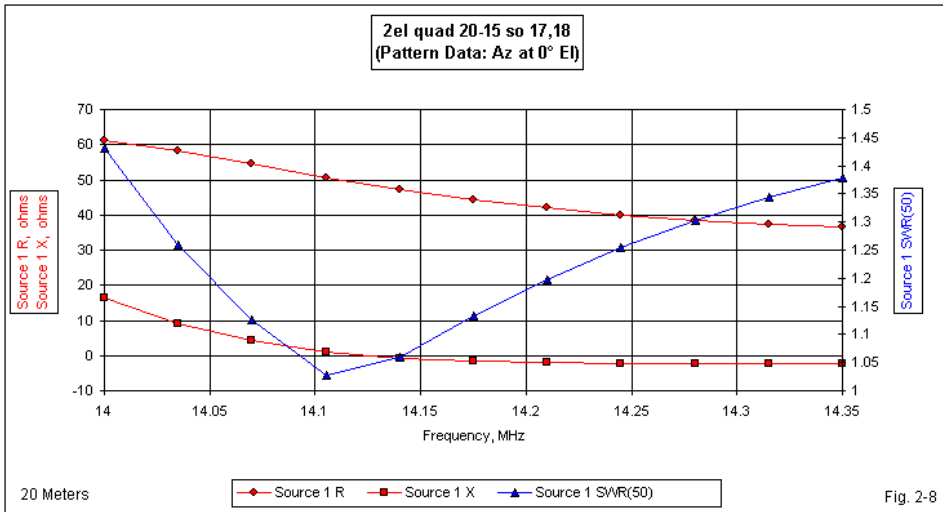
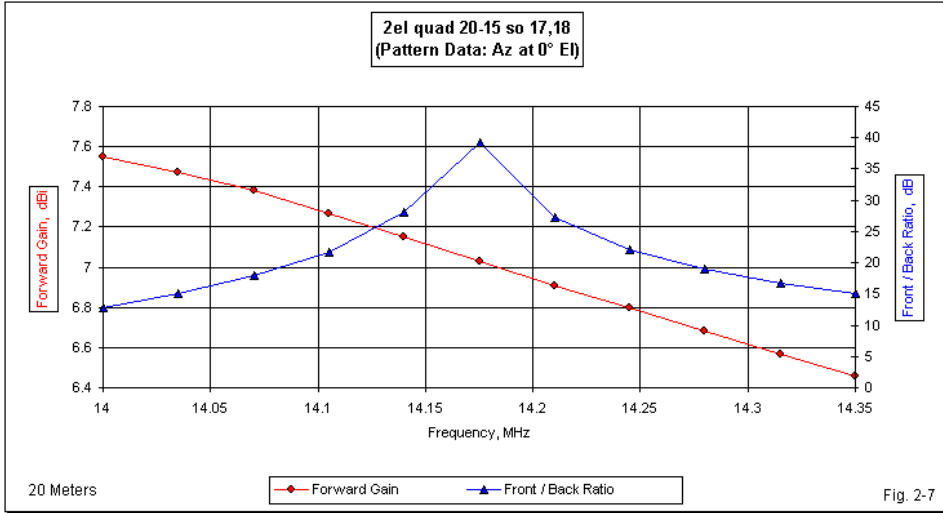
monoband values. For both bands in the dual-band quad, the pre-match feedpoint impedance values track well with the values for the other dual-band quads in terms of the reductions relative to monoband versions of the antennas.

Table 2-8. 2-Element 2-Band Quad Beams with Separate Driver Elements  
Each driver uses a  $\frac{1}{4}\lambda$  matchline of 75- $\Omega$  cable. See notes for exceptions.

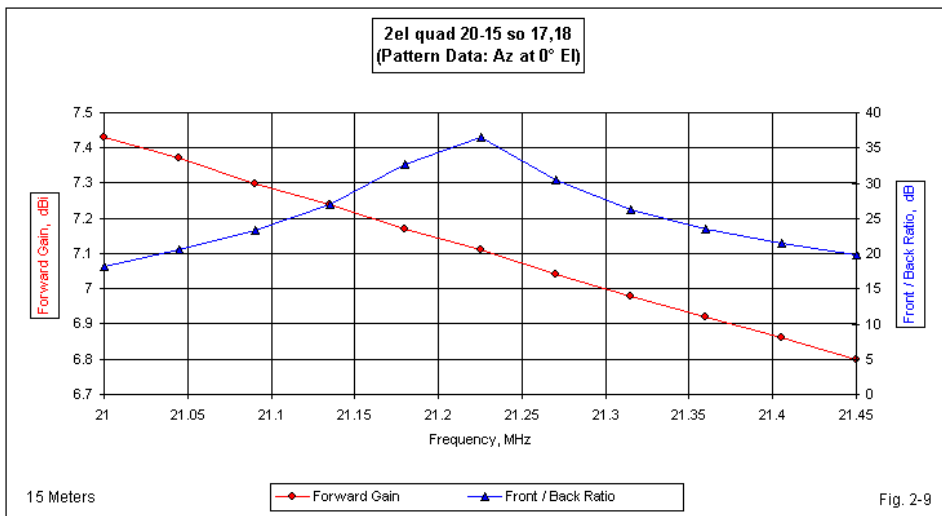
#### 20-15 Meters

20 Meters (Design Frequency 14.14 MHz)		Bandwidth: 2.47%		
Frequency MHz	14.0	14.14	14.175	14.35
Free-Space Gain dBi	7.55	7.15	7.03	6.46
180° Front-Back Ratio dB	12.81	28.17	39.12	15.15
Impedance (R +/- jX) $\Omega$				
Pre-Match Line	84.9 - j23.4	118.8 + j1.7	126.3 + j5.3	152.0 + j15.4
Post-Match Line	61.2 + j16.5	47.3 - j0.6	44.3 - j1.6	36.4 - j2.3
50-Ohm SWR	1.43	1.06	1.13	1.38
15 Meters (Design Frequency 21.19 MHz)		Bandwidth: 2.12%		
Frequency MHz	21.0	21.19	21.225	21.45
Free-Space Gain dBi	7.43	7.16	7.11	6.80
180° Front-Back Ratio dB	18.25	34.20	36.50	19.76
Impedance (R +/- jX) $\Omega$				
Pre-Match Line	87.0 - j29.0	108.1 - j0.6	111.9 + j4.0	135.1 + j30.1
Post-Match Line	57.0 + j18.6	51.4 + j0.5	49.7 - j1.4	39.4 - j7.4
50-Ohm SWR	1.45	1.03	1.03	1.34

Like the 15-meter section of the 15-10-meter quad, the 20-meter section of the new model shows the same drift upward in frequency, as shown in **Fig. 2-7**. The steeper gain curve of the 20-meter section relative to the monoband model results in the low end showing higher gain and the high end showing lower gain than in the monoband 20-meter antenna. The 20-meter front-to-back curve now peaks at mid-band rather than at the design frequency, with the low end of the band showing a front-to-back ratio of less than 13 dB.

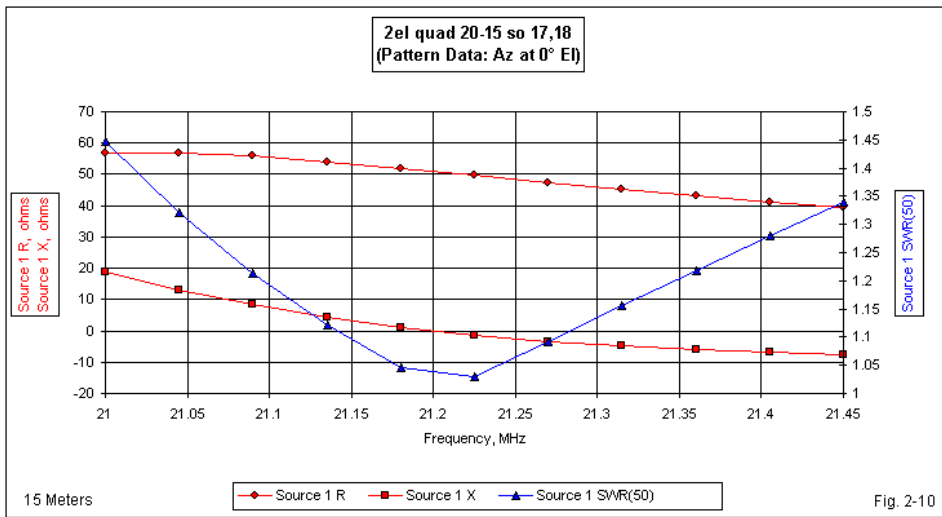


Allowing for a small difference in bandwidth as a percentage of the center frequency, the 20-meter dual-quad matched impedance values in **Fig. 2-8** are remarkably parallel to those of the 15-meter section of the 15-10-meter quad. The 50- $\Omega$  SWR curve is quite tame, since the outer section elements tend to reduce the reactance excursion across the band, relative to the monoband 20-meter quad. At the same time, the resistance range only moves upward slightly. Hence, SWR curve only peaks at 1.43:1 after a  $1/4\text{-}\lambda$  75- $\Omega$  matching line.



15 meters becomes the inner loop set on this dual-band quad. Not only is the gain curve somewhat shallower than on the monoband version, but as well, the curve is almost half as steep as the 15-meter gain curve on the 15-10-meter dual-band quad. The inner position of 15 meters also results in differences in the band-edge front-to-back ratio values. They are slightly better than the monoband values, but 4-5-dB better than the values for 15-meters when that band occupies the outer position in a dual-band situation. Compare the curves in **Fig. 2-9** with those of **Fig. 2-5**, along with the corresponding values in the relevant tables. Of course, we see the upward overall frequency shift in both performance categories.

With respect to impedance values, the inner position loses its advantage due to the greater drop in the resonant pre-match feedpoint impedance relative to a monoband quad. However, the fact that 15-meters is only 60% as wide as the first MHz of 10 meters allows the use of a standard  $1/4\text{-}\lambda$  75- $\Omega$  matching line with good results. The matched resistance and reactance curves are relatively flat, despite the 50- $\Omega$  excursion in the pre-matched reactance value. As a result, the 15-meter 50- $\Omega$  SWR curve is almost identical to the SWR curve for 20 meters in this dual-band quad. See **Fig. 2-10**.



The three dual-band quads that meet the basic requirements for this exploration all show the same patterns in physical and performance modifications relative to their monoband origins. The size of outer reflector increases, while outer drivers diminish. Inner reflectors require no change, whereas inner drivers shrink. The resulting performance patterns tend to shift gain and front-to-back curves slightly upward in the band, while allowing the pre-match feedpoint impedances to be near resonance on the original design frequencies. Both feedpoint impedances decrease, the outer by about 10  $\Omega$ , the inner by about 25

30  $\Omega$ . For the antennas derived from the original monoband designs, both bands of the dual-band versions allow use of a standard  $1/4\text{-}\lambda$  75- $\Omega$  line section for matching. However, for some bands, line length adjustment may yield a better match across a given band, especially for the inner quad of the pair.

The slight upward frequency shift in the gain and front-to-back curves may seem troublesome to someone seeking a perfect reproduction of the monoband curves. Further tweaking might indeed be possible. However, in most cases, I limited loop dimension changes to 0.1" increments, meaning a 0.8" inch change in the overall loop circumference. Anything more finicky would likely be impossible to replicate in most shops, and construction variables will likely override even the level of model precision that I used. Nevertheless, one may be able to move the gain and front-to-back curves downward in frequency slightly by making loop adjustments in 0.01" increments for each half side.

### **A 20-15-10-Meter 2-Element Quad Array Using Separate Feedpoints**

The terms of this exercise permit only 1 possible 3-band quad. Although 2-band quads are the main focus of the investigation, all of the basic materials were available to design the 3-band antenna. As well, a 3-band quad would answer—at least provisionally, since we would make only one model—some lingering questions about the 2-band versions. The physical and performance dimensions and values show very distinct patterns depending upon whether the loops for a given band are inner or outer quads. So one might relevantly ask the following questions. 1. Would the outer band loops remain at the same dimensions and with the same performance if we place 2 bands of quad inside? 2. Would the inner band loops retain their dimensions if we add 2 bands of quads outside them? 3. What happens to the dimensions and performance of the middle loops now that they are no longer either inner or outer loops? To obtain a first order set of answers, we must violate one of the guiding restraints. We must use a frequency ratio of 2:1 between the outer quad (20 meters) and the inner quad (10 meters). In advance, we might expect that the 20-meter loop might exert more influence on 10-meter dimensions and performance than the other way around. The 20-meter elements will be close to resonance as  $2\text{-}\lambda$  loops when we activate the 10-meter quad.

The tri-band dimensions appear in **Table 2-9** for comparison with several other dimensional tables in this part of our exploration. The 20-meter dimensions are exactly the same as they were in the dual-band quad using 20 meters as the outer band. The 10-meter reflector is the innermost element of that type and has the same dimensions as both the monoband and the dual-band quads. However, the 10-meter driver undergoes further shrinkage from the monoband 10-meter driver and is now shorter even than the driver for the same band as the inner loop in a dual-band quad. The further reduction in driver length is a likely function of two inseparable factors: the presence of the 20-meter driver and the required dimensional change in the 15-meter driver for its middle position in the array.

Table 2-9. 2-Element 3-Band Quad Beams with Separate Driver Elements

All dimensions in inches. Driver and reflector lengths are for  $\frac{1}{2}$  of each side. Multiply by 2 for full side length and by 8 for circumference. Band combinations based on a minimum frequency ratio of 1.3:1.

20-15-10 Meters			
Design Frequency	14.14	21.19	28.40
Driver	105.60	70.10	51.90
Reflector	109.90	73.50	55.62
Separation	128.34	87.24	65.70

On 15 meters, we encounter the most interesting dimensions. The driver is smaller than when it is the outer loop on a dual-band quad but larger than when it is the inner loop. Conversely, the reflector is longer than when it is an outer loop but shorter than when it is an inner loop.

**Table 2-10** provides a summary view of the performance of the tri-band quad.

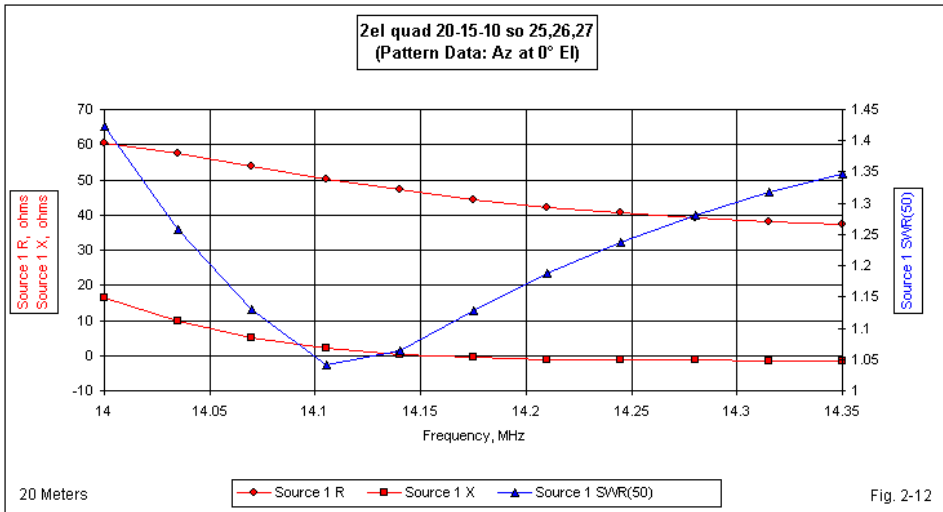
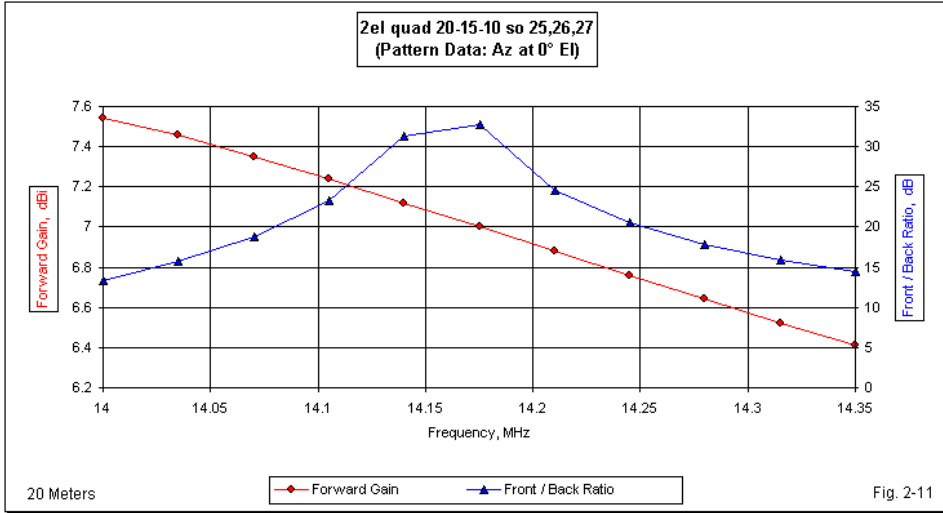
I shall reserve commentary on the band-by-band performance until we can survey the sweep graphs for each band. However, the pre-match impedances deserve special note. The 20-meter near-resonant impedance is the same as it was when 20-meters served as the outer quad on a 2-band antenna. The 15-meter pre-match impedance at the design frequency is closely comparable with the impedances of all of the inner drivers for the 2-band quads. On 10 meters, the pre-match impedance drops to 92  $\Omega$ , partly due to the further shortening of that element and—most likely—partly due to interactions of the 10-meter elements with the elements of both lower bands.

Table 2-10. 2-Element 3-Band Quad Beams with Separate Driver Elements  
Each driver uses a  $\frac{1}{4}\lambda$  matchline of 75- $\Omega$  cable. See notes for exceptions.

## 20-15-10 Meters

20 Meters (Design Frequency 14.14 MHz)		Bandwidth: 2.47%		
Frequency MHz	14.0	14.14	14.175	14.35
Free-Space Gain dBi	7.54	7.12	7.00	6.41
180° Front-Back Ratio dB	13.30	31.37	32.80	14.38
Impedance (R +/- jX) $\Omega$				
Pre-Match Line	85.8 - j24.0	119.2 - j0.8	126.4 + j2.3	149.5 + j11.4
Post-Match Line	60.4 + j16.5	47.1 + j0.4	44.4 - j0.6	37.2 - j1.4
50-Ohm SWR	1.42	1.06	1.13	1.35
15 Meters (Design Frequency 21.19 MHz)		Bandwidth: 2.12%		
Frequency MHz	21.0	21.19	21.225	21.45
Free-Space Gain dBi	7.49	7.11	7.03	6.57
180° Front-Back Ratio dB	16.88	37.31	28.18	14.96
Impedance (R +/- jX) $\Omega$				
Pre-Match Line	79.1 - j24.9	105.9 - j1.2	110.6 + j1.9	135.5 + j15.7
Post-Match Line	63.2 + j19.6	52.4 + j0.8	50.2 - j0.5	40.6 - j3.4
50-Ohm SWR	1.52	1.05	1.01	1.25
10 Meters (Design Frequency 28.40 MHz)		Bandwidth: 3.51%		
Frequency MHz	28.0	28.40	28.50	29.0
Free-Space Gain dBi	7.59	7.26	7.19	6.79
180° Front-Back Ratio dB	15.08	29.40	28.54	16.16
Impedance (R +/- jX) $\Omega$				
Pre-Match Line	66.6 - j49.1	91.9 + j1.6	98.6 + j12.9	131.7 + j62.3
Post-Match Line	46.8 + j31.0	61.2 - j4.1	57.6 - j11.2	36.9 - j22.8
50-Ohm SWR	1.88*	1.24	1.29	1.83
*10-meter matchline is 95", rather than 104".				

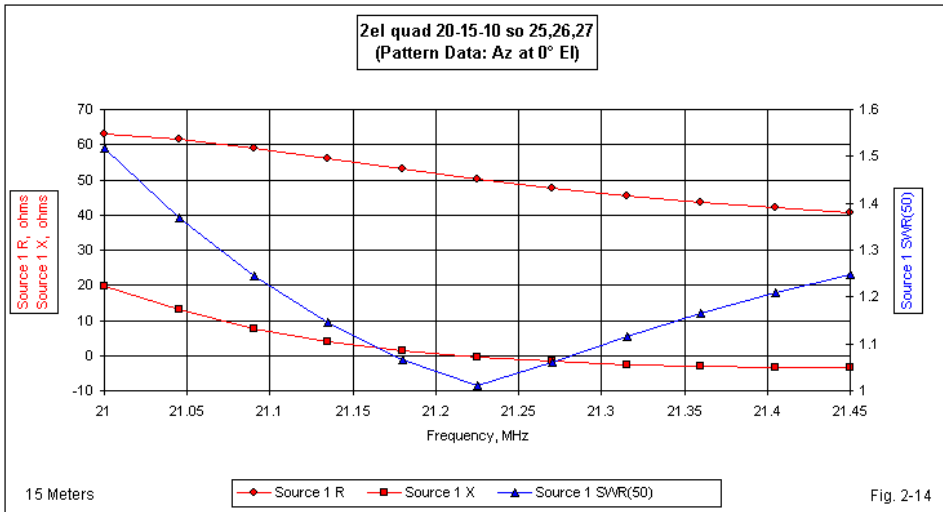
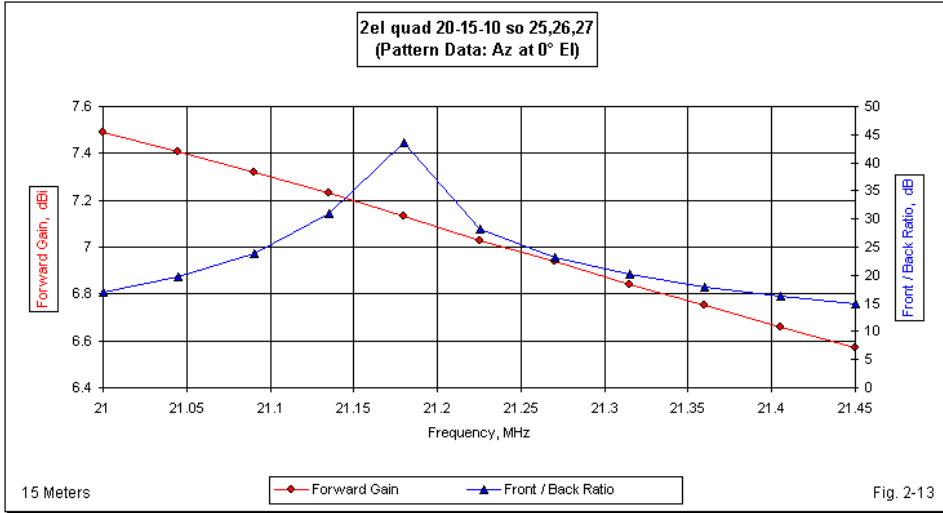
The 20-meter performance curves in **Fig. 2-11** are almost indistinguishable from those of the 20-meter elements in the 20-15-meter dual-band quad. The curves show the characteristic slight up-shift in frequency. Even the band-edge front-to-back ratio values are similar to those in the 2-band antenna.



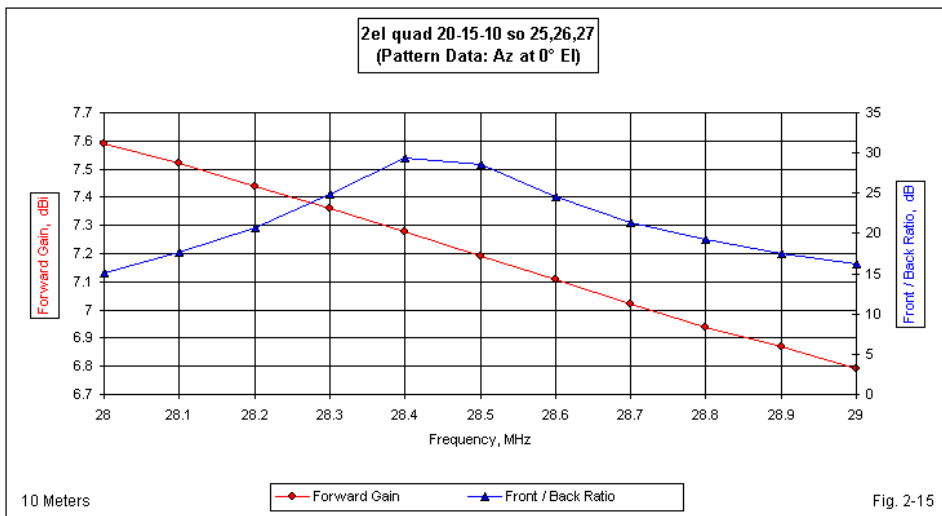
Equally similar to the curves for 20 meters in the 2-band quad are the tri-band 20 meter matched impedance curves in **Fig. 2-12**. The pre-matched resonant impedance on the design frequency is virtually identical to the value for the 2-band model, and the resistance and reactance changes across the band are within a few Ohms of those of the 2-band model. As a consequence, a  $1/4\text{-}\lambda$  75- $\Omega$  matching line provides a very satisfactory SWR curve with a maximum value of 1.42:1.

Since the 15-meter elements of the tri-band, separate-feed quad differ from both the monoband version and from the 2-band versions using either an inner or an outer position, we expect at least some difference in the performance curves. The rate of change in gain across the 15-meter band is one measure of similarity and difference. In the tri-band quad, the rate is greater than in the monoband 15-meter quad and also greater than when the 15-meter elements form the inner loops of a 2-band quad. However, the rate is lower than when the 15-meter loops form the outer elements of a 2-band antenna. See **Fig. 2-13**. Corresponding to these differences—which are small but distinct—are differences in the band-edge values of the  $180^\circ$  front-to-back ratio. In the tri-band version, they are lower than in the monoband version and lower than when 15 meters forms the inner elements of a 2-band quad. However, the values are higher than those for 15 meters as the outer quad in a 2-band antenna. Nevertheless, in both categories of performance, the central position of the elements allows us to return the curves to their monoband position, that is, with the front-to-back peak at or very near to the design frequency.

Despite the normalcy of the gain and front-to-back curves, the pre-matched impedance of the 15-meter band most resembles values that we obtain for the inner quad of a 2-band model, as shown in **Fig. 2-14**. As a result, the standard  $1/4\text{-}\lambda$  75- $\Omega$  matchline yields a 50- $\Omega$  SWR curve that is higher at the low end of the band. The curve is similar to the one for the 15-meter section of the 20-15 2-band quad, but with a slightly higher value at the low end of the band and a slightly lower value at the high end of the band. An adjustment to the matchline length would equalize the band edge values and reduce the maximum value below 1.5:1.



The 10-meter elements form the inner elements of the tri-band quad. The inner elements tend to show the lower rate of gain change in 2-band quads, and this trend continues in the tri-band model. See **Fig. 2-15**. The rate of gain change is lower than in both other models using 10-meter elements. The band-edge front-to-back ratio values match those of the 15-10 meter quad and are higher than the values shown by the monoband model. The overall front-to-back curve has a somewhat shallow appearance, especially when compared to the monoband version. The peak front-to-back ratio occurs on about 28.44 MHz, but it scarcely exceeds 30 dB, compared to a value of nearly 60 dB in the monoband version. (Of course, in a practical quad, the exceptionally sharp and narrow-band peak might not be obtained, even on a monoband quad.)



The pre-matched impedance of the 10-meter elements starts with a low resonant value (about 92  $\Omega$ ) and also shows rather wide excursions of both resistance and reactance across the wide 10-meter band. A 75- $\Omega$  matching line is not ideal for the situation, although using the prescribed length shown in **Table 2-10**, the 50- $\Omega$  impedance remains below 1.9:1 at both ends of the passband, as

shown in **Fig. 2-16**.

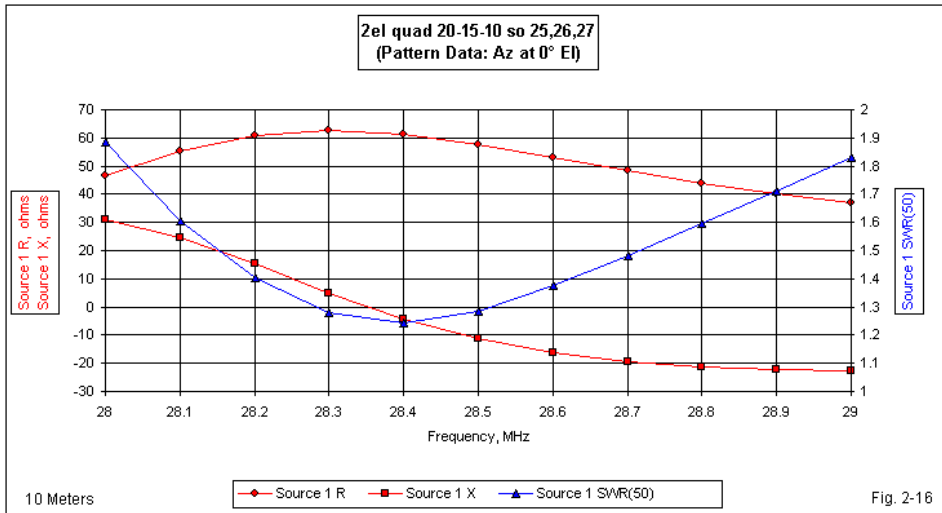


Fig. 2-16

The most usual strategy employed to improve the 10-meter SWR situation is to revise the 10-meter elements so that they provide a more acceptable—higher—resonant feedpoint impedance. However, the gain or the front-to-back performance may suffer as a result of these changes. Alternatively, one might lower the design frequency and limit the SWR passband to an upper frequency of about 28.8 MHz.

Despite the strain of obtaining an adequate SWR spread across the 10-meter band, the tri-band quad provides overall performance that is fully adequate to most needs on all 3 bands. Separate drivers and match-lines for each band allow for a remote switching system. As well, one may make fine (in contrast to basic) adjustments to loop lengths without significant change on the other bands. In the end, the performance of the tri-band quad is similar to the performance of the 2-band quads and of the monoband quads.

**Conclusion to Part 2**

In this part of our exploration, we have examined the physical and performance changes occasioned by combining monoband beams into several 2-band beams and one 3-band array, using separate drivers for each included band. Throughout, we remained true to the original monoband designs by retaining the element spacing. Thus, each spider quad shows almost identical angles between the driver and reflector elements for each band. The angles are close enough to each other so that non-conductive spacer rods can easily allow a builder to fix the spacing. However, in a quad (or other parasitic 2-element beam), the spacing tends to be less sensitive to change than the element lengths. An inch or so of element spacing at 20 meters is unlikely to create a noticeable change in array performance. However, changes in element circumference as small as an inch can move the performance curve, especially if we make the change in the reflector element of a 2-element quad beam.

The exercise has shown us what physical modifications occur as a result of simple element interaction between quads on the same support system when the frequency ratio between quads is between 1.3:1 and 1.5:1. Therefore, each sample quad has avoided the use of adjacent upper-HF bands, such as 20-17 or 12-10. After we have examined the question of a common feedpoint for these arrays, we shall return to the question of adjacent-band behavior in dual quads. At this stage, the wider frequency separation of the combined antennas provides us with variables that we may easily control and understand. This simplifying step has been necessary in order for us to be able to separate alterations of quad dimensions or of performance due to the use of a common feedpoint from alterations that are basic to placing 2 quads on the same arms.

In the third part of this exploration, we shall deal directly with 2-band quads using a common feedpoint. We have a useful collection of dual-band quad beams to use as comparators for the common-feedpoint models. In the next part of our journey, we shall encounter only 3 new models: 17-12 meters, 15-10 meters, and 20-15 meters. For reasons that will become clear in our examination of these models, we shall set aside the tri-band quad. However, in its place are a series of fundamental modeling questions. Therefore, we shall not begin the next part by

looking at 2-band quad performance. Instead, our first question will involve the proper way to model a common-feedpoint quad driver set.

## Chapter 3

### *Sneaking Up on 2-Element Common-Feed Quads*

### Part 3: Dual Band Quad Beams With Common Feedpoints

Finally. . .we are ready to tackle dual-band quad beams with common feedpoints. Like the dual band beams in Part 2 that used separate feedpoints, our new beams will rest ultimately on the series of monoband beam designs that we examined in Part 1. They will also adhere to the basic limits surrounding the study by using no more than 2 bands per beam where the bands have at least a 1.3:1 frequency ratio. Hence, our new combination beams will include versions for 17 and 12 meters, for 15 and 10 meters, and for 20 and 15 meters.

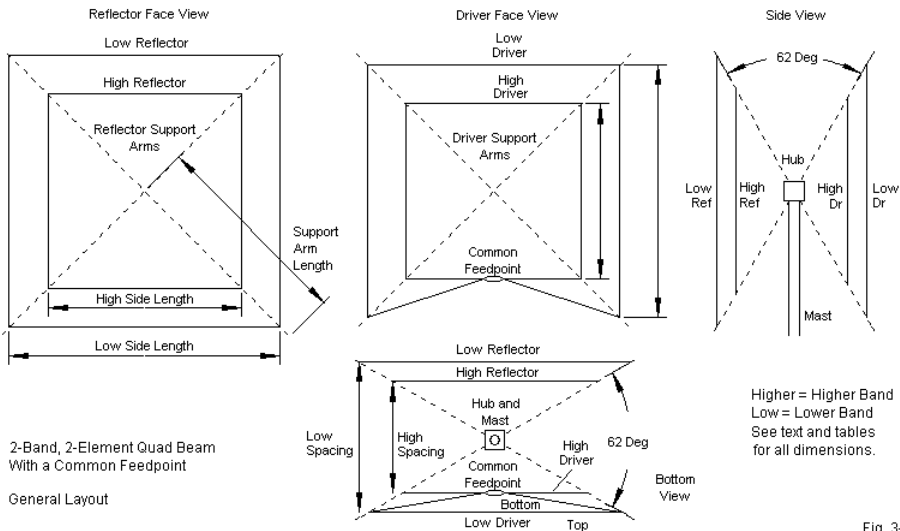


Fig. 3-1

**Fig. 3-1** provides a generalized sketch of the physical elements of the new set of beams. Like the versions using separate feedpoints, the new combinations will employ spider construction in order to maintain the spacing on each band used by the monoband beams. The angle between forward and rearward support arms is

an average of the angles calculated from the collection of monoband quads. As noted in Part 2, very small variations in spacing make very little difference to performance compared to equally small variations in the element lengths.

Perhaps the one item in **Fig. 3-1** that requires further comment is the arrangement of the feedpoint. For each combination beam, the inner or higher frequency driver will use a square loop. All loop-shape distortion will involve the driver for the lower frequency of the pair. The design decision rests on a number of factors, not the least of which is relative simplicity compared to finding an intermediate position for the feedpoint that distorts both driver loops equally. In addition, experience suggests (but does not prove) that driver distortion has fewer negative effects on the lower frequency driver than on the inner or higher frequency driver.

Table 3-1. 2-Element 2-Band Quad Beams with Separate Driver Elements  
All dimensions in inches. Driver and reflector lengths are for ½ of each side. Multiply by 2 for full side length and by 8 for circumference. Band combinations based on a minimum frequency ratio of 1.3:1. Second low-band driver figure indicates circumference for comparison with values in Table 2.

17-12 Meters		
Design Frequency	18.118	24.94
Driver	82.60/660.80	59.40
Reflector	85.90	63.24
Separation	101.40	74.54
15-10 Meters		
Design Frequency	21.19	28.40
Driver	70.65/565.20	52.10
Reflector	73.30	55.62
Separation	87.24	65.70
20-15 Meters		
Design Frequency	14.14	21.19
Driver	105.60/844.80	69.85
Reflector	109.90	74.29
Separation	128.34	87.24

To assess the quads that use a common feedpoint, we shall need some data at hand for reference. **Table 3-1** repeats the dimensions used on the same set of quads when using separate feedpoints. To the information presented in Part 2, I

have added the circumference of the driver for each lower frequency quad

All common-feed quad combinations sought to achieve the same goal used for the quads with separate feedpoints: restoration to the fullest extent possible of the performance of the monoband quads on which the designs rest. For immediate comparison of the physical results, **Table 3-2** provides the resulting dimensions for the common-feedpoint versions.

Table 3-2. 2-Element 2-Band Quad Beams with Joined Driver Elements  
All dimensions in inches. Driver and reflector lengths are for ½ of each side. Multiply by 2 for full side length and by 8 for circumference. Band combinations based on a minimum frequency ratio of 1.3:1. Starred driver elements are bent inward to join the lower-frequency driver and hence are longer than the half-side length would indicate. Second figure indicates total wire circumference for comparison with values in Table 1.

17-12 Meters		
Design Frequency	18.118	24.94
Driver	81.50/659.64*	61.00
Reflector	85.80	63.20
Separation	101.50	74.50
15-10 Meters		
Design Frequency	21.19	28.40
Driver	69.80/564.03*	53.60
Reflector	73.30	55.50
Separation	87.20	65.70
20-15 Meters		
Design Frequency	14.14	21.19
Driver	104.10/847.61*	71.20
Reflector	109.90	74.00
Separation	128.40	87.20

To obtain the circumference of any loop, we normally multiply the listed half-side length by 8. However, the models using a common feedpoint require us to add to the three linear sides the sloping and center sections of wire that create the feedpoint. Hence, the circumference forms an odd value relative to the half-side lengths.

Table 3-3. 2-Element 2-Band Quad Beams with Separate Driver Elements  
Each driver uses a  $\frac{1}{4}\lambda$  matchline of 75- $\Omega$  cable. See notes for exceptions.

## 17-12 Meters

17 Meters (Design Frequency 18.118 MHz)	Bandwidth: 0.55%		
Frequency MHz	18.068	18.118	18.168
Free-Space Gain dBi	7.18	7.04	6.89
180° Front-Back Ratio dB	27.07	36.00	25.21
Impedance (R +/- jX) $\Omega$			
Pre-Match Line	115.4 - j3.9	123.7 - j1.1	130.9 + j0.8
Post-Match Line	48.5 + j1.4	45.3 + j0.4	42.8 - j0.1
50-Ohm SWR	1.04	1.10	1.17

12 Meters (Design Frequency 24.94 MHz)	Bandwidth: 0.40%		
Frequency MHz	24.89	24.94	24.99
Free-Space Gain dBi	7.22	7.16	7.10
180° Front-Back Ratio dB	28.33	34.32	38.55
Impedance (R +/- jX) $\Omega$			
Pre-Match Line	98.8 - j3.7	103.0 + j2.2	107.1 + j7.8
Post-Match Line	56.0 + j2.1	53.9 - j1.0	51.6 - j3.4
50-Ohm SWR	1.13	1.08	1.08

## 15-10 Meters

15 Meters (Design Frequency 21.19 MHz)	Bandwidth: 2.12%			
Frequency MHz	21.0	21.19	21.225	21.45
Free-Space Gain dBi	7.56	7.14	7.05	6.47
180° Front-Back Ratio dB	13.64	30.69	34.87	15.13
Impedance (R +/- jX) $\Omega$				
Pre-Match Line	87.4 - j15.7	118.3 + j0.3	123.1 + j1.5	142.6 + j3.8
Post-Match Line	61.9 + j10.6	47.4 - j0.3	45.5 - j0.7	39.2 - j0.2
50-Ohm SWR	1.33	1.06	1.10	1.28

10 Meters (Design Frequency 28.40 MHz)	Bandwidth: 3.51%			
Frequency MHz	28.0	28.40	28.50	29.0
Free-Space Gain dBi	7.55	7.17	7.07	6.62
180° Front-Back Ratio dB	14.74	33.98	34.43	16.48
Impedance (R +/- jX) $\Omega$				
Pre-Match Line	73.4 - j46.2	100.7 - j0.8	107.5 + j8.9	138.3 + j50.4
Post-Match Line	53.5 + j33.0	55.1 + j0.8	51.3 - j3.6	35.4 - j10.5
50-Ohm SWR	1.88*	1.10	1.08	1.53

\*Shortening the matchline from 104" to about 100" will equalize band-edge 50- $\Omega$  SWR values.

## 20-15 Meters

20 Meters (Design Frequency 14.14 MHz)	Bandwidth: 2.47%			
Frequency MHz	14.0	14.14	14.175	14.35
Free-Space Gain dBi	7.55	7.15	7.03	6.46
180° Front-Back Ratio dB	12.81	28.17	39.12	15.15
Impedance (R +/- jX) $\Omega$				
Pre-Match Line	84.9 - j23.4	118.8 + j1.7	126.3 + j5.3	152.0 + j15.4
Post-Match Line	61.2 + j16.5	47.3 - j0.6	44.3 - j1.6	36.4 - j2.3
50-Ohm SWR	1.43	1.06	1.13	1.38

15 Meters (Design Frequency 21.19 MHz)	Bandwidth: 2.12%			
Frequency MHz	21.0	21.19	21.225	21.45
Free-Space Gain dBi	7.43	7.16	7.11	6.80
180° Front-Back Ratio dB	18.25	34.20	36.50	19.76
Impedance (R +/- jX) $\Omega$				
Pre-Match Line	87.0 - j29.0	108.1 - j0.6	111.9 + j4.0	135.1 + j30.1
Post-Match Line	57.0 + j18.6	51.4 + j0.5	49.7 - j1.4	39.4 - j7.4
50-Ohm SWR	1.45	1.03	1.03	1.34

Certain general patterns show up in the physical dimensions. For each combination, the inner reflector for the higher-frequency band remains either fully or close to unchanged. However, every inner driver shows increased length relative to the inner drivers for the quads using separate feedpoints. Likewise, the outer reflectors for the lower frequency show virtually no change in length. As well, the circumferences of the outer drivers for the common-feedpoint quads are very close in overall length to the circumferences of the outer drivers for the versions using separate feedpoints. The inner drivers undergo the most extreme change of any element when converting from separate feedpoints to a common feedpoint, and the amount of change is significant. It ranges from a 6" to a 12" overall circumference increase, depending on the models involved. The lower band element exerts much more influence over the higher band driver, despite (or perhaps because of) the distortion in the lower-band driver shape. At the same time, both types of dual band quads use independent loops for reflector elements. In general, the interactions between the reflector elements do not change significantly when moving from separately fed drivers to drivers with a common feedpoint. You may wish to consult Part 1 for the dimensions of the original monoband quads to determine the total amount of variation, although changes in that variation apply mostly to the inner or higher-frequency driver elements.

We shall also need to compare the performance values for the common-feedpoint quads to corresponding figures for versions with separate feedpoints. **Table 3-3** collects the performance data for all of the 2-band quads into one table for convenient reference. We shall have occasion to refer to this table as we encounter each of the dual-band common-feedpoint quad assemblies.

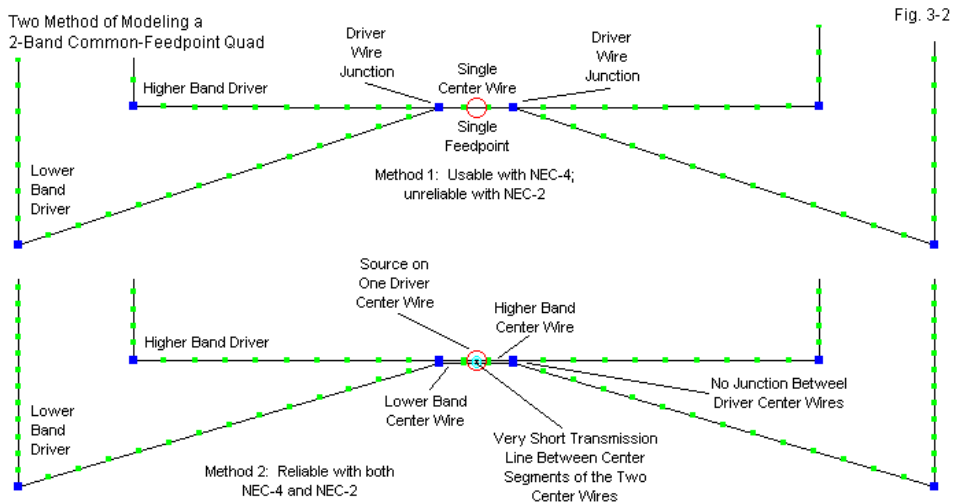
The data that we shall develop on the new set of quads comes from NEC models. Although I habitually use NEC-4, all of the quad designs that we have so far explored work well with NEC-2. Nothing in the designs challenges NEC limitations. Hence, each quad so far has shown an Average Gain Test (AGT) score between 0.998 and 1.002, indicating a high reliability. I have also subjected the models to convergence tests. These tests altered the segmentation of each wire uniformly. For dual-band quads, I varied both the inner and the outer wire segmentation so as to maintain the same ratio of segments in corresponding wires relative to inner and outer loops. The goal was always to maintain to the degree

possible an alignment between segment junctions. The results showed excellent convergence with relatively modest segmentation. Both the AGT and convergence tests are necessary but not sufficient conditions of model adequacy, but long use of wire quad models has resulted in their relatively high reliability. (The reliability of the models presumes that physical implementations do not use construction methods that introduce corner-fastening loops and other features that might detune an element relative to its model as a clean square.)

Given the high reliability of the models that we have used in Parts 1 and 2 of this exploration, we hope to achieve similar reliability for the common-feedpoint quads. However, the modeling itself presents a challenge.

### Modeling Common-Feedpoint Quads

The only critical region of a dual-band quad model using a common feedpoint is the set of wires coming together at the feedpoint wire. The most common method used for developing the model appears in the upper section of **Fig. 3-2**.



The inner driver "bottom" wire consists of 3 modeled wires. The center wire consists of 3 segments, with the source or excitation placed on the center segment. The adjacent segments are the same lengths as the source segment, providing for equal currents on each side of the source segment. At the ends of this wire, we connect the remaining lengths of the inner driver wire. We segment each of these wires so that the segment lengths are as close as feasible to the segment lengths on the center wire.

The ends of the center wire also form junctions with the wires for the outer driver. We segment each of these added wires so that the segment lengths are as close as feasible to the lengths of segments in the center wire and in the inner driver wires. For many applications, this technique suffices to produce highly accurate models. The current division between the 2 driver loops does not occur until at least one segment away from the source segment.

In the case of the quad loops, the inner and outer driver wires form an angle. The angle appears to be fairly wide. In fact, if we were creating a set of radials symmetrically arranged around a center junction, we might use much smaller angles and achieve high accuracy in the results from either NEC-2 or NEC-4. However, in the present situation, NEC-2 and NEC-4 show considerable differences in the results that they report from a single quad model. Given a test model for 17 and 12 meters using this modeling scheme, NEC-2 reports a free-space gain at 18.118 MHz of 7.88 dBi and 7.74 dBi at 24.94 MHz. Changing the core to NEC-4 yielded gain reports of 7.19 and 7.06 dBi for the two frequencies. If we check the AGT values, NEC 2 produces values of 1.215 on 17 and 1.212 on 12. These values indicate that NEC-2 gain reports are about 0.85 dB too high. In the same conditions, NEC-4 produces AGT values of 1.037 and 1.038 for the two bands, still overestimating gain by about 0.16 dB. In addition to misreporting the gain, the source resistance will also be in error. To correct the source impedance, multiply the reported value by the basic AGT score.

The initial models of common-feedpoint quads present two challenges. First, we should be able to develop models with a more ideal AGT score, a value much closer to 1.000 so that the gain reports require no adjustment. Second, the models should yield the same results under NEC-2 and NEC-4. Some years back, I

worked out an alternative scheme for modeling feedpoints that essentially are in parallel with each other. The technique is applicable to common-feedpoint quads, as shown in the lower part of **Fig. 3-2**. We begin by retaining the structure of the inner driver wire, but we shall make no wire connections to it from the lower frequency or outer driver. Instead, we shall create parallel 3-segment wires, one for each driver. The sloping wires of the outer driver will connect to their own center wire. We should use enough spacing between the two center wires so that they do not interact significantly. We shall be able to tell the minimum correct spacing from AGT scores for the final model. We can begin with relatively close spacing and increase the spacing until the AGT values approaches 1.0 as closely as we need for a given modeling exercise.

The next step is to place a source or excitation on the center segment of one and only one of the center wires. Between the source segment and the corresponding center segment on the other center wire, create a transmission line with the NEC TL facility or command. Give the line a characteristic impedance somewhere in the ball park of the anticipated impedance values, although the actual value will not be at all critical. The key to establishing a parallel connection is to assign the transmission line as short a length as a given implementation of NEC will permit. Many programs permit lengths as short as 1e-10 meters if using the TL command directly. You may use the same specification in whatever unit may be in use, if the interface translates those units into meters internally. Some programs have certain minimum values for some or all length specifications. Whatever the lower limit, use it. The goal is to set up a line length that creates virtually no impedance transformation between one end and the other end of the line. Remember that the line length that you specify is independent of the physical distance between the center segments that you set up when establishing the two center wires.

Using this modeling system, both NEC-2 and NEC-4 return the same gain and impedance reports, with AGT scores very close to 1.0, for the test quad combination for 17 and 12 meters. We shall examine that model's performance in more detail shortly. For the moment, the development of a relatively reliable method of modeling common-feedpoint quads is our concern.

Despite the nearly ideal AGT score for the revised method of modeling the quads, we cannot claim that the model is as reliable as the monoband models or the dual-band models with separate feedpoints. In this instance, reliability refers to our ability to transfer the results to a physical implementation of the quad designs. The model does not correspond perfectly to the geometry of a typical common-feedpoint as constructed for use. Such common feedpoints normally consist of a center insulator where the wires join. The distance between the junctions of the two drivers is likely to be smaller than the length of the 3-segment center wires unless we use a very high number of segments per wavelength. Therefore, any physical implementation of a common-feedpoint quad should take the modeled data as a starting point for final field measurements and adjustments. However, the revised modeling system should come a good bit closer to field measurements than the initial modeling system.

### **A 17-12-Meter 2-Element Quad Array Using A Common Feedpoint**

Because it involves a pair of narrow bands, the common-feedpoint 17-12-meter quad is the natural first experiment. The dimensions appear in **Table 3-2**. More pertinent to our interests here is **Table 3-4**, which provides the performance data. Compare the figures to those in **Table 3-3** for the 17-12-meter quad using separate feeders.

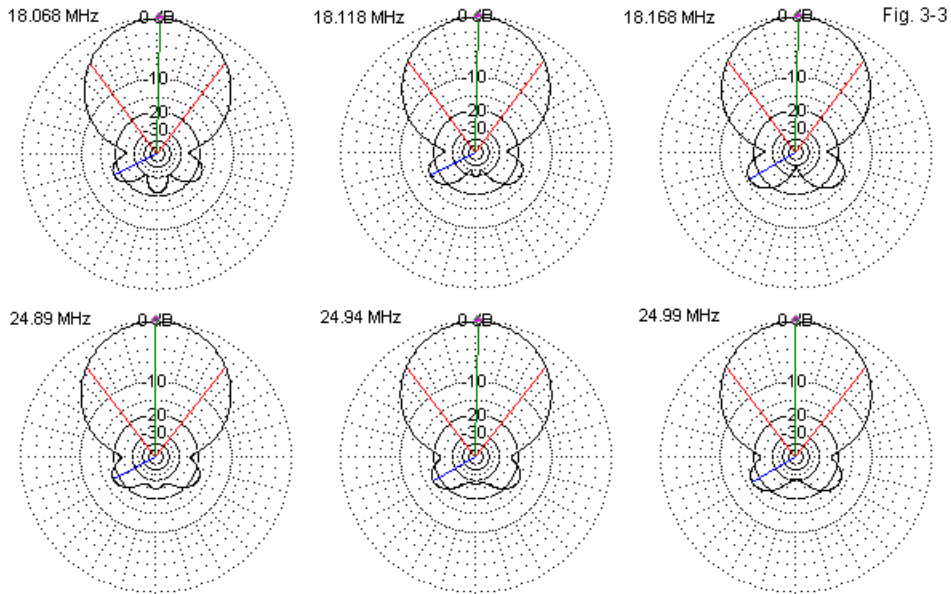
Compared to the separate feed model, the common feed 17-12-meter quad front-to-back curves appear to show an additional upward frequency shift. The 17-meter quad appears to reach peak value at the upper end of the band, while the 12-meter peak lies beyond the upper band limit. The gain levels are modest but well within expectations for a 2-element quad. Although the performance does not achieve the full monoband potential, the numbers and the patterns are fully appropriate for these bands. **Fig. 3-3** provides a gallery of free-space E-plane patterns for both bands to confirm this fact.

Table 3-4. 2-Element 2-Band Quad Beams with Joined Driver Elements

17-12 Meters: Common matchline 145" 75- $\Omega$  cable

17 Meters (Design Frequency 18.118 MHz) Bandwidth: 0.55%			
Frequency MHz	18.068	18.118	18.168
Free-Space Gain dBi	7.15	7.01	6.86
180° Front-Back Ratio dB	21.44	29.35	37.59
Impedance (R +/- jX) $\Omega$			
Pre-Match Line	115.6 - j15.2	126.2 - j9.4	136.2 - j4.9
Post-Match Line	47.3 - j1.7	44.5 - j5.2	41.8 - j7.3
50-Ohm SWR	1.07	1.17	1.27
12 Meters (Design Frequency 24.94 MHz) Bandwidth: 0.40%			
Frequency MHz	24.89	24.94	24.99
Free-Space Gain dBi	7.04	6.99	6.95
180° Front-Back Ratio dB	24.81	27.63	30.39
Impedance (R +/- jX) $\Omega$			
Pre-Match Line	116.4 + j17.7	122.4 + j24.3	128.3 + j30.4
Post-Match Line	47.6 + j8.9	44.3 + j8.9	41.4 + j9.2
50-Ohm SWR	1.21	1.25	1.32

The impedance behavior of the common-feed dual band quad holds a surprise: the mid-band feedpoint impedances are very similar for the two bands. The impedances specifically leave remnant reactances due to an interesting potential for the array. A single 75- $\Omega$  match-line can serve both bands in providing a satisfactory match to a 50- $\Omega$  main feedline. The model calls for a 145" (electrical) length, although in practice, a builder may have to experiment with the length that yields the best 50- $\Omega$  SWR curves on both bands. The modeled line is about 0.22  $\lambda$  on 17 meters and about 0.31  $\lambda$  on 12 meters. The matching line is an abbreviated form of series matching, for which Regier's work provides the most general solutions. The worst-case 50- $\Omega$  SWR is 1.32:1, a value that meets the most stringent SWR requirements on the amateur bands.



Free-Space E-Plane Patterns: 2-Band, 2-Element Quad Beam with Common Feedpoint

The ability to have a common feedpoint and a single match-line—along with the fully adequate performance on both bands—makes the dual-band 17-12-meter quad a prime candidate for actual construction and use. However, remember that the common-feed models require slight distortions of the physical geometry in order to meet modeling constraints. Therefore, one cannot approach such a project as if the model formed a final template.

### A 15-10-Meter 2-Element Quad Array Using A Common Feedpoint

The proper assessment the band-edge performance of the common-feedpoint quad requires that we examine models designed to cover wider bands. The 15-10-meter common-feedpoint quad provides one of two tests of the performance curves. **Table 3-5** gives us the summary data on the model's performance on both

bands for comparison with data for the separate feedpoint models in **Table 3-3**.

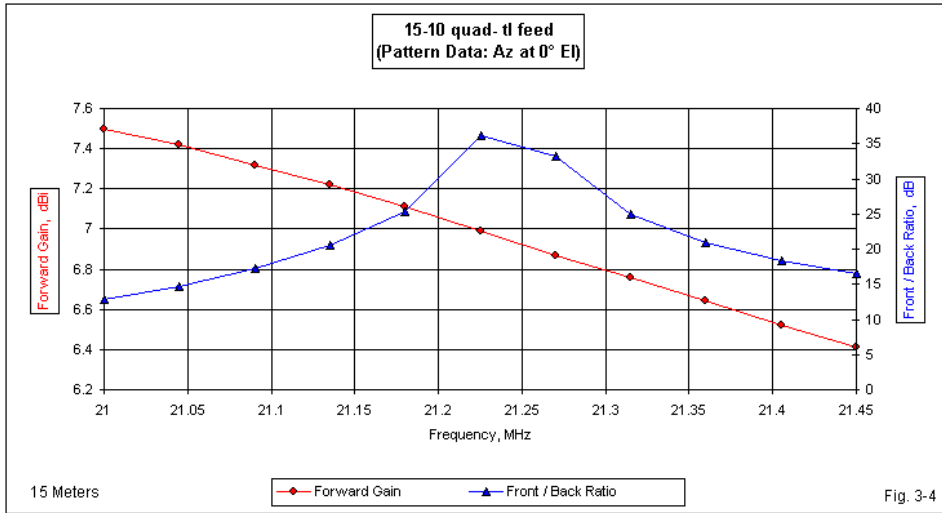
Table 3-5. 2-Element 2-Band Quad Beams with Joined Driver Elements

15-10 Meters: Common matchline 110" 75- $\Omega$  cable

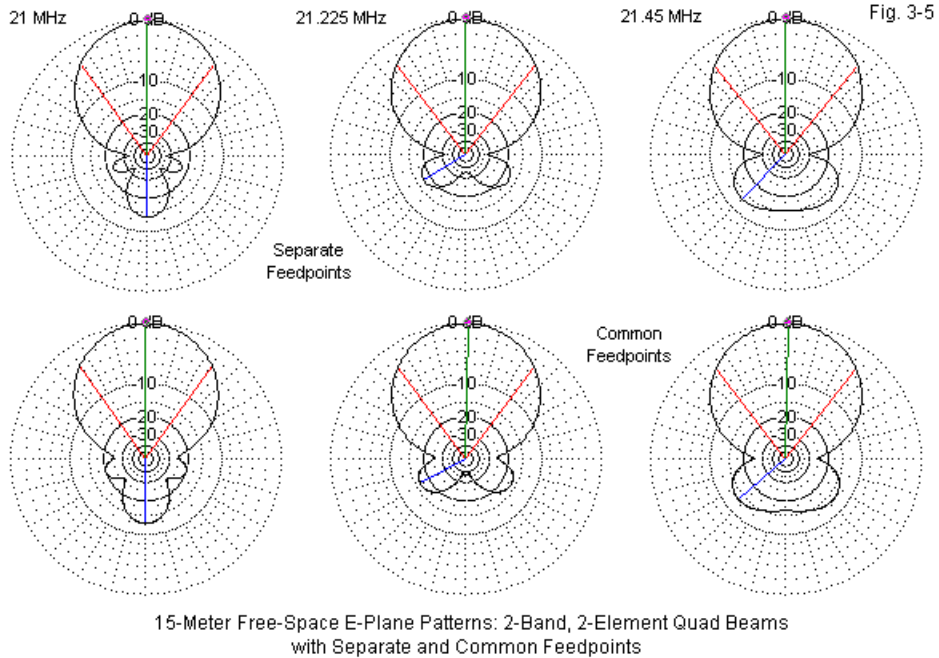
15 Meters (Design Frequency 21.19 MHz)		Bandwidth: 2.12%		
Frequency MHz	21.0	21.19	21.225	21.45
Free-Space Gain dBi	7.50	7.08	6.99	6.41
180° Front-Back Ratio dB	12.76	26.90	36.21	16.44
Impedance (R +/- jX) $\Omega$				
Pre-Match Line	89.3 - j33.6	124.8 - j9.2	131.1 - j6.5	163.0 + j1.3
Post-Match Line	48.8 + j6.2	46.7 - j12.7	45.2 - j14.5	37.4 - j19.1
50-Ohm SWR	1.14	1.31	1.38	1.69
10 Meters (Design Frequency 28.40 MHz)		Bandwidth: 3.51%		
Frequency MHz	28.0	28.40	28.50	29.0
Free-Space Gain dBi	7.31	7.07	6.99	6.64
180° Front-Back Ratio dB	13.74	25.49	30.86	18.80
Impedance (R +/- jX) $\Omega$				
Pre-Match Line	77.8 - j37.1	119.9 + j22.6	130.2 + j33.9	174.2 + j76.2
Post-Match Line	62.2 + j30.6	44.6 - j4.1	29.6 - j5.2	26.4 - j3.4
50-Ohm SWR	1.79	1.15	1.30	1.91

On 15 meters, the rate of gain decrease across the band is identical to the rate for the separate feed model. **Fig. 3-4** shows the gain and front-to-back curves for 15 meters. Relative to the separate-feedpoint model, the common-feedpoint version appears to show an added shift of the 180° front-to-back curve upward in the band, even though the gain curves for the two types of quads are very similar. The peak front-to-back value occurs just above the mid-band frequency.

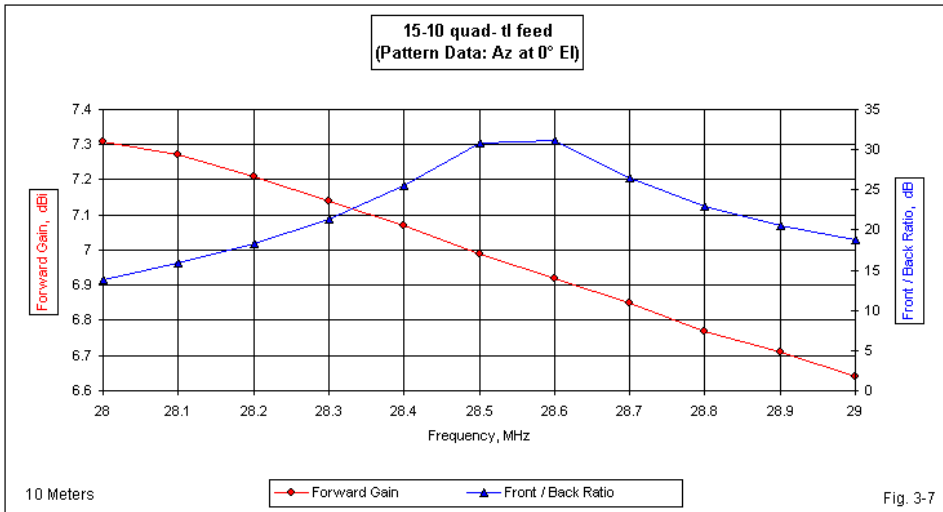
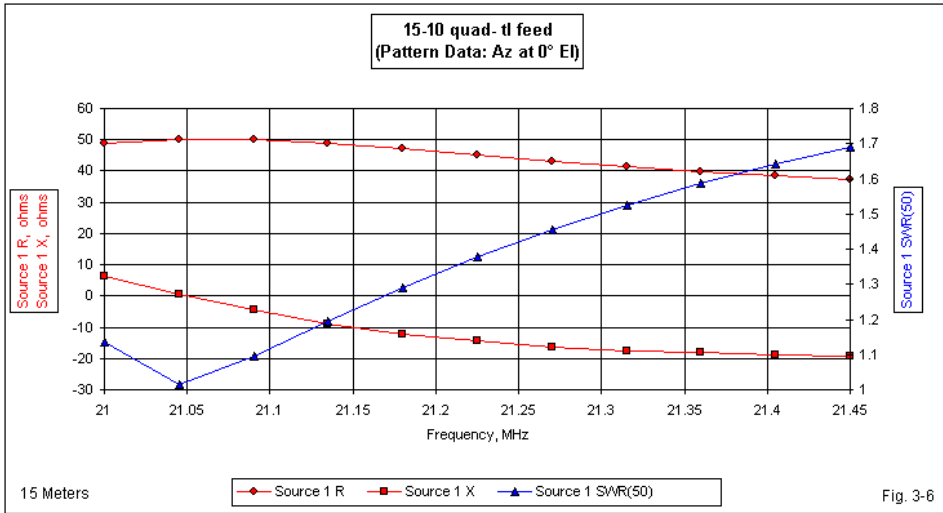
**Fig. 3-5** provides a gallery of free-space E-plane patterns for both the separate- and the common-feedpoint models on 15 meters. The clearest evidence of front-to-back upward frequency shift is the set of rear lobes that occur at 21 MHz. The common-feedpoint lobes are larger in all ways than those for the separate-feedpoint quad.



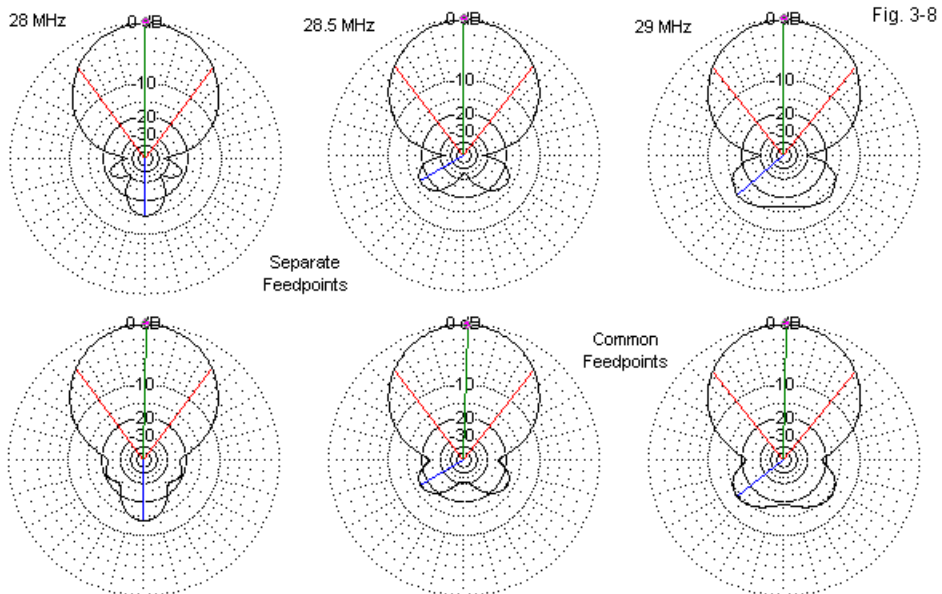
In **Fig. 3-6**, we see the post-match impedance curves for the 15-meter portion of the quad. The 110" (electrical length) 75-Ω match-line is about  $0.20 \lambda$  at the 15-meter design frequency. The result is an SWR curve that reaches its minimum value very low in the band. However, the upper band limit shows a maximum value that is under 1.7:1. Although we might change the length for a better match on 15, we have selected the length that yields the best compromise values for both 15 and 10 meters. The technique may not be ideal for the widest amateur upper-HF bands, but it is serviceable.



As the widest of the bands within our survey, the first MHz of 10 meters presents the greatest challenge to the common-feedpoint dual-band quad. The rate of gain decrease across the 10-meter band is actually lower than it is using separate feedpoints. The curves appear in **Fig. 3-7**. Once more, the common-feedpoint quad shows additional upward frequency shifting of the front-to-back curve relative to the separate-feedpoint model. The peak value of the 180° front-to-back ratio occurs at about 28.55 MHz.



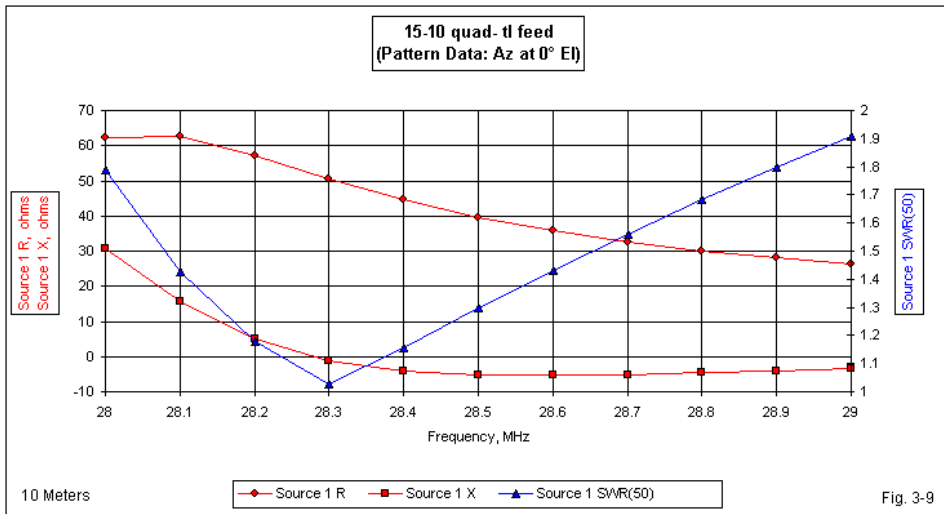
The upward frequency drift of the performance curves shows itself most vividly in a comparison of the 28-MHz free-space E-plane patterns for both the separate- and the common-feedpoint models in **Fig. 3-8**. The band-edge front-to-back value of the common-feedpoint model is less than 13 dB, and the pattern shows significant devolution compared to the 28-MHz pattern for the separate-feedpoint quad. In contrast, at 29 MHz, the separate-feedpoint model shows no signs of a  $180^\circ$  null, but the common-feedpoint model has a null that approaches 3 dB.



10-Meter Free-Space E-Plane Patterns: 2-Band, 2-Element Quad Beams  
with Separate and Common Feedpoints

Although the pre-match feedpoint impedance values of both 15 and 10 meters are similar in value, the post-match impedances show interesting differences. The post-match impedance performance curves appear in **Fig. 3-9**. At 28.4 MHz, the 110" 75- $\Omega$  match-line is about  $0.26 \lambda$ . Once more the minimum 50- $\Omega$  SWR occurs quite low in the band, with 29 MHz showing a value of 1.91:1—just barely within the

usual amateur 2:1 standard. The 3.5% bandwidth of 10 meters provides a considerable challenge for a compromise match-line length. However, in principle, the system does work. The quad design is subject to enough variables in the translation into a physical antenna that one could not certify the system without extensive field adjustment of the element lengths and the line length.



The 15-10-meter dual-band common-feed quad has its main function as a study model for observing the performance of the antenna under wide-band conditions. 10 meters provides the major challenge for the performance of the inner quad loops. There are potential outer band loops that must cover a wider bandwidth than the 2.1% offered by 15 meters.

**A 20-15-Meter 2-Element Quad Array Using A Common Feedpoint**

To confirm the general tendencies in wide-band performance of dual-band common-feedpoint quads, we may model a version for 20 and 15 meters. This combination places the challenge for coverage on 20 meters, the outer quad in the

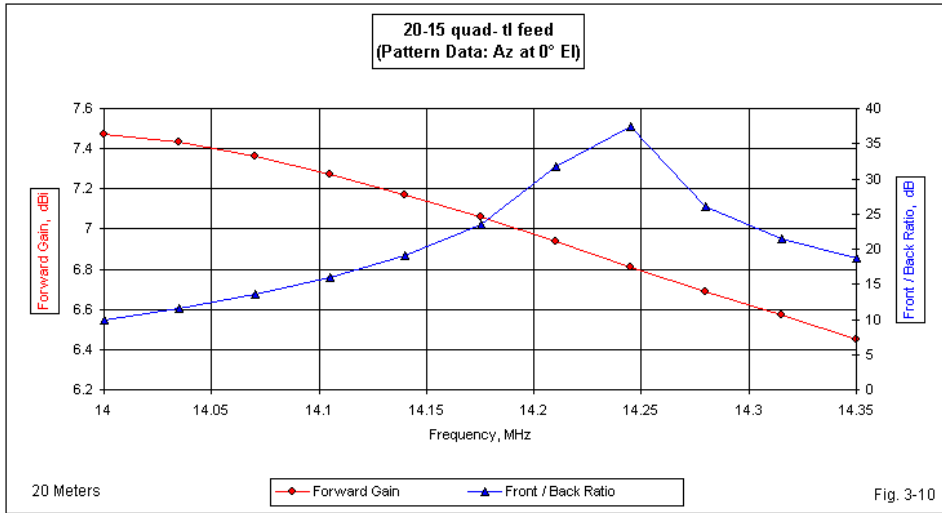
pair. As well, the frequency ratio is higher for this pair of quads: 1.5:1. **Table 3-6** provides the summary data about the performance of the pair.

Table 3-6. 2-Element 2-Band Quad Beams with Joined Driver Elements

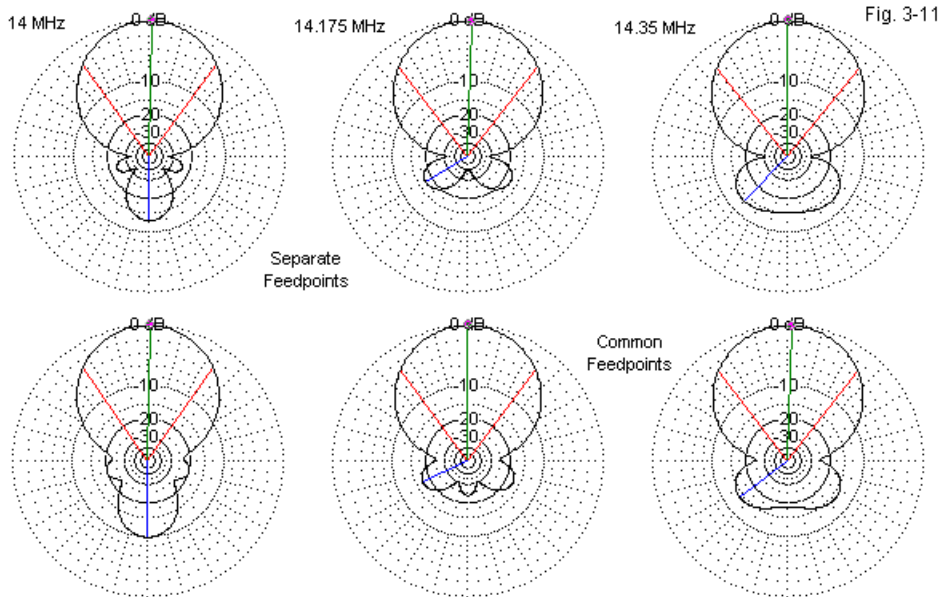
20-15 Meters: Common matchline 170" 75- $\Omega$  cable

20 Meters (Design Frequency 14.14 MHz)		Bandwidth: 2.47%		
Frequency MHz	14.0	14.14	14.175	14.35
Free-Space Gain dBi	7.47	7.17	7.06	6.45
180° Front-Back Ratio dB	9.82	19.02	23.42	18.63
Impedance (R +/- jX) $\Omega$				
Pre-Match Line	74.7 - j39.1	109.5 + j0.3	118.7 + j7.4	157.6 + j29.4
Post-Match Line	48.6 + j17.2	53.8 - j11.6	50.8 - j15.9	38.3 - j23.0
50-Ohm SWR	1.42	1.27	1.37	1.79
15 Meters (Design Frequency 21.19 MHz)		Bandwidth: 2.12%		
Frequency MHz	21.0	21.19	21.225	21.45
Free-Space Gain dBi	7.18	7.01	6.97	6.71
180° Front-Back Ratio dB	15.12	22.79	24.79	24.50
Impedance (R +/- jX) $\Omega$				
Pre-Match Line	78.9 - j26.0	105.5 + j6.2	110.4 + j11.1	139.9 + j37.3
Post-Match Line	79.7 + j25.9	54.8 + j9.8	51.5 + j9.4	37.8 + j11.2
50-Ohm SWR	1.85	1.23	1.21	1.46

As shown in **Fig. 3-10**, the rate of gain decrease across 20 meters is slightly lower for the common-feedpoint quad than for the version using separate feedpoints. However, the front-to-back curve slips further upward in frequency so that the peak value occurs at about 14.25 MHz. This slippage results in a continuing trend toward unequal front-to-back ratios at the band edges relative to the monoband model on which both dual-band quad beams rest.

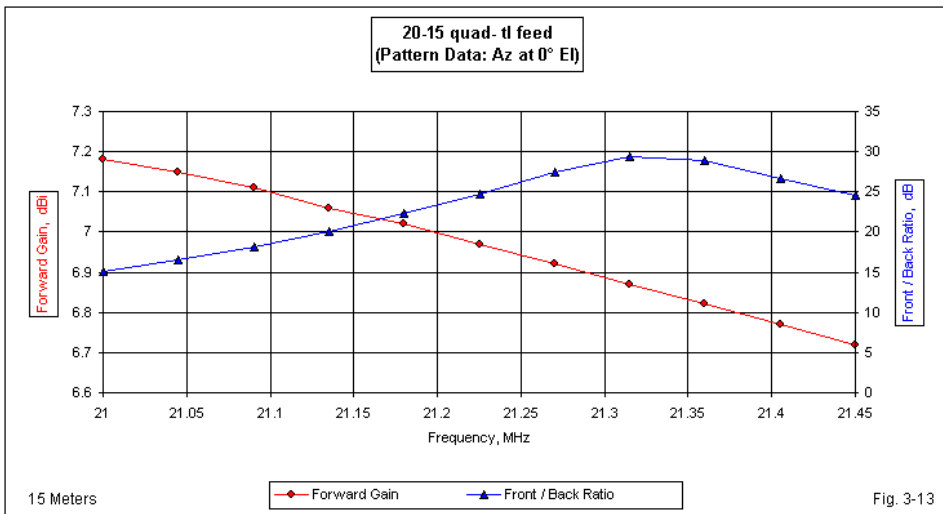
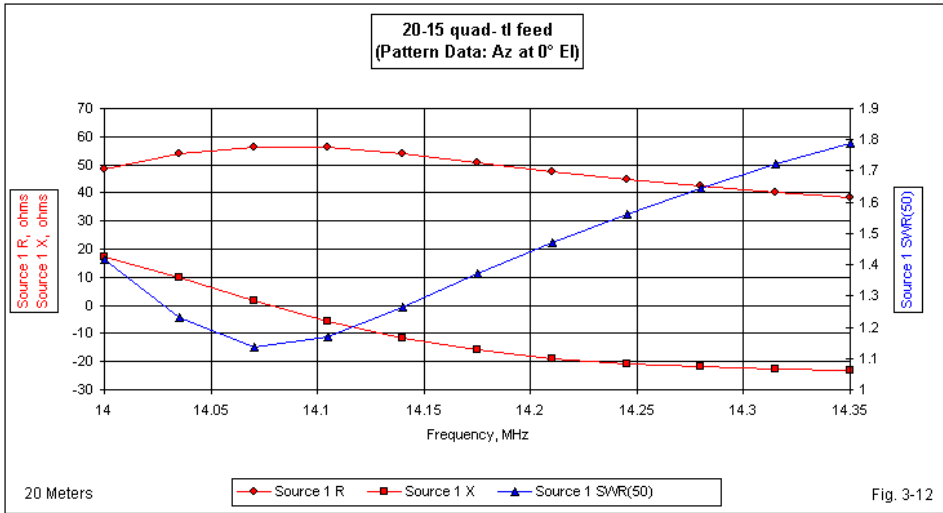


The gallery of free-space E-plane patterns in **Fig. 3-11** shows the degradation of the common-feedpoint rear lobe structure at the low end of 20 meters. The 180° front-to-back ratio has fallen below 10 dB, a value that is considered low even for a 2-element driver-reflector Yagi. It is not clear whether one may further refine the design to move the front-to-back curve lower in the band and still retain adequate forward gain and a usable feedpoint impedance. Remember that among the 2-element quad performance characteristics, the front-to-back ratio undergoes the greatest change over any bandwidth. Normally, one can more easily obtain a feedpoint impedance curve meeting any of the normal limits than one can obtain a broad front-to-back curve that meets any of the usual standards.



20-Meter Free-Space E-Plane Patterns: 2-Band, 2-Element Quad Beams  
with Separate and Common Feedpoints

The pre-match feedpoint impedance values on 20 meters (**Table 3-6**) are comparable to those for any of the other bands, with allowances for the bandwidth when comparing values. A 170" 75- $\Omega$  match-line is about  $0.20 \lambda$  at 14.14 MHz. It provides an adequate set of impedances for a 50- $\Omega$  feedline, although the upper band edge shows an SWR of 1.8:1. As in the case of the 15-10-meter combination, the 20-meter minimum SWR value occurs quite low in the band. See **Fig. 3-12**.



The rate of gain decline on 15 meters in the present combination is lower than when we use separate feedpoints. Although the gain at the low end of 15 meters—as shown in **Fig. 3-13**—is lower than for the separate feedpoint version, the gain values at the upper end of the band are nearly the same. The front-to-back ratio curve shows its anticipated upward shift. The separate-feedpoint version of the array showed a peak front-to-back value near mid-band. With a common feedpoint, the peak value occurs at about 21.3 MHz. As well, the peak value does not reach 30 dB. Obtaining very high and narrow bandwidth values of front-to-back ratio is not operationally very significant. However, it is a measure of the degree to which multi-band and common-feedpoint interactions among wires decrease performance peaks.

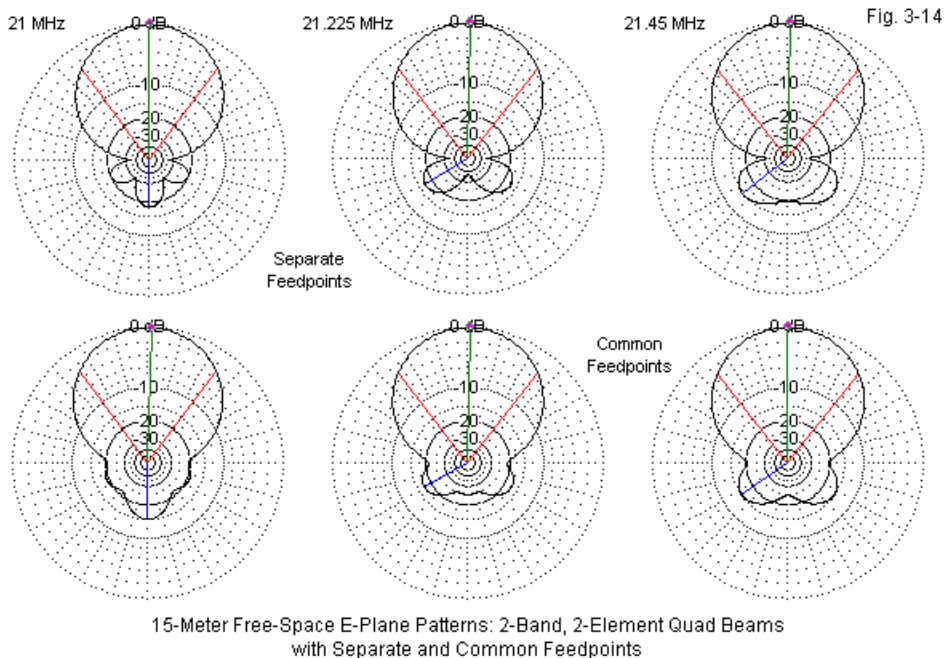
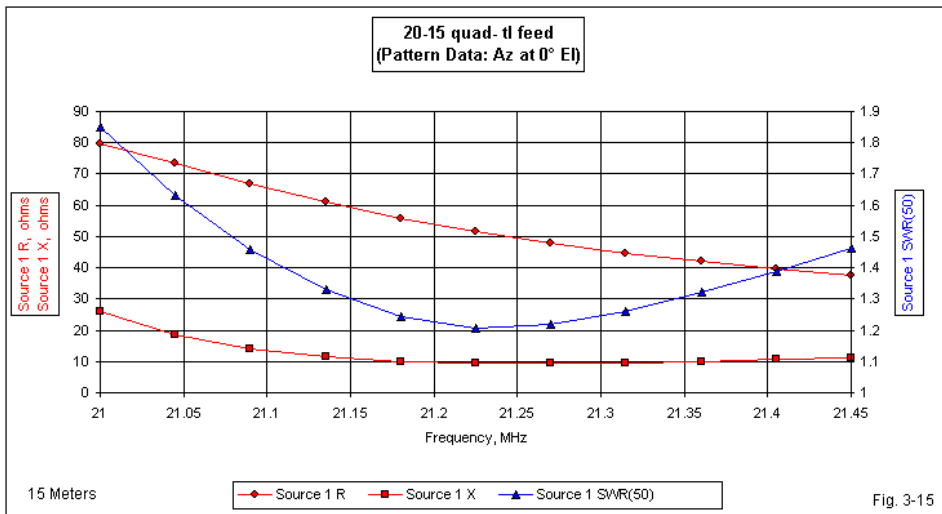


Fig. 3-14

The gallery of free-space E-plane patterns in **Fig. 3-14** provides a glimpse at

the types of azimuth patterns that one might obtain over ground. Our interest is in comparing the patterns for separate feedpoints with those for a common feedpoint. As in the other wide-band dual-band quads in this part, the pattern at the lower edge of the band (here, 15 meters) shows the greatest change of shape relative to patterns for the monoband and separate-feedpoint 15-meter beams. The front-to-back ratio at 21 MHz is down by about 3 dB relative to the separate feedpoint model. Overall, even though the common-feedpoint quad uses a design frequency of 21.19 MHz, performance appears to be best in the SSB portion of the 15-meter band.



The pre-match impedance spread resembles the curves for all of the other bands. The total change in resistance is lower than on 20 meters, while the total change in reactance is about the same. However, on 20 meters, we needed a 170" 75- $\Omega$  line to achieve a manageable 50- $\Omega$  SWR curve across that band. This same line length on 15 meters is about 0.31  $\lambda$ , somewhat longer than ideal for use as a single match-line for a common-feedpoint quad. Nevertheless, as shown in **Fig. 3-15**, the SWR curve fits, with a maximum value of 1.85:1. The peak value

occurs at the low end of the band, and the 50- $\Omega$  SWR never drops below about 1.2:1. Because 20 and 15 meters show peak SWR values at opposite ends of the band, any physical implementation of such a system is likely to require extensive field adjustment to work.

Like the 15-10-meter combination, the 20-15-meter common-feedpoint quad model is most useful in displaying the wide-band behavior of this type of quad. Perhaps the 17-12-meter version is the one most apt for construction, especially since coverage of those bands very often is an afterthought and uses beams of lesser capability than antennas for 20, 15, and 10 meters.

### **Conclusion to the Part 3**

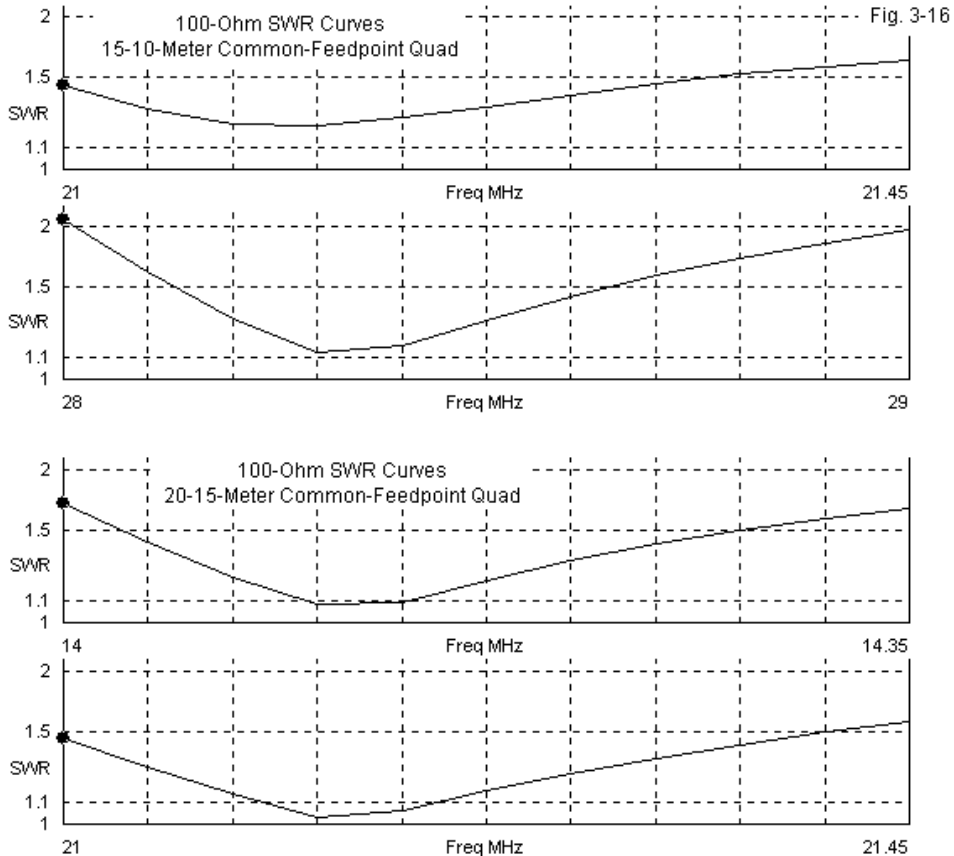
Our efforts to model dual-band common-feedpoint quads have produced a number of results, most of which may be smaller in scope than one might have imagined prior to the step-by-step process that we have gone through to arrive at these models. As we did in Part 2, we retained the spacing of the basic monoband quads and used spider construction so that the angle formed between the reflectors and drivers in a multiband quad remained constant. In all cases, we simply adjusted element lengths to obtain the closest approach possible to monoband performance. Throughout, we used quads with a frequency ratio of at least 1.3:1.

Part 2 showed that the largest physical adjustments to the dimensions of monoband quads occur by virtue of simple proximity of one quad to the next. Despite the use of separate drivers for each of the 2 bands in each assembly, we had to change some of the element lengths to restore performance. The three dual-band quads that meet the basic requirements for this exploration all show the same patterns in physical and performance modifications relative to their monoband origins. The size of outer reflector increases, while outer drivers diminish. Inner reflectors require no change, whereas inner drivers shrink. The resulting performance patterns tend to shift gain and front-to-back curves slightly upward in the band, while allowing the pre-match feedpoint impedances to be near resonance on the original design frequencies. Both feedpoint impedances decrease, the outer by about 10  $\Omega$ , the inner by about 25 to 30  $\Omega$ .

The modification of these models for a common feedpoint required only small dimensional changes. For each combination, the inner reflector for the higher-frequency band remains either fully or close to unchanged. However, every inner driver shows increased length relative to the inner drivers for the quads using separate feedpoints. Likewise, the outer reflectors for the lower frequency show virtually no change in length. As well, the circumferences of the outer drivers for the common-feedpoint quads are very close in overall length to the circumferences of the outer drivers for the versions using separate feedpoints. The inner drivers undergo the most extreme change of any element when converting from separate feedpoints to a common feedpoint, and the amount of change is significant. It ranges from a 6" to a 12" overall circumference increase, depending on the models involved. The lower band element exerts much more influence over the higher band driver, despite (or perhaps because of) the distortion in the lower-band driver shape. At the same time, both types of dual band quads use independent loops for reflector elements. In general, the interactions between the reflector elements do not change significantly when moving from separately fed drivers to drivers with a common feedpoint.

Adding a common feedpoint for a dual-band quad does affect the performance to some degree. The upward shift in the performance curves for gain and the front-to-back ratio continues the progression that we first saw in 2-band quads with separate feedpoints. One result on wider amateur bands, such as 20, 15, and 10 meters, is a degradation of the rear lobe confinement at the low end of each band.

In contrast, the near resonant feedpoint impedance at the design frequencies turned out to be very nearly the same for both bands of operation. The value of the resistive component is the value associated with the outer quad of separate-feedpoint dual-band quads. Although interesting, this result has limited utility if the impedance requires transformation in order to match the characteristic impedance of the main feedline. In the course of developing the common-feedpoint models, we saw that a single match-line length might serve 2 bands manageably, if not ideally.



The single match-line for a 50- $\Omega$  main feedline is not a necessary condition of common-feedpoint quad operation. It is possible to feed the quads with a balanced, shielded parallel line composed of series-connected lengths of 50- $\Omega$  cable. As the SWR curves for the two wide-band models show in **Fig. 3-16**, only 10 meters is wide enough to press the limits of the curve, even though the design frequency impedance is close to 120  $\Omega$ . The direct feed system has the advantage of being applicable to common-feed multi-band quads covering 3 or

more bands, so long as the impedance curves on each band are similar to those shown for the dual-band models.

The models that we chose as our baseline are not necessarily the best designs to implement for a multi-band quad using either separate or common feedpoints. I selected them because they presented the widest operating bandwidth of any 2-element quads using common wire elements. They offered us the best chance of seeing the dimension and performance changes that 2-band operation might create, while still maintaining recognizable performance curves. Along the way, the feedpoint impedance was not the limiting factor. The front-to-back ratio remains the quad's most changeable parameter as we scan any of the wider upper-HF amateur bands. If we wish full band coverage of 20, 15, or 10 meters, then we must decide if a relatively low front-to-back ratio at one band edge or the other is a satisfactory condition. If we only wish to cover a portion of these wider bands, then the 2-element quad becomes competitive with a 3-element short boom monoband Yagi and highly competitive with small multi-band Yagis using considerably longer booms.

One limiting factor in this entire journey into the dual-band quad and its feeding method has been the restriction of the frequency ratio between the two bands covered by the array. In all cases, we selected a minimum frequency ratio of 1.3:1. Hence, we have sample quads for 17 and 12, for 20 and 15, and for 15 and 10. The result of these selections has been the development of determinate but manageable modifications to the initial monoband designs, with resulting workable designs for dual-band quad beams. Still, any quad designer would carry away a number of questions if we ended the exploration at this point. The key question might have this form: How does the behavior of adjacent-band dual quads differ from the quads developed so far?

Five-band 2-element quad designs certainly exist in both homemade and commercially made varieties. Therefore, some designers appear either to have mastered any limitations presented by adjacent-band loops on a quad or to be satisfied with some form of lesser performance. If there are performance deficiencies, they most likely involve the front-to-back ratio and the feedpoint impedance. We have already seen that the front-to-back curve may be somewhat

steeper in a dual band quad than in the monoband version. The steeper curve results in lower front-to-back values at the band edges. Either additionally or alternatively, the feedpoint impedance may take a value that reduces the width of the 2:1 SWR passband.

Whether the design has mastered the art of handling adjacent bands in a quad or reduces performance in one or another way, we shall not be wasting our time to explore adjacent-band quad behavior somewhat more extensively.

## Chapter 4

### *Sneaking Up on 2-Element Common-Feed Quads*

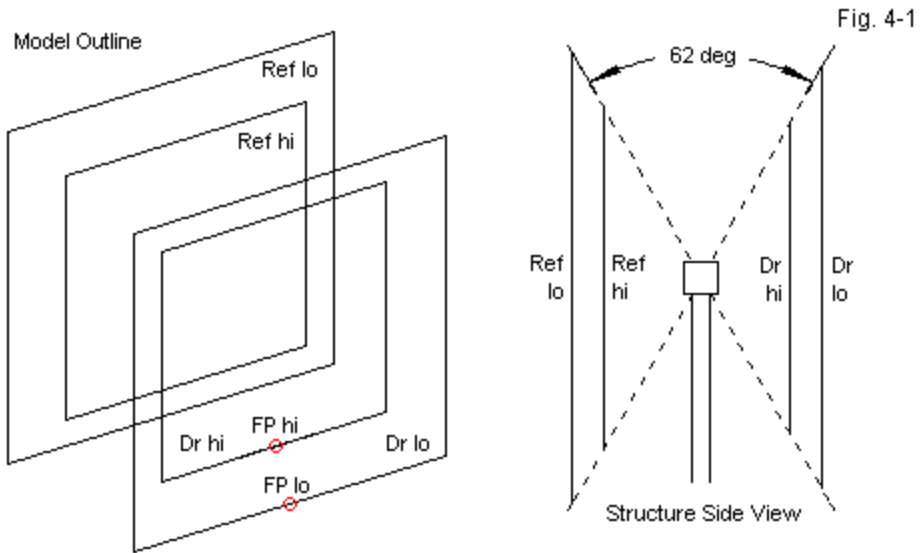
#### Part 4: Adjacent-Band Quad Behavior

In the study of quads that led up to some notes on dual-band antennas using a common feedpoint, I intentionally by-passed an important question. Dual-band quads required a frequency ratio of at least 1.3:1 for inclusion in the earlier notes. As a result, I omitted combinations such as 20 and 17 meters or 12 and 10 meters. The notes to this point have reached a number of conclusions about quad behavior based on consistent trends shown by the models that I did use. Foremost among the results was the observation that most of the major performance and dimension changes resulted from the simple proximity of the element loops, even when using separate feedpoints. The major dimensional change that occurs when using a common feedpoint instead of separate feedpoints is the lengthening of the inner or higher-frequency driver loop.

We are now positioned to fill in the gap in our exploration of dual-band quad behavior. The study can restrict itself to quads with separate feedpoints on each band, thus simplifying the required modeling. Most of the dimension and performance behaviors that we shall find interesting occur using separate feedpoints. **Fig. 4-1** shows the general parameters of the models used in this sequence of examinations. Of course, only one of the two feedpoints shown in the sketch will be active at any one time.

Like the earlier sequence of quad models, the new set will rest on the monoband quad designs derived by equations, as described in Part 1 of that study. Dual band models will presume spider construction, which calls for an angle of about  $62^\circ$  between the driver and the reflector support arms. Indeed, the only restriction that we shall remove is the minimum frequency ratio between bands. Hence, we can now see what trends develop as we change the ratio. By using combinations of 17 and 12 meters, 15 and 10 meters, and 20 and 15 meters, we encountered relatively small interactions that left the performance curves quite similar to those for the monoband beams, with variations only in the limiting values for each band. We also noted small variations that depended upon whether a loop was part of an inner or higher frequency beam or was part

of an outer or lower frequency beam.



General Outlines of 2-Element, 2-Band Quad Beams with Separate Feeds

To the collection of dual-band quads previously used, we may now add 4 other combinations: 20-17, 17-15, 15-12, and 12-10, where each designation is for an amateur band pair. We shall divide the trends into 2 parts. The first set of trends will involve the physical dimensions. The second (and longer) exploration will deal with performance.

### General Notes on Dual-Band Quad Dimensions

**Table 4-1** provides a summary of the dimensions, starting with those of the monoband beams. Along side each monoband beam are the dimensions of the loops and the spacing for all of the dual-band quads that we shall examine. As in past notes, all dimensions are in inches. Multiply the values by 0.0254 to obtain

dimensions in meters. The loop dimensions appear as circumferences in this table. A loop side is the value shown divided by 4. Spacing values are the distance between the front and rear loops for each band. As I did for the monoband beams, I used 14.14, 21.19, and 28.4 MHz as offset design frequencies so as to level the band-edge front-to-back ratio values to the degree possible. 17 and 12 meters are narrow enough to allow the band center frequency to serve also as the design frequency. All drivers are resonant at the design frequency within about  $\pm j1 \Omega$  of remnant reactance. In anticipation of potential trends, I extended the degree of element size precision to 0.05". All values of element spacing remain constant between the monoband and dual-band quads.

The dual-band quads are listed according to the bands covered, that is, as 20-17, 20-15, etc. Each combination shows the loop circumferences that result in a peak front-to-back ratio and near resonance at the design frequencies. The entries marked "d-Mono" show the difference between the required circumference of the element in its place within the dual-band quad and the corresponding monoband element. A positive value means that the dual-quad element is longer; a negative value means that it is shorter.

The dual quads fall into 2 groups. The 20-15, 17-12, and 15-10 models are wide, that is, have a greater spacing between the two element sets due to the larger frequency ratio. The ratios range from 1.34:1 up to 1.5:1. These patterns replicate what we uncovered in the previous study. If a driver is an outer (or lower frequency) element, then it will increase in length relative to the monoband value. For the upper HF bands used here, the amount and the range is small: 2.2 to 3 inches. If the driver is an inner (or higher frequency) element, then its length will decrease relative to a monoband quad. Again the amount and range are small: 3.8 to 4.3 inches.

Quad Dimensions: Monoband and Dual-Band										Table 4-1
All element dimensions are the circumference in inches.										
Design-Frequency Ratio:		1.499:1	1.377:1	1.340:1	1.281:1	1.170:1	1.177:1	1.139:1		
Version:		Monoband	20-15	17-12	15-10	20-17	17-15	15-12	12-10	
Band	Parameter									
20	Driver	842.40	844.80			846.40				
d-Mono			2.40			4.00				
	Reflector	886.64	880.40			874.80				
d-Mono			-6.24			-11.84				
	Spacing	128.33	128.34			128.34				
17	Driver	658.24		661.20		653.20	663.60			
d-Mono				2.96		-5.04	5.36			
	Reflector	693.92		687.20		695.20	677.20			
d-Mono				-6.72		1.28	-16.72			
	Spacing	101.39		101.40		101.40	101.40			
15	Driver	563.12	558.80		565.36		557.20	567.60		
d-Mono			-4.32		2.24		-5.92	4.48		
	Reflector	594.32	594.32		586.80		596.80	580.00		
d-Mono			0.00		-7.52		2.48	-14.32		
	Spacing	87.24	87.24		87.24		87.24	87.24		
12	Driver	478.72		474.80				473.60	483.60	
d-Mono				-3.92				-5.12	4.88	
	Reflector	505.92		505.92				508.00	489.20	
d-Mono				0.00				2.08	-16.72	
	Spacing	74.53		74.54				74.54	74.54	
10	Driver	420.64			416.80				415.20	
d-Mono					-3.84				-5.44	
	Reflector	444.96			444.96				448.00	
d-Mono					0.00				3.04	
	Spacing	65.71			65.70				65.70	

If a reflector is an outer loop, then it will be shorter than the corresponding monoband reflector. The amount is greater than for the other affected elements: 6.2 to 7.5 inches. In contrast, for the wide dual quads with higher frequency ratios, if a reflector is an inner loop, it requires no change from the monoband length.

The other group of dual quads includes 20-17, 17-15, 15-12, and 12-10 meters. The frequency ratios for this set run from a low value of 1.14:1 to a high value of 1.28:1. The average ratio is 1.21:1, in contrast to the average ratio for

the wide group: 1.42:1. The result, of course, is a 2:1 ratio of ratios.

For the narrow group, if a driver is an outer loop, then it increases in size relative to the monoband quad element and roughly in proportion to the ratio of ratios. That is, the driver range of increase is 4.0 to 5.3 inches. If the reflector is an outer loop, then it decreases in size, not only with reference to the monoband antenna, but as well by a factor greater than the ratio of ratios. Outer reflectors for the narrow group decrease their circumferences by 12 to 17 inches relative to the monoband models. In general, the closer the spacing between the elements of a dual-band quad, the more rapidly that a reflector becomes shorter to maintain the same performance points.

If a reflector is an inner loop, the wide dual-band quads required no change in circumference. However, with closer spacing, the narrow group of dual-band quads shows a small amount and range of increase relative to the monoband quads: 1.3 to 3 inches. Like the wide-group drivers, the narrow group drivers—when forming inside loops—require shortening relative to monoband values. However, the amount is less than proportional to the ratio of ratios. The range of 5.1 to 5.5 inches is only about 30% greater than the amounts required by the wide group.

Physically, then, the elements of dual-band quads show a varied pattern of changes as we shrink the spacing between loops by creating beams for adjacent bands. Some changes are roughly proportional to the ratio of ratios, while others are not. However, trends that first appeared for the wide group continue in the same direction as we decrease the loop spacing by using adjacent bands. (Of course, the one exception is the inner reflector, which showed no trend for the wide-group dual quads.)

Within reason, one might use the patterns shown in **Table 4-1** as a design aid if developing a dual-band quad. The exact amounts of change will themselves change if we alter the element diameter, that is, the wire size. A further variable prevents me from trying to codify the patterns into a set of design equations. The performance points listed as criteria for success at the design frequencies—peak front-to-back ratio and driver resonance—are not

perfect. The attainment of the peak front-to-back ratio at the design frequency is a judgment call within the limits of the increments of side-length change in the test models. As the frequency goes up, an increment of 0.05" per half-side length may not be sufficient to place the peak with precision. Operationally, such small departures from perfection are superfluous worries. However, they are enough to preclude final codification. Even regression analysis is not feasible, since it would apply to only one fixed wire size. A true set of design equations would require a survey that included a wide range of wire sizes. Such a survey is theoretically possible, and the results would amount to an extension of the existing monoband design equations, showing the modification of a monoband design for a dual-band quad for frequency ratios of perhaps 1.1:1 up to 1.5:1. However, the work involved so far does not seem to yield a sufficiently useful result.

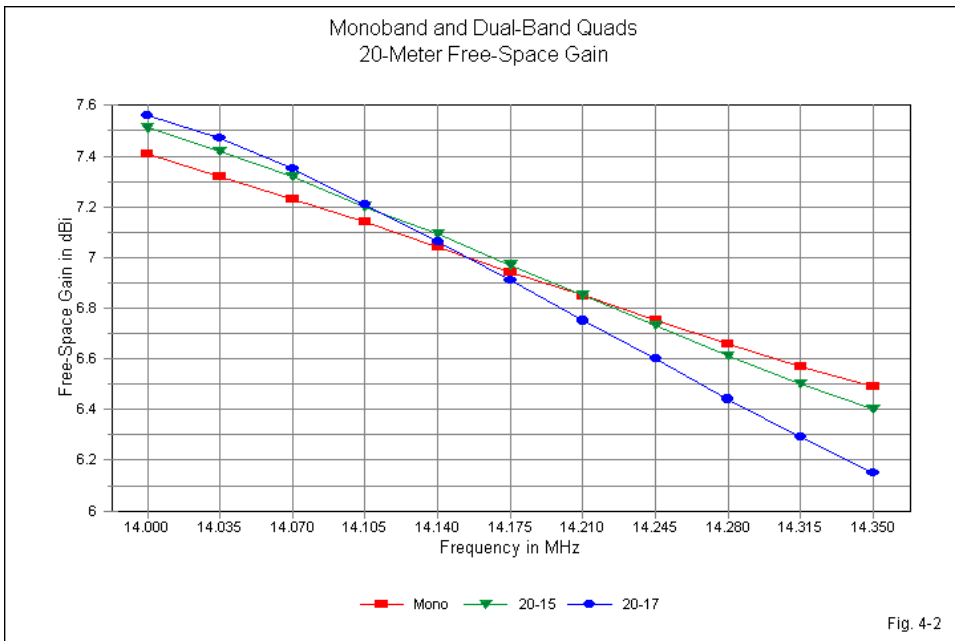
### **Band-by-Band Performance Trends**

The performance side of our adjacent-band behavior question requires a gallery of graphs. For each loop tuned to the design frequency on each of the upper-HF amateur bands, I plotted the following results across the band: gain, 180° front-to-back ratio, feedpoint resistance, and feedpoint reactance. Hence, there are 5 graphs for each parameter, one for each band. Each graph also contains the curve for the monoband quad as a reference. In all cases we shall be more interested in the slope or general shape of a curve than in precise values.

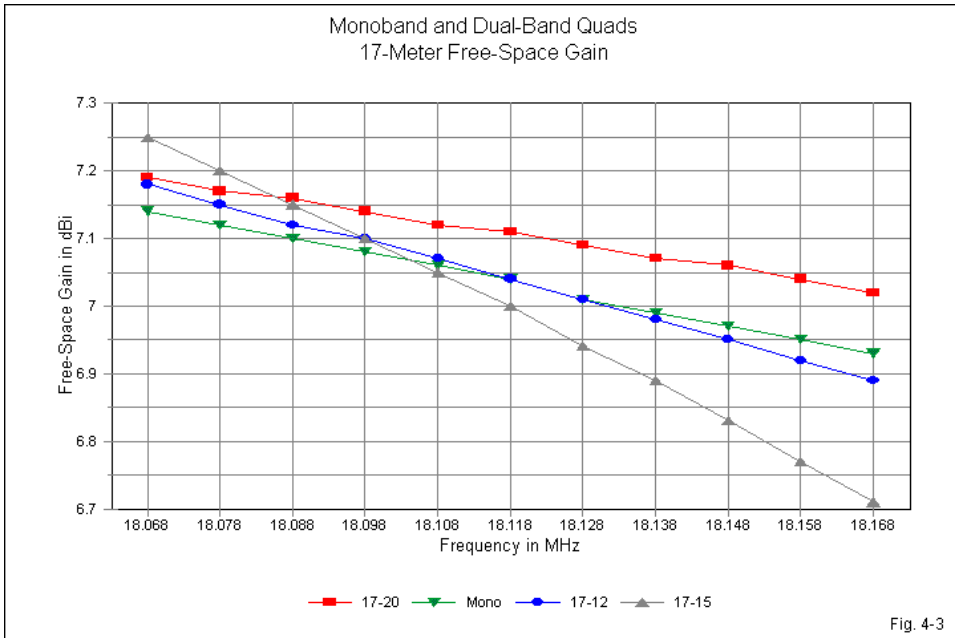
Each graph covers a different territory because not all wide and narrow group potentials appear in every graph. For example, the 20-meter graphs will show only 3 curves, and the two dual-band curves will apply only to loops that are outer elements, that is, lower in frequency than the accompanying band. 10-meter graphs show just the opposite in their 3 lines. Besides the monoband curve, we shall find only instances where the 10-meter elements are inner or higher frequency elements. Only 15 meters shows the full spectrum of potentials, with 2 outer loop and 2 inner loop cases to accompany the monoband curve.

The dimensional table used a single designation for each combination, for instance, 17-12. The graph legends use a modification of that system. The band of interest to the graph always appears first in the dual-band quad designation. Therefore, in the 17-meter graphs, we shall find the label 17-12, but in the 12-meter graph, we shall designate the same dual-band quad as 12-17.

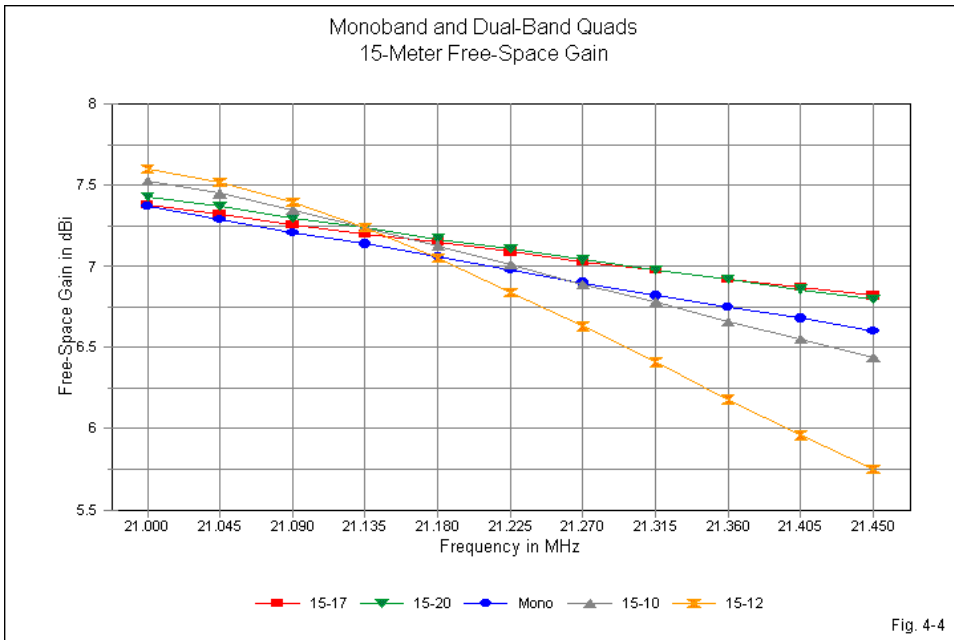
### Gain



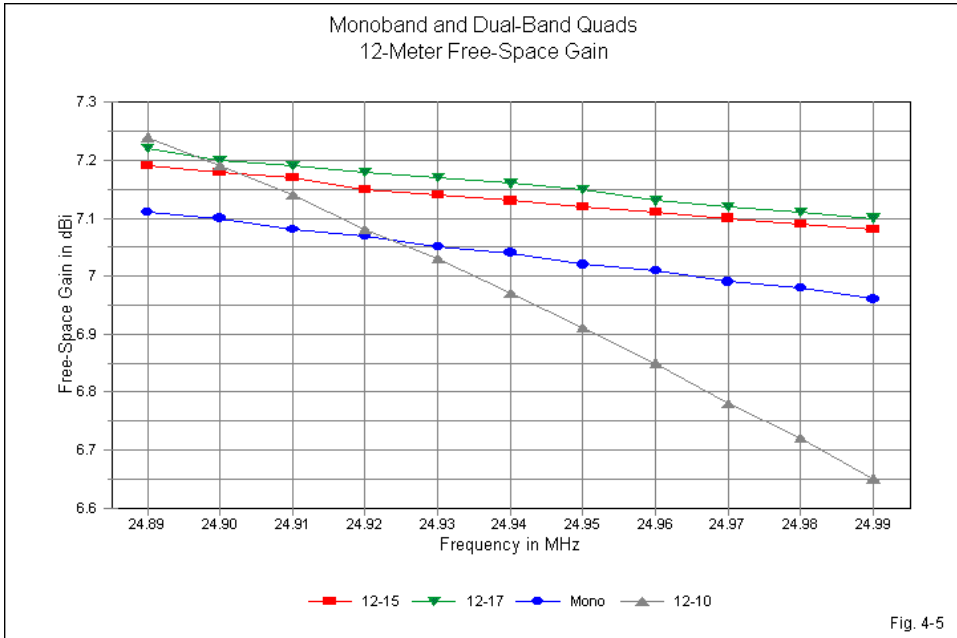
Both dual-band 20-meter curves in **Fig. 4-2** refer to outer elements in their pairs. The monoband curve shows the lowest rate of gain decrease across the band. Note that as we add a higher band—even widely separated—the rate of gain decrease becomes steeper. In addition, as we reduce the space between the 20-meter elements and the second set in the pair, the rate of gain decrease becomes even greater.



The 17-meter gain chart (**Fig. 4-3**) includes one instance where 17-meters is an inner element. In this case, the rate of gain decrease is slightly less than the rate for the monoband quad. For the two cases in which the 17-meter elements are outer loops, the rate of gain decrease is higher than the monoband rate. Once more, the more closely spaced elements result in a more rapid decline in gain than for the more widely spaced elements. Indeed, the slope angles for the two outer-loop cases are dramatic. In passing, we may also note that the monoband and the two outer loop curves do not vary in gain by much at the design frequency. However, the inner-loop case shows a numerically noticeable higher gain value (more than 0.1 dB).

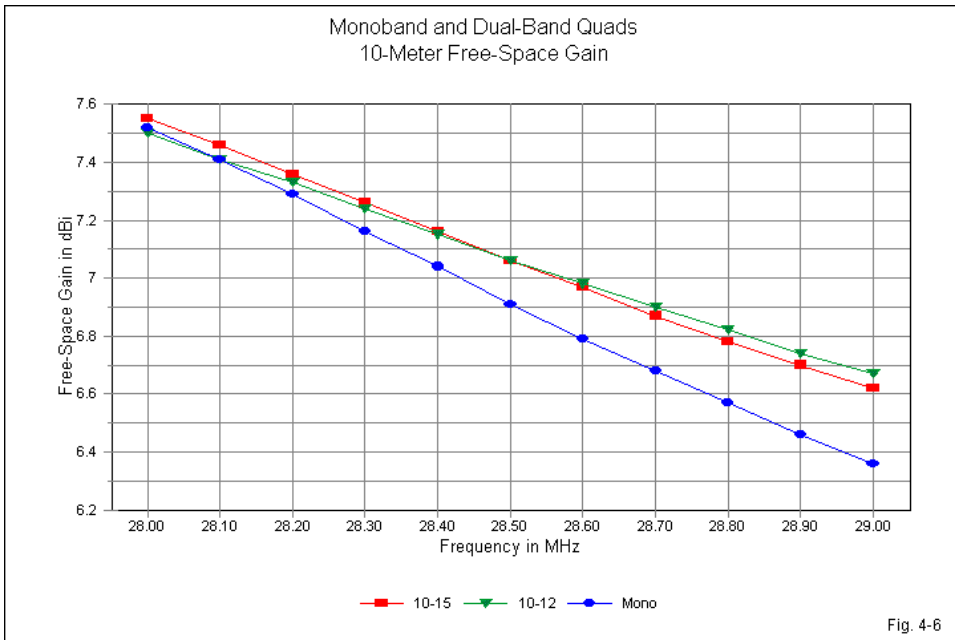


One reason for including graphs of the small 17- and 12-meter bands is that they show some fine detail better than graphs for the wider amateur bands. **Fig. 4-4** covers the gain situation on 15 meters, but the wide range of values may obscure some of the detail. When we pair 15 and 12 meters, the outer 15-meter loops show a very steep gain curve with a total gain decrease of nearly 2 dB across the band. When we pair 15 meters with 10 meters, the gain decrease range drops to just over 1 dB. The two cases where 15 meters forms the inner loop set (15-17 and 15-20) show gain decrease curves that are shallower than the monoband curve. With the scales used, it is difficult to see, but the 15-17 curve is slightly shallower than the 15-20 curve. Both inner loop curves show a slightly higher gain at the design frequency than the monoband quad. In short, the 15-meter gain curves reflect all of the trends shown for the other bands surveyed so far.



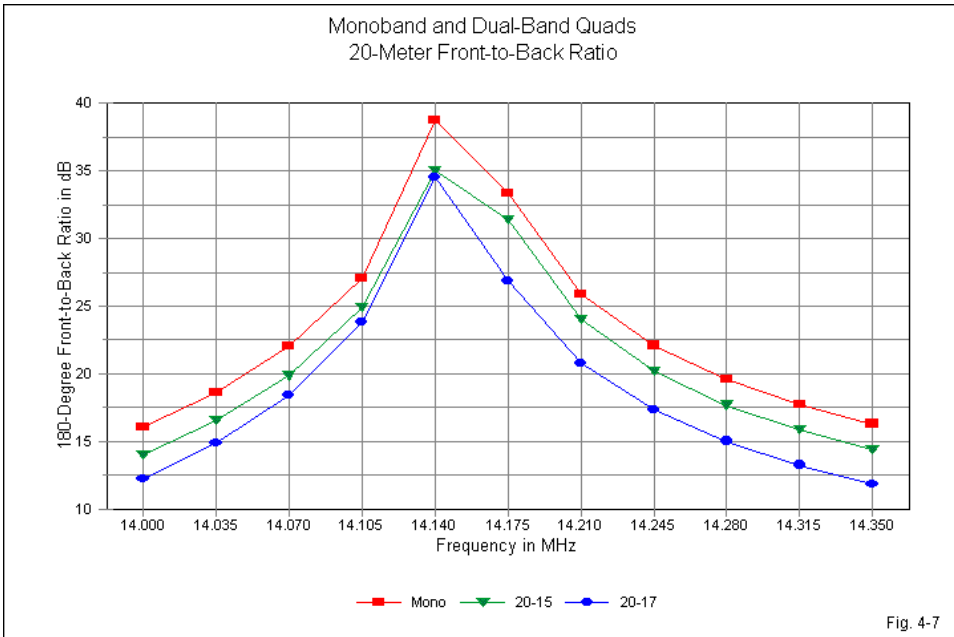
The 12-meter gain curves in **Fig. 4-5** provide us with only 1 case where the 12-meter loops serve as outer elements. The narrow spaced 12-10 combination produces a very steep gain decrease curve, even over the 100 kHz of the band. When the 12-meter elements are inner loops, they show slightly higher gain than the monoband quad. However, the curves for the 2 dual-band quads are too close together for any definitive conclusions regarding relative curve flatness.

Besides the monoband reference gain curve, the 10-meter dual-quad gain curves in **Fig. 4-6** are limited to cases where the 10-meter elements are inner loops. At 28.4 MHz, both dual-quad curves show a higher gain than the monoband quad. As well, the more widely spaced 10-15 combination shows a steeper curve than the narrow 10-12-meter pair.

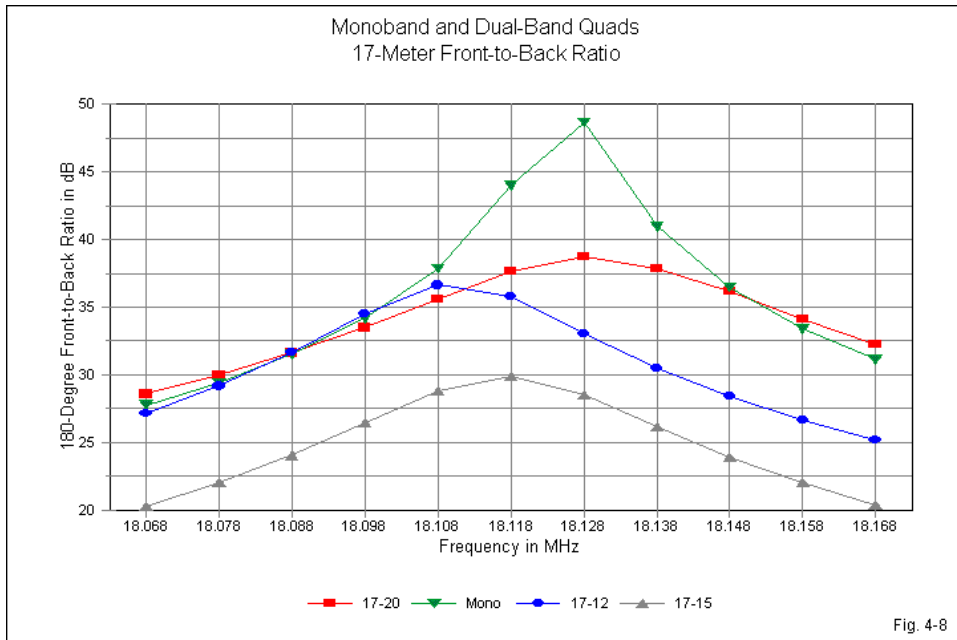


In general, then, the gain of inner loops at the design frequency is higher than the monoband value, and the rate of decrease is lower. Using adjacent amateur bands in a dual-quad results in a lower rate of inner-element gain decrease compared to using bands that more widely spaced. The situation for the outer loops in a dual quad is the reverse. Although the gain value at the design frequency does not vary significantly from the monoband value, the outer-loop gain curves are shallower. The closer the element spacing from one band to the other, the steeper the curve. However, outer-loop advantages over the monoband quad are generally too small to be operationally significant.

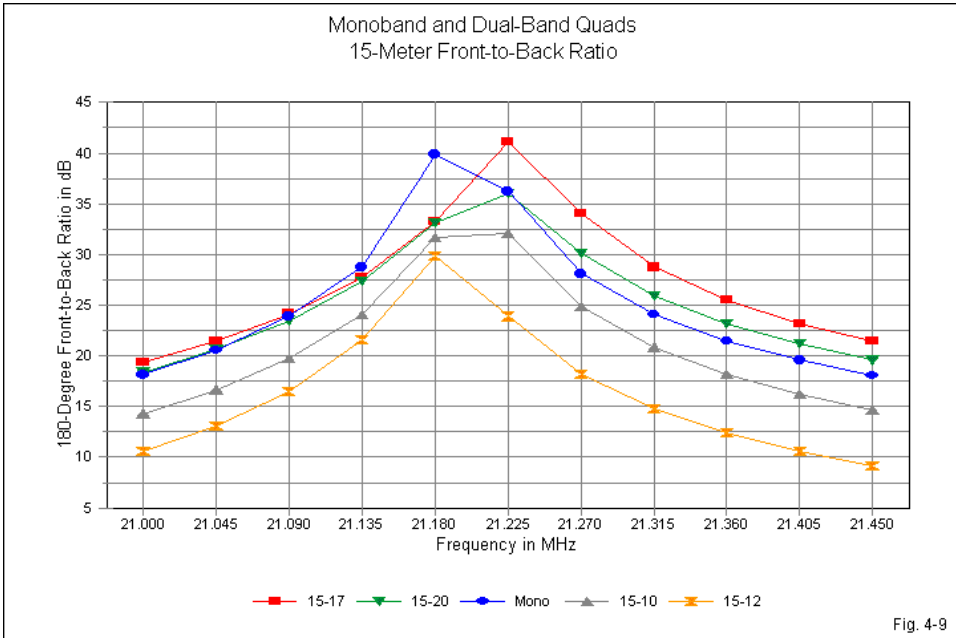
### 180° Front-to-Back Ratio



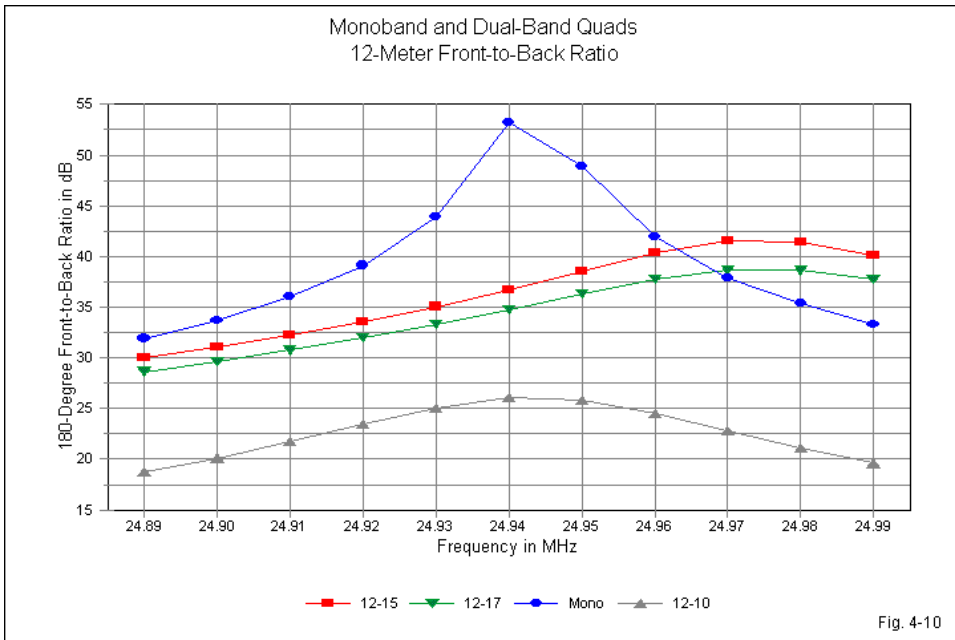
Within the limits of modeling described earlier, the 20-meter front-to-back curves are nearly congruent, as shown in **Fig. 4-7**. The monoband curve shows the highest peak value and the highest band-edge values. The dual-band quads show slightly lower peak values (although that appearance may be illusory, given the narrow-bandwidth of the actual peak). They also show very comparable band-edge values. However, as we decrease the frequency ratio of the 2 bands, the band-edge values decrease. Note that these remarks apply to the 20-meter loops as outer elements in the band pairings.



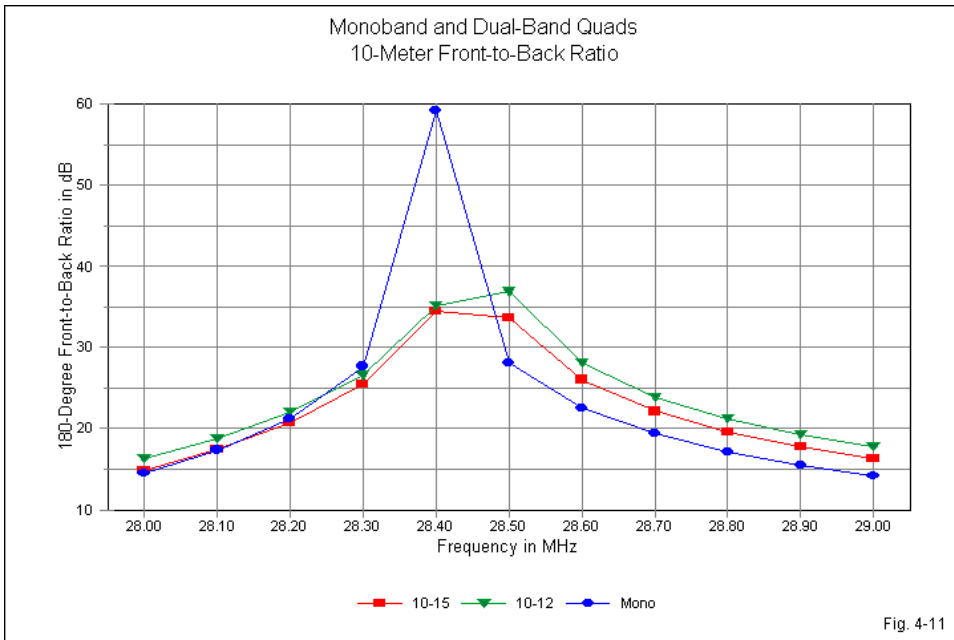
The front-to-back curves for the very small 17-meter band show the limitations of the data generation technique in **Fig. 4-8**. The divisions are 0.01 MHz apart, that is, less than 1/3 the increments used on 20 meters. Hence, peak front-to-back ratio displacements that would be invisible on 20 meters show clearly on the expanded 17-meter scale. The one instance where the 17-meter loops are inner elements (17-20) shows a lower peak value but higher band-edge values than the monoband curve. In both cases where the 17-meter elements are outer loop sets, the band-edge values are lower than the monoband values. As well, as the frequency ratio decreases, the overall front-to-back performance suffers, as shown by the 17-15 curve.



As we increase the quad frequency, we also encounter limitations in placing front-to-back peaks within the minimum increment of element length change. Hence, not all peaks appear at the 21.19-MHz design frequency, as shown in **Fig. 4-9**. Nevertheless, the curves continue to confirm and expand the trends already noted. When 15-meter elements are the inner loops, they show slightly higher band-edge values than the monoband beam—although not by an operationally significant amount. As well, the lower the dual-quad frequency ratio, the higher will be the band-edge front-to-back ratio. On the other side of the monoband curve, when the 15-meter elements are outer loops, we find significantly lower band-edge front-to-back values. The lower the frequency ratio when 15-meter elements are outer loops, the worse the overall front-to-back curve.



Unfortunately, the 12-meter band is too small for the graph in **Fig. 4-10** to tell us much in light of the modeling limitations imposed. The monoband curve and the 12-10 curve are well aligned. The 12-10 curve places the 12-meter elements as outer loops and the frequency ratio is small. Hence, we see the typical degradation of the front-to-back curve. Both instances where the 12-meter elements serve as inner loops have displaced peaks, so we can only guess that the band-edge values would be higher than the monoband values if the curves aligned perfectly. However, it is clear that the 12-meter curve for the 12-15 pair is generally higher than the 12-17 curve with which it aligns. Of course, the frequency ratio of the 12-15 pair is lower than the ratio for the 12-17 pair.



The misalignment of the 12-meter monoband curve with the 2 inner-loop cases is not quite accidental. The 10-meter curves appear in **Fig. 4-11**. The monoband quad model achieves a very high and steep peak value at the 28.4-MHz design frequency. The 10-12 and 10-15 dual quad pairs have peaks of unknown value near 28.45 MHz. Drawing the peak front-to-back ratio downward to the design frequency is a tedious task requiring exceptionally small increments of reflector length change. I have allowed the peak displacement since such tiny changes would be beyond the limits of most home shop facilities. Nevertheless, both inner loop 10-meters element sets show higher band-edge front-to-back values than the monoband quad, if only by a little. As well, the pair with the lower frequency ratio shows even more slightly higher band-edge values.

For all of the operating parameters, we have three interests in the curves

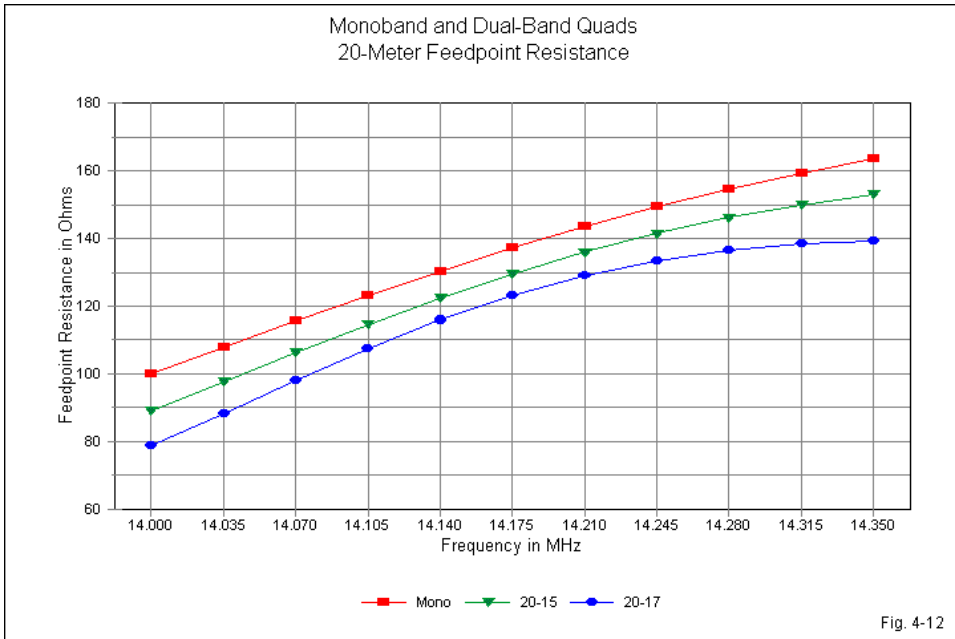
that appear in the graphs. First, we are interested in whether or not the curves for one band confirm the trends shown by the curves for another band. Within the limits of the sets, we can generally respond affirmatively, with no exceptions so far.

Second, we are interested in the differences in the performance levels depending on whether the elements for a given band form the inner or the outer set of quad loops. Throughout the front-to-back sequence, we have seen the outer loop sets generally yield poorer band-edge front-to-back values than the monoband beam. Because a quad front-to-back peak is so high, but only for a very narrow bandwidth, the band-edge values form a better overall marker of performance in this dimension than the peak value. Remember that a typical short-boom 3-element Yagi may be able to provide a 20-dB front-to-back ratio across any of the wider amateur bands. We tend to obtain slightly better band-edge front-to-back performance when the loops for a band are inner elements for a dual-band quad.

Finally, we are interested in the differences created by the frequency ratio between the loop sets of a dual-band quad. For outer loop sets, decreasing the frequency ratio between bands covered by the beam can result in a significant degradation of the front-to-back ratio across the band. Even the wider frequency ratios, such as between 10 and 15 meters, can yield noticeable decreases in the band-edge front-to-back performance. In contrast, when the loop set is an inner element set, the changes are operationally small, with numerically noticeable improvements in the band-edge front-to-back performance as we decrease the frequency ratio.

### *Feedpoint Resistance*

The next set of graphs will reveal the trends that we can expect from the feedpoint resistance as we move the position of elements from outer to inner locations in a dual-band quad and as we alter the frequency ratio between the loop sets in a pair. However, a fuller understanding of the overall feedpoint impedance requires attention to this section and to the next section that covers feedpoint reactance.



Both dual-quad curves for 20 meters in **Fig. 4-12** represent outer locations relative to the other band involved. Both curves show a systematic decrease in the feedpoint resistance relative to the monoband value. The lower the frequency ratio between the bands, the greater the decrease in feedpoint resistance in the outer loop. As well, the lower frequency ratio produces a less linear curve.

The 17-meter resistance curves in **Fig. 4-13** tend to confirm the patterns that we noted for the 20-meter resistance curves. As well, the new graph introduces the first instance of a curve for the loop set using an inner position. The curve is for a low frequency ratio (17-20), and it shows a progression of resistance values that are also lower than those for the monoband quad. In fact, they are the lowest in the graph.

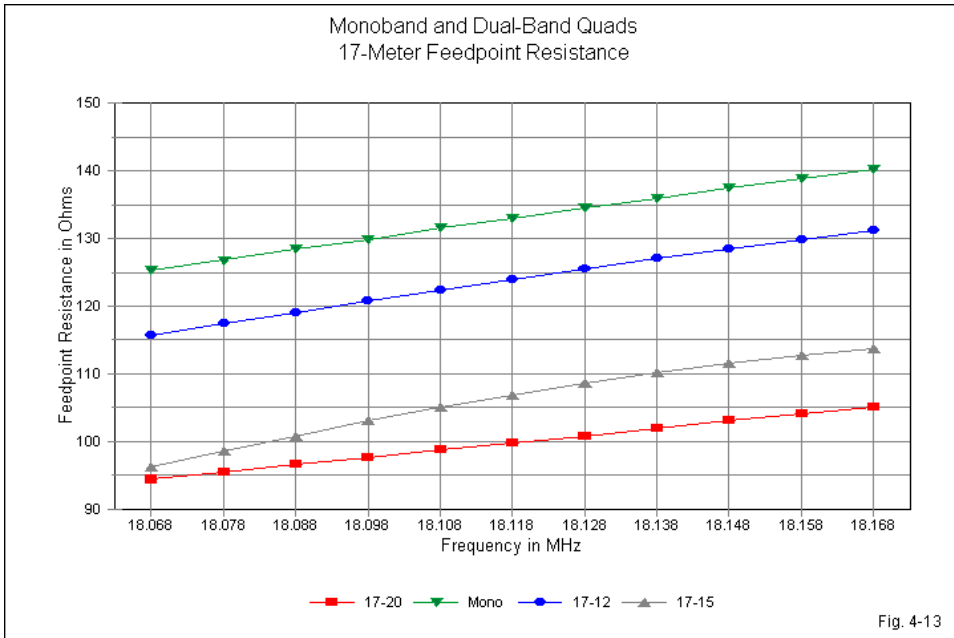
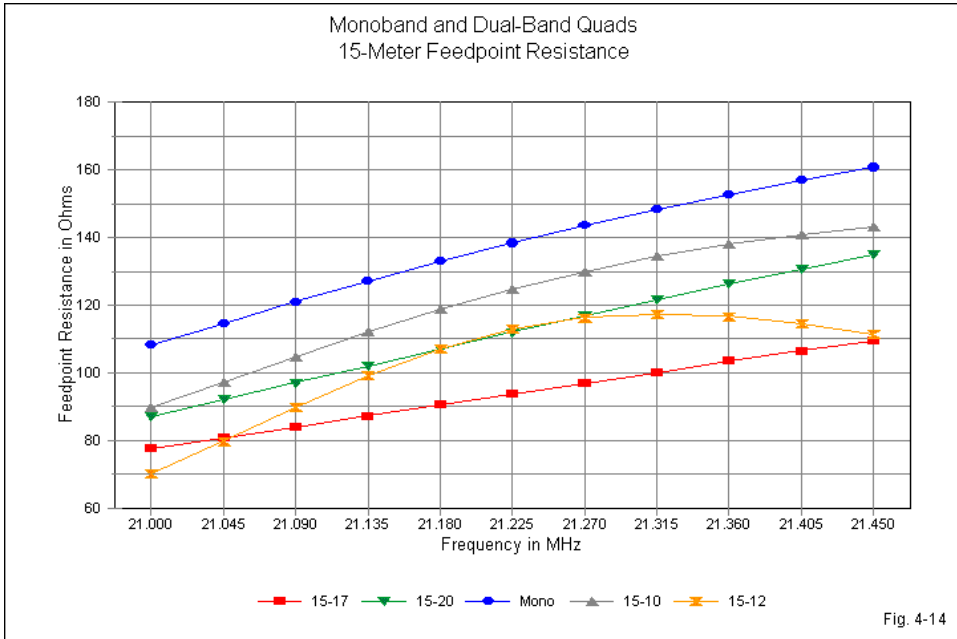
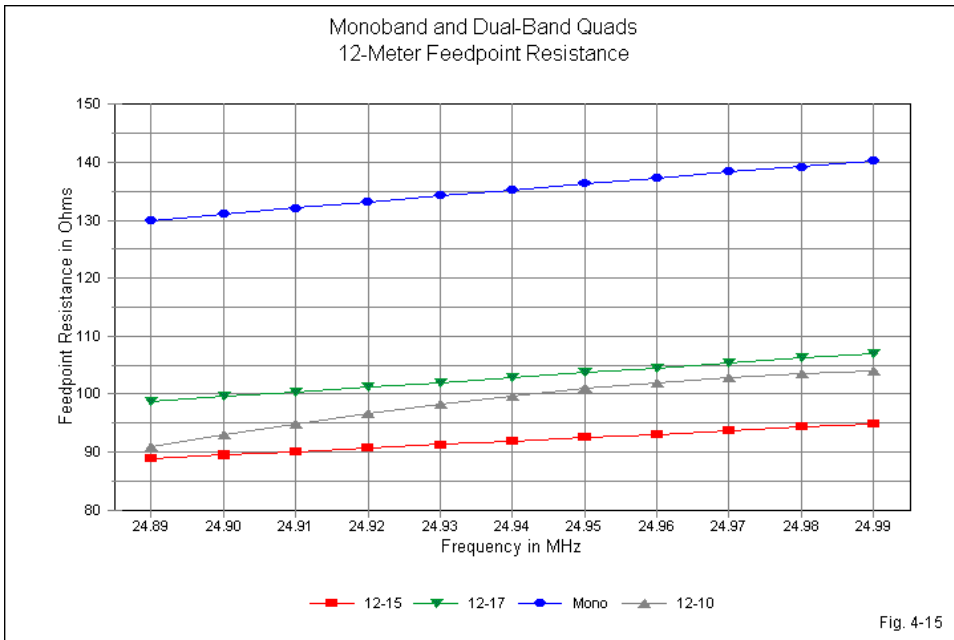


**Fig. 4-14** provides the resistance curves for 15 meters. All dual-band quad resistance values are well below the monoband values. When the 15-meter elements form outer loops, they show the same patterns that we saw on 20 and 17 meters. The curves show a growing non-linearity as we decrease the frequency ratio between the bands, and show in addition a greater reduction in value as we decrease the frequency ratio. When the 15-meter elements form inner loops, the curves are more linear, but decreasing the frequency ratio increases the reduction in the resistance values relative to the monoband quad.



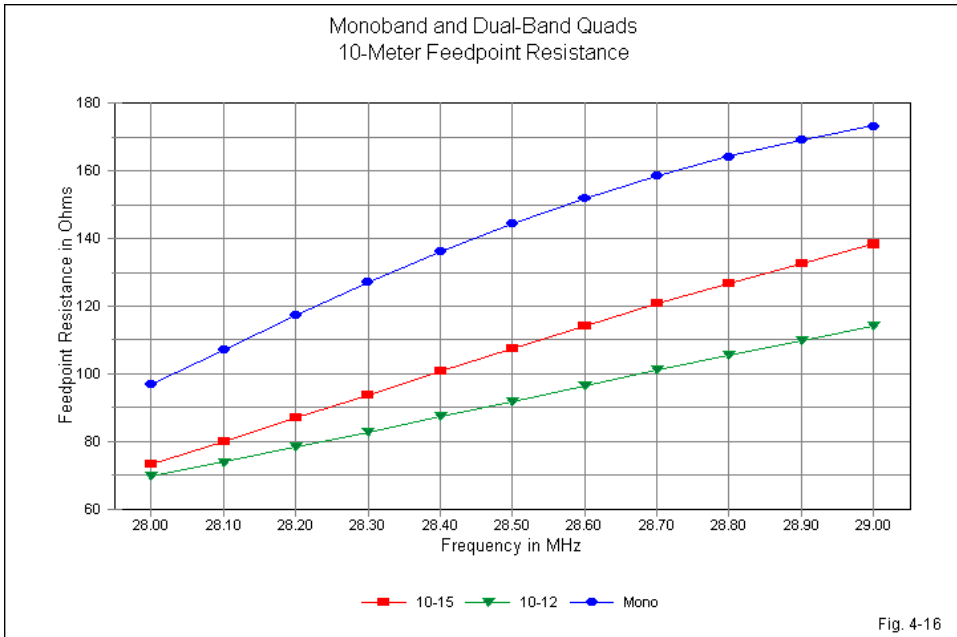
The narrow 12-meter band, shown in **Fig. 4-15**, allows us to examine the region of feedpoint resistance near the design frequency. In all cases, the dual-quad resistance is at least 30  $\Omega$  lower than the monoband value. As well, lower frequency ratios produce greater resistance reductions. Near the design frequency, the low-ratio inner loop curve has the lowest resistance. However, the low-ratio outer curves would show (as on 15 meters) a non-linear shape such that wider band edges would reveal values as low or lower than when the loops form a low-ratio inner element set.



The 10-meter graph in **Fig. 4-16** allows us only to examine dual-band quad feedpoint resistance when the loops are at inner positions. However, the band is wide enough at 3.5% bandwidth to reveal that even the monoband curve will show some non-linearity. In contrast, the inner-position dual band quads with 10-meter elements are more linear than the monoband curve with respect to feedpoint resistance. Once more, the lower the frequency ratio between the bands in the array, the greater is the reduction in feedpoint resistance relative to the monoband values.

The reductions in feedpoint resistance accompany dual-band quad elements regardless of whether they occupy inner or outer positions. The lower the frequency ratio between loops, the greater the reduction in resistance. This condition leads to attempts to design multi-band quads for direct feeding with 75- $\Omega$  feedline. Whether this tactic is completely feasible depends to a great degree

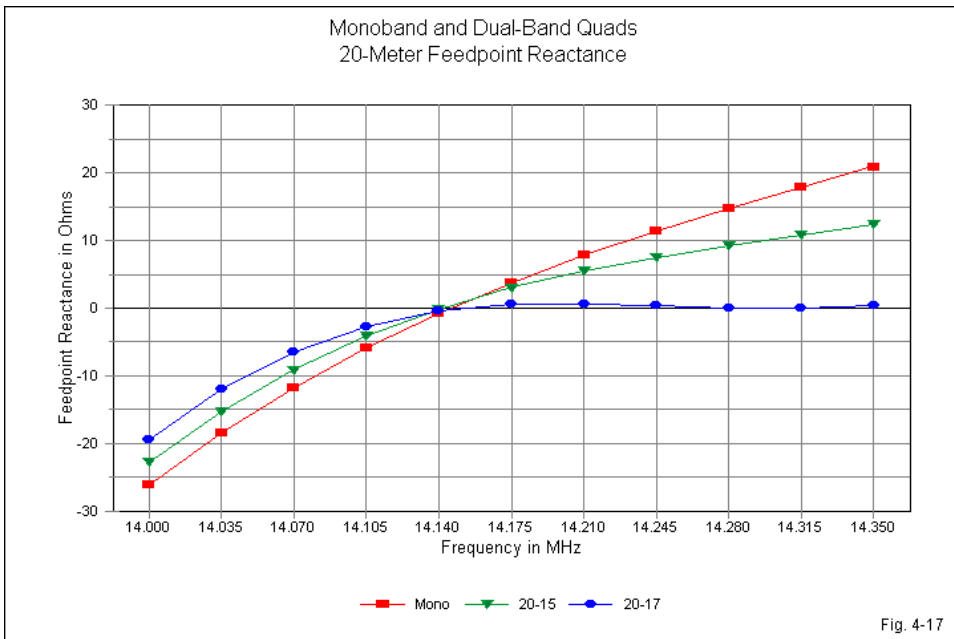
on the reactance excursions across the bands.



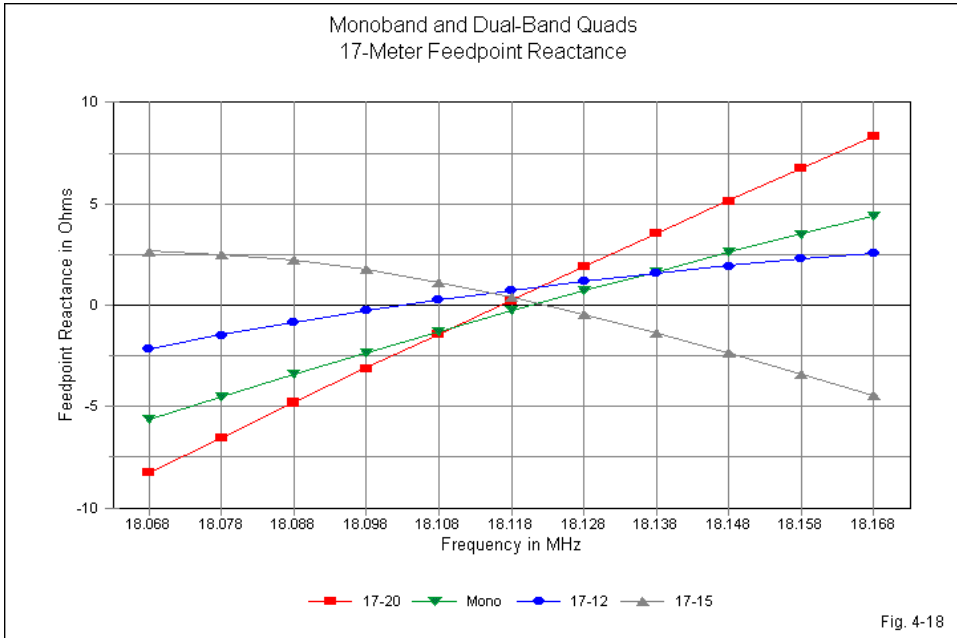
### *Feedpoint Reactance*

On 20 meters, as shown in **Fig. 4-17**, the monoband quad shows the greatest range of reactance. The other curves represent dual-band quads where the 20-meter loops have outer positions. The high-ratio curve for 20-15 has a slightly smaller range of reactance than the monoband curve due to the small non-linear shape. If we decrease the frequency ratio, as in the case of 20-17, the reactance curve flattens, limiting the total range of reactance change across the band. Each of the dual-band reactance curves is accompanied by a reduction in feedpoint resistance. The SWR relative to the resonant source impedance is a complex function of the ratio of reactance to resistance. The reduced range of reactance change offsets the reduction in resistance on 20

meters. Hence, the SWR curves for 20 meters tend to be similar in all 3 cases.

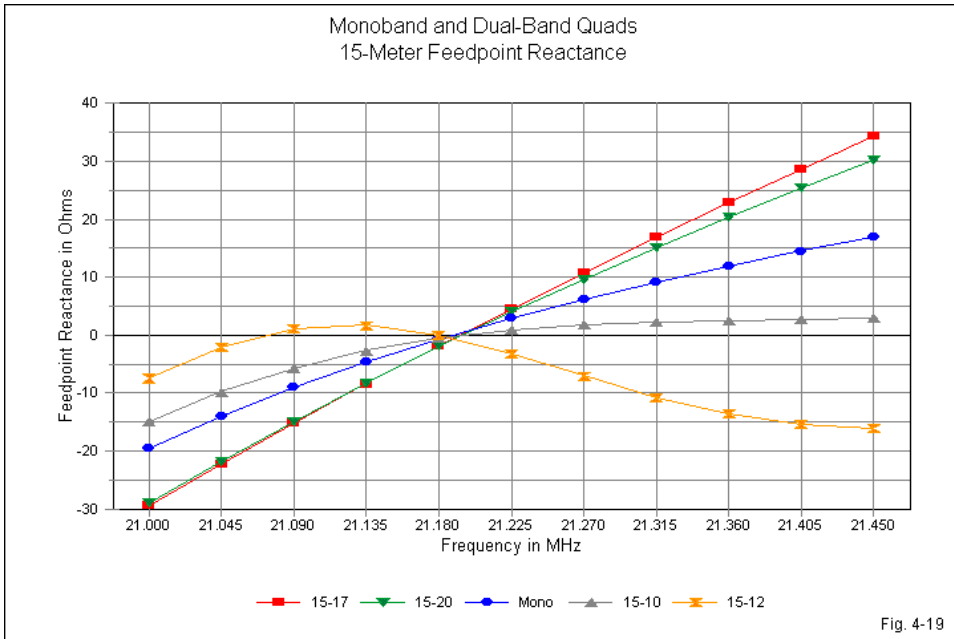


17 meters is so narrow, as shown in **Fig. 4-18**, that we may bypass curve shape and focus on basic properties. When 17-meter elements are outer loops with a high frequency ratio (17-12), the curve shows the flattening that we saw in the 20-meter loops. Likewise, when the 17-meter elements are inner loops (17-20) we see a higher slope to the reactance curve. However, when the 17-meter elements have an outer position with a low frequency ratio to the other band (17-15), the curve has a reverse slope. This situation provides an expanded view of the reactance behavior in the corresponding 20-meter case in which we saw a major bend in and flattening of the reactance curve as it passed the design frequency.

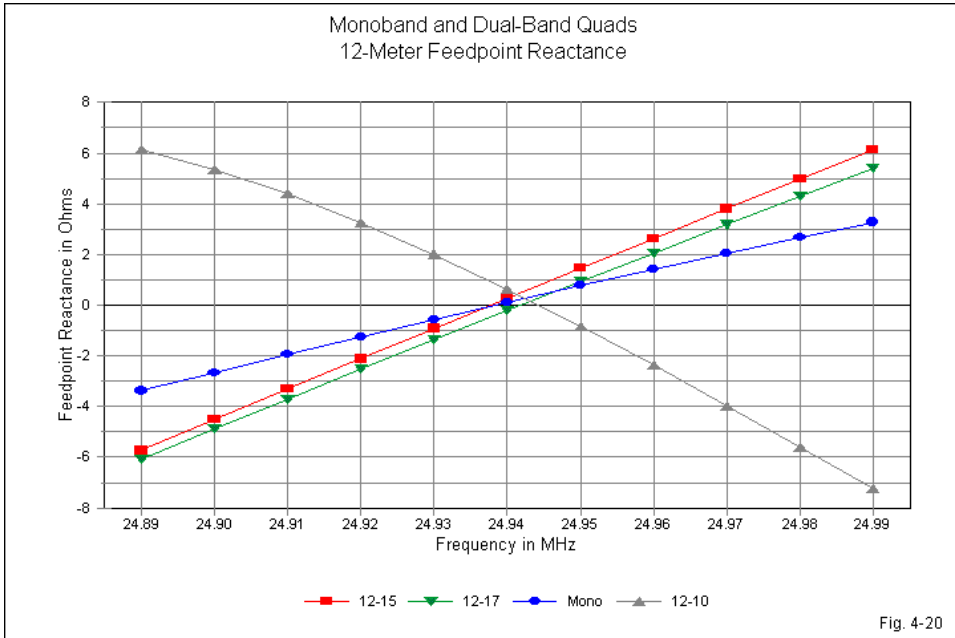


The 15-meter reactance curves in **Fig. 4-19** confirm the reactance behavior and allow us to view them over a greater bandwidth. When the 15-meter elements are inner loops, we find a steeper rate of reactance change than we find in the monoband curve. The change in frequency ratio between the 15-17 and the 15-20 cases produces only a small difference, with the lower frequency ratio showing the slightly steeper curve. More interesting are the curves for the 15-meter elements when they take an outer position. The 15-10 curve shows a slightly steeper rate of change below the design frequency. (This region also yields lower values of feedpoint resistance.) For the best SWR curve relative to the resonant impedance, one might wish to detune the 15-meter driver purposely to maximize the flatter portion of the reactance curve across the SWR passband. However, when we reduce the frequency ratio by pairing the 15-meter elements with 12-meters elements, we obtain greater self-limiting of reactance on the low side of the design frequency. Above the design frequency, the

reactance shows a fairly steep reverse curve, that is, a curve showing increasing capacitive reactance with increasing frequency.



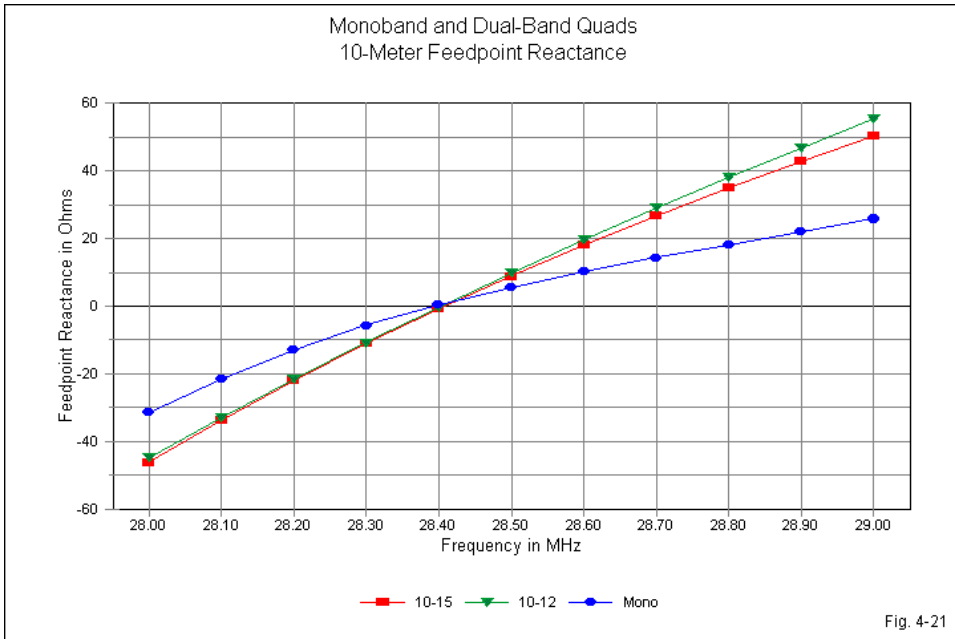
On 12 meters, as shown in **Fig. 4-20**, we find the expected behavior of the 12-meter loops when they have inner positions. The reactance change across the band is higher than for the monoband quad. However, when the 12-meter loops have an outer position with a low frequency ratio (12-10), they show a dramatic reverse curve across the narrow confines of this band. Indeed, the total change is higher than for any other case, although we should note that the maximum reactance excursion is only about 13  $\Omega$  for the 100 kHz passband.



The 10-meter curves in **Fig. 4-21** lose all drama because both dual-quads place the 10-meter elements in inner positions. Hence, the curves are nearly linear with a steeper slope than the monoband curve. The lower frequency ratio curve (10-12) shows a slight, nearly negligible, steeper slope than the higher frequency ratio curve (10-15). In both cases, the 1-MHz passband yields a total reactance change close to  $100 \Omega$ .

The reactance curves for dual-band quads present patterns that are considerably more complex than the patterns for many of the other operating parameters. When we use higher frequency ratios between bands in a multi-band quad, the behaviors are more nearly regular, relative to a monoband quad. Outer-position loops show flatter reactance curves, while inner-position loops show steeper curves. Hence, we may expect to have more difficulty covering all of 10 meters with an acceptable SWR than we encounter on 20 meters.

However, the outer position curves are less than linear, and that non-linearity increases as we decrease the frequency ratio between loops. The reverse curves with an increasing capacitive reactance as the frequency climbs offer considerable design challenge to the quad builder.



## Conclusion

We have taken a long look at dual-band quads using both higher and lower frequency ratios between bands. Our goal has been to detect reliable trends in major performance categories and in loop dimensions. The individual sections provide the best summaries of those patterns. In many categories of performance, the inner and the outer positioning of quad loops tend to produce reverse tendencies. However, the tendencies do not usually fully counter-balance each other for similar frequency ratios. Moreover, as we saw in the

case of reactance excursions, the inner and the outer position curves do not always form reverse versions of each other.

For the novice multi-band quad designer, there is a temptation to loosely believe that if we create a 3-band or a 5-band quad, the loops surrounded by other loops will simply neutralize the influences of the adjacent loops. However, the cautions that I just enumerated suggest that the surrounded loop may require more design effort, not less, in order to balance the unequal effects of the both inner and outer loops. The feedpoint resistance and reactance require special attention if we are to allow full coverage of all bands. The feedpoint resistance declines in the presence of any other loop (within the range of frequency ratios covered in these notes). If we cannot effect a suitable reduction of the total reactance change across the wider bands, the feedpoint SWR referenced to the resonant resistance will show a degraded curve.

Dual-band quad trends are instructive. However, they are not complete. For example, we have worked exclusively with spider-design quads that maintain a prescribed element spacing based upon calculations performed in wavelengths, not in feet or inches. Hence, these notes may or may not be applicable to planar quads that use a fixed physical distance between all drivers and reflectors. As well, these notes are only suggestive in terms of what actually occurs in 3-band and 5-band quads. As a data compendium, these notes represent only the barest beginning of systematic studies in the behavior of multi-band quad beams.

## Chapter 5

### A 3-Band, 2-Element Spider-Supported Quad Beam

One of the most difficult tasks in designing a multi-band 2-element quad beam is obtaining full band coverage. This problem has two dimensions. One dimension involves obtaining at the antenna an SWR that is less than 2:1 relative to the impedance of the main feedline all across each of the bands covered by the beam. The second dimension covers other important operating parameters, such as adequate gain and front-to-back ratio across each band.

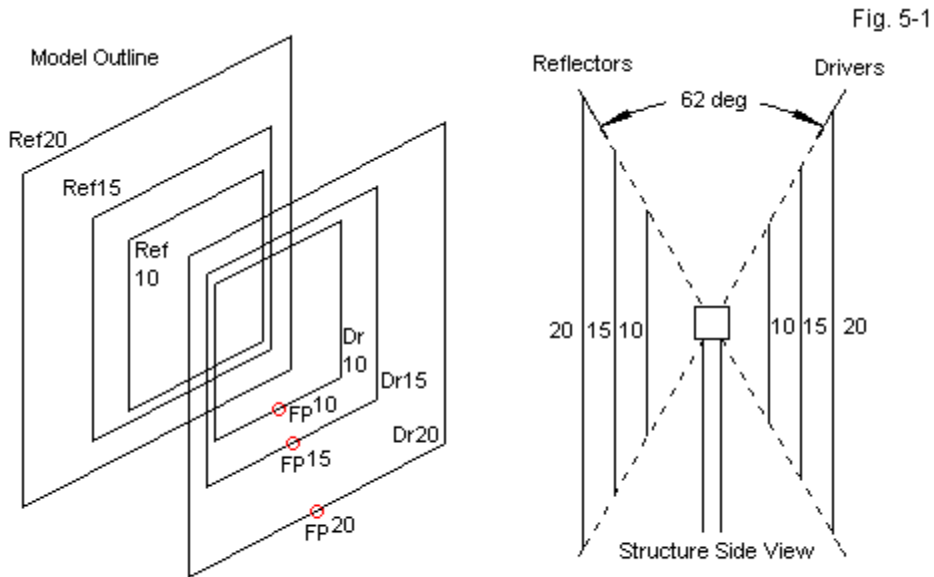
The design that we shall show covers only the widest amateur upper-HF bands: 20, 15, and 10 meters. For the narrower bands, 17 and 12 meters, one may use a dual-band quad with a common feedpoint, as shown in Part 3 of the chapters analyzing the element interactions and the use of a common feedpoint. The present beam uses separate feedpoints and restricts coverage to only 3 bands in order to obtain between adjacent bands the largest feasible frequency ratios. The result is relevantly similar band-to-band performance and a set of manageable feedpoint resistance and reactance values. By judicious use of a 75- $\Omega$  matching line on each band, the 50- $\Omega$  SWR values will be under 2:1 across all passbands.

The design specifically excludes the narrow bands, even though we might have thrown in loops for them. In the latter portion of our discussion, we shall examine a pair of 5-band designs previously analyzed in Volume 1 of *Cubical Quad Notes*. The exercise will clearly indicate why a 3-band limit within the upper HF range is desirable for a 2-element spider-based quad.

#### The Physical Design

The tri-band quad sketched in **Fig. 5-1** derives from the same set of monoband 2-element quads that we have used as the basis for dual-band quad behavior. In fact, it is simply a refined version of the sample tri-band, 2-element quad shown in Part 2 of "Sneaking Up on 2-Element Common-Feed Quads." The design frequencies for the 3 bands are 14.14, 21.19, and 28.4 MHz. At these frequencies, the monoband quads are set for resonance (within  $+/-j 1 \Omega$ ) and for peak 180° front-to-back ratio. At the design frequency, the free-space forward

gain is 7.04 dBi on all frequencies. The designs derive from calculations based on a large collection of models and regression analysis. The programs appear in Volume 2 of *Cubical Quad Notes* and require the designer only to input the element diameter and the design frequency. The model outline sketch on the left shows the positions of the 3 separated feedpoints, but not the match-line needed to feed the array with a 50- $\Omega$  main cable. Of course, only one feedpoint would be active at any one time, so the array requires a remote switch on the mast or 3 separate feedlines to the shack.



In adapting these monoband designs for a tri-band quad, I am using spider construction. It requires non-conductive support arms that "lean" forward and backward about  $31^\circ$  relative to a vertical line created by the mast as it reaches the hub (and virtually passes through to continue that line). This angle is the average

of the angles for each of the 3 bands. Since AWG #14 copper wire has a different diameter on each band if we measure it in wavelengths, the angle varies slightly from band to band. However, the small discrepancy in driver-to-reflector spacing will make no practical difference in the performance. The loop lengths are much more sensitive to changes. If a builder wishes to use the specified spacing between elements, he or she may attach a fiberglass or similar rod between the forward and rearward support arms near to the elements for each band.

Dimensions (Monoband vs. Tri-Band)						Table 5-1
Version:		Monobanders		Tri-bander		Match-Line
Band	Parameter	Side	Circum.	Side	Circum.	
20	Driver	210.60	842.40	211.40	845.60	209
	Reflector	221.86	887.44	220.10	880.40	
	Spacing	128.33		128.34		
15	Driver	140.78	563.12	140.30	561.20	130
	Reflector	148.58	594.32	147.00	588.00	
	Spacing	87.24		87.24		
10	Driver	105.16	420.64	103.70	414.80	95
	Reflector	111.24	444.96	111.40	445.60	
	Spacing	65.71		65.70		
Notes:	All wires AWG #14 (0.0641" diameter) copper					
	All dimensions in inches					
	All match-lines 75-Ohm, electrical length shown					

**Table 5-1** provides the required dimensions for the tri-band 2-element quad. All dimensions are in inches. The side lengths are for full sides. Modelers may need to divide those numbers by 2 in order to place a NEC or MININEC model at the center of the coordinate system. Later, all performance numbers will use free-space values. The gain of the array over ground will increase by about 5 or more dB (depending upon the actual height), but the front-to-back ratio will remain unchanged. If the array is at least 1  $\lambda$  above ground, the impedance will be virtually unchanged from the free-space value. Even at lower heights, the quad is less prone to ground-induced impedance changes than a beam using linear elements. The quad loop is actually two dipoles spaced about 1/4- $\lambda$  vertically, with the ends brought together at the zero-current points. When measured as a

function of the elevation angle of the main lobe and the same angle for a dipole or 2-element Yagi, the working height of a quad is about 2/3 of the distance from the bottom to the top horizontal wires. For non-critical purposes, the centerline or the hub height will do as the conventional marker of antenna height.

The dimensional table lists the sizes of the foundational monoband quads as well as the dimensions used in the tri-band version. For each band, the driver-to-reflector spacing remains unchanged. On 20 meters, the tri-band driver is longer than the monoband driver, but the tri-band reflector is shorter. On 10 meters—the innermost set of loops—the tri-band driver is shorter than the monoband driver, but the tri-band reflector is longer. In preceding chapter on dual-band interactions ("Adjacent-Band Quad Behavior"), I noted that when an element set undergoes interactions with both an inner and an outer set of elements, the middle set is not influenced equally. Hence, the effects on both the middle driver and reflector are not simply canceled out. In the case of the present tri-band design, the 15-meter driver and reflector are both shorter than in the monoband design on which they rest.

Each driver requires a match-line consisting of a length of 75- $\Omega$  cable. The 20-meter quad uses a relatively precise  $1/4 \lambda$ . On 15 meters,  $1/4 \lambda$  is about 139", while on 10 meters,  $1/4 \lambda$  or close to 104". The prescribed lengths for 15 and 20 are both shorter. When we examine the modeled performance data for the quad, we shall better understand why the lines use less than a full quarter- $\lambda$  of impedance transformation. Since the quad uses square rather than diamond construction, the match-lines (or even directly connected main feed lines) require support. I recommend the use of a UV-protected rope running from the hub through each feedpoint. You may then tape or otherwise clamp the match-lines to the rope, since coaxial cable is not designed to support loads—not even its own weight for very far. Of course, there is no rule that requires a coaxial match-line. Parallel 75- $\Omega$  transmission line—if available or if you can fabricate it—will work as well. However, at the remote switch or the transition to a 50- $\Omega$  coaxial feed line, you will need a 1:1 balun or ferrite-bead choke to suppress (or, more correctly, attenuate) common-mode currents. Such a device is good practice at the remote switch even if you use coaxial cables for the match-lines.

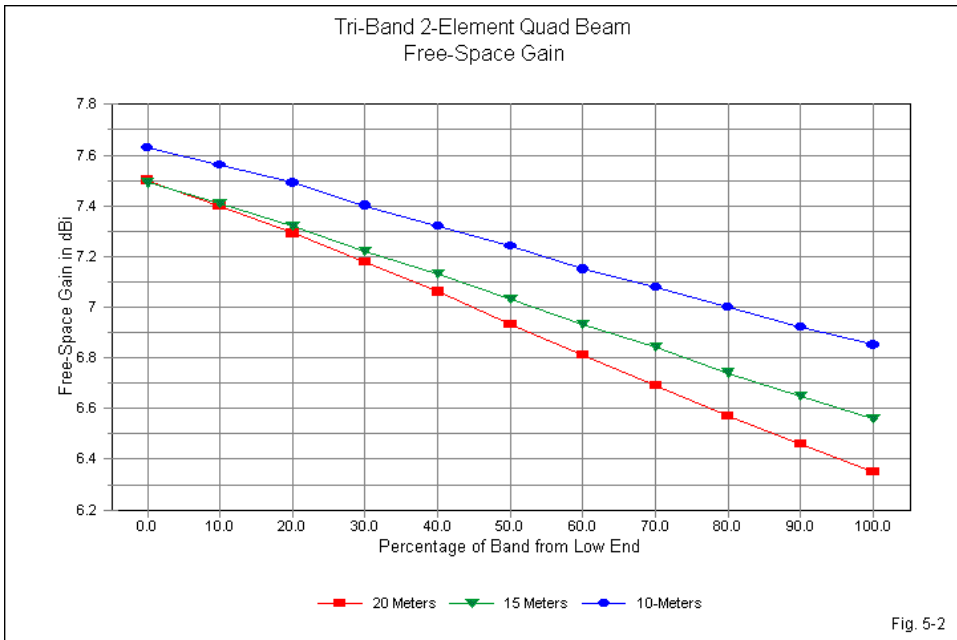
The dimensions for the tri-band quad are more finicky than those for a monoband quad (but less finicky than the dimensions for a 5-band quad). Therefore, you will wish to use careful construction methods to avoid the need for nearly endless field adjustments. The support arms should be non-conductive. As well, the method for attaching the elements to the arms at the element corners should make use of non-conductive materials or hardware. Metal clamps or loops can create 1-turn inductors at the element corners. The 4 required for each element may be enough to significantly detune the element. There are methods of compensating for such methods of fastening, but they tend to be long and tedious.

If you are constructing quads commercially, going through the compensation process once for each new design may well be worth the effort to obtain a desired set of corner fixtures. However, for a one-of-a-kind antenna that grows out of one's workshop, giving some extensive forethought to designing an effective means of arm-to-element attachment that involves only non-conductive materials may actually shorten the construction time considerably.

### **Tri-Band Performance**

The goal of the design was to obtain—to the degree possible—all of the performance potential offered by the monoband quads that form the basis for each element set. Studies in element interaction suggest that we may not be able to succeed completely. However, we may be able to develop a very good tri-band quad. As a yardstick, a short-boom Yagi will show about 7+ dBi free-space gain. Here, a short boom is about 8' on 10 meters and 16' on 20 meters. (A long-boom 3-element Yagi might develop just over 8-dBi free-space gain, where a long-boom on 20 is about 24' and on 10 is about 12'.) A 2-element driver-reflector Yagi may be able to manage about 6-dBi free-space gain. The 2-element Yagi front-to-back ratio will run between 10 and 12 dB across any of the wider amateur upper HF bands. However, a well-designed short-boom 3-element Yagi may achieve 20 dB across 20 and 15 meters and at least 17-18 dB across 10 meters. Although it is possible to design a 2-element driver-reflector Yagi for direct connection with a 50- $\Omega$  cable, most higher-performance Yagis below 6 elements require a matching network to raise a lower feedpoint impedance to the usual 50- $\Omega$  cable impedance. In general, a 2-element quad can match the gain of a short-boom (but not a long-boom) 3-element Yagi, but the quad suffers fairly narrow bandwidth for its front-to-

back performance. Under the best conditions, a monoband quad will show band-edge front-to-back ratio values somewhere between 12 and 18 dB, depending on the passband width. For this reason, I have used an initial monoband quad design with the broadest possible bandwidth for both the front-to-back and impedance performance.



Element interactions in a multi-band beam will limit our ability to achieve full monoband performance. However, gain is not one of those limitations. As shown by the graph in **Fig. 5-2**, the gain curves are normal or above normal for 2-element monoband quads. The design frequency is at the 40% marker on the steps up each of the bands. At that point, the monoband gain is about 7.04 dBi, and even the 20 meters elements achieve this level. The more inward loop sets manage slightly higher gain levels. However, the difference is not sufficient to be operationally noticeable. We may note in passing that the closer a set of elements

is to the outer position, the steeper is the slope of gain decrease with rising frequency.

Like all 2-element driver-reflector parasitic structures, the gain decreases as the frequency increases. The rate of descent of even the steepest curve is not far from the monoband curve. (Any parasitic array with at least one well-designed director will show a reverse curve, that is, one that increases in gain with rising frequency. For example a typical short-boom Yagi would show a curve that is virtually the reverse of the quad gain curves, but with very similar band-edge gain values.)

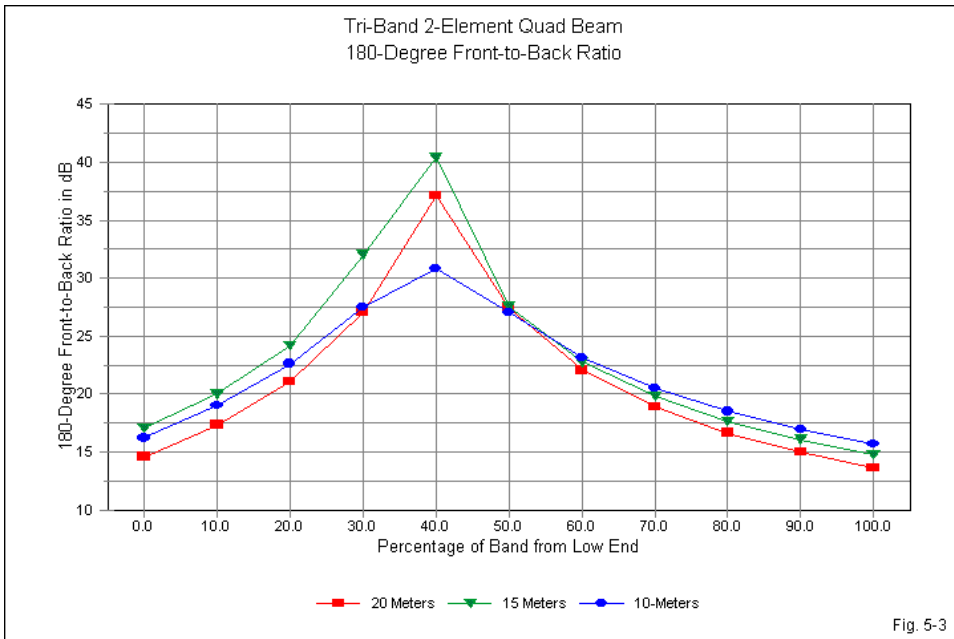


Fig. 5-3

One reason for tweaking the dimensions of the tri-band beam elements was to place the front-to-back peak as close as feasible to the design frequency on each band. The curves in **Fig. 5-3** measure the success of that move. I wanted to find

out if centering the front-to-back peak at the design frequency would yield relatively equal band-edge values, as the process did for the monoband quads. The band-edge front-to-back values are only slightly less equal than for the monoband beams on which this design rests.

For comparative purposes, the monoband 20-meter quad achieves about 16-dB front-to-back values at the band edges. The tri-band 20-meter elements fall from 1 to 2 dB below that value. The 15-meter monoband quad shows about 18-dB at the band limits. The 15-meter elements of the tri-bander are again about 1-2 dB lower. On 10 meters, the monoband quad reached a very high peak level, with about a 14-dB front-to-back ratio at 28 and 29 MHz. The inward position of the 10-meter elements in the tri-band quad prevents us from achieving the very high peak front-to-back value, but the band-edge values are 2 to 3 dB higher than for the monoband model.

We must add two notes to these reports of modeled performance. First, the actual peak front-to-back ratio—as a 180° value—will not be as operationally significant as it is dramatic in the graphs. Not only is the peak a narrow-bandwidth phenomenon, it is also a dimple in the overall rearward gain levels of the array. Second, the values appear in the graphs due to simple changes in the modeled array geometry. It is also unlikely that one will be able to precisely place the peak value with respect to frequency. (The best way to tell is to perform tests with a nearby patient friend, with the quad pointed directly away from that station.) The final construction-ending test is the adequacy of the front-to-rear overall performance, especially at the band edges.

The band-edge patterns are quite unlike those at the design frequency or at the nearby band center. To show the range of likely patterns, **Fig. 5-4** presents a gallery of free-space E-plane (azimuth) patterns for each of the bands, using the band limits and the band center as snapshot frequencies.

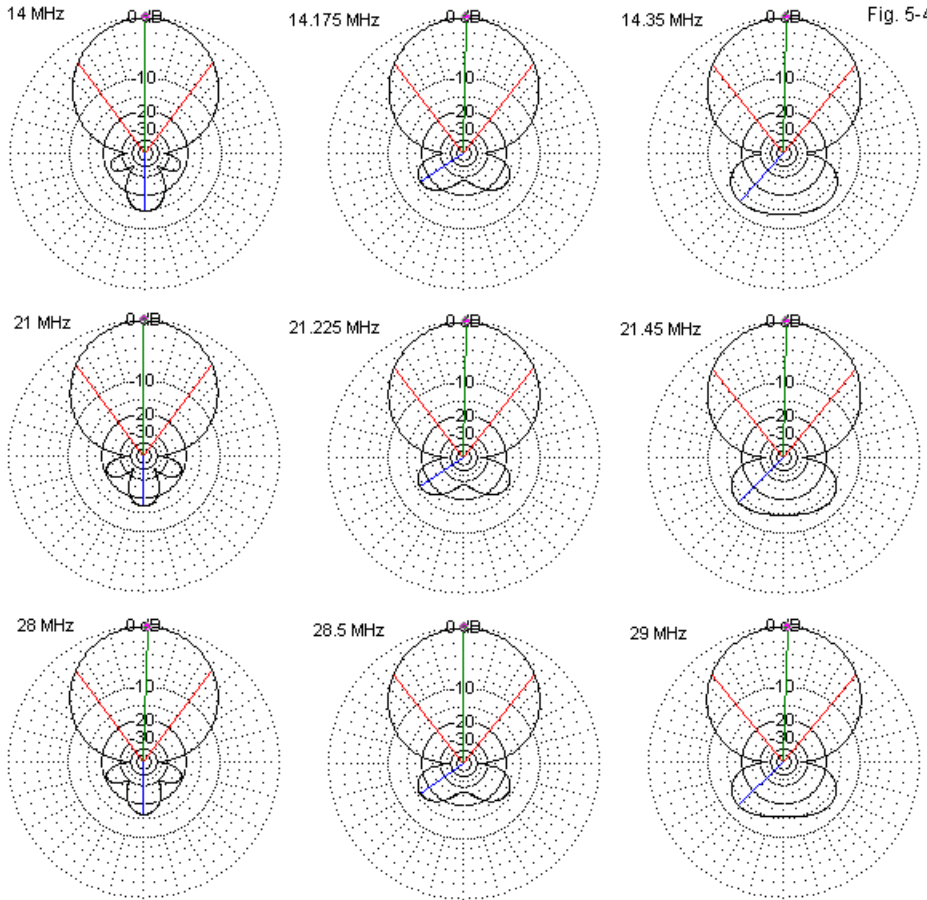


Fig. 5-4

Selected Free-Space E-Plane Patterns: 3-Band 2-Element Quad Beam

The patterns show both good and not quite so good things about 2-element quad performance in a tri-band array. The very good aspect of the gallery views is the fact that the patterns are very similar for corresponding positions in each band. The design constraints brought to the project have resulted in a quad that

performs in a similar manner on each of the included bands. Less than very good is a fundamental limitation in the rearward lobes of a quad when used on a wider amateur band. The lines that indicate the strongest rearward gain have similar values at the lower band edge and at mid-band: very roughly 15 dB below the main forward lobe. At the upper band edge, the worst-case front-to-back ratio is down to about 12 dB, even though the 180° value is somewhat higher. We find the same pattern of rearward lobes on monoband quads.

The next step in our review of tri-band quad performance takes us into the region of the feedpoint impedance. The monoband quads showed design-frequency resonant impedance values between 130  $\Omega$  at 20 meters to 136  $\Omega$  at 10 meters. Those values allow us to use a standard  $1/4\text{-}\lambda$  75- $\Omega$  match-line on any of the monoband quads to obtain a good match to a 50- $\Omega$  main feed cable and still have an acceptable SWR across each of the bands.

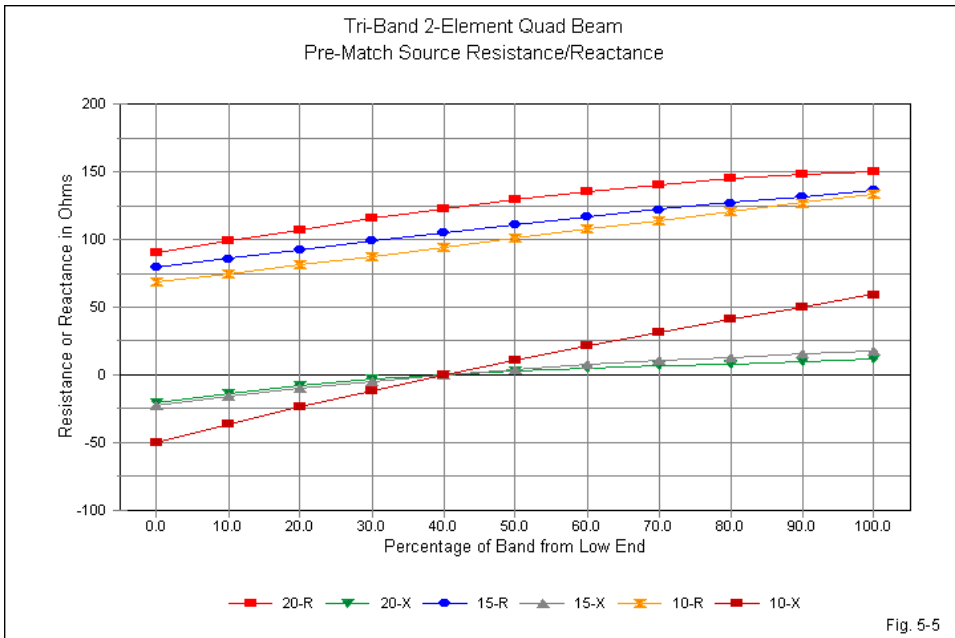
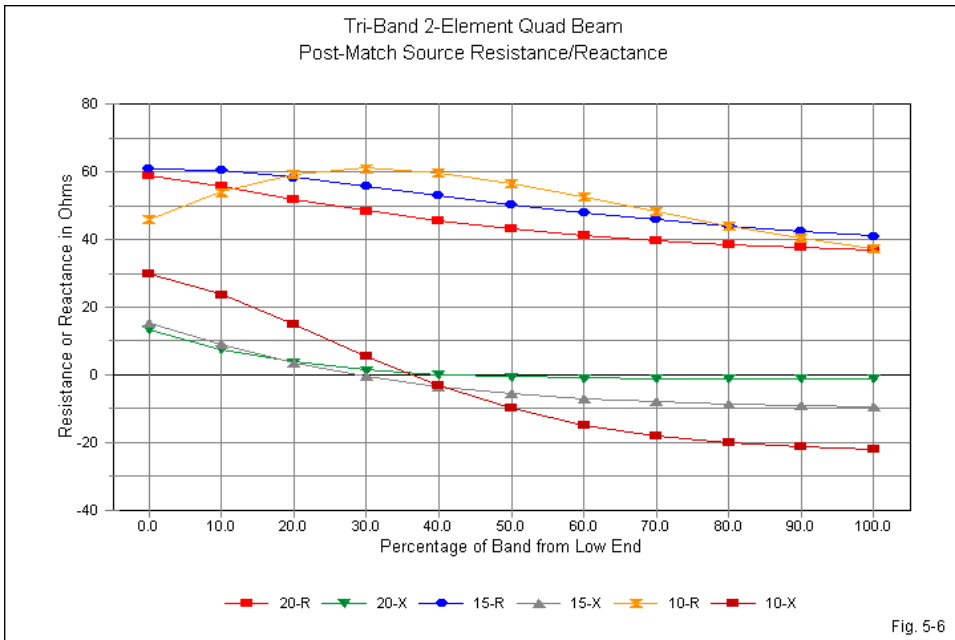


**Fig. 5-5** shows what happens to the feedpoint impedances in terms of resistance and reactance before we add any matching devices or networks. Again, the 40% marker represents the approximate design frequency for each band. At this point, we can see the crossing reactance lines at about  $j0 \Omega$ . As we learned in the study of adjacent-band quad behavior, it does not matter whether a multi-band loop set occupies an outer or an inner position. The feedpoint resistance will decrease. The 20-meter value is about  $123 \Omega$ . Perhaps the new information offered by the tri-band quad is that, as we add set of loops, the resistance decreases further as we move toward the innermost set. On 15 meters, the resonant impedance is only about  $106 \Omega$ , and on 10 meters, it has decreased to  $94 \Omega$ . We shall look at these values once more in the last part of these notes when we compare tri-band performance to 5-band performance.

The reactance curves are rather modest for 20 and 15 meters, partly as a function of having other element sets inward from them and partly because the bands are between 2.1% and 2.5% wide. In contrast, the 10-meter reactance curve undergoes the greatest excursion and virtually in a linear progression. The size of the excursion of reactance is a joint function of the added bandwidth (3.5% wide) and the fact that the 10-meter elements are the most inward of the bands included in this array.

**Fig. 5-6** shows the resistance and reactance at the shack-end of the match-line prescribed for each band. On 20-meters, we can employ a  $1/4\text{-}\lambda$   $75\text{-}\Omega$  line, which is about 209" at the design frequency. A corresponding 15-meter line would be about 139" long. However, a transmission line effects an impedance transformation at any length. By judicious line length selection, we can often achieve a more desirable set of resistance and reactance values across a given band. Note that the use of a 130" line on 15 yields band-edge resistance values that are very similar to those we obtain on 20 meters with the full  $1/4\text{-}\lambda$  line. At the same time, the reactance curve for 15 meters is nearly as flat as the one for 20 meters.



*Important Note:* The line lengths noted here are electrical lengths translated into inches. Multiply the listed electrical length by the velocity factor of the line actually used to arrive at the necessary physical line length. For most purposes, you may use 0.66 as the velocity factor for 75- $\Omega$  lines with a solid dielectric and 0.8 for lines with a foam dielectric. However, for best precision, it may be useful to measure the velocity factor of the line used.

On 10 meters, we have less than an ideal situation. A quarter-wavelength line does not yield an acceptable range of impedances, largely due to the wider range of reactance values that we encounter on this band. However, an electrical length of 95" will yield acceptable SWR values. As shown in **Fig. 5-6**, the resistance range is very similar to the range resulting from the 20- and 15-meter match-lines. However, the reactance curve is considerably wider than those for 15 and 20.

For most operators, the final measurement is simply the 50- $\Omega$  SWR at the junction of the matchline and the main feed cable. (I am avoiding all temptation to show values that might result from taking measurements 50, 75, 100 or more feet down an actual cable with its loss factors included. These shack-end SWR values will always be lower than the values at the point where the 50- $\Omega$  cable is closest to the antenna.) **Fig. 5-7** shows the modeled SWR curves. The match-lines use the NEC-provided lossless cable for the match-line. However, since each match-line is  $1/4\text{-}\lambda$  or less, the lossless values are a very good approximation of reality.

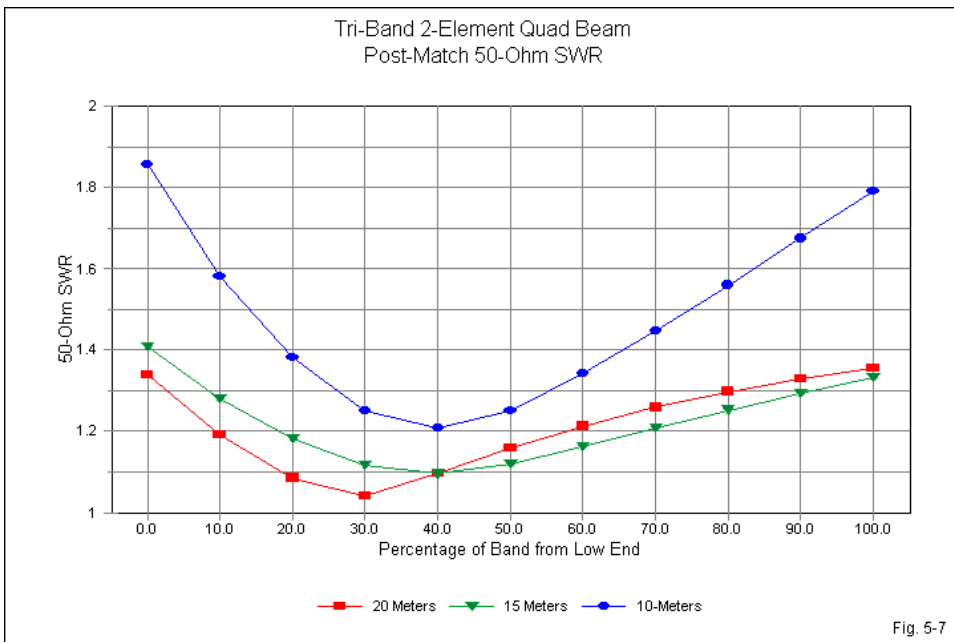


Fig. 5-7

The 50- $\Omega$  SWR curves 20 and 15 meters are very satisfactory, with the peak value just over 1.4:1. The 15-meter curve shows a lowest value that is higher than the lowest 20-meter value because the 15-meter match-line is a bit shorter than  $1/4\lambda$ . Had we used a perfect  $1/4\lambda$  line, the curve would have still been acceptable, but one end of the band would have shown a much higher value than

the other.

On 10 meters, we departed the farthest from  $1/4 \lambda$ , and the resulting SWR curve has a low value of about 1.2:1. At the band edges, the SWR is 1.8:1 or slightly higher. The result is an acceptable, but certainly not an outstanding 50- $\Omega$  SWR curve. However, in the world of multi-band 2-element quads, covering the entire first MHz of 10 meters with under 2:1 50- $\Omega$  SWR is itself a bit rare, especially if we wish to achieve any performance across this wide band.

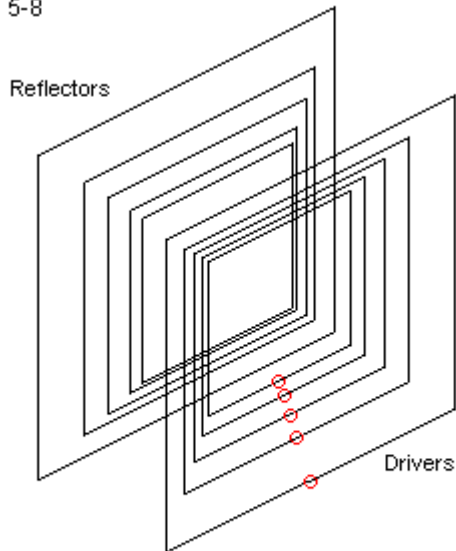
The tri-band spider quad based on wide-band monoband quad designs achieves its goals of providing close to monoband performance across all three included bands. Gain is standard. The front-to-back curves are what we might expect from a 2-element quad, and the band-edge values hold up better than in most designs. The use of match-lines for the separate feedpoints on each band allows us to obtain very good 50- $\Omega$  SWR curves on 20 and 15, with an acceptable curve on 10 meters.

We have a left over question that is more than trivial. Why not include all 5 upper HF amateur bands in the array? There is a very straightforward answer, but it may not be completely believable without a demonstration. Therefore, let's spend a little time exploring the performance of some typical 5-band spider quads.

### **3 Bands or 5 Bands**

In Volume 1 of *Cubical Quad Notes*, I reviewed the performance of two different but related 5-band 2-element quad beams. Both used spider construction and thus had the general layout shown in **Fig. 5-8**. The figure shows the positions of all of the feedpoints, but only 1 would be active at a time. The difference between the two beams rested on the spacing between elements. The narrow version used an element spacing of  $0.125 \lambda$ . The wide version used a spacing of  $0.174 \lambda$  or 6' at 10 meters.

Fig. 5-8

Model Outline: 5-Band  
2-Element Quad Beam

Both quad beams differed from the present design not only in spacing, but as well in the design frequency used for the wider amateur bands. The design frequency for all bands was the mid-band frequency: 14.175, 18.118, 21.225, 24.94, and 28.5 MHz. If I were interested in redesigning these arrays using the prescribed spacing today, I likely would lower the design frequency on each wider band to ensure equalized front-to-back ratios at the band edges.

However, our use of these older designs is not to produce a buildable design. The narrow version is attractive in some building circles because it results in a more compact array with arm supports that require less of an angle relative to a vertical line drawn from the mast upward. The required angle is about  $25.5^\circ$  or about  $51^\circ$  between the driver and reflector support arms. The wide version is actually slightly wider than the 3-band quad that we have reviewed in these notes.

Relative to a vertical line, the arm angle is a bit over 33°, or 66° total between driver and reflector support arms. Indeed, the wide version will be useful in showing differences between 3- and 5-band quads without having to replicate the newer design in a 5-band version.

Dimensions: 5-Band 2-Element Quads				Table 5-2	
Version:		0.125-wl Spacing		0.174-wl Spacing	
Band	Parameter	Side	Circum.	Side	Circum.
20	Driver	210.00	840.00	212.00	848.00
	Reflector	216.72	866.88	221.70	886.80
	Spacing	104.02		144.82	
17	Driver	163.92	655.68	165.30	661.20
	Reflector	168.72	674.88	173.80	695.20
	Spacing	81.43		113.25	
15	Driver	139.56	558.24	140.60	562.40
	Reflector	144.72	578.88	148.70	594.80
	Spacing	69.53		96.70	
12	Driver	118.80	475.20	118.60	474.40
	Reflector	122.40	489.60	126.70	506.80
	Spacing	59.16		82.28	
10	Driver	116.18	464.72	103.60	414.40
	Reflector	110.40	441.60	112.80	451.20
	Spacing	51.72		72.00	
Notes:	All wires AWG #14 (0.0641" diameter) copper				
	All dimensions in inches				

**Table 5-2** provides the dimensions for the 2 older 5-band designs. The chart shows both the side length and the circumference of the loops—as well as element spacing—so that you may directly compare the numbers to the corresponding dimensions for the 3-band quad in **Table 5-1**. Let's examine the basic free-space performance of these arrays as background for the critical conclusions that we shall draw from them.

*A 5-Band 2-Element Quad Using 0.125-λ Element Spacing*

The use of narrow spacing allows the quad array to achieve slightly higher gain levels than the 3-band version. The differentials average about 0.15 dB, which may not be operationally significant. The gain curves for the 3-wide bands of the array appear in **Fig. 5-9**. I have omitted the narrow bands from the performance review. More complete data appear in the original discussion.

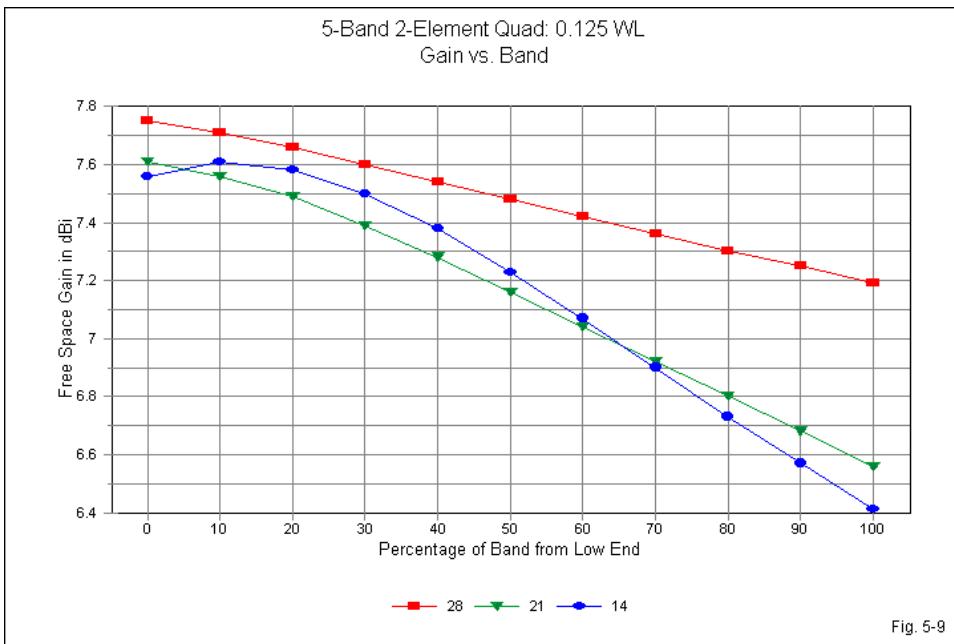
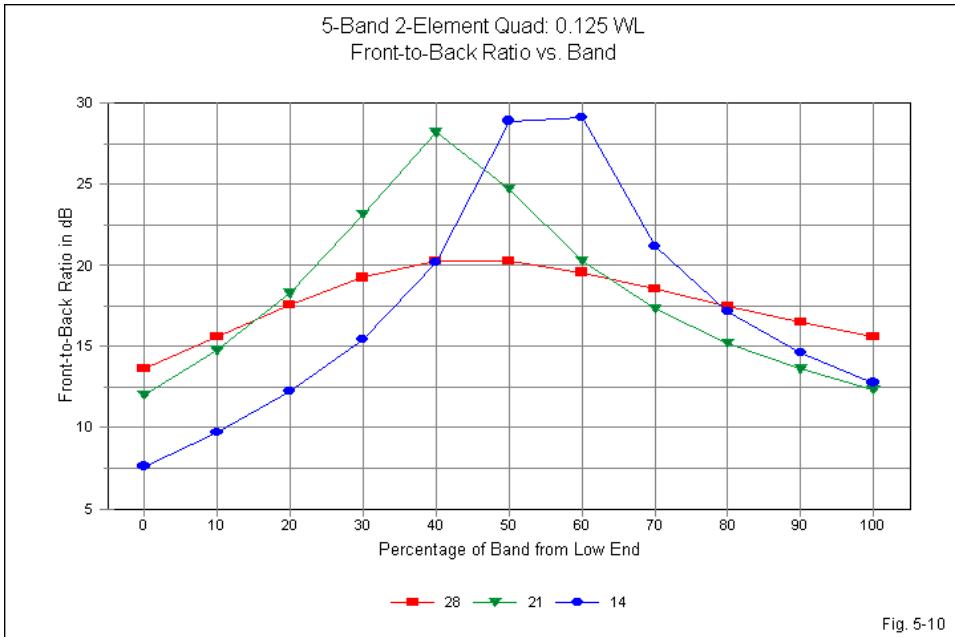


Fig. 5-9

Although the front-to-back peaks do not occur precisely at mid-band, as shown in **Fig. 5-10**, we can glean something about band-edge performance from the curves. Across the upper HF range, the band-edge front-to-back performance averages from 10 dB at 20 meters to about 15 dB at 10 meters. The corresponding values for the tri-band design at 14 and 17 dB, respectively. The difference is a joint function of the narrower element spacing and the proximity of

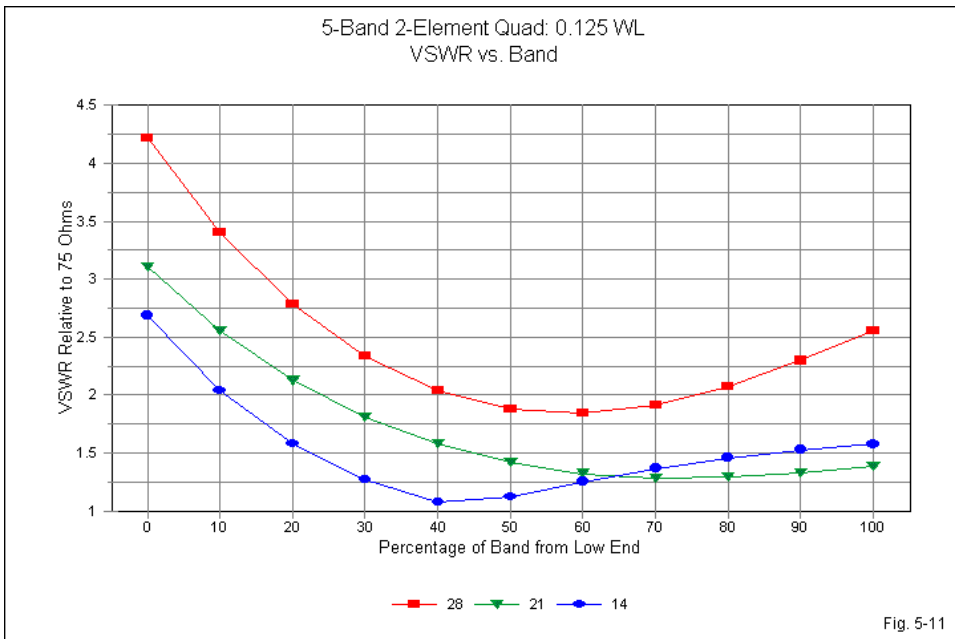
the loop sets in a 5-band quad beam.



One temptation that accompanies a 5-band quad design is to use direct feeding. The impedances suggest that a  $75\text{-}\Omega$  feedlines might be satisfactory for the array. **Fig. 5-11** shows the  $75\text{-}\Omega$  SWR curves of the array for each of the wider bands.

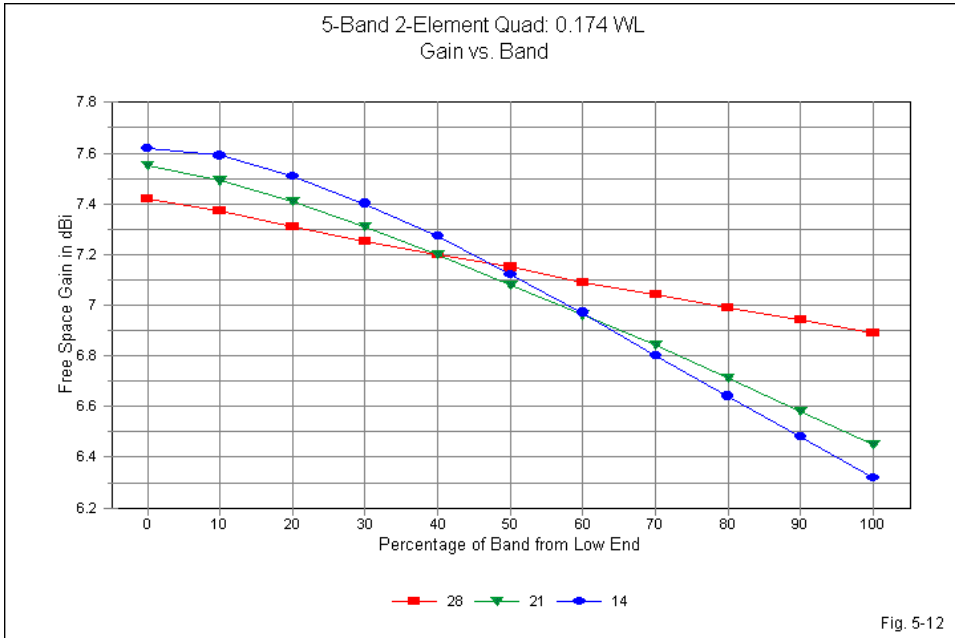
The results are not satisfactory from the perspective of full band coverage. On 20 meters, we manage to cover about 90% of the band, and with some juggling of the 20-meter driver, we likely would obtain full band coverage. The SWR curve for 15 meters, with resonance at mid-band, yields only about 75% coverage. However, the low SWR at the upper end of the band suggests that judicious redesign of the 15-meter driver might extend that coverage. However, 10 meters provides only about 30% band coverage. We shall see the reasons for this

difficulty after examining the wide 5-band quad array.

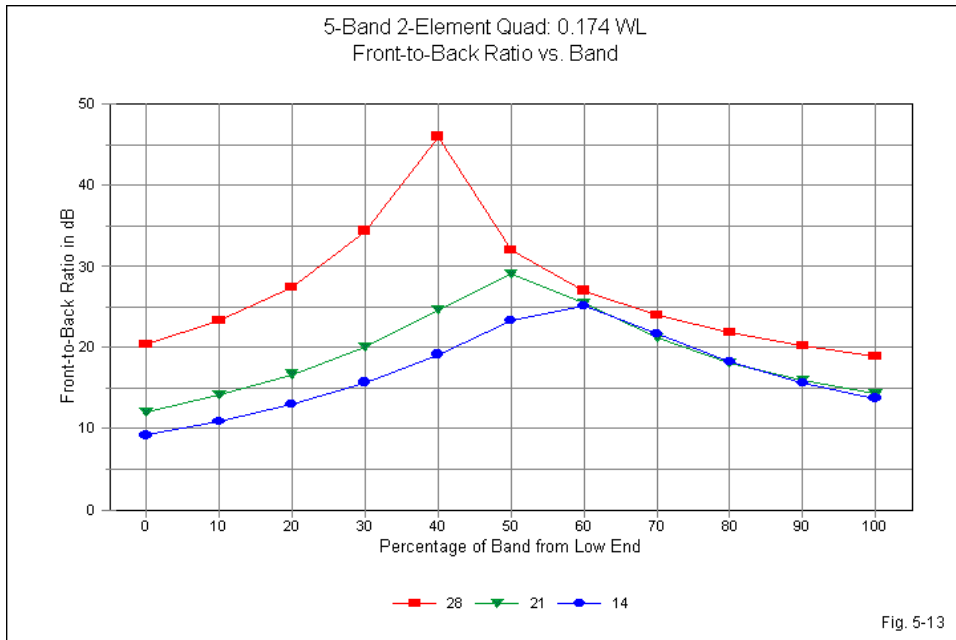


#### A 5-Band 2-Element Quad Using $0.174\lambda$ Element Spacing

Wider element spacing provides some improvement in the performance values. The wide 5-band array emerged before the development of idealized 2-element monoband models and hence uses a spacing just wider than optimum. However, as the curves in **Fig. 5-12** reveal, the gain values do not differ greatly from those of the tri-band model. The 5-band 20-meter curve is steeper than in the tri-band case, while the 5-band 10-meter gain curve is somewhat flatter. Both results stem from the closer proximity of loop sets in the 5-band model.

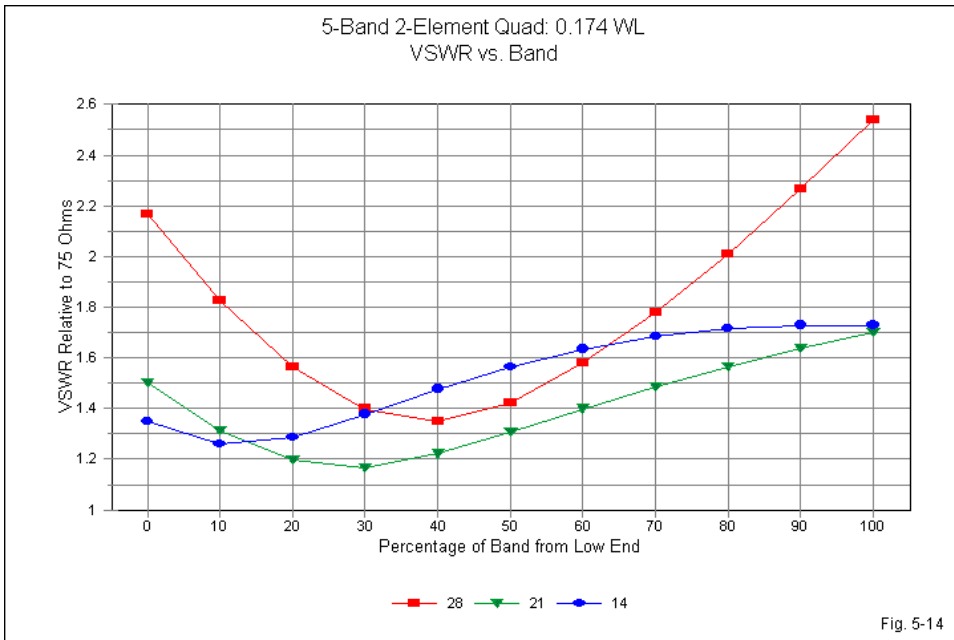


As shown by **Fig. 5-13**, the front-to-back performance again fails to place peaks precisely at the mid-band design frequencies. However, band-edge performance is fairly balanced. The 10-meter band-edge values average 19 dB—higher than for the tri-band version. However, the 20-meter band-edge values remain low, averaging about 11 dB. Thus, at the band edges, the band-to-band range of 180° front-to-back ratios is about 8 dB, compared to about 3 dB for the tri-band model. The results suggest (but do not definitively prove) that it may be more difficult to obtain even band-to-band 2-element quad performance when covering 5 bands with a lower frequency ratio between adjacent loop sets.



Direct 75- $\Omega$  feeding of the wide 5-band quad is tempting. In fact, **Fig. 5-14** shows that we obtain quite satisfactory 75- $\Omega$  SWR curves on both 20 and 15 meters. 10 meters remains the most difficult case, with only about 75% band coverage with less than a 2:1 75- $\Omega$  SWR ratio.

The wider 5-band quad achieves satisfactory gain values. Within general limitations of 2-element quad design, we might also rate the front-to-back performance as adequate at the band edges. However, the feedpoint impedances remain problematical. To see why, let's compare in a simple table (**Table 5-3**) the minimum and maximum resistance values for all three 2-element quad designs. For good measure, we shall also show the range of reactance values that accompany the resistance values across each of the wide upper HF amateur bands.



The first step is to compare the narrow and the wide 5-band quads. Since the frequency ratio between adjacent loops is the same for both beams, any differences are functions of the element spacing. The average differential in the feedpoint resistance between these two beams is 15 to 20  $\Omega$ , with the higher average on 10 meters. Accompanying the lower feedpoint resistances for the narrow beam is a higher range of reactance values across each of the bands. Narrow element spacing therefore has an obvious negative impact on the ability of the array to cover all of each band. The 5-band arrays also show a systematic lowering of the feedpoint resistance as we increase the frequency band. The inner loops show a systematic lowering of the feedpoint resistance relative to more outward loops. Hence, when we combine this effect with the larger reactance excursion for the inner loops, we obtain large difficulties in covering 10 meters with narrow spacing.

Resistance-Reactance Comparison				Table 5-3	
2 5-Band Quads and 1 3-Band Quad					
20, 15, and 10 Meters					
Antenna	Band	R Min	R max	Delta X	
5-B Nar	20	41	118	50	
	15	53	76	63	
	10	31	50	116	
5-B Wide	20	78	130	20	
	15	54	107	48	
	10	49	70	110	
3-Band	20	90	151	32	
	15	79	136	40	
	10	69	133	109	
5-B Nar = 5-band, 0.125-wl spacing					
5-B Wide = 5-band, 0.174-wl spacing					
3-Band = 3-band quad					
R Min = Minimum feedpoint resistance in Ohms					
R Max = Maximum feedpoint resistance in Ohms					
Delta X = Total change in reactance across band					

The table allows us to make a second comparison, this time between the wide 5-band quad array and the tri-band design that we featured earlier. Note the descending values of minimum feedpoint resistance for the 3-band model: about 90, 80, and 70  $\Omega$  for 20, 15, and 10 meters, respectively. Every multi-band quad shows a reduction in the feedpoint resistance regardless of loop position in the presence of loops for other bands. The lower the frequency ratio between loops, the greater the reduction in feedpoint resistance. The tri-band quad uses frequency ratios between 1.34:1 and 1.5:1.

In contrast, the 5-band wide quad uses frequency ratios between bands that average about 1.2:1. As a result, even the 20-meter minimum feedpoint resistance is lower than for the tri-band beam: about 80  $\Omega$  compared to the tri-band value of 90  $\Omega$ . The impedance value declines more rapidly as we move up in the HF region. On 10 meters, the differential between tri-band and 5-band minimum feedpoint resistance values is double that of 20 meters: about 70  $\Omega$  vs. about 50  $\Omega$ .

for the 5-band model. For reference, the reactance ranges for the wide 5-band model and for the tri-band model are comparable. You may repeat the exercises that we just ran using the maximum resistance values, although the minimum values are perhaps more critical.

The net result is that, as we move up the bands of a 5-band 2-element quad array, the feedpoint resistance drops much more rapidly than it does for a tri-band array that omits 17 and 12 meters. On 10 meters, the low resistance accompanied by a wide reactance range results in matching difficulties that are difficult to overcome. In most cases, we must de-rate the 10-meter coverage and even then rely on line losses of the main feedline to achieve a 2:1 SWR across the smaller portion of 10 meters. The comparisons provided by the numbers in **Table 5-3** provide a demonstration of a quite general phenomenon. Given pre-set upper and lower frequency limits, the more bands that we pack into a multi-band 2-element quad array, the lower will be the frequency ratio between adjacent loop sets. As we lower the frequency ratio, the feedpoint resistance drops more rapidly, even though the reactance range may not change very much. The higher the ratio between reactance and resistance, the more difficulties we encounter in effecting a match to a main feedline of a specified characteristic impedance, with or without matching devices or networks.

The tri-band quad begins with higher feedpoint resistance values on all bands. Hence, we require some form of matching. A 75- $\Omega$  (or similar) match-line that is  $1/4 \lambda$ —or shorter as necessary—allows us to match the quad on each band to a 50- $\Omega$  main feedline. As well, we may achieve full-band coverage on all 3 bands with an SWR value of less than 2:1 (without relying upon losses in the main feedline). In a nutshell, this small demonstration shows why I chose to design a tri-band 2-element quad beam rather than stretch for a 5-band model that would fail to provide full-band coverage on 20 through 10 meters.

## **Conclusion**

These notes have described and analyzed the structure and performance of a tri-band 2-element quad beam for the wider upper-HF amateur bands of 20 through 10 meters. The design rests upon wide-band monoband quad beams and

adjusts the dimensions to obtain as close to monoband performance on each band as feasible. In fact, the beam comes very close to replicating monoband performance. The array allows us to match the individual feedpoints to a 50- $\Omega$  main feedline by the use of 75- $\Omega$  lines of prescribed lengths, some of which are less than the usual  $1/4\lambda$ . The array presumes the use of a remote switch or separate feedlines for each band. The structure uses spider construction to sustain the required spacing between the driver and the reflector on each band.

My choice of a tri-band quad array, rather than a 5-band beam, results from previous studies of what happens to the feedpoint resistance as we add bands and consequently reduce the frequency ratio between adjacent loop sets. The following lines only summarize, but do not substitute for, a thorough review of the material in the previous chapters of this volume. The more bands that we add to a multi-band quad, the lower the frequency ratio becomes. The result is both a general lowering of all feedpoint resistance values and a greater differential between the feedpoint resistance values for 20 and 10 meters. Since the reactance ranges tend not to change by any great amount, we end up with a very high ratio of reactance to resistance on 10 meters. The ratio of reactance to resistance across the band tends to reduce matched coverage of 10 meters, regardless of whether or not we use a matching device or a network. By sustaining a higher frequency ratio between adjacent loop sets in a tri-band model, we may overcome (to an acceptable degree) the matching issue.

All of these notes presume that the general parameters of quad operation over the wide amateur bands are acceptable. A 2-element quad shows good gain with the typical driver-reflector parasitic-assembly decrease in gain with increasing frequency. However, the 180° front-to-back ratio shows considerable variability, with a relatively high mid-band peak but with band-edge values that are only somewhat higher than the ones that we obtain from a 2-element driver-reflector Yagi. Finally, full-band matching is achievable with an appropriate matching line for each band, but only if we begin with a basic design optimized for wide band coverage.

I intend these notes as general guidance for the individual who wishes to design and build his or her own multi-band quad beam. I do not have access to

the precise designs used by commercial quad makers. Hence, nothing in these notes has direct application to commercial designs or to the claims made for them by the makers.

## Chapter 6

### Why Not Use a 3-Band, 3-Element Quad?

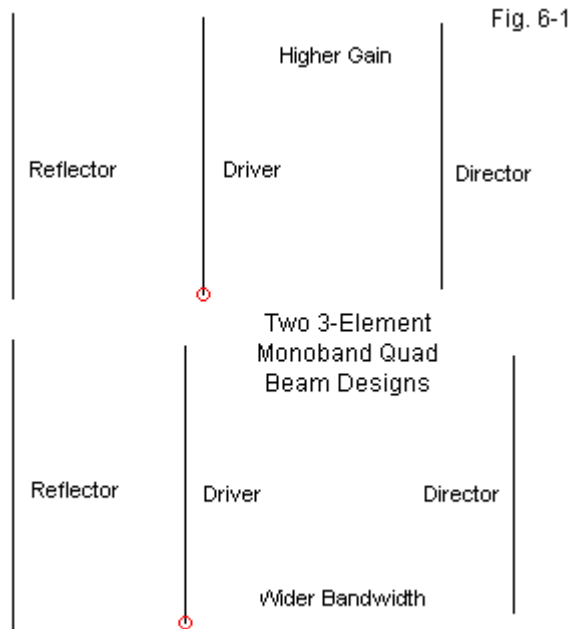
Although we can find a number of designs for 3-element monoband quad beams, we would have a difficult time uncovering tri-band or 5-band versions of them. There are both physical and electrical reasons for this lacuna in the range of available quad multi-band designs. We should spend at least a brief time discovering what the reasons are.

#### Monoband 3-Element Quads

Among 3-element quad beams, we can find both good and mediocre designs. In Volume 2 of *Cubical Quad Notes*, I offered computer programs for two types of 3-element monoband quads. One version stressed the widest obtainable bandwidth for both the front-to-back ratio and the SWR curve. The other version gave up bandwidth (but not altogether) in exchange for the maximum gain that we might obtain from 3 quad loops, commensurate with a reasonable front-to-back ratio at the design frequency. Both programs (along with a NEC-Win Plus NEC model that incorporated the equations) required only two input variables: the element (wire) diameter in the units in use and the design frequency. **Fig. 6-1** shows the outlines of the two beam types to provide an idea of their proportions.

The wide-band version is about 19% longer than the high gain model. Despite the greater length, the wide-band driver is closer to the reflector than the corresponding element on the high-gain version. The wide-band director is also considerably smaller in circumference than the high-gain director.

The wide-band version may be the easier antenna to mount. If you draw a centerline through the elements to represent a boom, then the mid-point of the boom will fall just beyond the "r" in the word "driver." However, since there would be two elements and their support arms left of the midpoint, the actual position for the boom-to-mast plate would fall somewhere within the word "driver." Alternatively, some builders have placed additional weights inside the director end of the boom to provide a mast position closer to the boom mid-point.



The situation is a bit more precarious with the high-gain version of the antenna. Here, the mid-point of the imaginary boom line falls close to the "d" in "driver." Since support arms tend to be flexible and an element wire extends across the face of the support mast or tower, builders tend to use counter weights inside the director boom end to arrive at a balance point that maximizes the flexing space for the driver support arms and wire.

Because the data will be significant when we explore the electrical properties of attempted tri-band 3-element quads, let's quickly review the potential performance of both types of monoband quads. Since all bands provide similar performance, except for bandwidth issues, we can illustrate performance by reference to the widest of the upper HF bands, 10 meters. **Table 6-1** provides the dimensions for both antennas. All dimensions are in inches, and the table lists full

side lengths and loop circumferences. The spacing dimension is referenced to the reflector.

Table 6-1. Dimensions of Two 10-Meter 3-Element Quads Derived from Models and Regression Analysis

Note: All dimensions in inches. Multiply by 0.0254 for meters.  
Design frequency: 28.42 MHz.

Wide-Band Version

Element	Side Length	Circumference	Space From Reflector
Reflector	110.02	440.08	----
Driver	105.06	420.26	65.73
Director	97.60	390.40	191.09

High-Gain Version

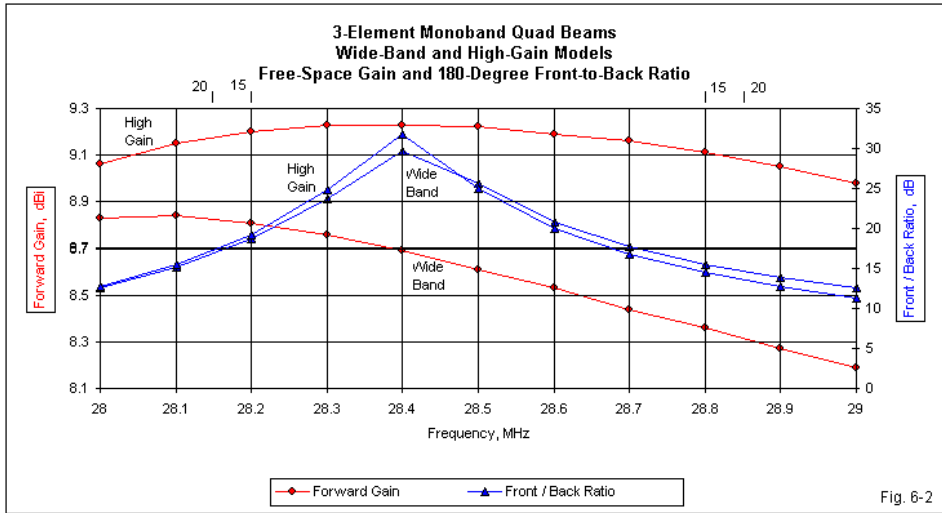
Element	Side Length	Circumference	Space From Reflector
Reflector	109.64	438.56	----
Driver	106.02	424.08	73.67
Director	101.96	407.84	166.29

The modeled performance in free space for both beams represents close to the best obtainable for 3-element quads of each type. **Table 6-2** samples the performance at the band edges and at the design frequency. Note that the worst-case and the 180° front-to-back ratios are the same at the band edges and differ only in the middle portion of the band, where the rear lobe shows a characteristic "dimple." Also notable is the difference in beamwidth between the two designs. As gain increases, beamwidth decreases. These properties are normal, not only for 3-element monoband quads, but as well for virtually any parasitic beam design.

Table 6-2. Modeled Performance of 10-Meter 3-Element Monoband Quads  
 Note: All values for free space.

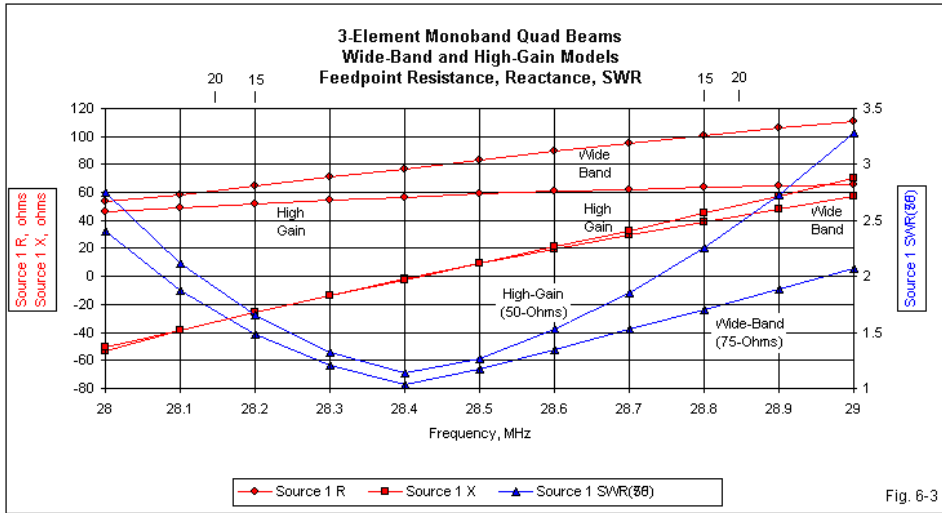
Version:	Wide-Band		
Frequency (MHz)	28	28.42	29
Gain (dBi)	8.83	8.68	8.19
Front-Back Ratio (dB)			
180°	12.52	29.79	12.51
Worst-Case	12.52	20.70	12.51
Beamwidth	64.8°	66.0°	63.1°
Feed Impedance ( $\Omega$ )	53.2 - j52.9	74.8 + j0.6	110.5 + j57.7
75- $\Omega$ SWR	2.40	1.05	2.07
Version:	High-Gain		
Frequency (MHz)	28	28.42	29
Gain (dBi)	9.06	9.23	8.98
Front-Back Ratio (dB)			
180°	12.79	31.02	11.27
Worst-Case	12.79	22.79	11.27
Beamwidth	63.0°	63.1°	61.3°
Feed Impedance ( $\Omega$ )	46.3 - j50.7	57.1 + j0.9	65.7 + j70.5
50- $\Omega$ SWR	2.75	1.14	2.65

We may correlate the main performance data in the table to the gain and 180° front-to-back curves for both models in **Fig. 6-2**. The high-gain version of the 3-element quad allows one to structure the design so that the maximum forward gain occurs at the design frequency, with lesser values at the band edges. Obtaining a high-gain curve of this shape with a Yagi is not normally possible. The high-gain quad model obtains in its 3 elements about the same gain as a long-boom 4-element Yagi. However, unlike Yagis that usually manage close to a minimum front-to-back ratio of 20 dB across the band, the quad shows the typically narrow-band nature of its front-to-back curve. The high-gain model manages 20-dB front-to-back ratio for only about 35% of the 10-meter band.



The wide-band version of the 3-element quad trades gain for a more acceptable feedpoint impedance range. The trade-off results in a gain level that is about 0.55 dB lower than the high gain model at the design frequency. The design frequency free-space gain level is close to the value obtained from a short-boom 4-element Yagi. In addition, the wide-band model shows peak gain at the low end of the band, with a decreasing gain curve toward the high end. However, the minimum gain value is about 8.2 dBi, about 1.5-dB higher than the minimum value for a 2-element monoband quad on 10 meters. Interestingly, the front-to-back curves for both the wide-band and the high-gain versions of the antenna are very similar. Differences would fall below the operationally noticeable level.

The graph also contains a pair of marks at each end—along the upper edge. Since the curves for all 3-element quads derived from the equation models would be very similar, the marks show the curve limits for the 20-meter and the 15-meter amateur bands. You may extrapolate the likely gain and front-to-back values for each band by using these limiting marks. The impedance data in **Fig. 6-3** contains the same marks for similar extrapolations.



The wide-band resistance curve centers at about 75  $\Omega$ . Although the resistance change across the band is higher than the corresponding change for the high-gain model, the reactance shows a much lower total change from 28 to 29 MHz. Hence, the wide-band model shows a 75- $\Omega$  SWR curve that covers about 900 kHz of the band with less than a 2:1 value. The same curve on 20 and 15 meters would show band-edge values well below 2:1.

The resonant impedance for the high-gain model is closer to 50  $\Omega$ , allowing within the limits of the antenna a direct connection to the typical main feedline (with a common-mode current attenuator, of course). However, the total range of reactance across the band limits the 2:1 50- $\Omega$  SWR operating bandwidth to about 600 kHz or about 60% band coverage. Since 20 meters is about 70% of the bandwidth of 10 meters, the curve would not quite allow 2:1 SWR use of that band. However, the curve would just about fit 15 meters, since it is about 60% of the bandwidth of 10 meters.

The monoband data will prove useful in evaluating the potential performance of any attempted tri-band 3-element quad. Tri-band 2-element quads managed to

produce performance levels on each band that are similar to monoband values for each band. The key electrical question will be whether or not we can expect similar results from a tri-band 3-element quad.

**Tri-Band 3-Element Quads: the Physical Questions**

Typically, there are two ways of constructing a multi-band quad: the spider and the planar methods. The spider method uses the distance between elements as measured in wavelengths as a constant. Therefore, the physical spacing between elements varies from one band to the next. **Fig. 6-4** shows a possible arrangement of elements for a tri-band quad in which the drivers form a plane and the reflectors and directors vary their distance in inches, feet, or meters as we change frequency band. The model uses the wide-band version of the monoband quad as the basis for the elements shown.

One Version of a 3-Element, 3-Band Quad  
Based on Optimized Wide-Band Monoband Quads  
Arranged as a Spider with Drivers in a Planar Arrangement

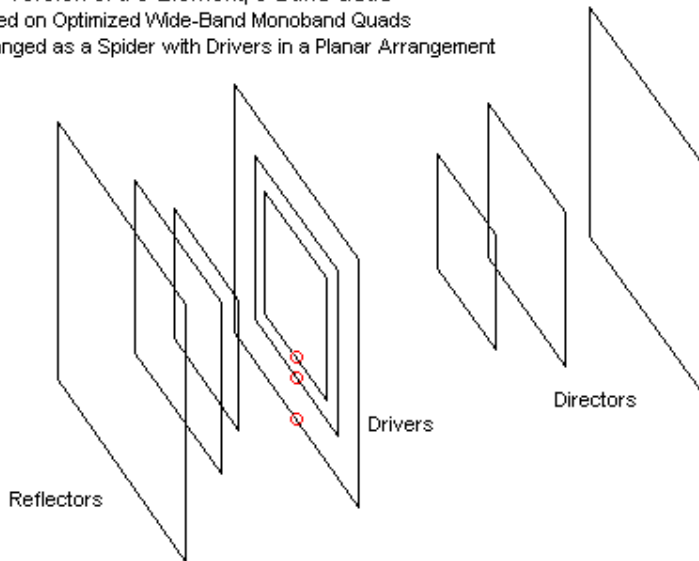


Fig. 6-4

The alternative construction method uses planar support arms for each element. **Fig. 6-5** shows the general outline for such a quad in terms of the element placement. Since the element spacing would be optimal for only one of the 3 bands—at most—the element spacing values will vary according to the design compromises used to create the structure.

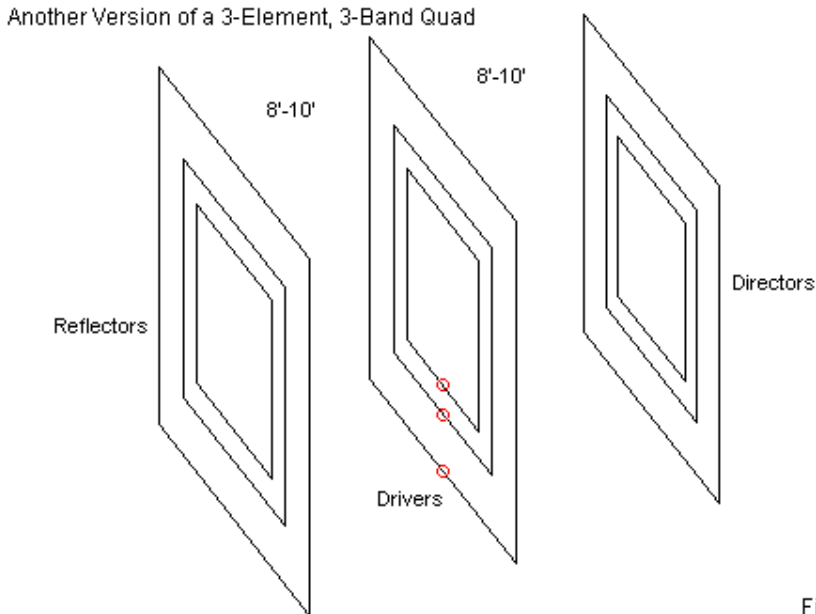
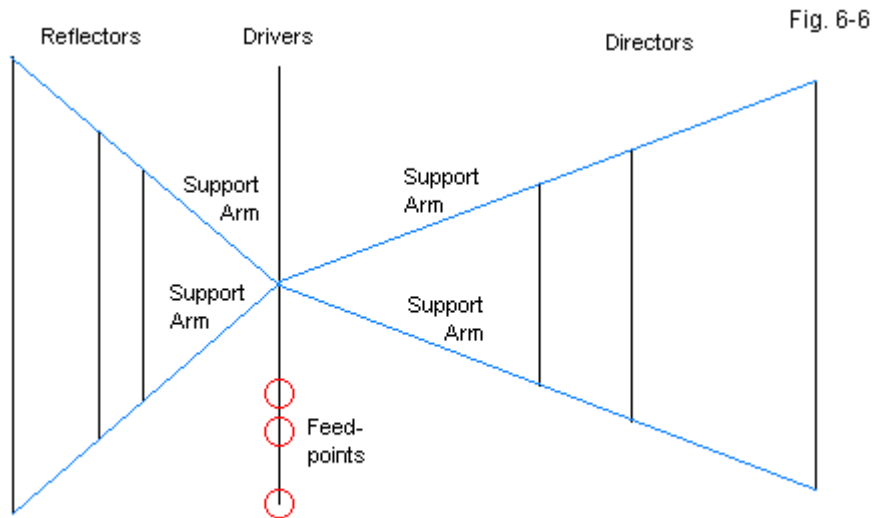


Fig. 6-5

At this juncture, we shall overlook performance questions to concentrate on the physical challenges presented by each design direction when constructing a tri-band 3-element quad. If we add support arms to the spider quad in **Fig. 6-4**, we obtain a sketch resembling the side view shown in **Fig. 6-6**.



The optimal angles for the parasitic support arms exceed what is wise (or perhaps, even what is possible) using the wide-band quad as a model. Quad support arms must be relatively light and strong, a combination that gives the arms considerable flexibility. When we exceed certain angles (that vary with the arm structure), flexibility turns into sag that tension rods between pairs of forward and rearward arms cannot overcome. We can modify the structure somewhat, perhaps by using the high-gain design with its shorter overall front-to-back dimension. However, even this design would show support-arm angles that threaten serious sag, especially if we add an ice load to the array. The next strategy might be seriously to reduce the spacing between elements. However, this tactic will either reduce the operating bandwidth or reduce the performance level below 3-element expectations.

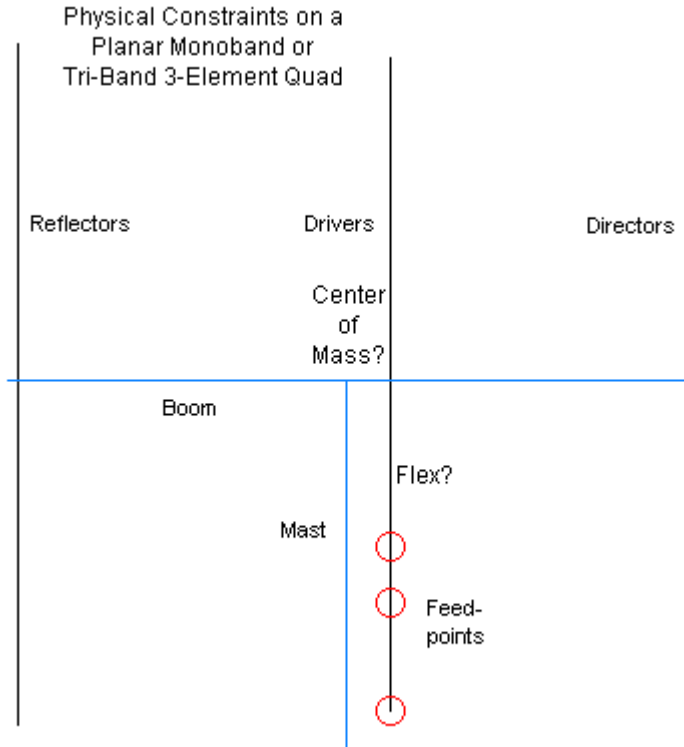


Fig. 6-7

**Fig. 6-7** shows the fundamental difficulty with all planar 3-element quads. The compromises called for in the electrical performance of this type of multi-band array tend to place the driver very close to the support mast. Typical reflector-to-driver spacing values for upper HF multi-band quads are from 8' to 10'. However, driver-to-director spacing values use the same range. Although support arm structures are lightweight and flexible, they still have some weight. Hence, even if we use different spacing values for the forward and rearward elements, we must adjust the mast-to-boom connection to compensate for the double X-structure on

one side of the mast. The net effect is to put the driver elements in jeopardy of contacting the mast or tower during normal wind loads.

For the reasons outlined, we find few 3-element tri-band quad designs available. Most builders prefer to move from 2 to 4 elements. Virtually all 4-element quad designs use planar construction. Hence, the load on each end of the boom, relative to the mast or tower, is equal. The reflector and driver elements go to the rear, while the directors ride in front. It is still important to mount the quad at its center of mass rather than using the boom-length center point. However, even that adjustment leaves several feet of space between the mast and the nearest set of element wires.

### **Tri-Band 3-Element Quads: the Electrical Questions**

There is more to dis-recommend a multi-band 3-element quad than just the mechanical details. Someone might well be able to overcome the physical constraints if the 3-element quad offered near-monoband performance on all bands, even if only in a 3-band version. However, we are unlikely to see such an antenna because the 3-element design—when multi-banded—presents some electrical problems.

To test the tri-band 3-element quad, I created a number of models using both planar and spider construction. All of the planar models failed to have either the gain or the bandwidth of the wide-band monoband 3-element quad. Since it is not possible in a finite lifetime to exhaust all of the possibilities, I cannot claim the survey to be exhaustive, although it has so far proven both exhausting and futile. Among spider models, the version of the antenna shown in **Fig. 6-4** and in **Fig. 6-6** proved to provide the best performance. **Table 6-3** samples that performance at the design frequencies. The table also lists the design-frequency monoband performance on all 3 bands to ease the task of making comparisons.

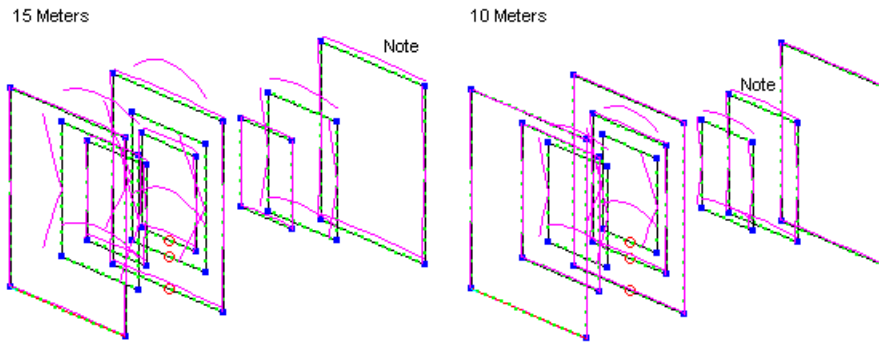
Table 6-3. Comparative Performance Values for 3-Element Monoband Quads and for a Spider Tri-Band Quad

Note: All values for free space. Wide-band designs used for both data sets.

Monoband Quads			
Frequency (MHz)	14.15	21.20	28.42
Gain (dBi)	8.59	8.64	8.68
Front-Back Ratio (dB)	29.05	29.38	29.79
E-Plane Beamwidth (degrees)	66.0	66.1	66.0
H-Plane Beamwidth (degrees)	79.1	79.1	78.9
Feed Impedance ( $\Omega$ )	77.4 - j0.2	78.1 + j0.0	78.4 + j0.6
Tri-Band Quad			
Frequency (MHz)	14.15	21.20	28.42
Gain (dBi)	8.52	8.01	7.38
Front-Back Ratio (dB)	22.95	17.14	21.44
E-Plane Beamwidth (degrees)	66.3	70.6	79.2
H-Plane Beamwidth (degrees)	79.0	86.8	99.3
Feed Impedance ( $\Omega$ )	76.3 - j4.1	61.9 - j8.8	60.1 - j8.2

The table clearly shows that we encounter a lower feedpoint resistance as we increase the frequency. However, the rate of decrease is lower than for 2-element tri-band quads. The reduced rate rests on a combination of factors, including the planar arrangement of the drivers and the fact that each driver has two elements that exert influence on the feedpoint impedance. Were it not for other factors, we might use this beam without further adjustment to the driver lengths.

Unfortunately, as we increase frequency, we also see a decline in the array gain. In fact, the 10-meter gain falls within the range that we can achieve with only 2 elements in a tri-band quad. As well, we also find a decrease in the front-to-back ratio. These numbers are not simply the product of a front-to-back peak that is on a different frequency. Rather, the decrease in front-to-back ratio is part of the same set of effects that yields the lower gain on each band above 20 meters. In fact, 20 meters is the only band on which we see near-normal (monoband) gain, and this fact provides a clue to what is happening.



Restrictions on Upper-Band Gain in a Tri-Band 3-Element Quad

Fig. 6-8

We can visualize the problem by examining **Fig. 6-8**, which shows the relative current magnitudes when we operate the array on 15 meters and on 10 meters. On the left, we find fairly high peak currents on the 15-meter elements, since the operating frequency is 21.2 MHz. There is one additional active element: the 20-meter director. Its current magnitude is over 1/3 the value of the 15-meter director current magnitude. Likewise, on 10 meters or 28.42 MHz, we find fairly high values of current magnitude on the 10-meter elements. As well, the 15-meter director is active at a current magnitude that is more than 1/2 the current magnitude of the 10-meter director.

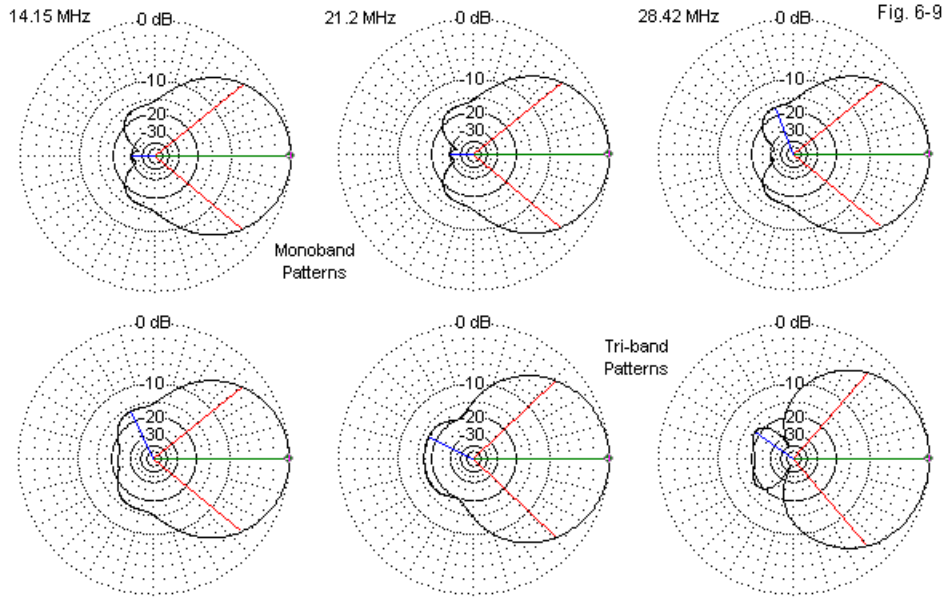
Current magnitude is not the sole determiner of what occurs with these elements. We must also consider the phase angle of the current. In the monoband versions of these 3-element quads, we find a relative current magnitude on the reflector that varies between 0.81 and 0.86 across 20 meters. The corresponding current phase varies from  $126^\circ$  to  $153^\circ$ . The modeled director current varies from 0.23 to 0.36 in relative magnitude, and a phase-angle range from  $-133^\circ$  to  $-151^\circ$ . At the design frequency, the current magnitudes and phase angles are about at the average of these ranges (0.85 at  $140^\circ$  for the reflector and 0.29 at  $-140^\circ$  for the director).

In the tri-band design, at 14.15 MHz, the reflector values are 0.84 at 131° and 0.27 at -149°—well within the range shown for the monoband beam. However, at 21.2 MHz, the tri-band reflector current is down to 0.68 at 133°, while the director current is 0.31 at -150°. The reflector relative current magnitude is low. At the same time, the 20-meter director shows current values of 0.11 at -11.6°. At 28.42 MHz, the 10-meter reflector current is 0.64 at 148°. The 10-meter director current values are 0.36 at -135°. While the combinations are not optimal, the key value is the low reflector relative-current magnitude. At this frequency, the 15-meter director shows current values of 0.20 at 20°.

If the parasitic element current magnitude and phase angle values are not radically out of line (with the possible exception of the 10- and 15-meter reflector magnitudes), then we may still be at a loss to explain why the forward gain drops so much, rather than just a little. The answer lies in understanding how currents and element functions go together. Clearly, reflector currents show a positive phase angle, while director currents show a negative phase angle in 3-element arrays. Although the exact number will change according to the precise design, the monoband ranges of magnitudes and phase angles give us ballpark values for any 3-element parasitic array. We should not neglect the driver current, which in all cases of this modeled sequence is 1.0 at 0°. Essentially, phase angle values near zero yield a driver element, and the two directors with unintended activity are closer to zero degrees than to values appropriate to reflectors or directors. In effect, the parasitically active directors for the next higher band are radiating energy, but without the direct influence of the parasitic elements that have been cut for the band in use.

The energy must go somewhere. For the subject design, the energy tends to go "up" and "down" relative to the wires in the loop as much as it goes forward and backward. In other words, we end up with wider beamwidth values, not only in the E-plane, but as well in the H-plane. Re-examine the data in **Table 6-3**. The tri-band 20-meter beamwidth values are nearly the same as the ones we derived for the monoband beam. In fact, all three monoband 3-element quads have almost identical beamwidth values. However, when we move to 15 meters, the E-plane shows a 4.5° wider beamwidth, while the H-plane value increases by about 8°. At 10 meters, relative to the monoband values, the E-plane beamwidth increases by

about 13°, while the H-plane beamwidth increases by over 20°. **Fig. 6-9** provides a gallery of H-plane patterns that show clearly the increasing beamwidth as we operate the 3-element tri-band quads on the upper bands.



Design-Frequency H-Plane Patterns: Monoband Quads and Tri-Band Combination

The exact degree of pattern deformation, relative to a standard derived from the monoband pattern, will vary with the multi-band quad design. However, every planar and spider 3-element quad design that I have examined has shown the same basic phenomena. At 15 meters, the 20-meter director is active, and at 10 meters, the 15-meter director is active. In both cases, being active means having a current magnitude of at least 10% the value of the driver. The activity is sufficient to prevent the quad from reaching its monoband performance levels on the upper two bands. Regardless of the precise design, the upper bands of a 3-element multi-band quad in some cases barely reach 2-element performance

levels.

Planar 3-element, 3-band designs are at a further disadvantage. 2-element designs exhibit only slow changes of performance with variations in reflector-to-driver spacing. However, the driver-to-director spacing (and element circumference) in a 3-element quad reacts to smaller changes in spacing. Hence, a 3-element tri-band quad tends more readily to show that fact that the element spacing is optimal at best on only one of the 3 bands and often not on any of them.

As a consequence, tri-band planar designs using 3 elements tend not to achieve a very significant gain over a 2-element quad. Optimized quad designs for the widest bandwidths easily show about 8.5-dBi free-space gain at mid-band. Optimized high-gain monoband quads top 9.0 dBi. A planar quad rarely achieves 7.8 dBi on any band.

I sampled tri-band 3-element planar quads using 3 different popular spacing values for boom lengths of 18' to 20'. One sample used 10' from reflector to driver and 8' from driver to director, while a second reversed those two numbers. A final sample used 10' for both the reflector-driver and driver-director spacing values. Although it may be possible to refine the performance further, **Table 6-4** shows the range of values at mid-band for the group of designs.

Table 6-4. Range of Tri-Band Planar 3-Element Quads Using 3 Popular Spacing Values

Note: Spacing values sampled were (from reflector to director) 10'-8', 8'-10', and 10'-10', resulting in an 18' to 20' boom length. Reported value ranges are at mid-band for each design.

Band	20 Meters	15 Meters	10 Meters
Gain (dBi)	7.57-7.81	7.76-7.85	7.44-7.85
Front-to-Back Ratio (dB)	13.5-18.4	21.5-44.0	11.8-14.0
E-Plane Beamwidth (degrees)	70.4-71.0	71.8-73.4	75.8-80.2
H-Plane Beamwidth (degrees)	88.5-87.9	88.5-91.1	92.0-98.8

The element spacing value range favors 15 meters over the other 2 bands. Hence, the overall 180° front-to-back ratio level is higher on that band. As well, the lowest gain value is higher than for either of the other bands. The planar

design also suffers in beamwidth in both the E- and the H-planes. Optimized monoband designs showed about a  $66^\circ$  E-plane beamwidth and a  $79^\circ$  H-plane beamwidth. As the table shows, all of the beamwidth values for the tri-band planar design are higher. In addition, the values increase with increasing operating frequency. Finally, the H-plane beamwidth shows considerable growth as the operating frequency increases. Given the associated physical challenges of a 3-element planar multi-band quad construction, most builders have concluded that there is no great sense in deriving 2-element performance from 3 elements.

### **Conclusion**

The only definitive point that these notes establish is that multi-band 3-element quads present both physical and electrical challenges that most quad builders find perhaps too daunting. Whether there are any sure-fire ways to overcome both sets of challenges, I frankly do not know. To this point, I have discovered none. That fact does not mean that no solutions to the electrical and mechanical problems exist. Rather, it means that I have so far lacked the stroke of ingenuity that might show the ways to reduce or eliminate the shortcomings of 3-element quads. Apparently, most quad builders have not found these ways either, since 3-element multi-band quads are far more rare than 4-element multi-band quads.

With 4 elements, a quad presents no major mounting problems other than the weight of the elements and their support arms. As well, the presence of the second director overcomes to a large measure the pattern distortions that tend to prevent 3-element quads from reaching monoband performance on the upper bands. Nevertheless, 4-element quads present their own challenges—and sometimes the means to overcome them. Virtually all 4-element quads use planar construction. The result will inevitably be that some bands have compromise performance values that emerge from using a boom length that is either too short or too long for optimal wide-band performance. At the same time, the presence of three parasitic elements per band allows the builder to offset some loop dimensions to increase the operating bandwidth with an acceptable SWR value. The challenge lies in finding the correct combination that yields operating bandwidth and reasonable performance that is worth the construction and adjustment effort. Many quad builders have found the benefit-cost ratio favorable

in 4-element designs while finding the ratio unacceptable for 3-element multiband quad designs.

## **Chapter 7**

### **The Quest for the Elusive TBWB4EQ (The Tri-Band Wide-Band 4-Element Quad)**

Tri-band quads for 20, 15, and 10 meters have a long history—about as long as hams have used quads. A number of longer tri-banders have periodically appeared in the literature. In these notes, I shall be very interested in 4-element quads of planar design, that is, with the elements for each band on a vertically oriented support frame. These designs use the same spacing between elements for all bands.

In the course of our exploration, I shall examine beams in the 30- to 35-foot boom range. Our first stop will be to examine a long-standing *ARRL Antenna Book* design to understand its limitations, especially its narrow operating bandwidth on at least one of the 3 bands that it covers. The results of this small study will form the basis for seeking out a design with a broader operating bandwidth on all bands. The first stop will be the 1983 design from W6PU, a design that has held persistent interest for two decades. The designer used the central pair of elements to form phase-fed dual drivers. My interest in this design covers two long-standing expectations of phase-fed dual driver quads: their gain and their operating bandwidth.

Next, I shall turn to designing a modified W6PU-quad that virtually anyone can replicate in model form. The goal will be to obtain full-band coverage of 20, 15, and 10 meters, with adequate gain and front-to-back performance. I shall use a few techniques not easily available to the design originator in order to simplify the array and to overcome some of the problems with the original version. Finally, I shall set up a reasonably fair set of comparative beam designs to evaluate whether anyone should go to the effort of actually building a tri-band wide-band 4-element quad beam.

#### **A Standard Tri-Band 4-Element Quad Design**

Many quad builders prefer to bypass the 3-element beam on their way up the ladder of performance. Odd numbers of elements tend to place the driver very

close to the support mast and tower, resulting in a conflict between electrical and mechanical requirements. An even number of elements places the mast equally distant between the center two elements, freeing the builder from at least one potential interaction problem.

Traditionally, quad designers have used a somewhat arbitrary spacing of the elements. 4-element quads for multi-band service often use equal spacing between all elements, with 8' and 10' being the most common values. A few designs have used a combination of these values, so that we can find 4-element tri-band designs with boom-lengths ranging from 24' to about 30' or so. The premise behind the spacing selection stems from the use of planar element assemblies. In terms of wavelengths, a fixed physical spacing between elements results in a different spacing for each band. For example, fixed 10' spacing between elements is about  $0.14\text{-}\lambda$  on 20,  $0.21\text{-}\lambda$  on 15, and  $0.28\text{-}\lambda$  on 10 meters.

The design of the quad then rests upon finding the element circumferences that will produce an acceptable combination of gain, front-to-back ratio, and feedpoint impedance, all with satisfactory operating bandwidths. Prior to the 1990s, the design effort was largely *empirical*, a term meaning trial and error. Indeed, most existing quad designs in amateur literature have their roots in the pre-computer-modeling period of antenna design.

One very interesting design appears in *The ARRL Antenna Book* for editions prior to the 19<sup>th</sup>. It appears in the table on page 12-2 of the 18<sup>th</sup> edition. The beam consists of 4 elements, each spaced 10' from the adjacent element. Hence, we have a total boom length of 30', plus whatever end lengths are necessary to handle the support-arm structures. **Fig. 7-1** supplies a basic outline of the quad's electrical structure. Throughout, the design of this quad, and the others that we shall examine, presumes separate feedlines for each band, with closed driver loops for each inactive band.

**Table 7-1** shows the element dimensions for the quad design. The antenna uses a direct feedline connection on 20 and 15 meters. However, 10 meters requires a quarter-wavelength  $75\text{-}\Omega$  matching section to transform its higher feedpoint impedance (above  $100\ \Omega$ ) down to the feedline's  $50\text{-}\Omega$  characteristic

impedance. The fixed element spacing creates a rising driver impedance as we move upwards through the HF bands. Although carefully choosing the element lengths can alter the impedance to some extent, there are severe limits to the range of adjustment. Trying to lower the 10-meter impedance for a direct 50-Ω feed tends to degrade the other performance parameters on that band.

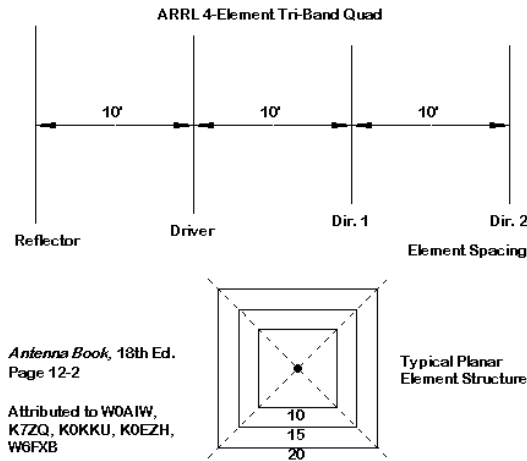


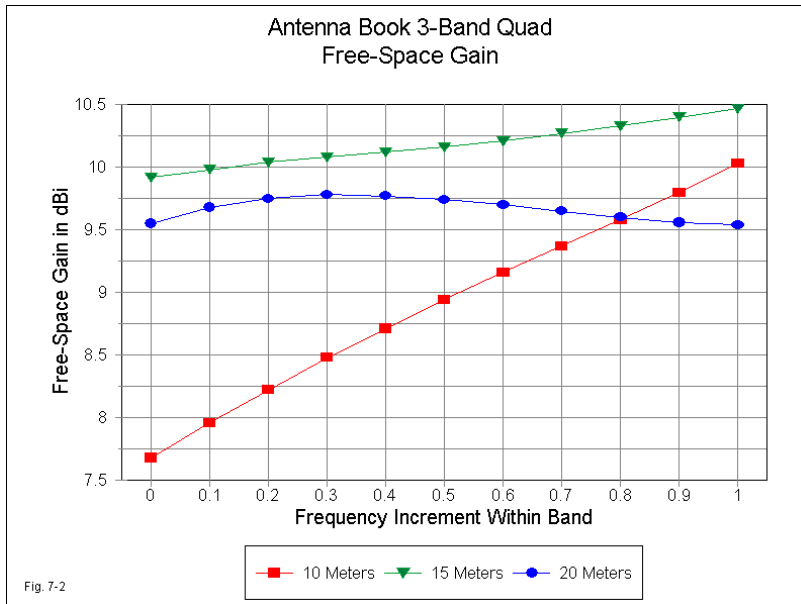
Fig. 7-1

Table 7-1. Dimensions of the ARRL *Antenna Book* 4-element, 30'-boom, tri-band quad

Element	Space from Reflector (feet)	Circumference in feet		
		20 Meters	15 Meters	10 Meters
Reflector	----	72.42	48.67	35.70
Driver	10.0	70.42 (70.80*)	47.33	34.70 (35.20*)
Dir. 1	20.0	69.08	46.33	33.60
Dir. 2	30.0	69.08	46.33	33.60

\* Dimensions in parentheses indicated modeling changes of the driver circumference to set the 50-Ohm SWR curve within the band limits. 20 and 15 meters use direct 50-Ohm coax connections; 10 meters uses a 1/4-wavelength 75-Ohm matching section to the 50-Ohm feedline.

In trying to model this antenna in NEC-4 using AWG #12 copper wire, I had to alter the published length of the 20-meter and the 10-meter drivers—both upward—in order to place the 50- $\Omega$  SWR curves within the band limits. 15 meters required no adjustment in the model. In part, this situation stems from the fact that the 15-meter dimensions result from interaction between the elements for that band and the elements for both of the other bands. The 10-meter and 20-meter elements interact mainly with only one other band. Key variables for those bands also include methods of assembly. Attaching elements to the support arms is subject to a number of variations, some of which result in the creation of small 1-turn inductive loops at each corner. Together, they can have an effect upon the electrical length of a loop, with the most pronounced effect on the driver, where the relative current magnitude is highest. The fact that I had to increase both driver lengths—which make clean corners in the model—by similar amounts suggests that the empirically derived design may take such mounting loops into account.



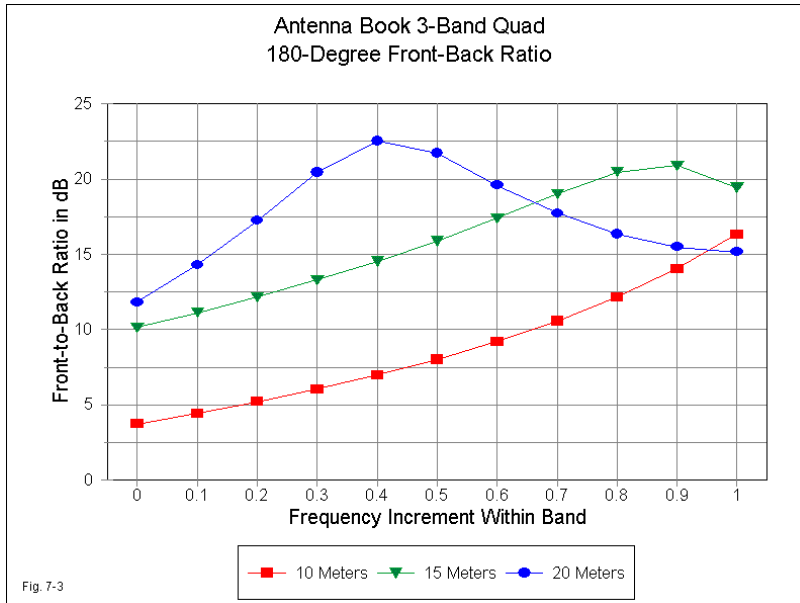
I modeled this traditional design in free-space as simply a guide to its anticipated performance level. All other beam designs that we shall consider also use free-space models, thus allowing a direct comparison of performance among them. **Fig. 7-2** shows the modeled forward gain performance of the array. This and other performance graphs subdivide each amateur band into 10 parts to permit combined presentations. 10 meters covers the 28- to 29-MHz portion of the band.

To make sense of the graph, we should note a few benchmarks that emerge from monoband beams. A short-boom 3-element Yagi (about 16' on 20 meters) achieves a free-space gain of over 7 dBi, while a long boom version of the array (about 24' on 20 meters) is capable of just over 8 dBi. These values are approximate, since 3-element Yagis show a rising gain value across the operating bandwidth. An optimized 2-element monoband quad achieves 7 dBi or so. We may optimize 3-element models for the widest operating bandwidth and obtain just over 8.5 dBi or for maximum gain and reach about 9.1-dBi free-space gain. An optimized 4-element monoband quad that uses #12 copper wire—like the other quads cited—is capable of just about 10 dBi maximum.

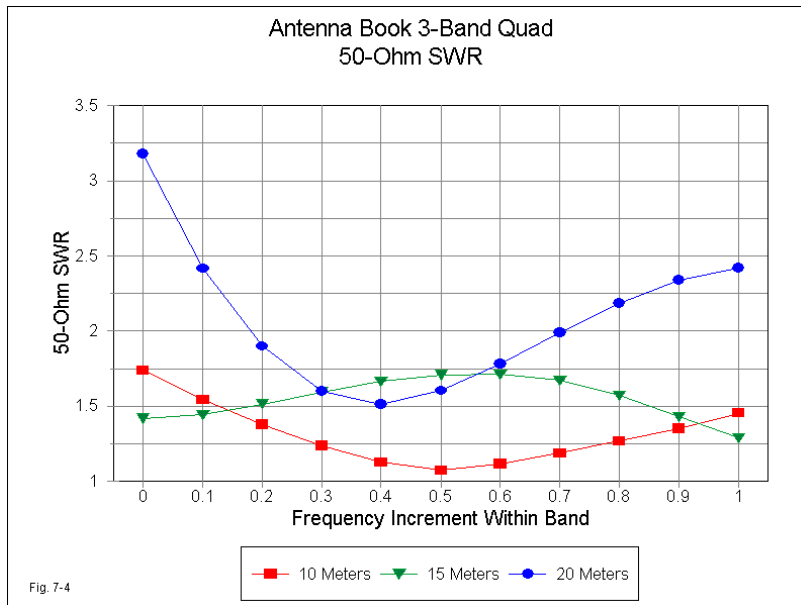
Since the boom length of the tri-band quad is considerably shorter than its monoband 4-element counterpart, we should not expect 4-element performance in the optimized monoband sense of the term. And we do not get it. However, we do obtain very respectable 20-meter performance in the 9.5-dBi range across the band. Helped by interactions with the surrounding elements for other bands and a longer boom as a percentage of a wavelength, the 15-meter gain performance does achieve the 10-dBi level. The 10-meter boom length is too long and thus shows a rising curve with a minimum value below 8 dBi. All in all, the quad design achieves quite good gain performance as a tri-band effort on a 30' boom.

Optimizing a monoband quad tends to bring the maximum 180° front-to-back ratio in close frequency-proximity to a desired gain level and the resonant feedpoint impedance of the array. Hence, these values are usually in excess of 20 dB and sometimes as high as 40 dB, although such a high peak front-to-back value is a narrow-band phenomenon. Most optimized monoband designs strive for relative equal band-edge values, and the exact band-edge front-to-back ratio will depend on the element diameter and the bandwidth of the passband as a function of its center

frequency. A tri-band quad does not have the luxury of such techniques, as **Fig. 7-3** will reveal.

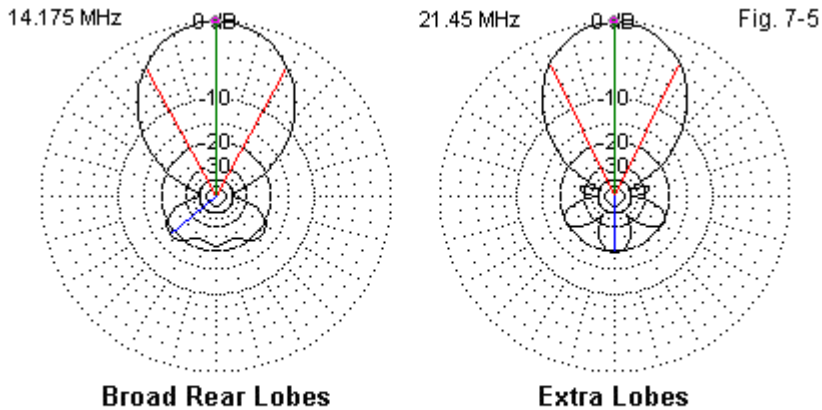


Both 20 and 15 meters show very respectable front-to-back curves, with minimum values between 10 and 12 dB, both at the low end of the bands. 10 meters shows the most problematical curve, with extremely low values in the CW portion of the band, but much improved values higher up. The coincidence of the rising gain and front-to-back curves suggests that one might go some distance in further optimizing performance for 10 meters within the first MHz of the band. However, every change in the 10-meter loop dimensions will force a change in the adjacent 15-meter element, with consequences for the outer 20-meter element. Hence, optimizing the present 10-meter portion of the design—with the potential pitfalls of ruining the 15- or 20-meter performance—is a significant task. It falls outside our use of the model as a representative existing design for comparative purposes.



The 50- $\Omega$  SWR curves appear in **Fig. 7-4**. Both 10 and 15 meters achieve less than 2:1 SWR across the bands. However, remember that the 10-meter driver includes a quarter-wavelength matching section that the model includes. Only the 20-meter SWR curve falls short of the mark, largely due to the fact that both the feedpoint resistance and reactance show large excursions. The resistance changes by 44  $\Omega$  across the band, while the reactance changes by 81  $\Omega$ . For comparison, the feedpoint resistance on 15 meters changes by just 6  $\Omega$ , while the reactance changes by 20  $\Omega$ . The 20-meter curve is a function of the fact that the loops for that band have no further lower-band loops with which to interact. Hence, they tend to show more normal monoband properties for the boom length and the element spacing than do the higher-band elements. Despite slight interactions with the 15-meter elements, the 20-meter elements display the narrow SWR bandwidth typical of monoband 20-meter quads on the same boom. The original tables for the ARRL quad design show separate dimensions for the CW and the SSB portions of the

band.



### Some Typical Multi-Band Quad Pattern Characteristics

Multi-band quads have a few other idiosyncrasies that do not show up readily in tables. Pattern shape is one of them, and **Fig. 7-5** displays some of them. However, the ARRL quad design is remarkably free of extreme pattern, and so the figures only modestly represent what we often see in more extreme forms. The pattern to the left shows a typical multi-band quad fantail. The rear lobes on multi-band quads often show considerable strength in rear quartering directions, resulting in worst-case front-to-back ratios that are considerably lower than the 180° front-to-back ratio. Inadequately designed LPDAs with too few elements for the frequency span covered tend to show a similar problem. It is likely that the fantail effect is a product of interactions with supposedly inert elements for other bands. Some have attributed the spread to the fact that there is a small vertically polarized component to the pattern, but this component does not result in forward beamwidths significantly wider than those we achieve from Yagis of similar gain potential. With respect to the relatively modest fantail shown in **Fig. 7-5**, the only function of the vertical radiation component is to reduce the deep side nulls that we might find for a Yagi.

The other pattern anomaly that accompanies multi-band design is the appearance of extra lobes, as shown by the 15-meter pattern in **Fig. 7-5**. In monoband design, it is possible to suppress secondary or forward side lobes through at least 6-element arrays. However, multi-band quads tend to show some extraneous lobes, even with only 3-4 elements per band. The most likely source of them is from the inactive elements for the other bands. As we increase loop size above about 1.5 wavelengths or decrease it below about  $0.75\lambda$ , the radiation tends to move from the desired broadside orientation toward the loop edges. Even low-level, induced activity in the supposedly inert loops can yield small lobes, such as the pair of side lobes shown in **Fig. 7-5**.

Nonetheless, the patterns of the ARRL quad show the anomalies only in small and relatively harmless ways. Moreover, the array shows very adequate levels of gain and front-to-back ratio. The 10-meter performance might withstand further optimizing, assuming one could achieve this goal without unduly disrupting the performance on 20 and 15 meters. Still, the task is one internal to the basic 4-element design itself.

We came to the ARRL 4-element, tri-band quad with the idea of using it as a comparator for reportedly improved designs. However, there are perhaps only two reasons for changing the basic design of the quad. One is to improve the operating bandwidth across 20 meters. The other is to see if we cannot achieve higher levels of gain and front-to-back ratio from a similar boom length. The next step in our exploration is to review an old design that seems to promise both improvements

### **The Original W6PU Dual Driver 4-Element Tri-Band Quad**

In the December, 1983, issue of CQ, Robert Martinez, W6PU, presented "The Evolution of the Four-Element Double-Driven Quad Antenna" (pp. 30-36). The article is absolutely typical of the period relative to antenna design. Without the benefit of well-calibrated computer calculation of antenna performance potentials, the era was filled with countless writers who handled decibels without due care.<sup>1</sup> Perhaps the most important of the W6PU claims are an improvement of 5.5 to 6.0 dB in forward gain and a 30-dB front-to-back ratio. Since the author refers to 2-element and 4-element quads for 40 through 10 meters, it is unclear over what the

new antenna showed the higher gain. However, we can model the W6PU 4-element, tri-band, dual-driver quad and see what we get. Since we have just reviewed a comparable model of a reasonably competent 4-element single-driver quad, we shall be able to tell if the builder effected any improvements by using dual drivers.

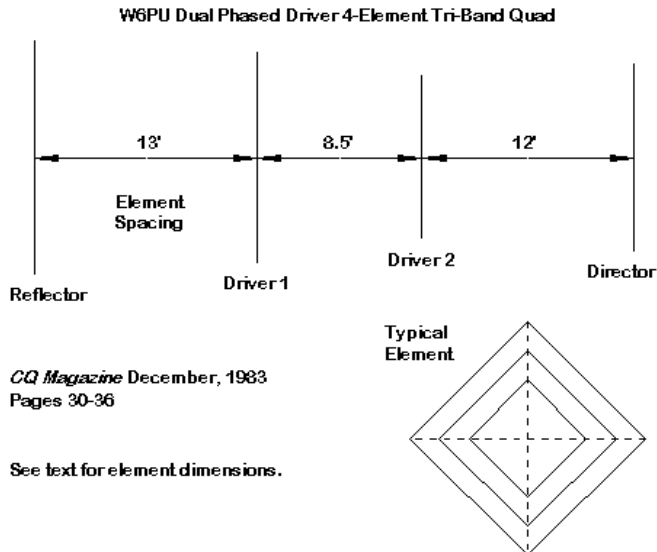


Fig. 7-6

**Fig. 7-6** shows the general outlines of the W6PU quad. The total boom length is 33.5' (plus the usual end additions for hardware). **Table 7-2** supplies the element loop circumferences used to construct the test model from the article description.

Table 7-2. Dimensions of the W6PU dual-driver, 4-element, 33.5'-boom, tri-band quad

Element	Space from Reflector(feet)	Circumference in feet		
		20 Meters	15 Meters	10 Meters
Reflector	----	75.42*	50.30*	37.24*
Driver 1	13.0	71.75	47.83	35.92
Driver 2	21.5	68.17	45.42	34.08
Dir. 1	33.5	68.67	45.83	34.42

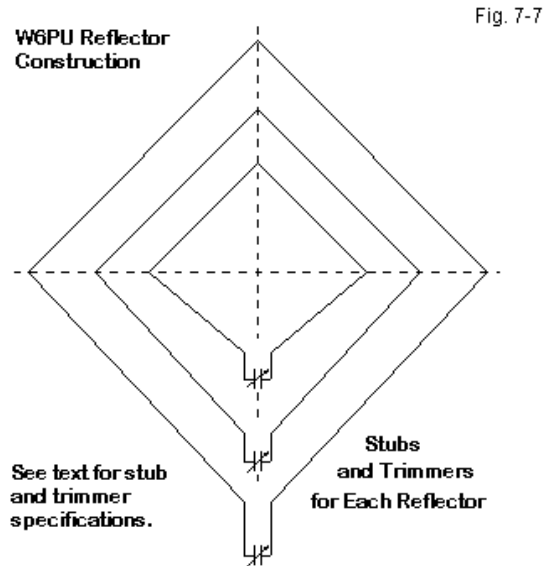
\*From Robert Martinez, W6PU, "The Evolution of the Four-Element Double-Driven Quad Antenna," CQ (December, 1983), pp. 30-36. Original specifications call for reflectors using the same circumference as the first driver, but with shorted transmission-line stubs and trimmer capacitors. The NEC-4 models use electrically equivalent full-size reflector loops, with the circumferences listed in the table.

The original reflector loop specifications called for loops identical in circumference to the ones used for driver 1. However, each reflector had a specified shorted transmission line stub with a trimmer capacitor across the short to tune the stub. See **Table 7-3** for the values involved and **Fig. 7-7** for the layout given in the article.

Table 7-3. Dimensions of the reflector stubs of the original W6PU quad.

Band	Stub Impedance In Ohms (see text)	Stub Length in feet	Trimmer Capacitor in pF
20	300	4.50	150
15	300	3.50	100
10	300	2.25	75

Note: article specifies 300-Ohm or 1.5" wide stub line. Reflector circumference for each band is identical to the listed value for the first driver circumference in Table 7-2.

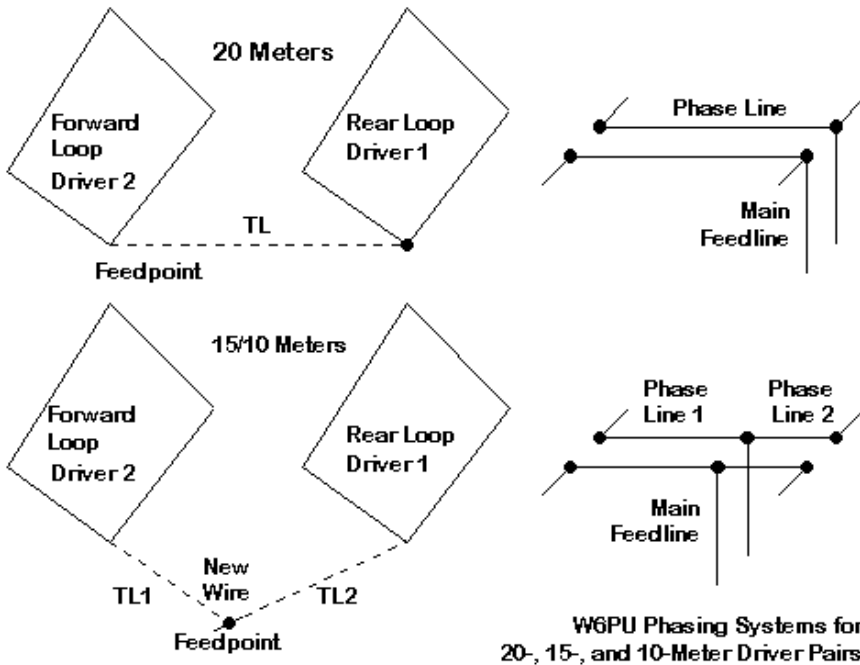


Unfortunately, the text gives the builder the alternative of using 300- $\Omega$  line or home-crafted lines spaced 1.5" apart. A stub made from AWG #12 copper wire and spaced 1.5" will have a characteristic impedance of about 435  $\Omega$ . Hence, for modeling purposes, it became impossible to know what sort of stub lengths and trimmer settings might have been used. The simpler method of proceeding was to use full size reflectors that are electrically equivalent to the stubbed and trimmed elements used in the original model. The values shown in **Table 7-2** resulted in the best gain and front-to-back performance across the band—without altering the other element sizes.

Note that the driver closest to the reflector is designated as driver 1, while the one closer to the director is called driver 2. This orientation is necessary to fully appreciate the sketch in **Fig. 7-8**. The right-hand side shows the phase-line arrangement between drivers for the 20-meter band—which uses a single line—and

the 10- and 15-meter bands—which use a split-line phasing system. The feedpoint, contrary to most phase-line systems used in horizontal arrays, is at or closer to the rear driver (driver 1). **Table 7-4** provides data on the specified line lengths. The original article carefully notes the use of 50-Ω (RG-8A/U) line with a velocity factor of 0.66. The electrical lengths used in the model of the antenna are the equivalent lengths for a velocity factor of 1.0.

Fig. 7-8



W6PU Phasing Systems for 20-, 15-, and 10-Meter Driver Pairs

Table 7-4. Phase-line lengths for each band for the W6PU quad.

Band	Line Route	Physical Length	Electrical Length	Feedpoint
20	Driver 2 to Driver 1	8.50'	12.88'	Driver 1
15	Driver 1 to Junction	7.17'	10.86'	Junction
	Driver 2 to Junction	14.58'	22.10'	Junction
10	Driver 1 to Junction	5.33'	8.08'	Junction
	Driver 2 to Junction	9.67'	14.65'	Junction

Note: All phase lines 50-Ohm, VF 0.66 coaxial cables. Driver 1 is the element closest to the reflector--that is, the rear driver.

Modeling a multi-band quad in NEC requires attention to a number of factors. First, the antenna wires require a bit more than minimal segmentation at the highest frequency. The model uses 7 segments per side or 28 segments per loop at 10 meters. Since the segment length should be relatively constant throughout the assembly, the 15-meter elements used 11 segments per side and the 20-meter elements used 15 segments per side. Second, the split phase lines require a junction segment to use for the antenna feedpoint. The technique appears in the left-hand side of **Fig. 7-8**. All wires are AWG #12 copper.

The structure is a diamond. Setting coordinates around the system involves calculating the support-arm length for each loop. For square loops, the corner coordinates are each simply the circumference divided by 8, so that each side is 1/4 of the circumference. For diamond loops, the arm length is the circumference divided by  $4 * \text{SQRT}(2)$  or 5.6569. To simplify adjustments when changing any loop size, I used software (NEC-Win Plus) with variables. **Fig. 7-9** shows part of the set-up of the page on which I assigned variables. **Fig. 7-10** presents a portion of the page on which I set up the wires by using variables instead of constants. An alternative view of the same program page would show the numbers created by the assignment of variables. Changing a loop size thus requires only one revised entry in the model. Since NEC-Win Plus uses NEC-2, I crosschecked the results of each run using NEC-4 software. The results are the same.

NEC-Win Plus+ [w6pu-orig-20.nwp]

File Edit Configure Commands Help

Frequency (MHz) Start: 14.14 End: 14.14 Step Size: .1

Ground: No Ground

Radiation Patterns: 0°<Az<360°,El=0°,Step=1°

Geometry: Zo = 50 Ohm

B12 79 Fig. 7-9

A	B	C	D	E	F	G	I
1	Var.	Value	Comment	Scratch Pad			
7	D =	145.66	20 dir				
8	E =	106.7	15 ref				
9	G =	101.47	15 dr1				
10	H =	96.34	15 dr2				
11	I =	97.23	15 dir				
12	J =	79	10 ref				
13	K =	76.19	10 dr1				
14	L =	72.3	10 dr2				
15	M =	73.01	10 dir				
16	N =	156	refl-dr1 space				
17	O =	258	refl-dr2 space				
18	P =	402	refl-dr space				

Wires Equations NEC Code Model Params

NEC-Win Plus+ [w6pu-orig-20.nwp]

File Edit Configure Commands Help

Frequency (MHz) Start: 14.14 End: 14.14 Step Size: .1

Ground: No Ground

Radiation Patterns: 0°<Az<360°,El=0°,Step=1°

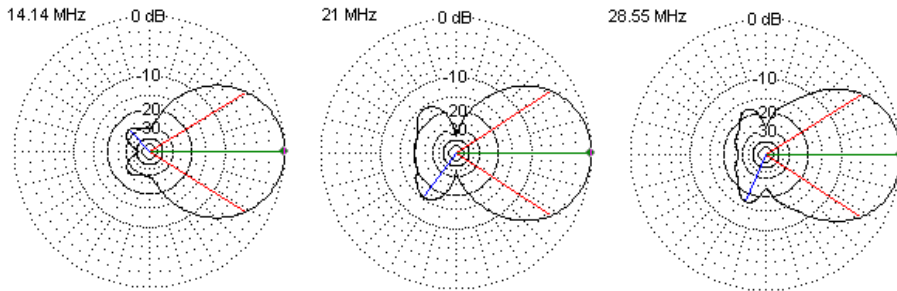
Geometry: Zo = 50 Ohm

N8 1/0 Fig. 7-10

Wire	Seg.	X1	Y1	Z1	X2	Y2	Z2	Dia.	Conduct	SrcLd
8	15	=N	0	=-B	=N	=-B	0	12 AWG	Copper	1/0
9	15	=O	=-C	0	=O	0	=C	12 AWG	Copper	0/0
10	15	=O	0	=C	=O	=C	0	12 AWG	Copper	0/0
11	15	=O	=C	0	=O	0	=-C	12 AWG	Copper	0/0
12	15	=O	0	=-C	=O	=-C	0	12 AWG	Copper	0/0
13	15	=P	=-D	0	=P	0	=D	12 AWG	Copper	0/0
14	15	=P	0	=D	=P	=D	0	12 AWG	Copper	0/0
15	15	=P	=D	0	=P	0	=-D	12 AWG	Copper	0/0
16	15	=P	0	=-D	=P	=-D	0	12 AWG	Copper	0/0
17	11	0	=-E	0	0	0	=E	12 AWG	Copper	0/0
18	11	0	0	=E	0	0	=-E	12 AWG	Copper	0/0
19	11	0	=E	0	0	0	=-E	12 AWG	Copper	0/0

Wires Equations NEC Code Model Params

Running the model on each of the bands produced the free-space E-plane patterns shown in **Fig. 7-11**. Each pattern represents my judgment of the best pattern on the band, with a record of the frequency at which it occurred. Besides the anticipated fantail rear lobes on the upper two bands, they are all well behaved. The question is whether we achieved anything with these well-shaped patterns.

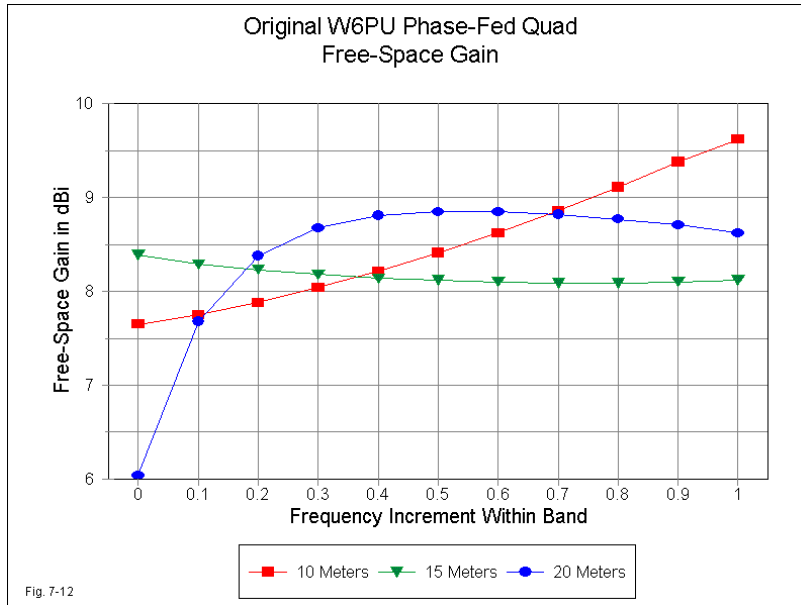


**Original W6PU Dual-Driver 4-Element Tri-Band Quad  
Best Free-Space E-Plane Patterns**

Fig. 7-11

**Fig. 7-12** graphs the free space gain of the array across each of the bands, using the same graphing scale that we applied to the single-driver ARRL quad beam. The 10-meter gain curve is very similar to the one obtained from the ARRL quad. The 15-meter curve is similar in its evenness, but at a level that is below the values that we obtained from the single-driver beam. The 20-meter curve peaks at mid-band. It descends very slowly above the peak frequency, but drops precipitously at the low end of the band.

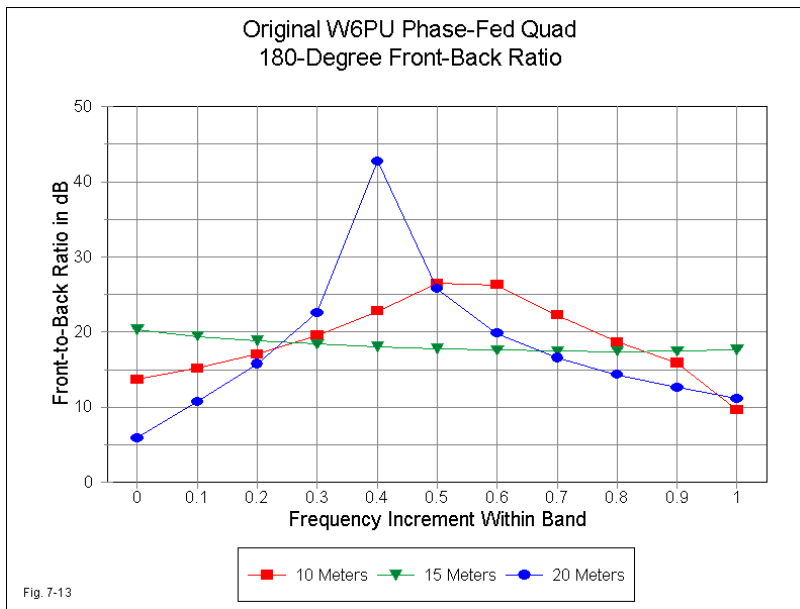
We can see the results for the 180° front-to-back values in **Fig. 7-13**. The values are not significantly different overall from those obtained from the single-driver array. Perhaps the one major difference lies in the very high peak value on 20 meters near 14.14 MHz. The pattern shape in **Fig. 7-11** reveals that the antenna has almost no rear lobes at all—just enough to recognize the deep 180° dimple. Accompanying this remarkable front-to-back value is a severe decrease in the front-to-back ratio at the low end of the band, corresponding to the great decrease in forward gain in the same frequency region.



One might surmise that W6PU created the antenna to obtain a coincidence of maximum gain and maximum front-to-back ratio for a small portion of the 20-meter spectrum. 10 meters also shows a mid-band front-to-back ratio peak, but of much smaller proportions. 15-meters is flat. However, the array design using phase-fed drivers fails to produce any gain over the single driver quad explored earlier in these notes. Since we do not know the design of the quad against which he made his gain comparisons, any further conclusions than this one would be speculative.

We need not speculate about the feedpoint impedances obtained with the model of the W6PU array. They are all too low to graph against a 50- $\Omega$  standard. All of the reported impedances have a very low reactive component, with the maximum range over the 3 bands going from  $-j8 \Omega$  up to  $+j11 \Omega$ . However, the resistive component is problematical. On 10 meters, it runs from 9 to 20  $\Omega$ . On 15, the range is 9 to 11  $\Omega$ . On 20, it runs from 1.5 to 15.5  $\Omega$ . The diagrams all show a

direct connection to a 50- $\Omega$  feed line. However, the model suggests that a 1:4 transformer would be necessary to achieve a 50- $\Omega$  impedance across even part of the bands. With such a transformer, 15 meters would show under 2:1 50- $\Omega$  SWR across the band. 10-meters might provide about 800 kHz of coverage, since the feedpoint resistance rises very slowly across the first half of the band and much more rapidly thereafter. On 20, the SWR would be satisfactory only over the upper or SSB portion of the band. Of course, this speculation assumes the use of a 1:4 transformer with high efficiency.



The number of times that the W6PU dual-driver array has been brought to my attention suggests that numerous antenna planners are using the beam as a potential foundation for their own antenna work. Yet, we are left with a quandary. If the dual-driver system aimed to increase gain over a single driver, it failed. If it aimed to produce a wider passband than the single driver array, it also failed.

In arrays using phase-fed dual drivers, the constraints of phase feeding the drivers make maximum gain and a wide passband virtually contradictory. It is possible to set the current magnitude and phase on the two elements so that they yield very high gain—over 7 dBi in free-space models of 2-element phased horizontal arrays—over a very narrow passband and at a very low impedance. It is also possible to set the driver current magnitudes and phases to achieve maximum front-to-back ratio, but only at a lesser gain, perhaps just below 6 dBi. The required current magnitudes and phases for a given pair of elements are very different for the two conditions. In phase-fed Yagi studies, I have used the high-gain setting with a director to achieve further gain and a very good front-to-back ratio—but only at the cost of a low feedpoint impedance and a bandwidth only suited to the so-called WARC bands.<sup>2</sup>

Obtaining a wide operating bandwidth tends to require a set of current magnitude and phase conditions that fall in between those needed for the extremes of gain and of front-to-back ratio. The improvement in horizontal arrays using linear elements tends to be only marginal, usually to the front-to-back ratio over the entire passband, relative to Yagis with similar spacing and the same number of elements. The gain remains at or just under the levels achieved by a well-designed Yagi of the same boom length and the same number of elements.<sup>3</sup>

Since it is unlikely that the phase-fed dual driver system can achieve any gain advantage over the single-driver ARRL quad array, perhaps the rightful place for the W6PU array lies in providing full band coverage with good gain and front-to-back values for all of the bands—including 20 meters. However, if we hope to achieve a wide-band, 50- $\Omega$  feed system, the array will have to undergo considerable redesign.

### **A Modified W6PU Dual Driver 4-Element Tri-Band Quad**

Designing a simple 2-driver log-cell Yagi begins with the design of the phased drivers. When we add parasitic elements to the driver set, we ordinarily do not disturb the drivers. Instead, we set the length and spacing of each parasitic element for a desired set of performance curves over the selected passband. Finally, we either accept the feedpoint conditions presented by the phased drivers,

or we take the entire array through a number of iterations attempting to preserve the performance curve while attaining a desired feedpoint impedance curve. In theory, designing a dual-driver monoband quad would follow the same scenario.

Our subject antenna, however, is not a monoband quad, but rather a tri-band quad with preset element spacing. Our goal is to discover if we can adapt the basic design to a reasonably high performance array, using the ARRL quad as an initial measuring stick. As well, the goal is to find out if we can extend the passband so that we obtain full band coverage on 20 and 15 meters and full coverage from 28 to 29 MHz on 10 meters. The task has some limiting factors. First, the element spacing, even between drivers, varies from one band to the next as a function of a wavelength. Second, the interactions among the active elements and the passive ones may complicate not only the sizing of the parasitic loops, but as well, the phase line for the active band. Indeed, because changes in the phase line length on one band will affect the activity of the elements when passive, we have an additional variable that will affect the outcomes. Hence, we shall require a considerable number of iterations to assure that we attain the project goals.

Refer to **Fig. 7-5** for the general outline of the modified W6PU phased-driver array. The elements of that sketch do not change in the process of modification. However, we do change the phase-line scheme to a more conventional one that uses a single line between drivers for each band. As well, we feed the forward driver, as shown in **Fig. 7-14**. These moves are for convenience of design and do not invalidate the use of split lines to effect the desired phasing. The goal is to find a ratio of current magnitude on the drivers and a set of relative phase angles that will yield acceptable performance.

A phased pair of drivers requires relative current magnitudes and phase angles of certain orders for any given performance curve. The current magnitudes are normally close to but hardly ever precisely equal. The current phase angle between the two elements varies with the spacing, with the rear element showing a positive angle relative to the forward element. The wider the spacing, the larger the phase-difference required for a given result.

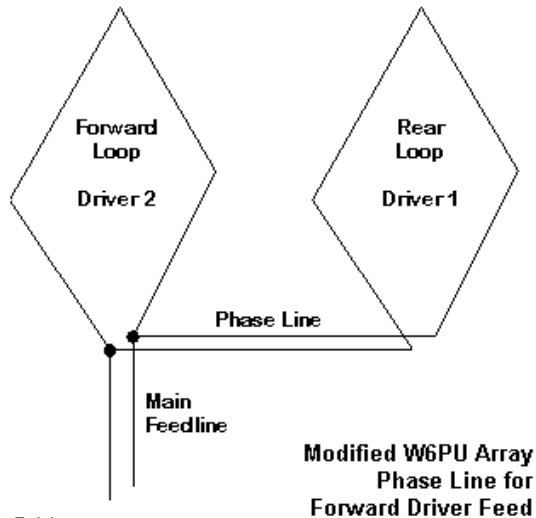


Fig. 7-14

At the same time, we wish the feedpoint to exhibit an acceptable impedance. In our test case, the target is  $50\ \Omega$  resistive, with slow variations of both resistance and reactance as we move away from the design frequency. For a system that uses a single line between the drivers, we may presume a constant voltage at the junction of the forward element and the phase-line end. The parallel connection forms a current divider. The forward element feedpoint impedance sets the current level and phase angle for the forward element. However, the impedance on the phase-line side is determined by the impedance of the rear element, as transformed along the phase line. Hence, the phase-line characteristic impedance and length play a role in determining what impedance appears at the junction. This impedance, in parallel with the forward element impedance, determines the current division. The transformation of the current and its phase angle working back toward the rear element determine the current magnitude and phase angle at that point. The parallel combination of the phase-line forward-end impedance and the forward element impedance yield the feedpoint impedance of the array.<sup>5</sup> If we use a split pair of phase lines, with a length forward to the front element and another length

back to the rear element, we only complicate the situation by one more set of transformations along an added transmission line.

The presence of parasitic elements and of interactive undriven elements for inactive bands assures that the simple calculations will not yield usable results. Therefore, when all else fails, one uses the method of experimental iteration, also known as trial and error. By a series of trial phase-line lengths and characteristic impedances, accompanied by judicious re-sizing of some element circumferences, one can see trends in performance, as well as the limits of improvement made by further changes of the same type. The initial stage involved finding settings for the individual bands, followed by re-adjustments occasioned by the fact that changes to one band required additional changes to the other bands.

Table 7-5. Dimensions of the modified W6PU dual-driver, 4-element, 33.5'-boom, tri-band quad

Element	Space from Reflector(feet)	Circumference in feet		
		20 Meters	15 Meters	10 Meters
Reflector	----	73.07	50.30	37.24
Driver 1	13.0	72.12	49.97	36.06
Driver 2	21.5	67.41	46.20	33.00
Dir. 1	33.5	67.88	45.83	34.42

**Table 7-5** provides the dimensions of the final model for the modified W6PU array. The most notable changes are the enlargement of the rear drivers and the shrinkage of the 20-meter and 10-meter forward drivers. The 15-meter forward driver is actually larger than in the original array. Changes to the circumferences of reflectors and directors tweak performance or the position of performance peaks within the passband.

A 50-Ω phase line proved satisfactory for all bands, but its length is not what we expect of a 2-element phase-line. We are used to the trick of reversing the connections of a short phase line to accrue the impedance transformation of a longer line, for example, giving a half twist to a 45° line to effect a 135° line.

Because early principles in amateur circles stressed the impedance transformation rather than the current transformation in the phase line, we have mis-labeled the effect of the half twist. A 45° line with a half twist does not transform to 135 degrees, but instead to -45 degrees—or 315 degrees, if counting always in a positive direction. Of course, the current transformation is only 45 degrees if the rear element has an impedance value that matches the characteristic impedance of the phase-line.

The spacing between the two drivers in our array does not permit the use of a very short line. Hence, we need to use longer lines without the twist for our phase lines. The shortest line must be at least 8.5' long, plus a small addition to clear the supporting mast for the array. On 20 meters and 15 meters, the required 50-Ω lines are considerably longer. In this exercise, I shall pass over the difficulties of physically controlling the route taken by the longer lines.

Table 7-6. Phase-line lengths for each band for the modified W6PU quad.

Band	Driver Spacing Wavelengths	Line Electrical Degrees	Physical Length		
			Length feet	VF=.66	VF=.80
20 (14.175)	0.1225	44.10	31.25'	20.63'	25.00'
15 (21.225)	0.1834	66.02	25.83'	17.05'	20.67'
10 (28.5)	0.2463	88.67	13.33'	8.79'	10.67'
10 (alt)*	0.2463	88.67	30.59'	20.19'	24.47'

Note: All lines are 50-Ohm without reversal, except 10 (alt)\*, which uses a reversed 50-Ohm line. For all lines, the route is from Driver 1 (rear) to driver 2 (forward), with the feedpoint at driver 2.

**Table 7-6** presents the required line lengths for the phase lines for all 3 bands. On 10 meters, the 8.79' line may be too short for routing around the mast. Therefore, I have included its reversed counterpart, which is similar in length to the 20-meter line. The table also contains some other useful information, such as the spacing between drivers for each band measured as a function of a wavelength and in electrical degrees—both at the middle of each band. As well, I have shown the physical lengths of the lines assuming velocity factors of 0.66 and 0.80 as a rough guide to the actual line lengths a builder might encounter. Anyone contemplating

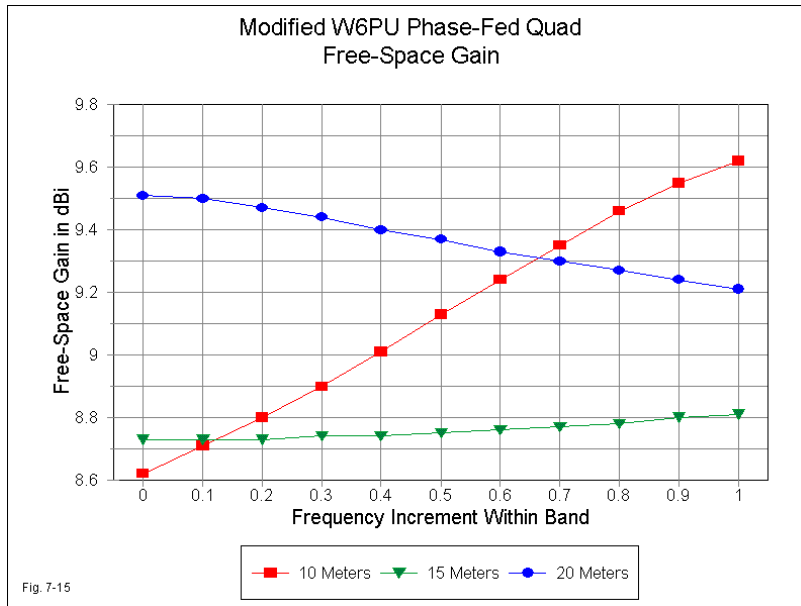
building this or any other phased array is well advised not to trust the published velocity factor values, but to measure the velocity factor of the actual material being used.

Table 7-7. Current phasing data.

Freq. MHz	Differentials Between Rear Driver and Forward Driver		Line Length Degrees
	Current Magnitude Ratio Rear-to-Forward	Relative Current Phase Rear (Forward = 0.0)	
14.175	1.365:1	103.2	162.1
21.225	0.779:1	131.3	200.7
28.5	0.856:1	150.3	139.1

One more table completes the data necessary to understand something of the complexity of a multi-band, dual-driver quad array. **Table 7-7** provides information on the modeled mid-band differentials between the two drivers in terms of their current magnitudes and phase angles. The data may provide some appreciation of how element interactions complicate matters in tri-band phased arrays. The lines for 20 and 15 meters are considerably longer than we might expect for the spacing between driver, while the 10-meter line is shorter. (These expectations are based on the erroneous rule of thumb that a spacing of  $0.125\lambda$  requires a phase line of 135 electrical degrees.) Indeed, the 15-meter line, under the influence of both the 10- and 20-meter inactive elements, is longer than  $1/2$  wavelength (180 degrees).

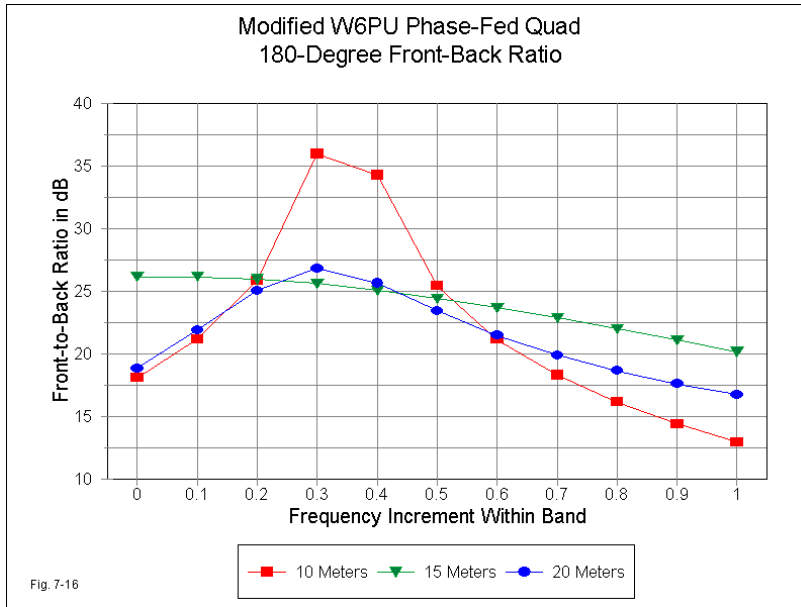
The current ratios initially look to be well off of any ideal ratio, where something close to 1:1 might be expected. However, I experimented extensively with the 20-meter drivers and obtained peak performance with exactly equal currents and a phase difference of 110 degrees. The improvement was exactly 0.01-dB increase in gain and 3 dB in front-to-back ratio. Since the front-to-back ratio at the center of 20 meters already exceeds 23 dB and since the added gain is not obtainable with a commonly available transmission line, I ended the tests.



The question that follows this foray into the design parameters for a multi-band, phase-fed quad array is what we obtained for our efforts. In terms of free-space gain, **Fig. 7-15** provides the results. Relative to the original W6PU design, we obtain higher gain across each of the three bands. 20 meters shows a smooth gain curve, with no major drop-off at either band edge. 10 meters shows the cross-band rise that we saw in the original design, but at a high average level. 15-meter gain is flat across the band and slightly greater than in the original design.

If we compare array gain with the ARRL quad with which we started this investigation, we find the 20-meter results to be very comparable, with the ARRL single-driver quad having an average 0.1-dB advantage. However, the ARRL quad shows an average advantage of about 1.3 dB over the dual-driven array on 15 meters. The 10-meter gain curve largely offsets that advantage, since the ARRL version is much steeper. It has about a full dB less gain at the low end of the band and only just exceeds the modified W6PU array at the top end. In essence, this

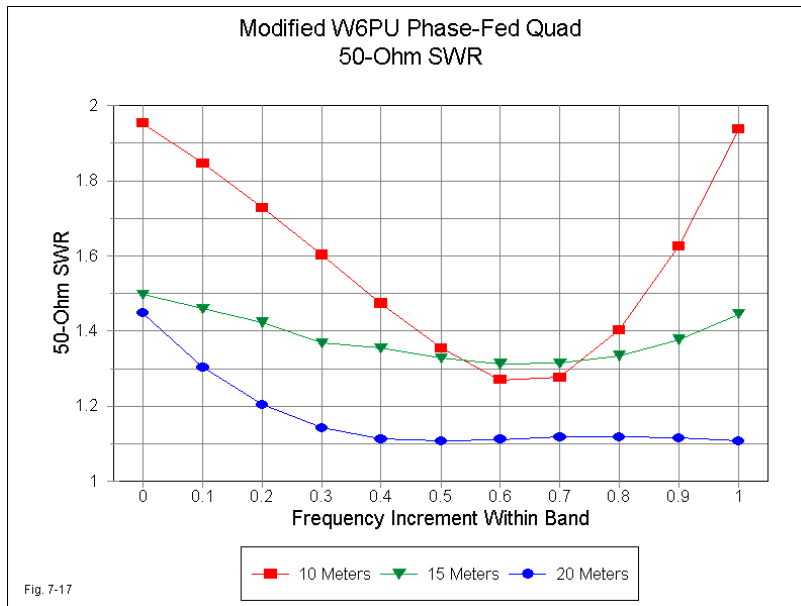
result establishes that a phase-fed quad array has no particular gain advantage over a more conventional single-driver array of about the same boom length and using the same number of elements.



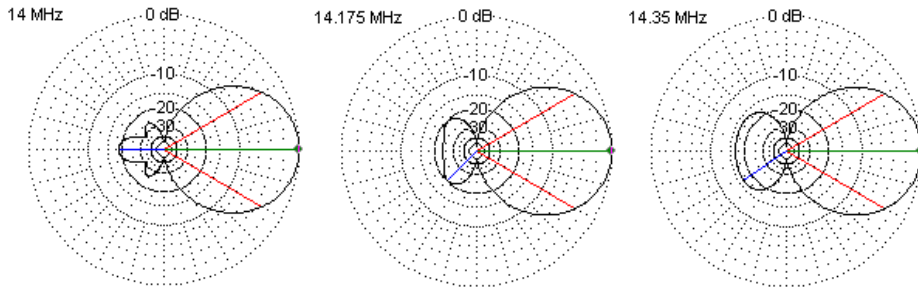
The 180° front-to-back ratio results appear in **Fig. 7-16**. The original W6PU array has a very sharply peaked 20-meter front-to-back curve with very poor values at the low end of the band. In contrast, the ARRL quad 20-meter front-to-back curve almost parallels the modified array curve, although the latter has somewhat better low-end values. On 15 meters, the modified array shows a value above 20 dB all across the band. The original W6PU array was several dB lower at all points in a parallel curve. The ARRL front-to-back curve rises from 10 dB to 22 dB across the band, in contrast to the smooth results for the modified phase-fed design.

On 10 meters, the modified and original W6PU designs again show parallel curves. However, the modified design manages to increase the front-to-back ratio

by at least 3 dB everywhere in the band. Unfortunately, the ARRL array requires significant improvement in its 10-meter front-to-back performance, with a curve that runs from 4 dB at the low end of the band to only 14 dB at 29 MHz. Although the gain differentials among the designs may be operationally moot in most cases, the modified phase-fed array has superior performance in the front-to-back category over both of the other arrays.



Since the motivation for this design exercise was to determine if phase-feeding a quad array could improve the operating bandwidth, especially on 20 meters, we should examine **Fig. 7-17**. The graph settles the question immediately. On 20 and 15 meters, the 50- $\Omega$  SWR curve is 1.5:1 or lower everywhere on each band. Although the 10-meter SWR curve remains below 2:1 across the first MHz of the band, it does not match the corresponding 10-meter SWR curve of the ARRL quad. However, that single-drive quad does not match the phase-fed array on either 20 or 15 meters, with 20 meters being very deficient in coverage.

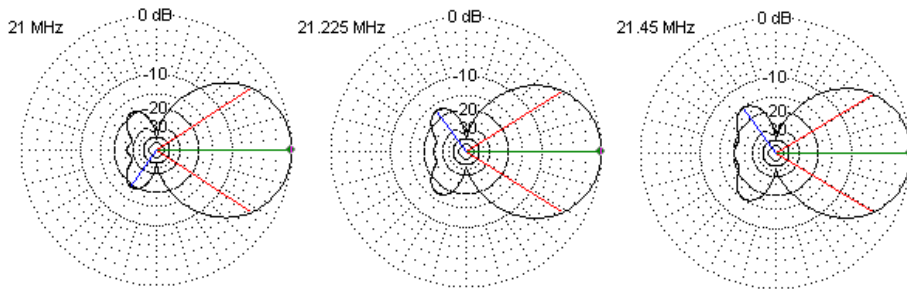


**Modeled 20-Meter Free-Space Azimuth Patterns  
Modified W6PU Quad Array**

Fig. 7-18

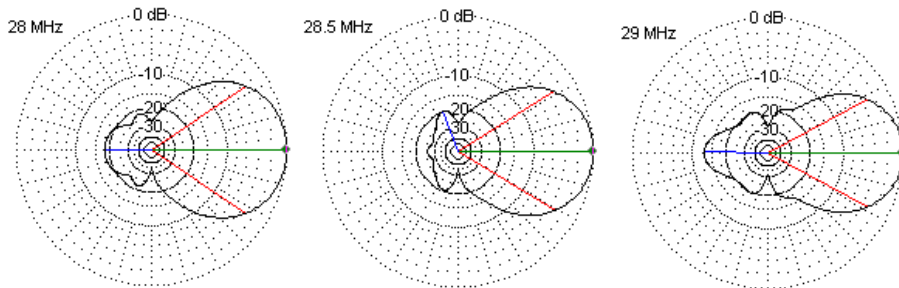
As I indicated early on in the investigation, multi-band quads require attention not only to levels of performance, but as well to pattern shape. Therefore, I am including some modeled free-space E-plane patterns that will closely resemble the azimuth patterns one might achieve with such an antenna at least 1 wavelength above real ground. **Fig. 7-18** samples the 20-meter patterns at the band edges and in the middle of the band. Perhaps the only way to describe these patterns, relative to our expectations from a comparable monoband Yagi, is that they are clean and well behaved.

In **Fig. 7-19**, we find the corresponding patterns for 15 meters. The forward lobes are once more clean. The rear lobes show a minor tendency toward fan tailing as we increase the frequency within the band, so that the worst-case front-to-back ratio is about 15 dB at the high end of the band. Compared to many multi-band quad designs, the 10-meters patterns in **Fig. 7-20** are quite free from anticipated abnormalities. The rear lobes, while not as diminutive as we might like from a monoband Yagi, are free from quartering sidelobes that would yield a ratio of less than 20 dB. From 28.5 MHz to 29 MHz, the forward lobe shows small bulges, indicating an incipient but undeveloped secondary forward lobe.



**Modeled 15-Meter Free-Space Azimuth Patterns  
Modified W6PU Quad Array**

Fig. 7-19



**Modeled 10-Meter Free-Space Azimuth Patterns  
Modified W6PU Quad Array**

Fig. 7-20

All in all, then, the modified W6PU phase-fed driver multi-band quad offers in principle reasonably good performance on all three of the wide upper HF amateur bands. It is broadband in its full coverage of each band, and its gain and front-to-back levels are very respectable for quad arrays with a 33.5' boom. The modified version overcomes the shortcomings that appeared in models of the original W6PU design, while generally equaling or bettering the performance curves for the ARRL design (except for 15-meter gain).

In the final analysis—and apart from prejudices for or against quads—the design

leaves us with a final question: how does the anticipated phase-fed quad performance stack up over and against the performance of a comparable multi-band Yagi design?

### **The Modified Phase-Fed Quad vs. 2 Multi-Band Yagis**

The modified W6PU phase-fed quad uses 12 elements in 4 groups of three on a 33.5' boom. To evaluate its performance fairly, we need to compare the figures that appear in the graphs (**Fig. 7-15, 7-16, and 7-17**) with those from an array with which the quad might be competitive as a design of similar complexity, similar coverage, and similar size. Hence, monoband quads and Yagis are not suitable comparators in the evaluation. The potential gain figures for the monoband antennas, cited at the beginning of this study, serve only to reveal to what extent the multi-band quad (or other multi-band antennas) achieves (or fails to achieve) monoband performance.

A more suitable comparator for a first-order competitive comparison would be a multi-band Yagi having a similar boom length to the one used in the quad, something in the range from 30' to 35'. Over the years, I have developed models of at least two possible designs. Although the models have roots in the measurement of dimensions of actual antennas, they are not models of the antennas themselves. Instead, they are modeling idealizations, using uniform-diameter elements, in contrast to the normal stepped-diameter element structures used in upper-HF horizontal arrays. Hence, the element lengths do not coincide with those of actual antennas. As well, both models use complex feeding systems so that the user requires only one feedpoint and cable. All such systems depend for the impedance transformations on not only the element lengths and spacing, but as well on the element diameter. The idealization of the model to uniform-diameter elements requires alterations in the feed structure to simulate the actual one. As a consequence, the performance curves that emerge from the models may differ in detail from those obtained with real antennas of roughly similar outlines. These cautions result in a disclaimer: for true models of any antenna, commercial or otherwise, one needs to consult the maker or the maker's literature.

In addition, various antenna makers use different methods and test set-ups for

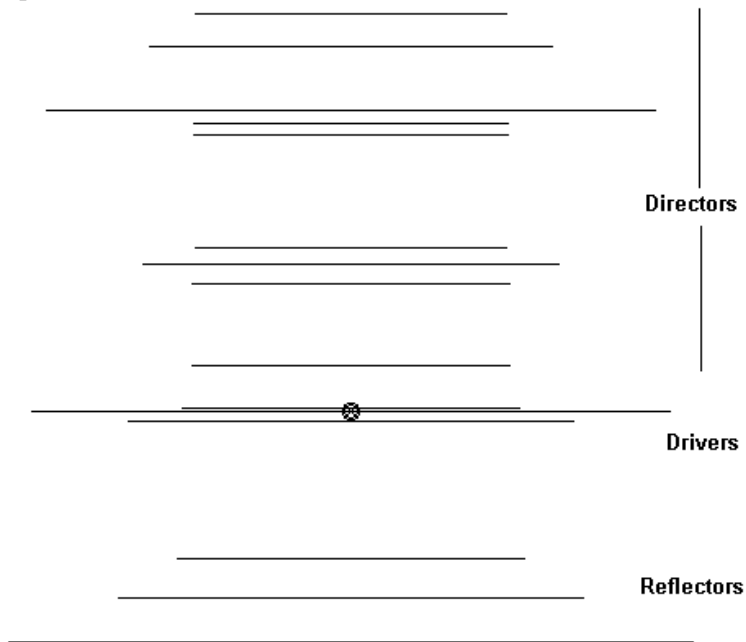
obtaining performance results that eventually appear in one or another form of print. The modeling results that I shall present stem from simple free-space models. Hence, they may not coincide with numbers that may appear for similar-looking antennas. As well, makers modify and improve designs with time, and the models used here may be dated relative to their roots.

Nevertheless, we may use these idealized models for a limited purpose: to gather basic data on the potential performance of multi-band Yagis in the 30-35-foot category. We shall limit the use of the data to seeing how the modified quad design stacks up with these modeled Yagis. The comparison may tell us whether the quad design is roughly competitive, vastly superior, or embarrassingly inferior. If one needs finer shades of evaluation, one must build all of the arrays and test them on a rated range.

One question that the evaluation will not tell us is whether the quad enjoys in fact its reputation as a band opener and closer. Such a study involves more than the basic modeled performance of the antenna, since it likely depends on propagation phenomena as well as on radiation pattern phenomena. Consequently, these notes will remain silent on that perennial issue in the Yagi vs. quad discussion.

*A 15-element tri-band Yagi using a master driver and two slaved drivers:* The first of our multi-band Yagis uses a boom just over 31.5' long, plus such end extensions as may be needed to mount the element-to-boom hardware. The general outline appears in **Fig. 7-21**, with the model dimensions shown in **Table 7-8**. The design uses 3 20-meter elements, 4 15-meter elements, and 8 10-meter elements. This type of listing is conventional and based on the length of the elements. However, as in all multi-band Yagi designs, the elements for inactive bands relative to one being used are active to some degree.

Fig. 7-21

**15-Element Tri-Band Yagi Using a Master and 2 Slaved Drivers**

20-meter elements are particularly troublesome to 10-meter operation, since they can be not only active, but may control 10-meter performance. The length of a 20-meter element as it approaches a full wavelength on 10 meters tends to be long in terms of what the 10-meter portion of the array requires, even from a full-wave element. The effect is to drag the performance curves lower in frequency, preventing full high-band coverage. The normal compensation is to add a 10-meter director immediately to the driver side of the 20-meter director. As well, one usually needs to place a further 10-meter director on the other side of the 20-meter director. Although less of a burden in this respect, similar treatment usually accompanies the placement of 15-meter directors, as these elements can also

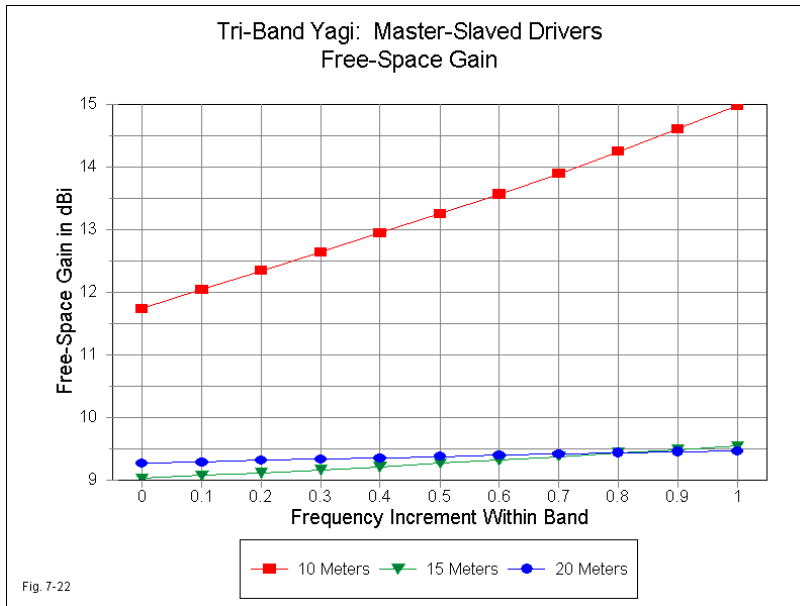
affect 10-meter performance. Signs of such design maneuvers appear in **Fig. 7-21**.

Table 7-8. General dimensions of a 15-element, master+2 slaved drivers, tri-band Yagi

El. #	Function	Length (feet) (feet)	Diameter (inches)	Distance from Reflector (feet)
1	20-m reflector	34.50	0.625	----
2	15-m reflector	23.33	0.50	2.17
3	10-m reflector	17.50	0.40	4.17
4	15-m slaved driver	22.33	0.50	11.09
5	20-m master driver	32.17	0.625	11.60
6	10-m slaved driver	16.97	0.40	11.79
7	10-m director 1	16.00	0.40	13.92
8	10-m director 2	15.92	0.40	18.00
9	15-m director 1	20.92	0.50	19.00
10	10-m director 3	15.58	0.40	19.83
11	10-m director 4	15.83	0.40	25.50
12	10-m director 5	15.83	0.40	26.08
13	20-m director 1	30.67	0.625	26.75
14	15-m director 2	20.33	0.50	30.00
15	10-m director 6	15.67	0.40	31.58

A second reason for surrounding lower-band directors with high-band directors is the fact that in developing a design, directors for different bands—especially for 10 and 20 meters—seem to "want" to be in the same place. The design at hand does not use traps to resolve the placement issue. Instead, the fore-and-aft high-band director treatment settles the issue.

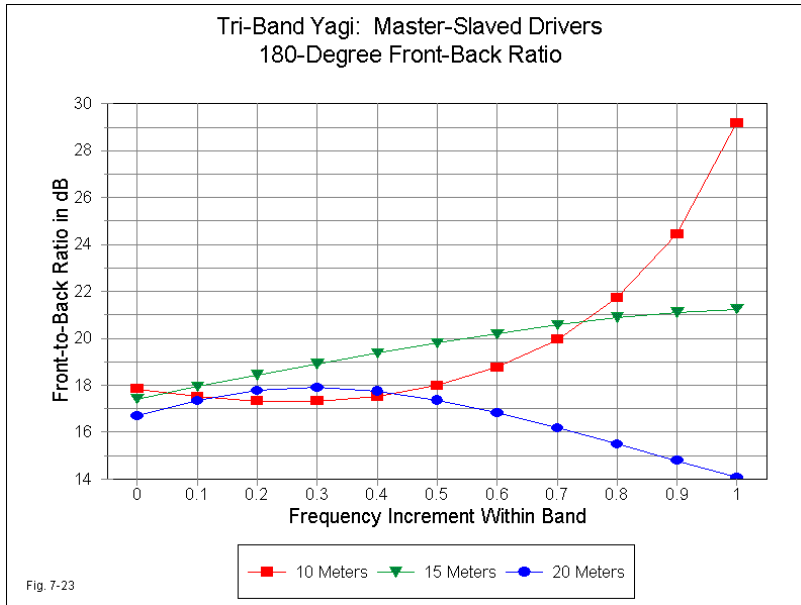
The driver section of the antenna employs a master 20-meter driver. Closely spaced slaved drivers for 15 meters and 10 meters require no connection to the master driver to perform their function. Such systems depend upon the mutual coupling between elements—all of which are highly dependent upon element length and spacing of the slaved drivers relative to the master driver—to provide the higher-band energy for the array and to show a suitable impedance value at the master driver on all three bands.



Such a design is capable of high levels of performance on all three upper-HF bands. **Fig. 7-22** shows the modeled free-space gain of the array. The values for 20 and 15 meters form smooth curves and range from just above 9 dBi to about 9.5 dBi. The boom length is long for 10 meters and is filled with directors that increase gain in addition to compensating for interactions with elements for other bands. Hence, 10-meter gain is considerably higher than for the lower bands, ranging from about 11.7 dBi to nearly 15 dBi across the first MHz of the band.

**Fig. 7-23** shows the modeled 180° front-to-back performance of the array. From monoband beams, we expect to see values above 20 dB everywhere within the band covered. Although the front-to-back ratio of a tri-band beam may peak over the 20-dB marker level, the average front-to-back ratio averages in the range between 17 and 20 dB. In the test model, the 20-meter ratio drops to just above 14 dB at the high end of the band, while the 10-meter ratio appears headed for a sharp peak just beyond 29 MHz. Nonetheless, the curves are important also for what they

do not show: the extremely low values at one or another band edge that often attach to some conventional multi-band quad designs. For example, the lowest value on 20 meters—where the array uses 3 elements—is well above what we might obtain from a 2-element driver-reflector Yagi design.

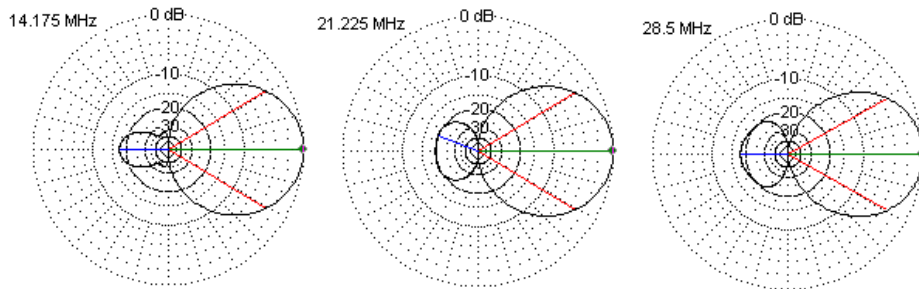


The 50-Ω SWR performance appears in **Fig. 7-24**. On 20 and 15 meters, the array achieves an SWR well below the conventional standard of 2:1 at the antenna feedpoint. The antenna also manages to cover all but the last 100 kHz of the 10-meters, as defined in terms of its first MHz. Some improvement in the 10-meter curve may be possible by judicious adjustments to the length and spacing of the 10-meter slaved driver relative to the master 20-meter driver. However, my experience with 2-band antennas using the same type of driving system suggests that without beneficial element interactions that broaden an operating curve, reduced coverage is natural. The means taken to isolate 10-meter gain and front-to-back performance from problematical interactions with lower-band elements also limits

the SWR passband. All multi-band antennas ultimately demand compromises and decisions as to which properties receive priority.



Multi-band Yagi designers are as concerned with pattern shape as with the basic performance numbers. **Fig. 7-25** provides a sample pattern from each band—taken at the band center frequency—to create a quick check on this property. In all cases, the patterns are clean, that is, typical Yagi patterns for the level of gain and front-to-back ratio.



**15-Element Tri-Band Yagi Using a Master and 2 Slaved Drivers**  
**Representative Free-Space E-Plane Patterns**

Fig. 7-25

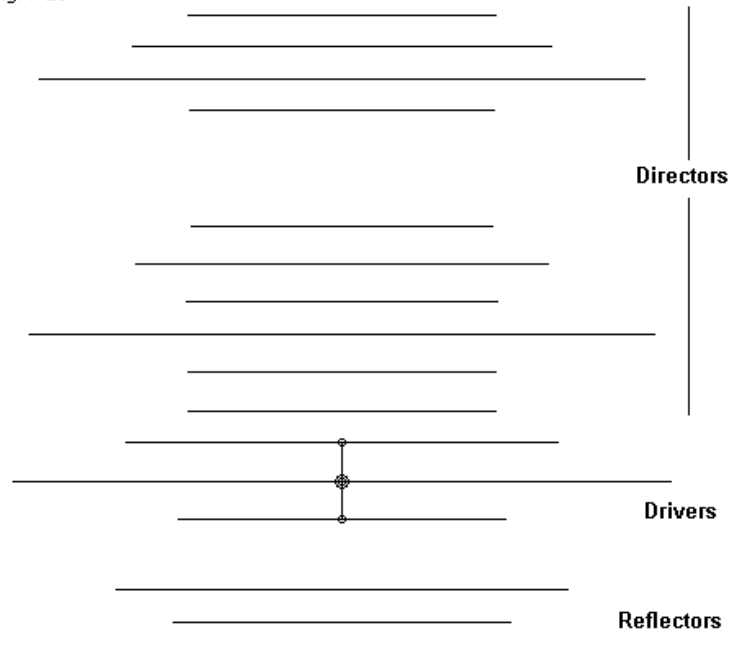
*A 16-element tri-band Yagi using directly coupled drivers:* A single multi-band Yagi design might be an aberration from the norm, so I am including a second tri-bander using a boom nearly 33' long. It employs 16 elements: 4 for 20 meters, 4 for 15 meters, and 8 for 10 meters. Lest one think that the design is a clone of the 15-element Yagi, a comparison of **Fig. 7-26** with **Fig. 7-21** will reveal that the element placement is quite different throughout. What this array shares in common with the first one are two major design features. One is the use of surrounding 10-meter directors for the 20- and 15-meter directors. The other is the general progression of elements, which is a factor controlled by the frequencies covered more than a simple decision of the designer.

The 16-element array differs from the 15-element Yagi in several important ways. The 4<sup>th</sup> 20-meter element changes the relationships among all of the directors, allowing a wider spacing between the 10-meter directors and the lower-band directors. As well, the array places the 10-meter driver behind the 20-meter driver, with the 15-meter driver in front. The result is a slight reduction in 10-meter gain and an enhancement of 15-meter gain, relative to what would be possible had one reversed the drivers.

The positions of the drivers also result from the feed system, which directly couples energy from the master driver's feedpoint to each of the other two drivers via a low-impedance transmission line. This system uses close driver spacing, but

not as close as in the master-slaved driver system. Nonetheless, the higher-band drivers receive both direct energy and mutually coupled energy from the 20-meter driver. Hence, the higher-band driver lengths and spacing are critical to the success of the feed system. **Table 7-9** provides the dimensions of the model that uses uniform-diameter elements. Compared to the 15-element Yagi, the 16-element Yagi uses much fatter elements, especially on the upper bands.

Fig. 7-26



**16-Element Tri-Band Yagi Using 3 Directly Coupled Drivers**

Table 7-9. General dimensions of a 16-element, directly coupled drivers, tri-band Yagi

El. #	Function	Length (feet) (feet)	Diameter (inches)	Distance from Reflector (feet)
1	20-m reflector	34.68	0.70	-----
2	10-m reflector	17.29	0.55	1.64
3	15-m reflector	23.24	0.625	3.28
4	10-m driver	16.77	0.55	6.89
5	20-m driver	33.74	0.70	8.86
6	15-m driver	22.16	0.625	10.83
7	10-m director 1	15.73	0.55	12.47
8	10-m director 2	15.73	0.55	14.44
9	20-m director 1	32.17	0.70	16.40
10	10-m director 3	15.99	0.55	18.04
11	15-m director 1	21.27	0.625	20.01
12	10-m director 4	15.47	0.55	21.98
13	10-m director 5	15.66	0.55	27.89
14	20-m director 2	31.17	0.70	29.53
15	15-m director 2	21.58	0.625	31.17
16	10-m director 6	15.73	0.55	32.81

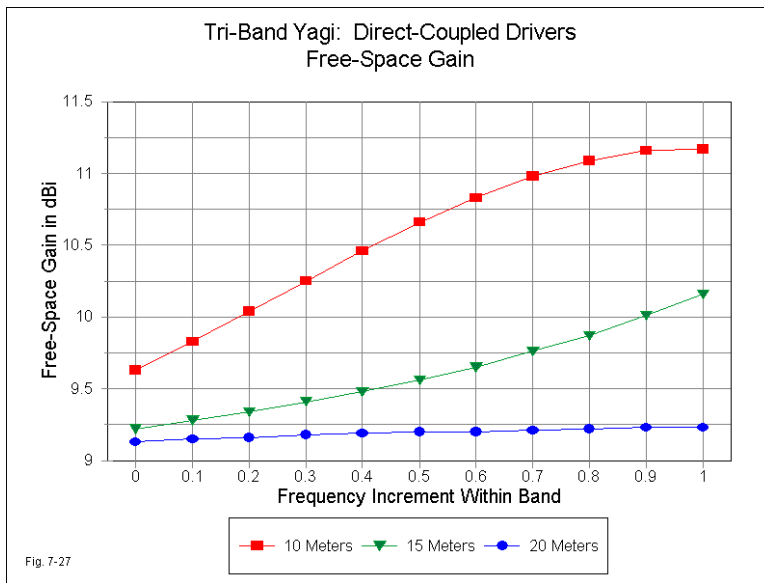
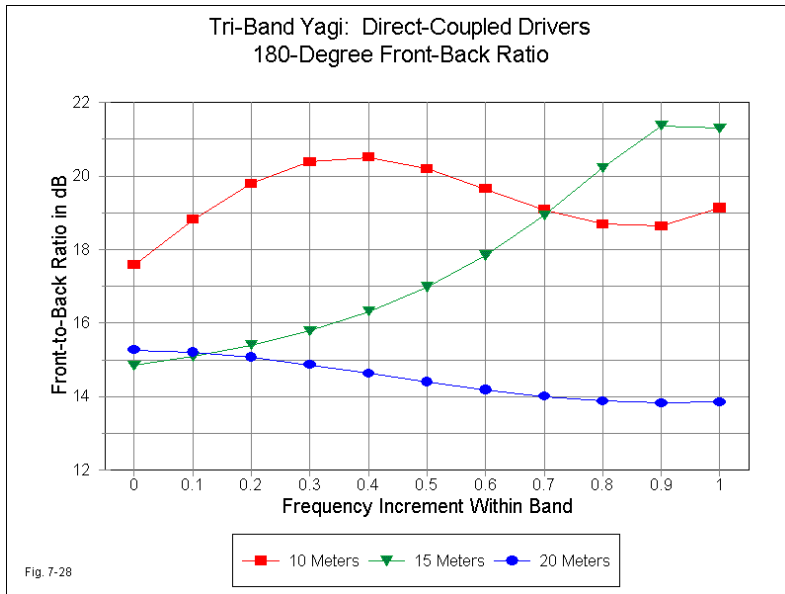


Fig. 7-27

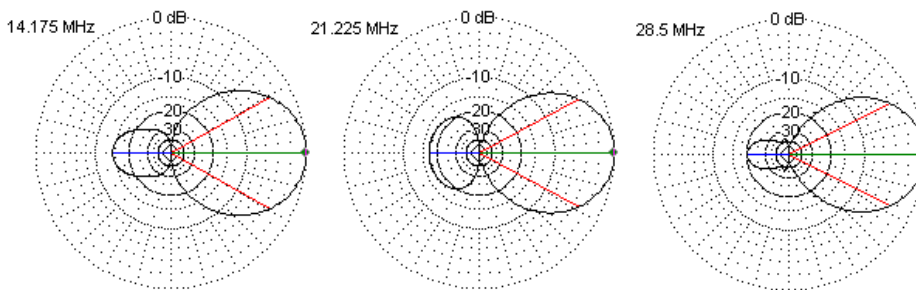
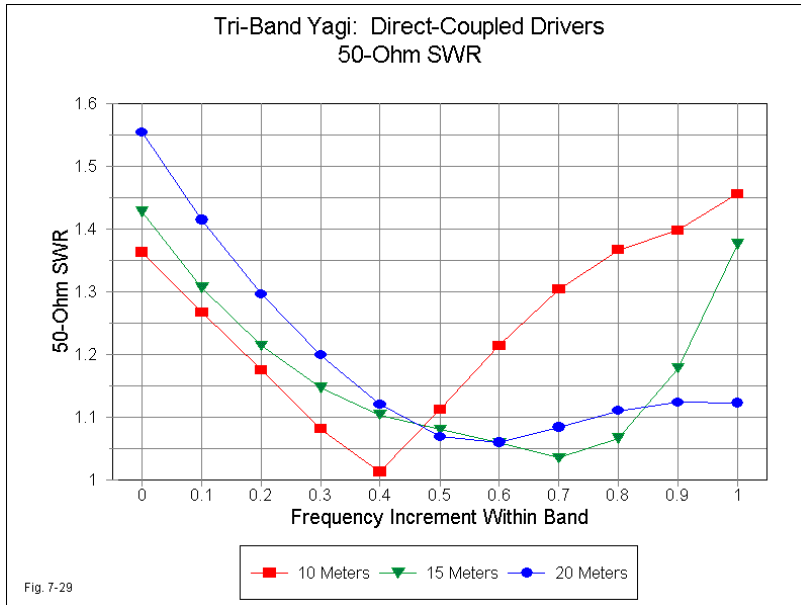
The gain that we obtain from the model of the 16-element array appears in **Fig. 7-27**. The 10-meter gain shows the steeply rising curve common to most multi-band designs, but at a somewhat lower level than for the 15-element design. In contrast, the 15-meter curve is slightly higher. 20-meter gain levels are comparable within about 0.2 dB.



**Fig. 7-28** shows the modeled 180° front-to-back ratio results. Overall, the front-to-back ratio fluctuates within the 14 to 22 dB range. No sharp peaks appear in the graph, although one might exist between 21.36 and 21.45 MHz in the last tenth of the 15-meter band.

The advantages of the directly coupled drivers—used by more than one maker these days—appear in **Fig. 7-29**. Although the graph indicates a few 50-Ω SWR values above 1.5:1, the curve shapes strongly suggest that with judicious adjustment of the drivers, all of the curves would settle in with band-edge values

well below 1.5:1. To go with the performance curves, the 16-element array patterns all classify as clean and well behaved, as revealed by the samples in **Fig. 7-30**.



**16-Element Tri-Band Yagi Using 3 Directly Coupled Drivers  
Representative Free-Space E-Plane Patterns**

Fig. 7-30

*The comparison and conclusion:* The two multi-band Yagi designs, as modeled here, are sufficiently similar to form a basis for evaluating whether the modified W6PU phase-fed quad array is competitive. By competitive, I simply mean that it is capable of sufficient performance to warrant a move from abstract modeling design to planning a physical implementation. A review of the performance curves for all three antennas is necessary for detailed evaluation, but we can gain something of value by summarizing the average performance figures. **Table 7-10** provides the averaged data for free-space gain, 180° front-to-back ratio, worst-case front-to-back ratio, and 50-Ω SWR. The insertion of the worst-case figure provides for the tendency of the quad to show a fantail rear lobe structure on some bands, such as 15 meters.

Table 10. Some average values of performance parameters by bands:  
modified W6PU quad array and 2 tri-band Yagis

Band	Free-Space Gain dBi	180-Degree/Worst-Case Front-to-Back Ratio dB	50-Ohm SWR
Modified W6PU 4-element phase-fed Quad			
10	9.13	22.17 / 18.28	1.59
15	8.76	23.94 / 16.95	1.38
20	9.37	21.48 / 19.74	1.17
15-element, master+2 slaved drivers, tri-band Yagi			
10	13.29	19.97 / 18.68	1.64
15	9.27	19.62 / 19.18	1.43
20	9.37	16.56 / 16.56	1.66
16-element, directly coupled drivers, tri-band Yagi			
10	10.55	19.32 / 19.32	1.25
15	9.61	17.64 / 17.17	1.18
20	9.19	14.47 / 14.47	1.20

Clearly, the Yagis win the gain contest on 10 meters by a wide margin, due to the ability to add the extra directors on a 30-35-foot boom. On 15 meters, the Yagis

hold a slight gain margin—about 0.5 dB—but 20 meters is a dead heat. In the 180° front-to-back category, the quad is superior by a margin that ranges from slight—that is, a fraction of a dB—to a margin that might be operationally significant—5 dB. When it comes to worst-case front-to-back ratios, the field is split, with each antenna in the table taking top honors once. All of the arrays cover all bands with less than 2:1 50- $\Omega$  SWR, with the exception for one Yagi of the top 100 kHz of the first MHz of 10 meters.

Although it is dangerous to make decisions based on such summary figures, the averages do indicate that the phase-fed 4-element quad is sufficiently competitive with tri-band Yagis of similar boom length to rank as neither vastly superior nor embarrassingly inferior. Hence, quad aficionados might be attracted to the design or to some offshoot of it. A myriad of mechanical features that may influence such a decision go uncovered in this study. Certainly, quad hardware is readily available. However, even some seemingly minor construction details can affect performance. For example, the creation of loops at the fastening points of the loops to the support arms can detune a loop from its modeled dimensions. In addition, one would need to carefully handle the long phasing lines between the drivers. For many operators contemplating a new antenna in the size range that we have been considering, one final fact may prove decisive. A quad design of the sort investigated here is a home-brew effort, whereas the Yagi models have commercial counterparts that require only assembly in accord with detailed instructions.

This investigation began with an evaluation of the ARRL quad as a well-designed single-driver quad in order to establish two things: whether it has limited band coverage and whether the use of phase-fed dual drivers would provide any gain or band-coverage advantages over a single-driver quad. The initial modeling of the most prominent dual-driver 4-element quad developed by W6PU failed to provide the promised 50- $\Omega$  feedpoint impedance, although the general design showed promise in other operating categories. Some judicious redesign of the phasing system and the element dimensions yielded a promising design with full-band coverage on 20 through 10 meters. However, the exercises laid to rest the old claim that driver phasing significantly increases array gain. The truer function of driver phasing is to obtain a wider operating bandwidth while sustaining other

performance figures, such as the front-to-back ratio.

Our final question was whether or not the resulting quad design is electrically competitive with multi-band Yagis of similar boom length. The general answer is affirmative, although specific properties of one or another type of array may tip the balance. Since all multi-band arrays are filled with compromises occasioned by element interaction, the quad is neither decisively superior nor decisively inferior to comparable Yagi designs from a strictly electrical perspective.

About the intangibles that form both the quad and the Yagi mystiques, I must close with a prudent "no comment."

### **Notes**

1. Without casting a single aspersion on the antenna that W6PU created, we may note that he gives the basic quad loop a 2 to 2.5 dB advantage over the a dipole. (The actual advantage when using the same element wire-diameter is 1.0 to 1.1 dB.) He attributes a much lower radiation elevation angle to the quad over a Yagi, when both are mounted at the same height. (The effective height of a quad is about two-thirds of the distance upward from the lowest point to the highest, a net increase in effective height that fails to lower the radiation angle significantly relative to the Yagi.) W6PU gives the diamond shaped quad loop a gain advantage over the square loop. (The differential is negligible in electrical terms, although some builders prefer the diamond for its support of feed cables along its arms and its ability to withstand winter weather.) Finally, he tends to add up all of the small gains to reach a value for his antenna that is their simple sum.

If any problematical tendency has remained from the early 1980s in antenna work, it is the temptation to sum up the theoretic gains from individual modifications to a basic antenna and then to claim that the gain of the new antenna is that sum. In most instances, the new antenna will not achieve the performance level of the claims derived from simple summing. In some cases, a basic modification will dominate the performance, negating the gains of other modifications. In other cases, modifications will cancel each other rather than re-enforcing each other. The only way to have confidence in performance levels is to create the entire new

antenna structure and then to test it. Accurate modeling is one route to testing antenna ideas before building and, equally important, before making claims about the design.

The period from about 1950 up to almost 1990 is fraught with dangers for the relative newcomer to antenna design and performance. After 1990, both NEC and MININEC saw wide distribution and the rectification of many earlier over-estimates of antenna performance. In the earliest part of the period, antenna builders would compare their designs to what they thought were standard Yagi beams. In most cases, performance claims for the Yagis specified close to theoretical perfection for the home-built design, despite the absence of adequate measurement or rigorous calculation. Very often, the Yagi performance fell well short of theoretically possible levels. Builders often mistook a healthy front-to-back ratio for forward gain. When a different design, such as the ZL-Special, would outperform a 3-element Yagi, builders attributed the situation to the seeming fact that the non-Yagi design had more gain than the claimed Yagi gain (in contrast to the actual Yagi gain). The consequence, which reached its peak in the 1980s, was a wholesale inflation of gain figures. 2-element horizontal arrays claimed free-space gain values of 8-9 dBi (or its equivalent in dBd). Similar claims accompanied quad arrays and beams with  $\frac{1}{2}\lambda$  elements bent in a forward V. Reality proved to be far more modest. Pride prevented many antenna builders from accepting the accuracy of computer antenna design and analysis software until the new millenium. More quietly, serious commercial antenna makers subjected their designs to careful computer scrutiny and modified both their antennas and their performance claims.

There are numerous useful antenna designs from the latter half of the 20<sup>th</sup> century, and many appear in articles and handbooks of the period. However, before accepting any performance claims about these antennas, model them carefully on one of the many NEC or MININEC programs that are readily available today.

2. For fuller information on phase-fed horizontal arrays, see the 4-part series "Some Notes on Two-Element Horizontal Phased Arrays," in *The National Contest Journal*, beginning in Nov/Dec, 2001 and concluding in May/June, 2002.
3. For further background on antennas using phase-fed driver cells and linear

elements, see "Some Aspects of Long-Boom, Monoband Log-Cell Yagi Design," *QEX* (Jul/Aug, 2001), pp. 11-22.

4. See "Modeling and Understanding Small Beams: Part 5, The ZL Special," *Communications Quarterly* (Winter, 1997), pp. 72-90, for some of the equations relevant to an analysis of action along an array phase line.

## Chapter 8

### Notes on Designing Large 5-Band Quads

The design of large 5-band quad arrays has a number of facets, each of which deserves attention by the would-be quad user. We can divide them into three general groups.

1. The use of antenna modeling software as the design vehicle: how do we set up the model for effective design work?
2. The performance of the quad as designed: how can we use the modeled performance as a guide to evaluating and improving designs?
3. The transition from model to physical antenna: what factors play a role in determining if and how the modeled array should be built?

Although it is not possible to provide definitive answers to all of these questions, we can run through a design exercise and extract as much guidance from it as possible. Although not exhaustive, the amount of guidance will be considerable.

For our project, let's consider the design of one or more large 5-band HF quad arrays. By large, I mean an array with at least 4 elements per band.

#### **Setting Up the Design Project**

The availability of NEC-based antenna modeling programs has moved much of the design process from the antenna tower to the computer. However, the process of design may prove daunting unless we approach it in a somewhat systematic manner.

*Constraints:* Designing a large quad array involves some concessions to reality from the start. For example, multi-band quad arrays typically employ planar groups of elements, that is, flat, 4-arm non-conductive structures to support an element for each of the bands of concern. Consequently, the designer cannot for each band

select the optimal spacing between elements for maximizing key performance parameters, such as gain, front-to-back ratio, and SWR bandwidth. Every performance outcome will be a compromise whose foundation lies in the initial spacing decisions for the sets of support arms.

Equally limiting will be the fact that quad arrays typically use wire elements. At the outset, I shall specify #12 AWG copper wire as the material of choice for this exercise. However, that very choice will limit and direct the design effort. As I have shown in Volume 2, the gain and the operating bandwidth (in terms of both the front-to-back ratio and the 2:1 SWR curves) are functions of the element diameter when specified as a fraction of a wavelength. In the upper HF region, #12 wire is a small fraction of a wavelength. Achieving full operating potential requires element diameters approaching about 0.5" at 10 meters and 1" at 20 meters.

However, the planar arrangement of elements does permit the quad designer to achieve—at least on some bands—a higher level of performance than would be provided by a monoband version of the array using similar dimensions. The effects of element interactions on the large quad array will be among the phenomena that we shall examine in the course of the work.

*A Starting Point.* Because so many examples of large quad array design already exist, we need not begin at random. One of the better designs available is the product of Danny Mees, ON7NQ. (See "Improving the Cubex Three-Element, Five-Band Quad," *Antenna Compendium*, Vol. 6, pp. 119-20.) It consists of 3 elements on 20, 17, and 15 meters, with a fourth element added for 12 and 10 meters. As a 3-element quad on the lower three bands, the array uses one of the standard set of element spacing values. As shown in part of **Fig. 8-1**, the reflector is 10' from the driver, with a director 8' forward of the driver. On 12 and 10 meters, Danny added new elements, 5' each from the reflector and the driver. The new element structure became the driver set for the upper two bands, with two directors to the front of it. **Table 8-1a** supplies the modeled dimensions of the ON7NQ 3-4-element quad. The set of tables also contains the dimensions of the larger quads that we shall explore (in **Table 8-1b** and in **Table 8-1c**), so we shall return to it from time to time. **Fig. 8-2** shows the general outline of the entire ON7NQ array.

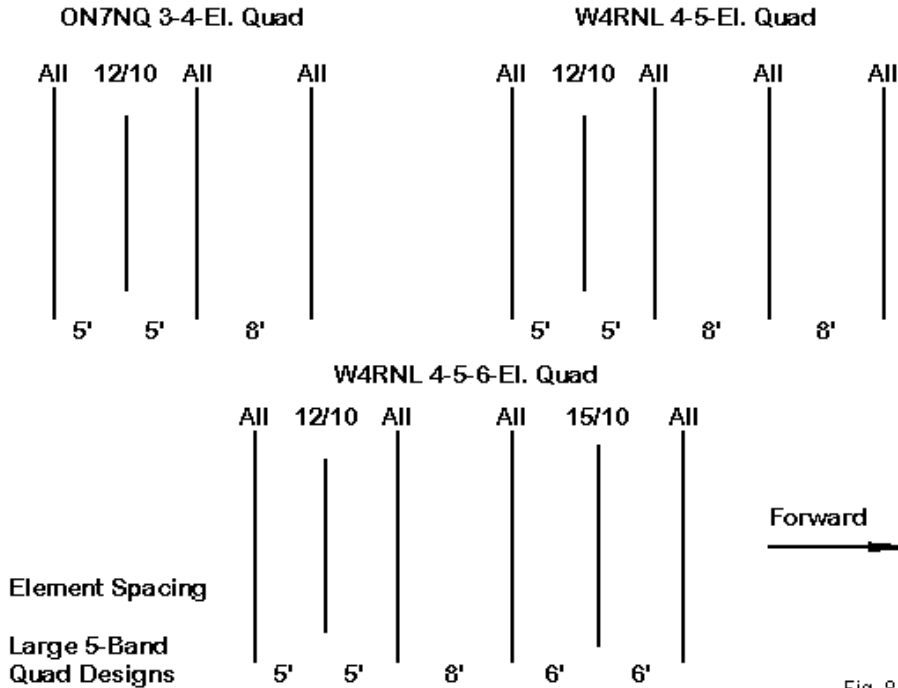


Fig. 8-1

Since one facet of quad design is reducing the number of variables with which we must deal, it may prove useful to accept the initial spacing selections of the ON7NQ array as a starting point. Then we shall add one or more elements to each band. **Fig. 8-1** shows the spacing for the first of the two resulting arrays. An additional director has been added, once more at the somewhat standard 8' spacing from the ON7NQ forward element, resulting in a 26' boom. Thus, we have a 4-5-element array. **Fig. 8-3** shows an outline sketch of the full set of elements.

Table 8-1a. ON7NQ 3-4-Element 5-Band Quad  
Dimensions (Inches)

Antenna Part	Side Length	Loop Circumference
20 Refl	217.0	868.0
20 Dri	213.7	854.8
20 Dir 1	205.0	820.0
17 Refl	168.5	674.0
17 Dri	166.3	665.2
17 Dir 1	159.8	639.2
15 Refl	144.8	579.2
15 Dri	142.0	568.0
15 Dir 1	138.0	552.0
12 Refl	122.4	489.6
12 Dri	119.9	479.6
12 Dir 1	118.2	472.8
12 Dir 2	118.7	474.8
10 Refl	110.68	442.7
10 Dri	105.8	423.2
10 Dir 1	104.6	418.4
10 Dir 2	103.99	416.0

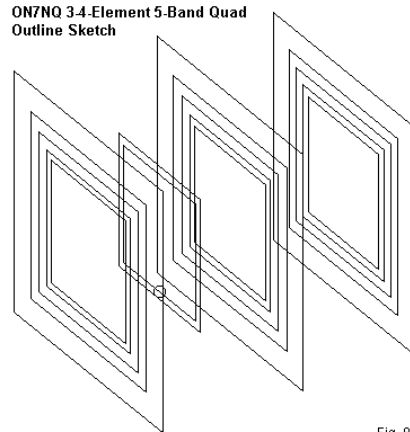


Fig. 8-2

See text and Fig.8-1 for element spacing data.

When the model reports suggested that we might achieve additional performance benefits from using a wider spacing for the new director, the third spacing sketch in **Fig. 8-1** came into play. It places the forward elements 12' from the ON7NQ forward elements for a 30' boom length. However, for reasons that will become clear as we proceed to analyze the design, it became necessary to add another partial element set equi-spaced between the two most forward full element sets. The new support holds elements only for 15 and 10 meters. The end product is a 4-5-6-element quad array, an outline sketch of which appears in **Fig. 8-4**.

Table 8-1b. W4RNL 4-5-Element 5-Band Quad  
Dimensions (Inches)

Antenna Part	Side Length	Loop Circumference
20 Refl	217.0	868.0
20 Dri	213.0	852.0
20 Dir 1	195.0	780.0
20 Dir 2	196.0	784.0
17 Refl	168.5	674.0
17 Dri	165.6	662.4
17 Dir 1	159.8	639.2
17 Dir 2	159.8	639.2
15 Refl	145.4	581.6
15 Dri	141.4	565.6
15 Dir 1	139.5	558.0
15 Dir 2	139.3	557.2
12 Refl	122.4	489.6
12 Dri	120.6	482.4
12 Dir 1	118.2	472.8
12 Dir 2	119.8	479.2
12 Dir 3	118.6	474.4
10 Refl	110.0	440.0
10 Dri	105.8	423.2
10 Dir 1	104.4	417.6
10 Dir 2	105.0	420.0
10 Dir 3	104.0	416.0

See text and Fig 8-1 for element spacing data.

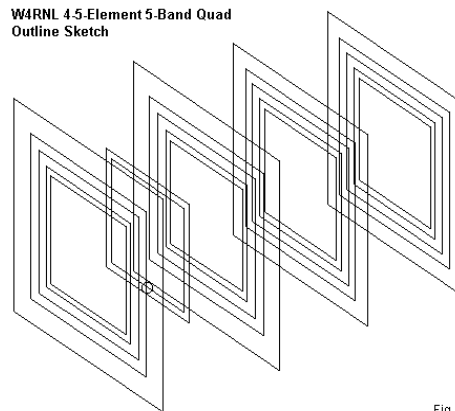


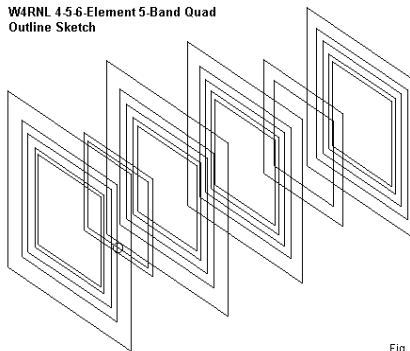
Fig. 8-3

**Specifications:** The design process might proceed without a set of goals, but then, one would never know when to stop. A set of clear specifications, based on reasonable expectations that emerge from experience, can direct the work of optimizing a design, converting an endless task into a merely long but finite one. For the design project at hand, the following specifications were set for the 4-5-element quad.

Table 8-1c. W4RNL 4-5-6-Element 5-Band Quad  
Dimensions (Inches)

Antenna Part	Side Length	Loop Circumference
20 Refl	217.0	868.0
20 Dri	213.0	852.0
20 Dir 1	201.2	804.8
20 Dir 2	194.8	779.2
17 Refl	168.5	674.0
17 Dri	165.6	662.4
17 Dir 1	160.2	640.8
17 Dir 2	159.6	638.4
15 Refl	145.8	583.2
15 Dri	141.4	565.6
15 Dir 1	139.0	556.0
15 Dir 2	138.8	555.2
15 Dir 3	138.4	553.6
12 Refl	121.8	487.2
12 Dri	120.2	480.8
12 Dir 1	119.4	477.6
12 Dir 2	120.2	480.8
12 Dir 3	117.4	469.6
10 Refl	110.6	442.4
10 Dri	105.7	422.8
10 Dir 1	104.4	417.6
10 Dir 2	104.8	419.2
10 Dir 3	104.8	419.2
10 Dir 4	104.2	416.8

W4RNL 4-5-6-Element 5-Band Quad  
Outline Sketch



See text and Fig.8-1 for element spacing data.

Fig. 8-4

**Gain:** The average free-space gain of the 4-5-element quad should be about 0.7 dB higher than the ON7NQ array on each band. This goal is likely to be achieved on all but 20 meters, where the boom length is short for 4 elements. The length is adequate for a monoband optimized Yagi, but the fixed spacing of the quad array limits improvements. First, a monoband quad generally requires greater spacing than a monoband Yagi to achieve its full gain potential for any element diameter. Second, on 20 meters, the elements do not have other elements outward from which to potentially derive a modicum of performance enhancement. Third,

the individual element spacing may not be optimal.

When the spacing was increased to the 30' boom length for the 4-5-6-element array, the gain specification was raised by about 0.2 dB as the design goal.

**Front-to-Back Ratio:** It is almost impossible to obtain a 20-dB front-to-back ratio from a wire quad on any HF band (except for the non-harmonic or WARC bands). Consequently, that standard, long applied to monoband Yagi designs, had to be set aside. More realistic is the goal of achieving a 15 dB front-to-back ratio across the bands. Even this reduced standard cannot be achieved on every band with every configuration. Part of the analysis will deal in why some bands with some array configurations fall short of the goal.

The front-to-back specification is given in terms of the 180E front-to-back ratio. Due to element interactions and the fixed spacing of the elements, a full front-to-rear evaluation will only sometimes match the 180E front-to-back ratio. A front-to-rear evaluation examines the entirety of the radiation pattern to the rear of the beam. Large multi-band quad array rear patterns can range from good to exceptionally "messy."

**Feedpoint Impedance:** Since the ON7NQ array was designed for direct feed with a 50- $\Omega$  coaxial cable, the larger arrays also used this feedpoint impedance as a specification. The usual 2:1 SWR standard will be applied to determine if the feedpoint impedance falls within the range limits.

**Bandwidth Coverage:** Although the ON7NQ array was optimized for the CW end of each of the HF bands covered, the goal for the larger arrays was to allow operation on all of each band. In the performance analysis, we shall find limitations to this goal. 20 meters is especially resistant to full coverage within the other performance specifications. As well, 10 meters was limited to coverage of the first 800 kHz (from 28.0 to 28.8 MHz), since broader coverage required a severe reduction of performance levels. This decision was made in the process of design, as we shall later see.

*Strategy:* The discussion of a starting point and a set of specifications involve

basic "whats" but do not tell us anything of the "how" of design. Design work with antenna modeling software requires something of a strategy if the work is to proceed effectively, if not efficiently. Modeling a 5-band quad of more than 3 elements per band results in a large model for most amateurs.

Moreover, each element that will be modified in the design process involves—assuming a free-space model—the alteration of 16 coordinate values for each and every change. For the task at hand, modeling software that permits the use of variables as coordinates can simplify the work of alteration to a single operation. Consequently, the design work was performed on NEC-Win Plus, which permits 24 variable assignments—just enough for the entire project without resorting to work-arounds.

Another strategic issue is the segmentation of the element loops. Ideally, a good NEC model attempts to align segment junctions to achieve maximum accuracy. As well, since all wires are to some degree active on all bands, the 20-meter elements should have about twice the number of segments as the 10-meter elements so that each segment is about the same length at the highest frequency to be used. Since 5 segments per side is about the minimum level of segmentation to assure accurate results with a closed loop structure, the overall segmentation becomes a matter of number juggling. If we place 7 segments on each side of a 10-meter element and if we increase the number by 2 for each lower band in order, we arrive at 15 segments per side on the 20-meter elements. **Fig. 8-5** sketches the elements and the suggested level of segmentation for 1 set of elements for 5 bands. This segmentation scheme comes close to meeting the desired 2:1 ratio of segments between 20 and 10 meters and yields as close an alignment of segment junctions from one band to the next as is practical to achieve.

The resulting arrays are large in both the number of wires and the number of segments. A fully segmented ON7NQ array requires 68 wires and 724 segments, already more sizable than the limits of some widely used software. The 4-5-element array needs 88 wires and 944 segments, while the final 4-5-6-element quad calls for 96 wires and 1016 segments. Since the time required for each run of the modeling core goes up by powers of both the number of wires and the number of segments, core runs for the largest array approached the duration within which

the designer might easily lose interest in the project.

**Full Segmentation Scheme: 7 to 15 Segments per Wire**

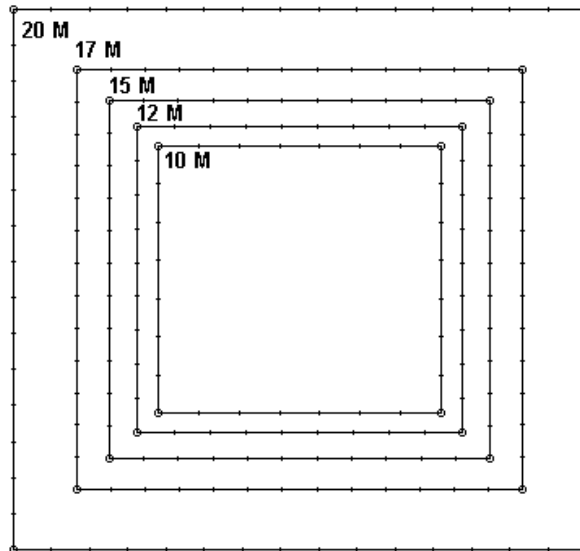


Fig. 8-5

The solution is to use a lower level of segmentation, but only after verifying its adequacy, if not its accuracy. Therefore, I ran a set of comparative curves on the ON7NQ array using full segmentation and a lower level: 5-segments per side for the upper 3 bands and 7 segments per side for the lowest 2 bands. The resulting models produced operating bandwidth performance data such that in only two instances was a final small adjustment required using the fully segmented model. However, the actual gain and front-to-back figures were sufficiently off that only the performance curves were used to optimize the model. The performance tables to follow reflect the numbers yielded by the fully segmented models.

**Table 8-1** (b and c) provides the dimensions that emerged for the larger arrays. Without adequate preparation as outlined above, the few hours of work needed to produce these figures might well have been lengthened into the work of many weeks.

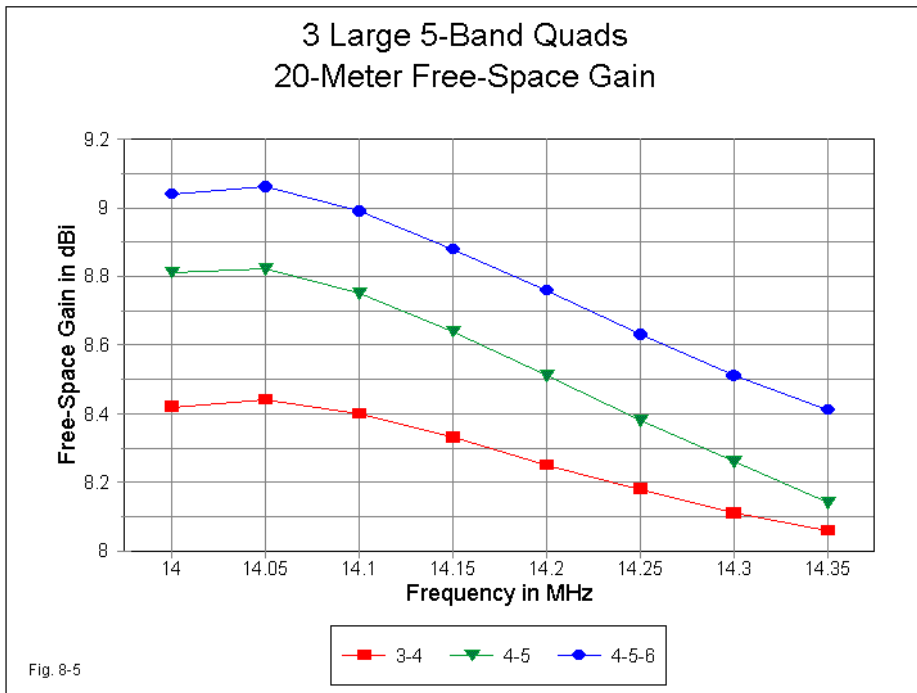
### Design Evaluation

In the course of the design exercise, a number of interesting properties of large quad arrays emerged. Some of the patterns that make up the properties might not have been so easily discovered without the efficiency of computer-aided design, although automated design might also have obscured some of them. Let's analyze the designs band by band to see what we might uncover. We shall use a mixture of tabular and graphic data to examine each band, with performance curves being most applicable to the wider HF bands.

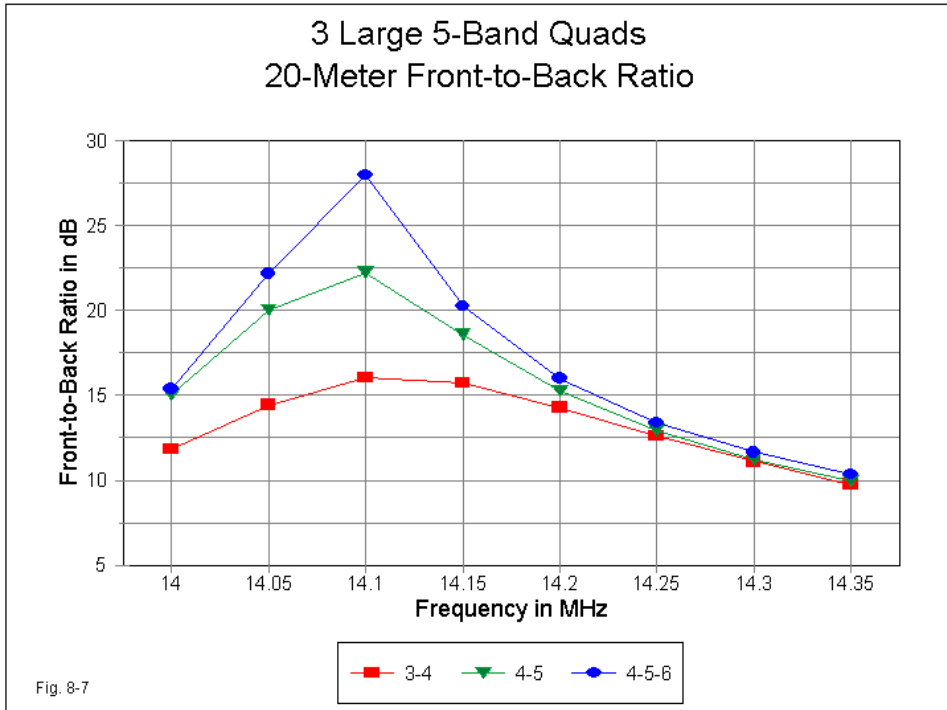
Table 8-2. 20-Meter performance of 3 quad arrays.

Freq. MHz	Gain dBi	Front/Back dB	Impedance R +/- jX	50-Ω SWR
ON7NQ 3-4-Element, 5-Band Quad				
14.0	8.42	11.83	37.6 - j 18.5	1.66
14.175	8.29	15.06	44.3 + j 4.4	1.17
14.35	8.06	9.76	34.8 + j 36.5	2.50
W4RNL 4-5-element, 5-Band Quad				
14.0	8.81	15.02	33.6 - j 20.5	1.88
14.175	8.58	16.76	51.9 + j 10.0	1.22
14.35	8.14	9.96	57.8 + j 33.8	1.89
Average gain over 3-4: 0.25 dB				
W4RNL 4-5-6-element, 5-Band Quad				
14.0	9.04	15.37	31.7 - j 18.4	1.89
14.175	8.82	17.82	54.9 + j 12.8	1.29
14.35	8.41	10.36	56.6 + j 35.3	1.94
Average gain over 4-5: 0.25 dB    Average gain over 3-4: 0.50 dB				

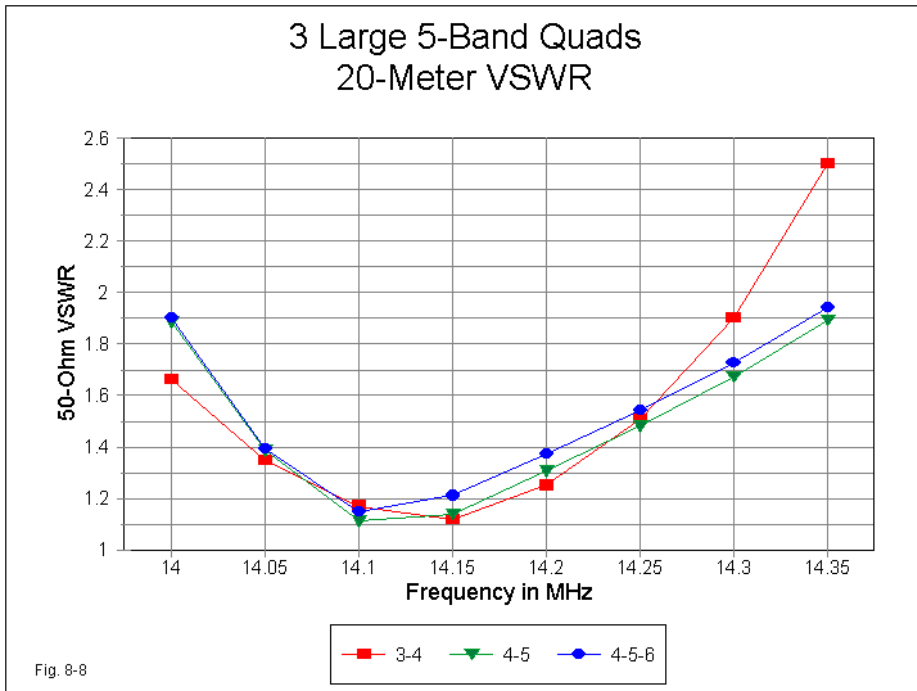
*20 Meters:* With respect to gain, all of the large arrays show a steady increase with each step upward in frequency band. Of all the bands, 20 meters shows the least improvement as we enlarge the array. **Table 8-2** provides the data at check points for the band edges and the middle of the band. **Fig. 8-6** sweeps the band to provide a fuller picture of the free-space gain.



At the low end of the band, the 4-5 array shows a significant increase over the 3-4 version. The gain increase tapers off as we move up the band so that the average gain margin between versions 3-4 and 4-5 is the same as between version 4-5 and 4-5-6. However, the gain of version 3-4 had been optimized at the expense of full-band coverage. Both 4-5 and 4-5-6 provide full coverage of 20 meters, even if at lesser levels at the high end of the band.



The front-to-back ratio curves for all three quad versions appear in **Fig. 8-7**. The curves are roughly congruent, but the increasing boom length of the array as we move from one version to the next yields a higher peak value at about 14.1 MHz. Although both larger arrays have a higher ratio than the original array at the low end of the band, all three pass the upper end of the band with similar values. Likewise, as shown in **Fig. 8-8**, the 2 larger arrays have similar SWR curves that barely fit within the band at less than 2:1 SWR relative to 50  $\Omega$ . In this feature, they are superior to the original ON7NQ array, since its SWR curve cannot be moved sufficiently to cover the entire band without a significant reduction in peak gain.



Adding a second director to the initial ON7NQ starting point thus allows an improvement of gain of modest amounts, with the longer-boom model showing additional gain. The added director permits coverage of the entire 20-meter band by judicious selection of director loop sizes, which differ as we change the boom length. Without major changes in individual element spacing, further significant performance improvement is unlikely, since the first director has two functions. In combination with the driver and the reflector, it sets the feedpoint impedance. In combination with the second director, it sets the operating bandwidth for the major parameters. Hence, the 2 4-element 20-meter sections use very different director sizes, although the driver and reflector remain constant. All in all, both larger 20-meter sections have boom lengths that remain well under  $0.4 \lambda$ , which is a short for a 4-element parasitic array.

*17 Meters:* Because 17 meters is such a narrow band (100 kHz), the data in **Table 8-3** will suffice to permit an evaluation of the performance of the arrays on this band. Three factors allow the 17-meter portions of the larger arrays to achieve significant gain over the initial 3-element quad. First, the boom length increases as a fraction of a wavelength so that the two new designs bracket a half wavelength of boom length. Second, the extra element is well suited to setting the element mutual coupling for a higher gain level. Third, the 17-meter band is narrow, permitting the operating performance to be well focused.

Table 8-3. 17-Meter performance of 3 quad arrays.

Freq. MHz	Gain dBi	Front/Back dB	Impedance R +/- jX	50-Ω SWR
ON7NQ 3-4-Element, 5-Band Quad				
18.068	8.47	21.80	42.7 - j 5.1	1.21
18.118	8.42	25.52	43.5 - j 0.3	1.15
18.168	8.36	20.90	43.2 + j 4.6	1.19
W4RNL 4-5-element, 5-Band Quad				
18.068	9.24	22.03	36.0 - j 1.7	1.39
18.118	9.18	21.26	39.3 + j 5.7	1.31
18.168	9.10	17.39	42.3 + j 12.5	1.37
Average gain over 3-4: 0.75 dB				
W4RNL 4-5-6-element, 5-Band Quad				
18.068	9.45	18.43	42.7 + j 0.7	1.17
18.118	9.39	21.33	47.9 + j 6.5	1.15
18.168	9.31	20.50	42.4 + j 10.8	1.24
Average gain over 4-5: 0.21 dB    Average gain over 3-4: 0.96 dB				

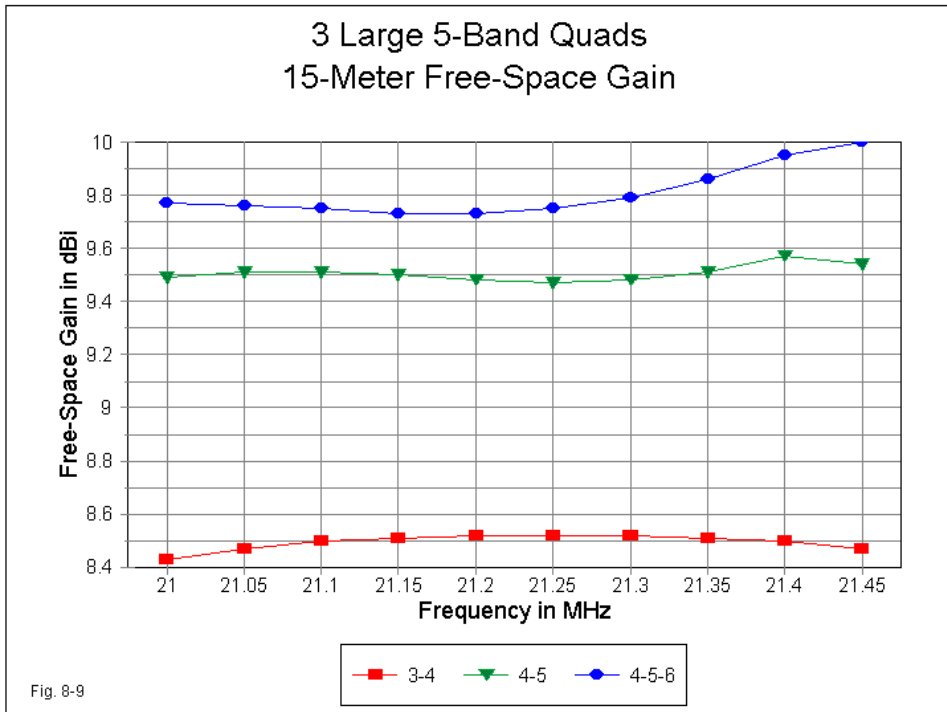
Nevertheless, the 30' boom version requires different element lengths than the 26' version for the 2 directors in order to achieve the final 0.2-dB gain increment. However, the added length also permits the designer to obtain feedpoint impedances closer to 50 Ω, even though both 4-element sections have comparable front-to-back ratio values.

Despite the factors that allow the 17-meter section to achieve gain in excess of the specifications for the larger arrays, the gain differential between the 17-meter and 20-meter sections calls for brief comment. The longer boom length in terms of a fraction of a wavelength and the narrow band requirements on 17 meters contribute to the gain excess over 20 meters. However, the 17-meter elements in their planar supports are surrounded on both sides by elements for other bands. Changes in the 20-meter and 15-meter elements do affect the performance curves of 17 meters—much more of an effect than changes to the 17-meters elements have upon the 20-meter performance curves. In general, being surround by elements for other bands tends (but not without exceptions) to improve gain but also to slightly reduce the front-to-back ratio and SWR bandwidth.

Table 8-4. 15-Meter performance of 3 quad arrays.

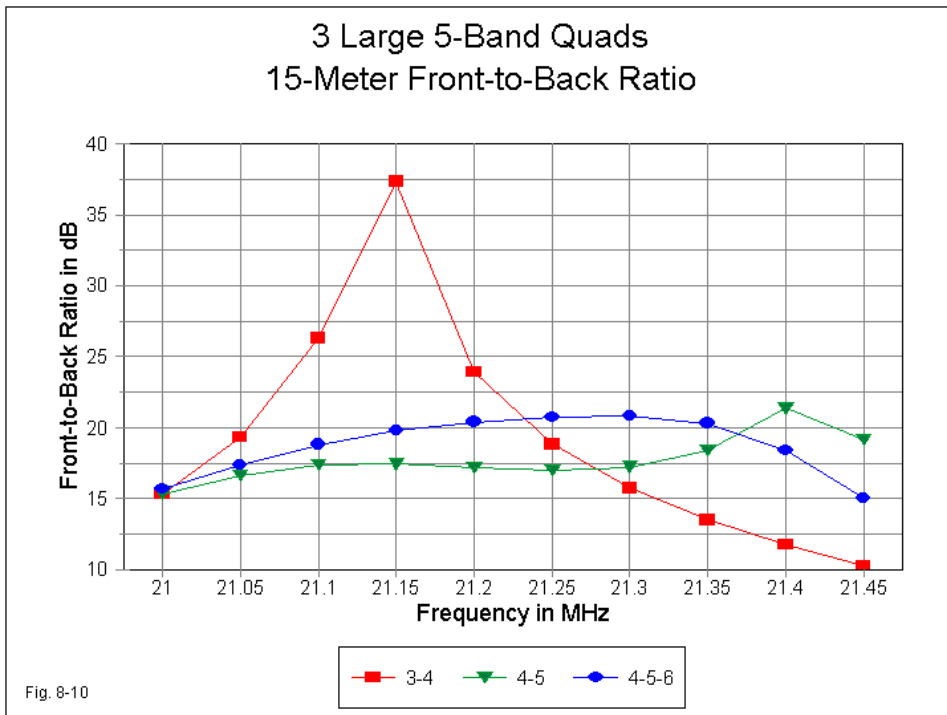
Freq. MHz	Gain dBi	Front/Back dB	Impedance R +/- jX	50-Ω SWR
ON7NQ 3-4-Element, 5-Band Quad				
21.0	8.43	15.28	49.7 - j 20.1	1.49
21.225	8.52	20.98	46.4 - j 0.0	1.08
21.45	8.47	10.24	36.2 + j 30.7	2.16
W4RNL 4-5-element, 5-Band Quad				
21.0	9.49	15.33	41.4 - j 15.6	1.47
21.225	9.47	17.04	57.0 + j 7.5	1.21
21.45	9.55	19.16	31.3 + j 9.9	1.70
Average gain over 3-4: 1.03 dB				
W4RNL 4-5-6-element, 5-Band Quad (before adding 5th element)				
21.0	9.36	11.43	46.4 - j 19.8	1.51
21.225	9.65	22.65	58.1 - j 8.8	1.25
21.45	9.95	15.68	28.2 + j 8.7	1.85
W4RNL 4-5-6-element, 5-Band Quad (after adding 5th element)				
21.0	9.78	15.70	46.9 - j 7.6	1.19
21.225	9.74	20.57	63.4 + j 1.0	1.27
21.45	10.00	15.03	35.0 + j 11.9	1.57
Average gain over 4-5: 0.34 dB    Average gain over 3-4: 1.37 dB				

**15 Meters:** As shown in **Table 8-4** and in **Fig. 8-9**, 15 meters is marked by remarkable gain stability in all 3 versions of the arrays. The gain improvement on the 4-5 array over the 3-4 array is in excess of 1 dB, with another 1/3 dB added by the increased boom length of the 4-5-6 quad. However, the values, which are in excess of expectations for the 4-5-6-element design, required the addition of a new director 6' between the first and second directors for 20 and 17 meters. **Table 8-4** provides the best gain values obtained with the longer boom, but without the added director. Obviously, the longer boom—about  $5/8 \lambda$ —was insufficient to provide stable gain across the band without an intervening director.



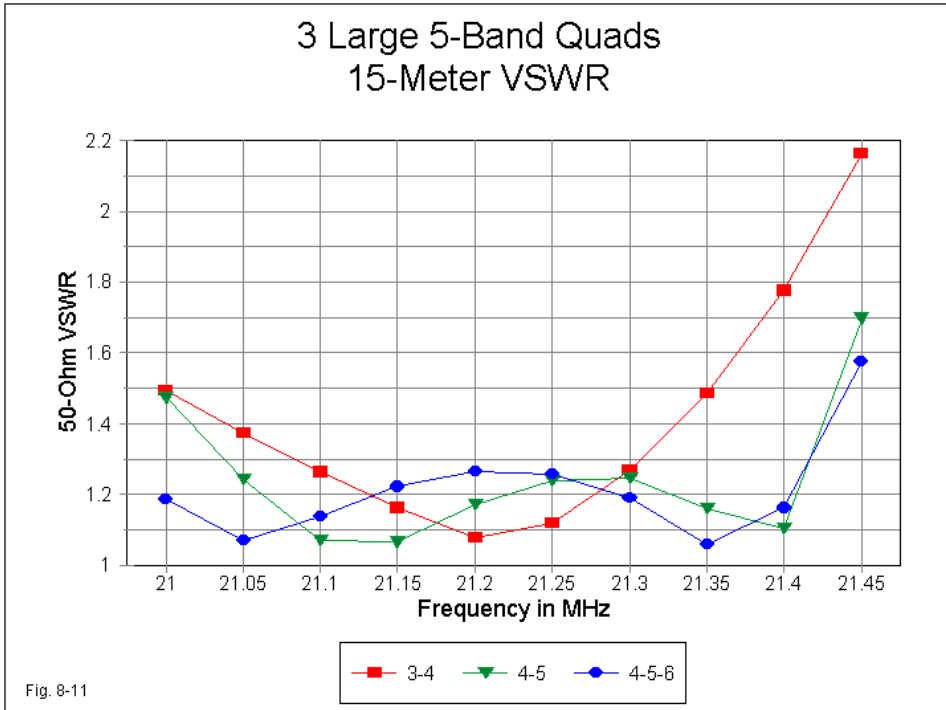
The front-to-back curves for 15 meters, shown in **Fig. 8-10**, are equally

interesting. The initial 3-4 array, with a single director for 15 meters, shows the typical "spike" in the front-to-back value. However, both longer-boom models provide much smoother performance across the entire band. The smoother performance is also reflected in the feedpoint impedance values in the tables. The 3-4 array can be adjusted for less than 2:1 SWR across the band, but it cannot approach the leveled values for the longer boom arrays.



Part of the reason for the impedance and SWR situation is revealed in **Fig. 8-11**, the 50- $\Omega$  SWR curves for the three arrays. The 3-4 array shows the typical curve of a 3-element beam, with a single point at which SWR is minimum. Both the 4-5 and the 4-5-6 element arrays display two SWR minimums at distant points

within the band. The double-dip curve is a mark of "wide-band" tuning of a parasitic array, as the term is defined in the series of Yagis designed by NW3Z and WA3FET.



The 15-meter array spaces the reflector and the first director at nearly optimal distances from the driver to set the feedpoint impedance for wide-band 50- $\Omega$  operation. The reflector is about  $0.216 \lambda$  behind the driver, while the first director is about  $0.173 \lambda$  ahead. The additional director or directors, as reflected in the dimensions for those elements in Table 8-1, then provide gain. The additional director in the 30' model permits the designer to achieve smoother wide-band performance in all categories at a boom length that is beyond the capabilities of a

single director. Both larger quads call for a smooth decrease in the sizes of the directors, although some wide-band applications with 5 elements may require that the second director be equal to or slightly larger than the first director. This phenomenon is an indicator that the forward 2 directors are used as the principal determinants of the bandwidth for the gain and front-to-back curves.

Table 8-5. 12-Meter performance of 3 quad arrays.

Freq. MHz	Gain dBi	Front/Back dB	Impedance R +/- jX	50-Ω SWR
ON7NQ 3-4-Element, 5-Band Quad				
24.89	9.26	22.72	35.1 - j 2.1	1.43
24.94	9.22	18.92	41.1 + j 2.3	1.27
24.99	9.18	16.70	47.6 + j 4.8	1.12
W4RNL 4-5-element, 5-Band Quad				
24.89	10.27	21.77	38.6 + j 5.2	1.33
24.94	10.29	19.80	40.2 + j 9.1	1.34
24.99	10.25	16.77	41.9 + j 14.3	1.43
Average gain over 3-4: 1.04 dB				
W4RNL 4-5-6-element, 5-Band Quad				
24.89	10.34	18.78	25.9 + j 3.5	1.94
24.94	10.37	20.98	37.0 + j 7.9	1.42
24.99	10.25	21.69	49.1 - j 2.5	1.06
Average gain over 4-5: 0.06 dB Average gain over 3-4: 1.10 dB				

*12 Meters:* For all three arrays, 12 meters is the lowest band to use a driver spaced 5' from the reflector, with the element at the 10' mark becoming a director. **Table 8-5** provides the operating figures for this 5-element section. The 4-5 (26') array provides more than 1 dB gain improvement over the 3-4 (18') array on 12, with similar front-to-back and SWR curves.

When increasing the boom length to 30', the forward director moves from 0.2 to 0.3  $\lambda$  ahead of the second director. The larger spacing is near the limit of the ability

of the forward two directors to control both gain and front-to-back ratio, even on a narrow band such as 12 meters (100 kHz). Indeed, without a further director, one can improve either the gain or the smoothness of the front-to-back ratio—but not both. As shown in **Table 8-5**, the design approach used for the 4-5-6 array was to raise the lowest level of front-to-back ratio by about 2 dB—a value that just verges on operational detectability.

As a result of this design decision, the gain of the longer-boom array increases insignificantly over that of the 26' model. However, since the overall gain increase, relative to the initial 3-4-element array, was well in excess of 1 dB, the decision seems appropriate. For the same reason, a new director was not added to the support arms used for the added 15-meter director. The absence of an added director for 12 meters illustrates once more the different requirements for the narrow and wide amateur HF bands.

*10 Meters:* Of all the HF bands, 10 meters is the widest. From the outset, it was apparent that a thin-wire quad array could not be pressed at any reasonable gain level to cover even the full first MHz of 10. An 800 kHz operating bandwidth is much more feasible goal, and all three arrays achieve it, as shown in **Table 8-6**.

On average, the 4-5-element quad shows better than 0.8 dB more gain than the 3-4 array. The 30' boom model adds more than 0.4 dB further gain (using a fourth director), for a 1.25 dB total improvement over the original 18' quad design. However, these figures—as averages—may be deceptively simple in view of the wide operating bandwidth on 10 meters.

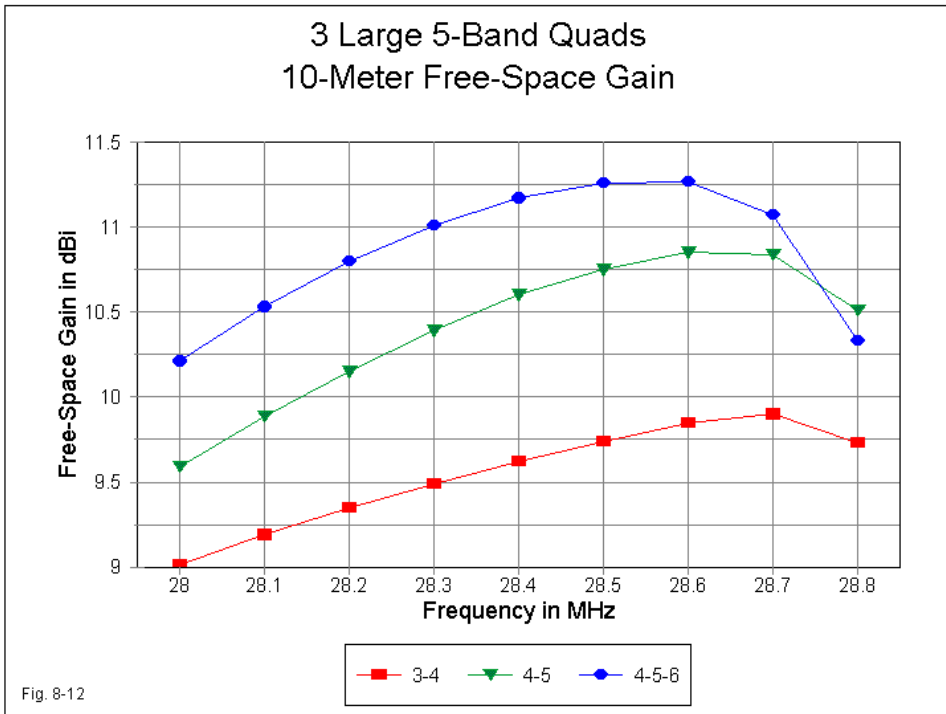
Despite the best efforts to achieve a smooth gain performance, 10 meters exhibits the highest differential between minimum and maximum gain for all three of the arrays. The differential runs between 0.9 dB and 1.1 dB, depending on the version of the array. The 4-5-6-element array would have shown an unacceptably high differential—more than 1.5 dB—had the final design not included a new director on the same support arms as the added 15-meter director. **Fig. 8-12** show the gain curves for all three final designs. Even with the new director, the 4-5-6 version displays a more rapid gain fall-off at the upper end of the band than the other two quads.

Table 8-6. 10-Meter performance of 3 quad arrays.

Freq. MHz	Gain dBi	Front/Back dB	Impedance R +/- jX	50-Ω SWR
ON7NQ 3-4-Element, 5-Band Quad				
28.0	9.01	18.40	43.8 - j 31.6	1.96
28.2	9.35	25.89	45.3 - j 11.0	1.29
28.4	9.62	30.72	51.3 + j 6.8	1.15
28.6	9.85	22.80	58.7 + j 9.6	1.27
28.8	9.73	12.38	31.1 + j 8.1	1.68
W4RNL 4-5-element, 5-Band Quad				
28.0	9.59	12.15	40.7 - j 27.4	1.88
28.2	10.15	17.00	49.3 - j 12.7	1.29
28.4	10.60	20.50	47.1 - j 2.8	1.09
28.6	10.85	19.76	42.6 + j 18.0	1.52
28.8	10.51	29.74	64.9 + j 12.1	1.40
Average gain over 3-4: 0.83 dB				
W4RNL 4-5-6-element, 5-Band Quad (before adding 6th element)				
28.0	9.54	18.64	41.3 - j 19.4	1.59
28.2	10.22	43.18	40.0 - j 1.3	1.25
28.4	10.72	20.43	39.2 + j 23.6	1.78
28.6	11.04	16.89	59.1 + j 55.3	2.70
28.8	10.67	11.37	56.4 - j 19.1	1.46
W4RNL 4-5-6-element, 5-Band Quad (after adding 6th element)				
28.0	10.21	13.85	58.9 - j 31.2	1.80
28.2	10.80	20.75	51.9 - j 21.9	1.54
28.4	11.17	26.41	47.1 + j 0.6	1.06
28.6	11.27	31.30	62.3 + j 16.0	1.43
28.8	10.33	12.67	34.0 + j 1.7	1.47
Average gain over 4-5: 0.42 dB    Average gain over 3-4: 1.25 dB				

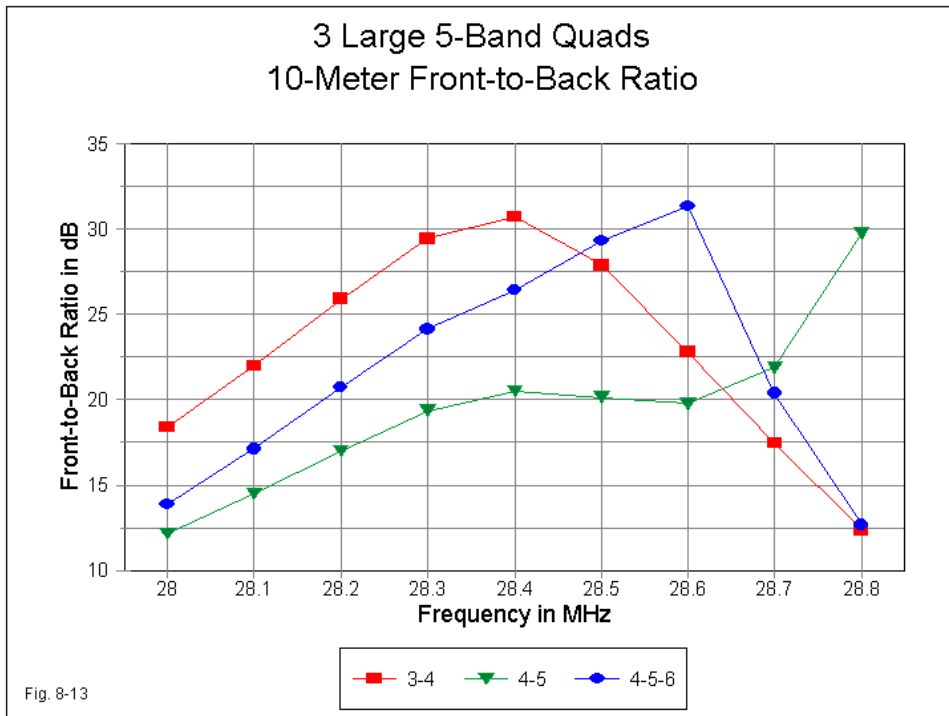
The front-to-back curves in **Fig. 8-13** show something about where to place the peak front-to-back value for optimal performance—if there is design room to vary it

without adversely affecting other properties. The 3-4-element array centers the curve. The 4-5-element version moves the maximum 180E front-to-back ratio to the upper end of the band. The result is lesser performance at the lower end of the band. However, the 180E front-to-back ratio is not the sole determiner of placement. The general shape of the rearward lobes and the strength of rearward side lobes can also play a role in the design decision. Placing the maximum front-to-back ratio at the high end of the band in the 4-5 array provided the best overall front-to-rear performance across the band.



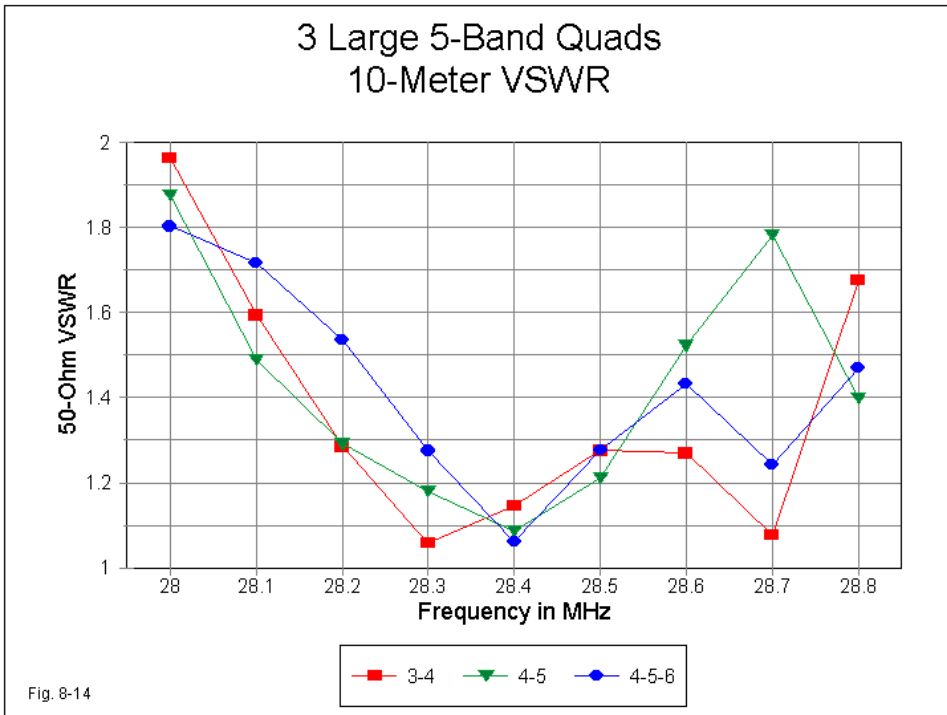
The additional director to make the 10-meter section a 6-element array was prompted by the front-to-back performance as much as by the gain curve of the

array without the added director. **Table 8-6** shows the high in-band peak front-to-back ratio without the new director. The consequence is a relatively poor front-to-back performance except for a small portion of the band. With the added director, the front-to-back performance curve spreads the higher levels of performance over a greater portion of the band, although the band edges fall below the target levels given on the specifications.



The added 10-meter director also resolves another problem. Without the director, the elevated level of SWR between the two wide-band minimums rises too high and exceeds the 2:1 level by a considerable amount at 28.6 MHz. As shown in **Fig. 8-14**, all three of the final versions of the arrays achieve the double-minimum

wide-band curve, although in different patterns. The 4-5-6-element 30' array achieves the flattest curve of all, but all three curves remain below the 2:1 SWR level for the entire operating bandwidth. In both the 4-5 and 4-5-6 arrays, the first director plays its most significant role in setting the feedpoint impedance of the array and hence turns out to be smaller than the second director.



*Overall Evaluation:* The 4-5-element and the 4-5-6-element 5-band quads achieve most of the operating goals set forth in the original specifications for array gain. Each array exhibits increased gain as we change bands upward in frequency. Only 12 meters fails to provide at least 0.2 dB gain more for the 4-5-6 array over the 4-5 version. Only 20 meters fails to meet the goal of the 4-5 quad in providing

at least 0.7 dB more gain than the array used as the starting point. The front-to-back ratio goals—with cautions that we shall further discuss—are generally met except for the upper end of 20 meters and the passband edges of 10 meters. Both the 4-5-element and the 4-5-6-element quads cover all of the assigned passbands with under a 2:1 SWR relative to a  $50\text{-}\Omega$  standard. However, in several cases, the limit is pressed on one or the other end of the band, and on 20 meters, on both ends of the band.

Within these restrictions, then, the overall design is reasonably successful in achieving a design for a larger 5-band quad array. Indeed, more important than this overall evaluation are the design principles and limitations discovered along the design road. The notes on these matters give us some further insight into how multi-element, multi-band quads operate. Moreover, it is critical to understand that the designs emerged from some initial constraints of wire size and fixed element spacing. Revising the element spacing among sets of elements might yield differences of front-to-back ratio curves and SWR curves. Consequently, the designs are now suited to the application of both incremental and genetic optimizing routines. The incremental routines may provide further tweaking of the element sizes in the direction of perfected performance curves. Genetic algorithms might well uncover unsuspected potentials for the array designs.

Even if we accept the declaration of relative success in designing 4-5-element and 4-5-6-element quad arrays, the design process is far from over. First, there are some further general cautions about multi-band quads that deserve to be addressed. Second, although the use of antenna modeling software shows good efficiency in developing a design, if the design cannot be translated into an effective physical antenna with adequate performance, the exercise is idle. The interface of models and quad construction is an important aspect of the modeling-design process itself.

### **Limitations, Cautions, and Correlation Techniques**

The numbers that emerge from an antenna-modeling program used to design a large quad array can be deceptive unless we use extreme caution in reading them and in using them to construct a physical version of the array. In this final part of

the exercise, I want to explore at least some of the limitations and cautions that attach to the design model and to its transferal into wire and fiberglass.

*Patterns:* The basic design work has been done with free-space models. Hence, all gain figures require readjustment relative to a proposed height for the array above a specific ground quality. Ordinarily, the front-to-back ratio or rearward lobes and the SWR curve will hold good if the array is more than  $1/4 \lambda$  above ground. Quads are less sensitive to ground influences on the feedpoint impedance and other operating characteristics than are arrays with open-ended linear elements. Of course, the exact gain of the strongest lobe and the elevation angle of that lobe will be functions of antenna height as measured in wavelengths or a fraction of a wavelength above ground. With the exception of quite low mounting heights, azimuth patterns taken above ground will closely resemble at the elevation angle of maximum radiation the free-space patterns that we can take directly from the design model. However, we must adjust our expectations for such patterns to reflect a recognition of the high levels of interaction among the concentric elements of the array. Not all bands produce patterns that we have come to expect from monoband Yagis.

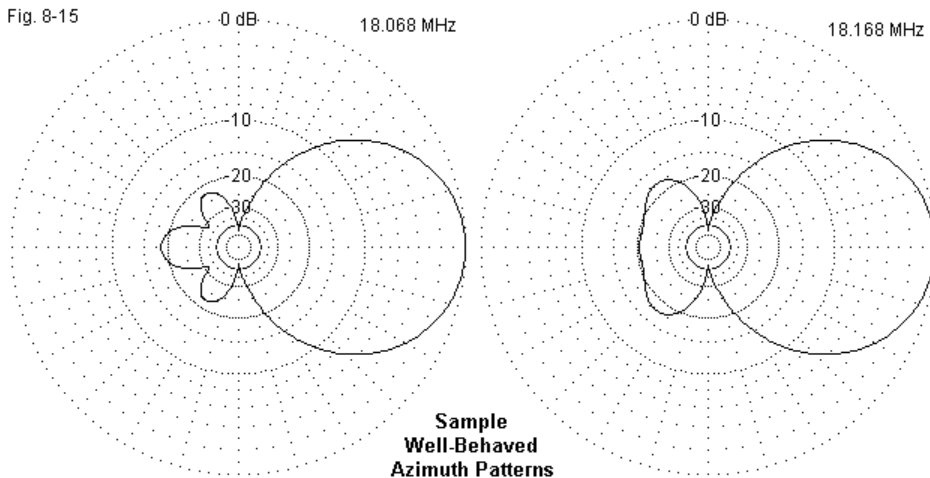
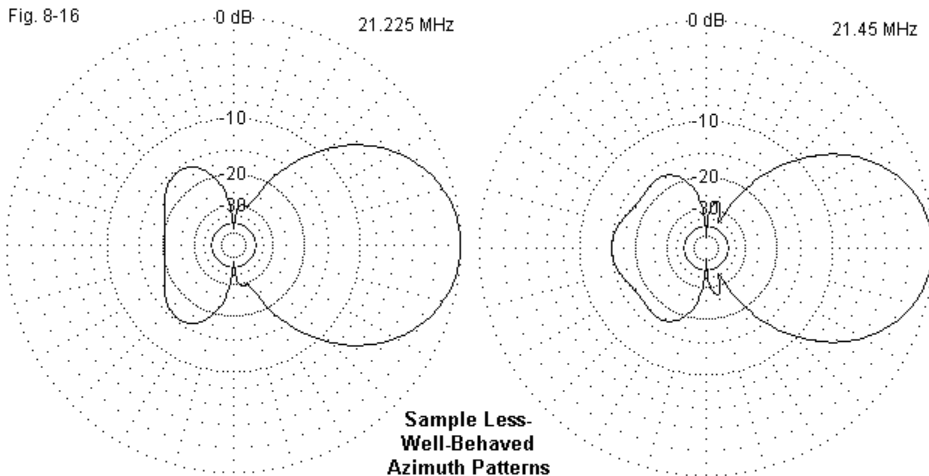


**Fig. 8-15**, for example, might represent both the 20-meter and 17-meter bands for the 4-5-6-element array. In both cases, we have well-behaved patterns, with single forward lobes and no forward side lobes. As well, we have radiation to the rear that follows fairly standard progressions of showing either 3 small rearward lobes or a single broad lobe or something in between the two. However, even the pattern for 18.168 MHz reveals a good reason for the quad array designer to look at each pattern within the list of check frequencies. The rearward pattern at the upper end of 17 meters shows a worst-case front-to-back ratio of about 17.5 dB, despite a 180E front-to-back ratio of better than 20 dB.



Above 17 meters, the patterns—both forward and rearward—can grow considerably less well behaved. In the progression from the middle of 15 meters to the upper end (**Fig. 8-16**), we find the development of forward side lobes. Although they remain diminutive at 15 meters, on higher bands, the side lobes can grow to proportions that affect the overall forward beamwidth of the array between -3 dB power points. In addition, the merely large rear radiation patterns, with a worst-case ratio to the forward lobe of 15 dB, evolve into very broad patterns. The broader pattern may have operational consequences, since response to the rear would no

longer be to a pair of narrow directions, but instead would cover most of the rear quadrants. Needless to say, pre-construction evaluation of a large quad array design must include an evaluation of whether or not the patterns (as well as the performance numbers) are satisfactory for the intended operation.

*Efficiency.* The NEC core that is the heart of most common antenna modeling software provides a power budget that lists a value for efficiency. The efficiency of an antenna is simply the power radiated (without regard to where it goes) to the power supplied to the antenna—and then converted to a percentage. The calculation does not include anything not modeled, for example, matching sections or networks, feedline losses, etc. However, it does include material losses within the antenna elements as a result of their resistivity, and it also included resistive losses associated with any traps or reactive loads. This latter category of losses does not apply to the quad arrays, but wire losses do apply, since we are using #12 AWG copper wire. The wire size is as important as the material, since skin effect is partially a function of element surface area. In fact, with high levels of surface area, such as with the use of aluminum tubing, material losses can be minimal. For example, there are models of 6-element Yagis in my collection with efficiencies approaching 99%.

The thinner the wire as a fraction of a wavelength and the higher the frequency, the greater will be the losses and the lower the efficiency of an antenna. These general rules would reveal themselves if we developed a sequence of simple monoband Yagis by which to test them. However, the large quads that we have been exploring display complex interactions among the elements. In doing so, they reveal another dimension to antenna efficiency that is not as well appreciated as element diameter and frequency.

**Table 8-7** lists the calculated mid-band efficiencies of each of the quads we have reviewed. Note that the highest efficiency is considerably lower than that for a "fat-element" Yagi. Although we can detect a drift in the general direction claimed by the rules, the set of numbers does not clearly correspond with expectations bred by the rules. Especially noticeable is the very low figure for 12 meters on the largest array.

Table 8-7. Radiation efficiencies of 3 large quad arrays.

Band Meters	Frequency MHz	Antenna Efficiency (%)		
		3-4-Element	4-5-Element	4-5-6-Element
20	14.175	93.6	94.6	94.4
17	18.118	93.9	92.7	93.3
15	21.225	94.1	92.7	93.7
12	24.94	90.1	87.7	80.4
10	24.4	93.6	91.9	90.7

Note: Efficiency is the ratio of power radiated to the power supplied to the antenna and does not include matching or line losses.

If we return to **Table 8-5**, we would discover that the 12 meter portion of the largest array provided less than 0.1 dB gain advantage over the next shorter quad, with most other characteristics being roughly equal between the two. What limits the gain is the inability of the elements on their fixed spacings to achieve the most effective inter-element coupling to yield a higher gain. If the larger array had resulted in significantly larger rear lobes, the efficiency might have been higher. Had it resulted in higher forward gain—or even a wide beamwidth—we might also see a higher efficiency value. However, we often neglect a third possibility: the current distribution in all elements is such that the sum of radiation in all directions does not increase, but instead, the current levels are higher in regions of the antenna where losses exceed contributions to radiation. The result is lower efficiency without a change in wire size, wire lengths, or frequency. For the 12-meter case, one might raise efficiency somewhat by adding the fourth director (as was done on 10 meters), even though it would add to wire losses. As well, one might optimize further the relative spacing of the 12- and 10-meter drivers from the reflector.

Efficiency is (or can be) an indicator of possible design improvement. However, it does not affect the reported gain of the array, since that gain already takes into account the radiation efficiency of the total antenna model. Indeed, attaching the wrong significance to efficiency can result in a misuse of the data.

For example, achieving 99% efficiency in a directional array, where the added radiation is to the rear or sides, would not amount to a design improvement.

*Element Precision:* An array with highly interactive parasitic elements requires considerable precision in construction to achieve the design results. One aspect of construction precision is understanding which elements can be adjusted and which should be precisely built and then left alone. The following guidelines may be useful, although their application may vary from one design to another.

1. Reflector-driver-first director: For arrays with 2 or more directors on a band, fine-tuning the reflector-driver-first director combination tends to function predominantly in setting the source impedance across the band in question. Once set, it is useful not to perform further adjustments on this set of elements—with one exception. The driver can be adjusted to shift the reactance levels. However, reductions in driver size will normally also reduce the resistive component of the feedpoint impedance, and increases in size will raise the feedpoint's resistive component. In constructing a given large array design, adjustments here should be near to last.

2. First director: Where there are 2 or more directors, the size of the first director may be sufficiently critical that, once set, it should not be altered. On some bands, under a 1" change in the first director can create large changes in the performance within a given passband, and these large changes may involve any of the key operating parameters: gain, front-to-back ratio, or SWR curve. In general, the further forward the changes, the less critical they are for a given amount of change.

3. The two forward-most directors: As **Table 8-1** (a through c) may reveal by comparing dimensions among arrays, one can go far toward controlling the characteristics of any band served by a large array by changing the forward directors. For wide-band service, the most forward director becomes shorter to enhance high-end performance and the next director to the rear become larger to enhance low-end performance. Both moves tend to raise the feedpoint resistive component a bit, which is why hasty adjustments to the driven element should be avoided.

Obviously, where there are too few elements to adhere to these guidelines, other measures are required. For example, a band with 4 elements may require a slight enlargement of the reflector to enhance low-end performance. However, this move may require re-adjustment of the driver and first director to restore or obtain a desired feedpoint impedance and SWR curve across the band. A 3-element band becomes a ballet of interactions among the elements such that the reflector is normally used to control both radiation resistance and low-end performance, while the director controls high-end performance, with the driver sized to create the best possible situation for the antenna feed. Since large multi-band quad arrays normally begin with fixed spacing, there are many instances where meeting design specifications may not be possible.

*Correlations between models and reality.* Because many dimensions within a large multi-band quad array require precise measurement of the loop circumference to within less than 1", constructing such an array is not a casual endeavor. Indeed, it may lie beyond the realm of simple backyard build-and-play techniques. However, with some care, trials, and testing, constructing a modeled design is perfectly feasible. The key lies in understanding both the model and the realities of a proposed construction technique. The two can be correlated.

**Fig. 8-17** sketches loosely some of the ways in which many builders attached quad loop corners to the support arms. In two of the versions, we have metal rings wrapped around the non-conductive support arm. In many cases, the wire will be wrapped at the corner to reduce abrasion. Whether or not directly connected, we have a small closed 1-turn coil in close proximity to the quad loop corner. The current at a quad loop corner is significant, in fact, higher than the current magnitude on a linear element the same distance from center. The closed loop may function as a load on the quad loop, and it does not take much of a load to detune the element relative to the original model of the loop. Similarly, when quad arms are composed of combinations of aluminum and non-conductive material, the aluminum may be close enough to the loop corner to create a slight detuning, equivalent to adding a very small load to the wire loop.

Of the 4 variations on wire attachment to a support arm, the cable-tie system comes closest to matching the computer model, although an anti-abrasion sleeve

may constitute a small distance over which the wire can be considered insulated. Insulated wire creates a velocity factor for the wire, making the physical and electrical length of the wire unequal. Corner sleeves may turn out to be harmless relative to the complex operation of a large multi-band array, but they should never be presumed to be harmless.

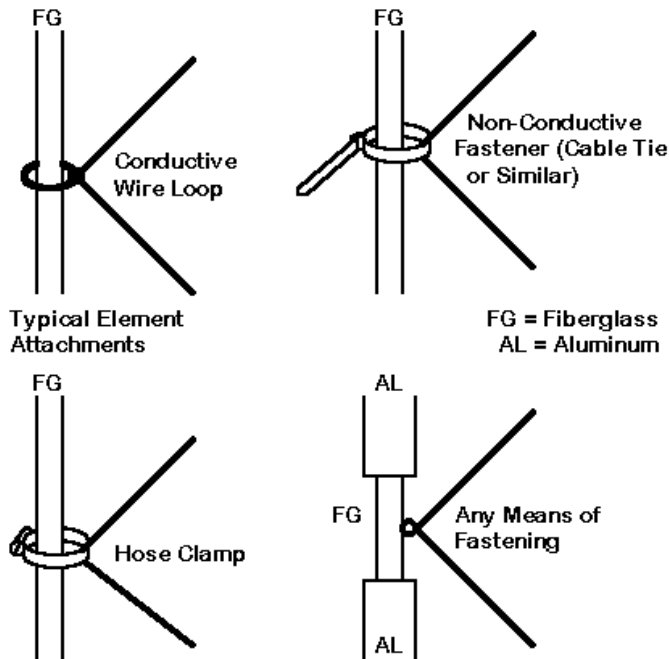
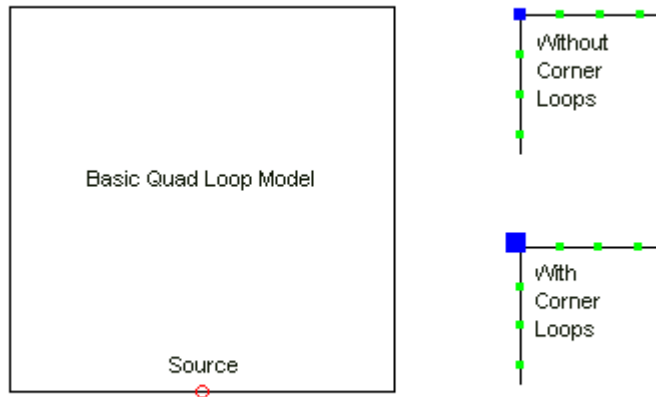


Fig. 8-17

To demonstrate the degree of detuning that is possible, consider a model of a square quad loop that is resonant when modeled without accounting for the ring connectors. The subject model is for 28.5 MHz and uses AWG #14 wire for the element. **Fig. 8-18** shows the general outline of the quad loop, along with two variations.

Fig. 8-18



Test Modeling What We Normally Do Not Model

The top-right partial outline shows one corner of the basic loop as normally modeled. The lower sketch shows the same corner with a 1" square loop attached, simulating the ring connector often used in physical quads. Since the quad loop is about 109.56" per side exclusive of the loops, the small additions seem insignificant, even when we multiply the one shown by four. **Table 8-8** tells another story.

Table 8-8. A Quad Loop With and Without Corner Attachment Loops

Version	Impedance (Ohms)	Max. Gain (dBi)	AGT	AGT-dB
Without	125.4 - j 0.5	3.30	1.002	0.01
With	128.1 + j24.5	3.29	1.001	0.01

The reactive component of the impedance may at first sight seem manageable. In reality, the test quad loop model required a reduction in the side length to 108.52" to return the loop to resonance with the corner loop appendages. In terms of circumference, the loop's wire length required a 4.2" change. At 10 meters, this

value amounts to 1% of the loop's circumference.

The sample will not exactly correspond to the loops and construction methods in any particular case, since the effect of virtual corner loops will vary with frequency, with the corner-fastening material, and with other variables. Still, it does show the degree to which the model may depart from reality in that reality contains loops the size of the ones included in the revised model. For every case of omitting details from models, the prototype will require adjustment to center the performance curves where the design model intended them to be. The problem becomes more acute with parasitic elements. One may use either a detailed or a shortcut procedure. The shortcut simply applies the percentage of change to the driver loop length to each of the parasitic elements.

There is a tedious but straightforward way to determine to what degree construction practices may affect the operation of a quad relative to the "clean," bare wire model on which it may be based. First, model only the driven element assembly or assemblies. Determine as precisely as feasible the resonant frequency of each driver. Second, build as precisely as possible the driver assemblies in accord with the proposed method of construction and elevate them to a good height. Determine the resonant frequency of each driver. Either the resonant frequencies will match those of the model or a pattern of offsets will become evident. The absence of a pattern will likely be good reason for reviewing the initial driver construction.

Relative to the measured resonant frequencies, add loads of the appropriate reactive amounts to each of the 4 corners of each driver so that the model resonates at the same frequency as the driver assembly tested. For each band, adding the same loads to each of the four corners of quad loops on that band will be a quite accurate approximation of the construction technique effects on the entire set of elements. Now readjust the dimensions of the model to restore the performance curves of the original model. The resulting dimensions should result in correct operation of the array on all frequencies.

I can only state that they "should result in correct operation," but the effectiveness of the technique will rest upon the precision with which the array is

constructed during both the test and "final" construction phases of the operation. Large quad arrays such as the ones discussed in these notes require dimensional precision to within an inch on some elements. Even small amounts of loading or detuning on some elements may throw the array off the desired performance curve on some bands.

Variations of the technique suggested here for correlating modeled quads and physical quads are adaptable to many other types of antennas. More important is the general thesis that models—usually using bare wire and with no modeled detuning effects—require correlation to the physical construction methods employed by the builder if the models are to be adequate guides to antenna design. Any success in building a large multi-element, multi-band quad of the order discussed in these notes will depend upon this step as much as any other in the design process.

The design of a large multi-band quad array intended for eventual construction can be enhanced by the proper use of antenna modeling software. However, as we have seen, the task is not an idle modeling exercise. It must be preceded by careful consideration of constraints, specifications, and modeling strategies to ensure reasonable results. Moreover, the task is not completed unless the final design model is carefully evaluated and then correlated to the proposed construction methods. These notes have had as their goal to make the process orderly, but by no means brief.

### *Conclusion*

In this long exercise, we have traced the design evolution of a 3-4-element quad into longer versions, in the end, settling on a 30' boom with between 4 and 6 elements, depending on the band. The initial design for our work began with 4 X-braces to support element for various bands, while the final version required 6 X-braces. The shorter intervening structures did not hold elements for the same bands.

In design terms, the final product met or exceeded almost all of the initial design specifications. The design failed to meet a few desired performance results

as a consequence of the limitations imposed by pre-setting the element spacing for the planar support structures. Note that the design goals did not use abstract figures, such as a minimum front-to-back ratio of 20 dB. Rather the goals used were suited to the general nature of parasitic quad beam capabilities.

More significant to the exercise were two facets of design work. One involved the use of antenna modeling software to develop the design. All such software operates well only within guidelines specific to the programs involved. Any design work that does not honor these guidelines is subject to significant error. The other aspect of design is an appreciation of the degree to which the elements of a planar quad design interact. These interactions require multiple adjustments of many bands to optimize a given performance parameter on one band without adverse affect to other bands. As well, the interactions also limit the behavior of the patterns that we may obtain from a large multi-band quad beam.

Equally important to the design exercise is a recognition of the move that we must eventually make from the design to a prototype. Construction variables almost always dictate a requirement for field adjustments that tend to grow exponentially as we add band to the array. As we noted in the final section, there are some construction facets that we may incorporate indirectly into the models themselves—but at a cost of increased model complexity.

## Chapter 9

### What Have We Learned?

In these 3 volumes of notes on the cubical quad, we surveyed a number of quad designs ranging from monoband mini-quads to standard 2-element 5-band quads. The second volume turned to re-thinking the monoband quad in order to overcome a limitation that appeared with virtually every design in the first volume: narrow operating bandwidth in more than one operating category. The volume featured computerized programs to allow calculation of 1-element to 4-element quads that would stand up to the rigors of computer analysis via NEC and MININEC software. However, that volume also explored some of the avenues used to design longer quad beams of up to 6 elements.

This volume has explored only one of the directions left open at the end of volume 2. We have taken a long, but not exhaustive, look at multi-band quads, beginning with 2-element versions and ending with quads with different numbers of elements on different bands. The jump from 2 element quads to larger arrays also changed the physical planning. We moved from spider construction that placed elements at optimal electrical distances from each other to planar construction that used standard physical increments between elements. In the progression of quad designs, we confirmed a number of conclusions reached in the earlier volumes and established some new ones.

1. In the development of ever-larger quads, we discovered that once a quad beam reaches about 4 elements, it loses its gain advantage over a Yagi. The parasitic interactions among quad loops are not identical to the interactions of linear elements. The larger quad requires a greater boom length to achieve its maximum gain than a Yagi with the same number of elements. Hence, for both mono-band and multi-band quads and Yagis, designs having similar boomlengths have similar gain performance.

2. In the HF region, one key limiting factor of quad designs is the necessary use of thin conductors. The average quad element conductor is less than 0.1 the diameter of the average Yagi conductor, even allowing for the element-tapering schedule used in HF beams. The result is a narrower operating bandwidth. In

general, quad gain curves show higher rates of change across the wider HF bands than well-designed Yagis. As well, obtaining a 2:1 50- $\Omega$  SWR curve for the wider bands becomes more difficult. Optimized 2-element designs with separate feedpoints can overcome the SWR limitation, even when transferred to a 3-band or a 5-band beam. However, longer quads, especially using planar construction, have more difficulty with this operating parameter.

3. Although the thin conductors of HF quads contribute to the narrow front-to-back ratio passband of most quad designs, that feature is endemic to the quad configuration. Even though very fat conductors—usable in VHF and UHF quads—can extend the front-to-back curve, no design to this time has yet achieved the level of front-to-back performance that Yagis routinely achieve in good designs.

4. Like the design of multi-band Yagis, the design of multi-band quads is not so much a science as it is an art. The process requires patient trial-and-error design work that inches toward a successful design. Despite the similarity in the design procedures for multi-band quads and Yagis, the two processes do have at least one important difference. In multi-band Yagi design work, we must spend much energy eliminating unwanted interactions among elements, especially with respect to harmonically related bands like 20 and 10 meters. Hence, we find the use of control directors whose job is less to contribute to the array's gain than it is to prevent the adjacent 20-meter director from shifting the 10-meter passband downward in frequency.

In contrast, the quad designer must spend equal effort trying to use element interaction to enhance performance. Element interaction under good control can add to the array's gain and help place gain peaks within the passband. More significantly, interactions can aid large planar quads show wider SWR passbands than roughly equivalent monoband quads.

Multi-band Yagi and quad design share other features. First, the needs for special elements on some bands may appear at any time. This need tends to wash out the desire for a simple mechanical design. Second, the dimensions of some elements—especially select directors—may become very finicky. Third, the construction method becomes one of key elements that increases the difficulty in

translating a computer-generated model into a physical reality. The challenges that the Yagi designer faces in the boom-to-element junction have their counterparts in the quad designer's attachment of loop elements to non-conductive support arms.

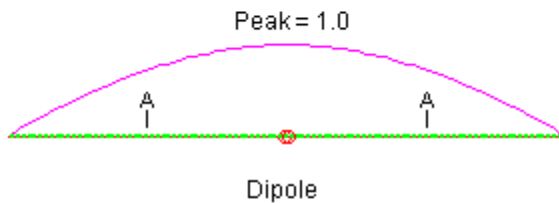
Hopefully, we have also made some strides in this volume with respect to understanding element interaction, at least at the rudimentary level of 2-element quads. Sorting out interactions that occur because of element proximity and frequency ratio from interactions that may occur when using a common feedpoint required systematic modeling using optimized initial monoband reference designs.

We managed to see patterns of required element adjustments that accrue to both adjacent-band designs and to combinations of more widely spaced bands. One of the critical patterns that emerged involved the lowering of the feedpoint impedance for inner loops, a pattern aggravated by adding more bands to an array or using adjacent band loops. The individual who desires to design and build his or her own multi-band quad is more likely to achieve success with a modest 2-element 3-band design. The narrower bands (12 and 17 meters) are ripe for a common-feedpoint quad, since the required passbands do not face any major challenges that a little feedpoint network ingenuity cannot overcome. The correlate proposition for one who purchases a commercial 5-band quad is to assemble the unit as precisely according to instructions as possible and to place it within the recommended height range specified by the maker.

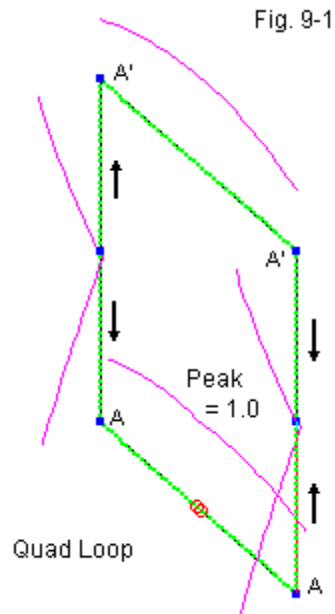
The systematic work of this volume has gone only a small distance toward understanding quad behavior. Although we might with suitable hubris like to think that we have made good strides in understanding quad behavior, the truth is that the results of our work tend to reveal more of what we do not yet know. The patterns that we have uncovered have little theoretical foundation beyond the calculating abilities of NEC-4 software. Codifying results into tabular patterns and into equations developed through regression analysis may have some practical utility, but such work does not yet constitute an explanation in sound theoretical terms. At this stage of development of our understanding of quads, we are still identifying factors that play (or may play) a role in the differences that we see between parasitic loop and parasitic linear element properties.

One factor that may play such a role is the difference in current distribution along the double-dipole wires of a quad loop in contrast to the linear wire of a dipole. **Fig. 9-1** shows the current distribution along these wires in graphic form. Note that the quad loop has been restructured from its normal 4-wire simplification into a 6-wire structure with the upper and lower bent dipoles terminated but connected at the horizontal centerline.

Current Magnitude/Distribution  
Along a Dipole and Along  
a Quad Loop



Quad arrows indicate model  
construction method.  
A = Quad corner and dipole  
equivalent position.



The points marked A are important, since they mark on the dipole the segments corresponding to the corner segments on the quad loop, where the lossless 0.1"-diameter wires in each resonant 28-MHz model use 100 segments per half-wavelength. Working from the feedpoint outward, the dipole shows relative current magnitudes of 0.737 and 0.716 in adjacent segments. The phase angles are  $-3.05^\circ$  and  $-3.14^\circ$ , respectively. The end segments of the dipole have magnitude and phase angle values of 0.025 and  $-4.84^\circ$ , remembering that these

values are not at the exact element tip, but along a length that is 1% of the total dipole length. Of course, the series source of the dipole shows relative current values of 1.0 and 0.0°.

With the same source method, the quad loop shows successive corner magnitude values of 0.725 and 0.703. The corresponding corner phase angles are -6.68° and -6.93°. These values apply to the lower corners of the quad loop. Even with lossless wire in a free-space model, the current distribution along the upper wire is not identical to what we find on the lower wire. The upper wire center segments show 0.996 and -1.40°. The upper corners show successive magnitude values of 0.716 and 0.695, with phase angles of 1.06° and 1.34°, working from the horizontal wire to the vertical wire.

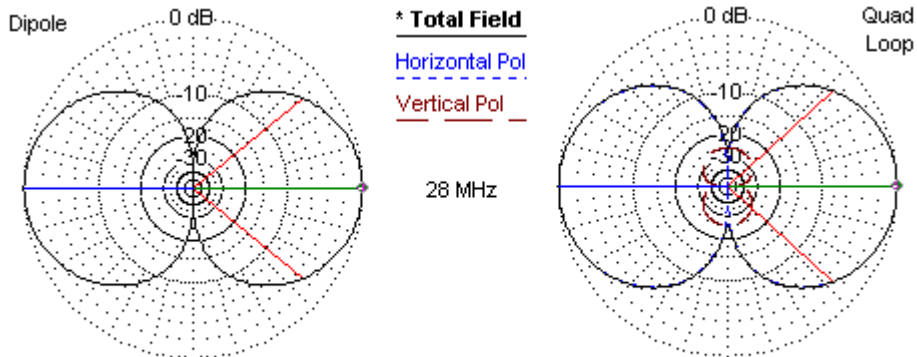
The differential in current magnitude at the corners and the corresponding successive dipole segments is very close to the same (0.021 vs. 0.022). However, the phase-angle changes are very different: 0.09° for the dipole and 0.25° for the quad loop. As well, by the time we arrive at the corner position, the quad loop current has undergone a phase shift that is more than double the dipole shift. That phase shift continues until we reach the junction of the vertical wires at the centerline of the quad. The joining segments show phase shifts of about 77°, with the actual junction in a truly balanced quad loop with both top and bottom in-phase feeding showing a 90° shift each way.

Our normal cursory scan of parasitic element currents usually focuses only upon the center segment, although we are very much interested in the current magnitude and phase angle on this segment. However, this interest normally applies to linear elements. It may not apply equally to quad-loop elements. We can show through large collections of models that a 2-element driver-reflector Yagi obtains maximum front-to-back ratio with the elements about  $0.125 \lambda$  apart. For the same condition, a driver-reflector quad requires between  $0.16$  and  $0.17 \lambda$ . A detailed study of just how this difference relates to the different current distribution conditions along the two types of elements might enlighten our understanding of both kinds of parasitic beams—and their counterparts with one or more directors.

There is one more subject connected to quads—or more specifically, the quad

vs. Yagi discussion—about which silence is the most discrete policy. In the early years of amateur quad use, persistent reports arose about the ability of quad beams to "open and close bands" as propagation shifted in the early morning and late afternoon. Some folks have simply dismissed the tales (usually, Yagi users). However, others have noted that the reports are too numerous and well corroborated to be so easily dismissed. (Unfortunately, this claim also attaches to UFO sightings.) Over the decades, we have been treated to innumerable explanations ranging from scratch-pad calculations of quad surface area to estimates based on the peculiar skewing of signal polarization during dusk and dawn periods of skip phenomena.

In fact, the patterns of basic dipoles and quad loops do show a small difference, even though we popularly hold that the bottom-fed quad loop is a horizontally polarized antenna. **Fig. 9-2** shows free-space E-plane patterns of both types of antennas. Within the available resolution, we find no trace of a vertically polarized component in the dipole pattern. In the pattern for the quad loop, we find the radiation consequences of the fact that the loop side wires have current levels ranging from zero to a relative magnitude of about 0.7.



Free-Space E-Plane Patterns: Dipole and Quad Loop

Fig. 9-2

- - - RADIATION PATTERNS - - -

Table 9-1

- - ANGLES - -		- POWER GAINS -			- - - POLARIZATION - - -		
THETA	PHI	VERT.	HOR.	TOTAL	AXIAL	TILT	SENSE
DEGREES	DEGREES	DB	DB	DB	RATIO	DEG.	
90.00	0.00	-131.72	■ 2.14	2.14	0.00000	90.00	LINEAR
90.00	10.00	-131.72	1.95	1.95	0.00000	90.00	LINEAR
90.00	20.00	-131.72	1.37	1.37	0.00000	90.00	LINEAR
90.00	30.00	-131.72	0.39	0.39	0.00000	-90.00	LINEAR
90.00	40.00	-131.72	-1.00	-1.00	0.00000	90.00	LINEAR
90.00	50.00	-131.72	-2.88	-2.88	0.00000	90.00	LINEAR
90.00	60.00	-131.72	-5.39	-5.39	0.00000	-90.00	LINEAR
90.00	70.00	-131.72	-8.97	-8.97	0.00000	90.00	LINEAR
90.00	80.00	-131.72	-15.04	-15.04	0.00000	90.00	LINEAR
90.00	90.00	-131.72	-131.72	-128.71	0.00000	45.00	LINEAR
90.00	100.00	-131.72	-15.04	-15.04	0.00000	-90.00	LINEAR
90.00	110.00	-131.72	-8.97	-8.97	0.00000	-90.00	LINEAR
90.00	120.00	-131.72	-5.39	-5.39	0.00000	90.00	LINEAR
90.00	130.00	-131.72	-2.88	-2.88	0.00000	90.00	LINEAR
90.00	140.00	-131.72	-1.00	-1.00	0.00000	90.00	LINEAR
90.00	150.00	-131.72	0.39	0.39	0.00000	90.00	LINEAR
90.00	160.00	-131.72	1.37	1.37	0.00000	-90.00	LINEAR
90.00	170.00	-131.72	1.95	1.95	0.00000	-90.00	LINEAR
90.00	180.00	-131.72	■ 2.14	2.14	0.00000	-90.00	LINEAR
90.00	190.00	-131.72	1.95	1.95	0.00000	-90.00	LINEAR
90.00	200.00	-131.72	1.37	1.37	0.00000	-90.00	LINEAR
90.00	210.00	-131.72	0.39	0.39	0.00000	90.00	LINEAR
90.00	220.00	-131.72	-1.00	-1.00	0.00000	-90.00	LINEAR
90.00	230.00	-131.72	-2.88	-2.88	0.00000	-90.00	LINEAR
90.00	240.00	-131.72	-5.39	-5.39	0.00000	90.00	LINEAR
90.00	250.00	-131.72	-8.97	-8.97	0.00000	-90.00	LINEAR
90.00	260.00	-131.72	-15.04	-15.04	0.00000	-90.00	LINEAR
90.00	270.00	-131.72	-131.72	-128.71	0.00000	-45.00	LINEAR
90.00	280.00	-131.72	-15.04	-15.04	0.00000	90.00	LINEAR
90.00	290.00	-131.72	-8.97	-8.97	0.00000	90.00	LINEAR
90.00	300.00	-131.72	-5.39	-5.39	0.00000	-90.00	LINEAR
90.00	310.00	-131.72	-2.88	-2.88	0.00000	-90.00	LINEAR
90.00	320.00	-131.72	-1.00	-1.00	0.00000	-90.00	LINEAR
90.00	330.00	-131.72	0.39	0.39	0.00000	-90.00	LINEAR
90.00	340.00	-131.72	1.37	1.37	0.00000	90.00	LINEAR
90.00	350.00	-131.72	1.95	1.95	0.00000	90.00	LINEAR
90.00	360.00	-131.72	■ 2.14	2.14	0.00000	90.00	LINEAR

We may confirm the essential horizontal polarization of the dipole by looking at the NEC-4 radiation pattern in **Table 9-1**. The table uses 10° increments for brevity. The vertical gain component is uniformly -131.72 dBi or a power ratio of about 6.7E-14. This value is a calculation artifact. Made evident by looking at the relative gain values for both components at a phi angles of 90° and 270°.

Equally significant in the table is the NEC classification of the polarization as linear, based on the axial ratio calculation of 0.0. The axial ratio is (within NEC) the ratio of the value of the minor axis to the major axis of the ellipse of rotation of transmitted or received electromagnetic waves. True circular polarization would show an axial ratio of 1.0, while elliptical polarization shows values between 0 and 1.0.

In fact, for many directions in a standard free-space E-plane pattern, a quad loop is elliptically polarized. **Table 9-2** confirms this fact with a radiation pattern for our basic quad loop, again using 10° increments. The sense of the polarization shifts from left to right and back again every 90° around the E-plane circle. Only at points of minimum horizontal gain and at points of minimum vertical gain do we find true linear polarization.

Lest this condition spark a new wave of theories about quads that tries to create a correspondence between skip energy skewing and elliptical polarization, we must call attention to the axial ratio column of the table. First, the maximum value for the axial ratio is 0.01796 or well under 2%. Second, the maximum gain of the vertical component is -22.07 dBi, but that occurs at right angles to the loop plane. Along the plane of the loop, the vertical component is much weaker, and it drops to -134 dBi broadside to the loop. In the end, the fact of elliptical polarization does not provide evidence of any phenomenon capable of explaining and confirming the tales of quads opening and closing the DX bands.

There is one more possible source of the reports, one that is perhaps plausible, if not true in detail. We may note in passing that, during the sunspot peak near the turn of the millenium, we did not hear tales of quad performance and its superiority over Yagis. In fact such reports emerge largely in the 1970s and 1980s.

- - - RADIATION PATTERNS - - -

Table 9-2

- - ANGLES - -		- POWER GAINS -			- - - POLARIZATION - - -		
THETA	PHI	VERT.	HOR.	TOTAL	AXIAL	TILT	SENSE
DEGREES	DEGREES	DB	DB	DB	RATIO	DEG.	
90.00	0.00	-134.16	■ 3.31	3.31	0.00000	90.00	LINEAR
90.00	10.00	-36.27	3.15	3.15	0.00064	-89.39	LEFT
90.00	20.00	-30.47	2.66	2.66	0.00132	-88.74	LEFT
90.00	30.00	-27.31	1.83	1.83	0.00208	-88.00	LEFT
90.00	40.00	-25.30	0.61	0.62	0.00301	-87.10	LEFT
90.00	50.00	-23.95	-1.08	-1.06	0.00424	-85.90	LEFT
90.00	60.00	-23.06	-3.42	-3.37	0.00609	-84.06	LEFT
90.00	70.00	-22.49	-6.84	-6.72	0.00947	-80.64	LEFT
90.00	80.00	-22.17	-12.81	-12.33	0.01796	-71.23	LEFT
90.00	90.00	■ -22.07	-134.16	-22.07	0.00000	0.00	LINEAR
90.00	100.00	-22.17	-12.81	-12.33	0.01796	71.22	RIGHT
90.00	110.00	-22.49	-6.84	-6.72	0.00947	80.64	RIGHT
90.00	120.00	-23.06	-3.42	-3.37	0.00609	84.06	RIGHT
90.00	130.00	-23.95	-1.08	-1.06	0.00424	85.90	RIGHT
90.00	140.00	-25.30	0.61	0.62	0.00301	87.10	RIGHT
90.00	150.00	-27.31	1.83	1.83	0.00208	88.00	RIGHT
90.00	160.00	-30.47	2.66	2.66	0.00132	88.74	RIGHT
90.00	170.00	-36.27	3.15	3.15	0.00064	89.39	RIGHT
90.00	180.00	-134.16	■ 3.31	3.31	0.00000	-90.00	LINEAR
90.00	190.00	-36.27	3.15	3.15	0.00064	-89.39	LEFT
90.00	200.00	-30.47	2.66	2.66	0.00132	-88.74	LEFT
90.00	210.00	-27.31	1.83	1.83	0.00208	-88.00	LEFT
90.00	220.00	-25.30	0.61	0.62	0.00301	-87.10	LEFT
90.00	230.00	-23.95	-1.08	-1.06	0.00424	-85.90	LEFT
90.00	240.00	-23.06	-3.42	-3.37	0.00609	-84.06	LEFT
90.00	250.00	-22.49	-6.84	-6.72	0.00947	-80.64	LEFT
90.00	260.00	-22.17	-12.81	-12.33	0.01796	-71.22	LEFT
90.00	270.00	■ -22.07	-134.16	-22.07	0.00000	0.00	LINEAR
90.00	280.00	-22.17	-12.81	-12.33	0.01796	71.22	RIGHT
90.00	290.00	-22.49	-6.84	-6.72	0.00948	80.64	RIGHT
90.00	300.00	-23.06	-3.42	-3.37	0.00609	84.06	RIGHT
90.00	310.00	-23.95	-1.08	-1.06	0.00424	85.90	RIGHT
90.00	320.00	-25.30	0.61	0.62	0.00301	87.10	RIGHT
90.00	330.00	-27.31	1.83	1.83	0.00208	88.00	RIGHT
90.00	340.00	-30.47	2.66	2.66	0.00132	88.74	RIGHT
90.00	350.00	-36.27	3.15	3.15	0.00064	89.39	RIGHT
90.00	360.00	-134.16	■ 3.31	3.31	0.00000	90.00	LINEAR

In a long footnote to Chapter 7, I explored some of the reasons for the gain-claim explosion that occurred in the two decades prior to 1990. One significant part of that note recorded the fact that many of the commercial and homemade Yagis of the day in fact fell far short of theoretically possible Yagi performance. Indeed, operators might easily confuse front-to-back ratio for gain in the absence of true range tests. Early quads enjoyed success in terms of living up to their billing, although comparisons with Yagis of the day led to claims that 2-element quad beams surpassed long-boom 3-element Yagis in performance. In fact, 2-element quad beam performance—when optimized—equals the gain of a short-boom 3-element Yagi, which may be a full dB lower than the gain of a well-designed long-boom Yagi. (For this note, a long-boom 3-element Yagi has a boom that is about 1.5 times the length of its short-boom cousin. This value amounts to 24' vs. 16' at 20 meters or 12' vs. 8' at 10 meters.)

In terms of many (but certainly not all) Yagis of the 70s and the 80s, we might easily have found well built quads that could show more gain and thus open and close bands. The situation did not stem so much from some magical property of the quad as it did from deficiencies in many of the Yagis of the period. As we moved into the era of computer-aided antenna design in the 1990s and now into the 21<sup>st</sup> century, the stories have abated. And perhaps this is as it should be. Quad beams work very well indeed within their constraints. We need no magic to justify the effort and care that goes into the design and construction of a technically sound array, regardless of whether it is a quad or a Yagi. Indeed, I hope that the future of quad investigation sets aside speculative explanation and puts in its place straightforward systematic study using all of the resources to which we have access.

Our understanding of quad beams has not ended. It has just begun.

*Special Note on Models*

Attached to this volume on the CDROM is a special directory for the models used in these studies. The folder has a subdirectory for each chapter. In these folders, you will find the actual models that I used to develop these notes. Most of the models are in EZNEC (.EZ) format, although you may find a few in NEC-Win Plus (.NWP) format as well.

If you are interested in the models, I recommend that you transfer the entire set of folders to your hard drive. When you open the files and inevitably modify them, you can save the changes. The CDROM does not have write-back capability, but forms a long-term archive of the models with which you start.

## Other Publications

We hope you've enjoyed this Volume 3 of the **Cubical Quad Notes**. You'll find many other very fine books and publications by the author L.B. Cebik, W4RNL in the **antenneX Online Magazine BookShelf** at the web site shown below.

---

*Published by*  
**antenneX Online Magazine**  
<http://www.antennex.com/>  
**POB 271229**  
**Corpus Christi, Texas 78427-1229**  
**USA**

---

Copyright 2007 by **L. B. Cebik** jointly with **antenneX Online Magazine**. All rights reserved. No part of this book may be reproduced or transmitted in any form, by any means (electronic, photocopying, recording, or otherwise) without the prior written permission of the author and publisher jointly.

ISBN: 1-877992-80-1

---